The Decay Constant of ^{87}Rb

and A Combined U-Pb, Rb-Sr Chronology of Ordinary Chondrites

by

Ethan David Rotenberg

A thesis submitted in conformity with the requirements

for the degree of Doctor of Philosophy

Graduate Department of Geology

University of Toronto

The Decay Constant of ^{87}Rb

and A Combined U-Pb, Rb-Sr Chronology of Ordinary Chondrites

Ethan David Rotenberg

Degree of Doctor of Philosophy, 2009

Department of Geology, University of Toronto

Abstract

The ^{87}Rb-^{86}Sr system is a widely used long-lived isotope geochronometer. ^{87}Rb, the naturally occurring radioactive isotope of Rb, undergoes β-decay to stable ^{87}Sr with a half-life of approximately 50 Ga. Decay of ^{87}Rb to ^{87}Sr results in variable $^{87}Sr/^{86}Sr$ in minerals with different Rb/Sr, and measurement of $^{87}Rb/^{86}Sr$ and $^{87}Sr/^{86}Sr$ allows for the determination of the age of the rock. Accurate ages depend both on the quality of the isotopic analysis and on the accuracy of the ^{87}Rb decay constant, λ_{87}.

Although the currently accepted value for λ_{87} of $1.42 \times 10^{-11} a^{-1}$ has been in use for over 30 years, there is growing evidence that it is not accurate. Recent attempts to refine λ_{87} and its precision have not reached a consensus. This thesis describes a new experiment to measure λ_{87} by ^{87}Sr accumulation over a period of about 30 years, and the preparation of a $^{84\text{-}86}Sr$ double-spike in conjunction with that experiment. Radiogenic ^{87}Sr produced in aliquots of a $RbClO_4$ salt was

measured by isotope dilution thermal ionization mass spectrometry. An average of 31 measurements yields a value of $1.398 \pm 0.003 \times 10^{-11} a^{-1}$. This requires a substantial revision from the previously accepted decay constant and makes Rb-Sr ages calculated with it 1.5% older.

A Rb-Sr and U-Pb isotopic chronometry study was carried out on thirteen ordinary chondrites – the most common type of meteorite, the origin and history of which are still unclear. Some meteorites appear disturbed, possibly by recent shock during breakup of the parent body, whereas others yielded accurate and precise U-Pb and Pb-Pb ages. For example, L5 Elenovka yielded distinct ages for silicates (4555 Ma) and phosphates (4535 Ma), allowing the cooling rate of this meteorite from approximately 1055 K to 759 K to be constrained to 15 ± 3 K/Ma. Rb-Sr yielded less precise ages than U-Pb, but using the new decay constant allows accurate comparison between the two methods. This study creates a firm foundation for future studies in thermal history of chondrites and terrestrial metamorphic complexes using Rb-Sr together with other isotopic chronometers.

Acknowledgements

There are many people without whom I would not have accomplished this work. First I must thank my supervisors Don Davis and Yuri Amelin for their guidance and advice, for sharing with me their accumulated wisdom from years of experience in isotope geochemistry, and for giving me the opportunity to work on interesting projects which allowed me to regularly handle rocks from outer space. My committee members, Ed Spooner and Mike Hamilton have given me valuable advice along the way. Jon Patchett graciously travelled from Arizona to act as the external appraiser for the thesis, and to share with me how his trip to New Jersey gave him deeper insight into the music of Bruce Springsteen.

It has been a great pleasure working with, and learning from, everyone at the Jack Satterly Geochronology Laboratory: Kim Kwok, Sandra Kamo, Tom Pestaj, Bohdan Podstawskyj, Chris C. and Abin, and all the others who have passed through the lab. I would especially like to acknowledge the scientific advice and good humour of Tom Krogh and Oleg Bogdanovski, and I hope that my work will serve as a testament to their memories.

Mike Gorton has exhibited infinite patience and displayed encyclopædic knowledge in answering my myriad questions, many related to my research and many more not. James Brenan granted me access to his laboratory and materials, and Grant Henderson has kept me in good spirits with his fascinating hallway conversations.

Grazie mille to the recent graduates and others who kept me sane and gave me encouragement when I most needed it as my seemingly impossible deadlines loomed: Darlene, Halan, Lesley, Steve, and Chris K, Thomas, and Charly – I could not have pulled down the home-stretch without you. And Vera – thank

you for always cheering up everyone who finds themselves working in the department late at night.

The Royal Ontario Museum generously provided the meteorite samples that I studied. Mal, Ian, Bob, and Katherine were always helpful, and and always interested in my studies. Dr. David Gregory generously provided samples for study, and has done an incredible job of building the meteorite collection at the ROM. And thank you Aron for regularly allowing me into the museum for free.

The Department of Geology staff are wonderful and friendly and have always been there to take care of whatever problems popped up: Lynn, Ampy, Riaz, Silvanna, Karyn, Tasha and Jim C. Silvanna, thank you especially for making sure that I always got paid.

My thanks go to Barbara Shu and Elizabeth Glover – librarians at the physics library across the street. Barbara helped me track down my grandmother's PhD dissertation[*][❁] the first week I showed up at U of T. I frequently sent Barbara and Elizabeth down to physics library storage on wild goose chases for outdated German journals, and in the end they always managed to find what I was looking for.

I can't name all students – grad and undergrad – who have made my time at the department interesting and pleasant and fun. Thanks to all of you, and especially everyone who has made a temporary home in 2113, 2108, and most of all, 2105 – the best office. Leonie, all I have to say to you is: Nerf basketball, crossword puzzles, and Play Four.

---

[*] Levi, Miss M. (1922) On Photo-electric Conductivity of Diamond and Other Fluorescent Crystals. *Proc. and Trans. Royal Soc. Can.*, 3rd Ser. **XVI,** 241 – 257.

[❁] Levi, Miss M. (1924) On the Characteristic X-Rays from Light Elements. *Proc. and Trans. Royal Soc. Can.* 3rd Ser. **XVII,** 159-178.

Sheila Hall taught me the most important thing I learned in graduate school: the recipe for Halan's chocolate chip cookies – the best in the world.

Josiah *&* Gila, Nitai, Hallel, Honi, Sheer and Shemaiah, Elizabeth *&* Michael and Sidonia – thanks for everything. (New niece or nephew, you missed getting in here by just a few days).

Most of all, I must thank my parents, אבי מורי and אמי מורתי, for their support in this and all my other endeavours. They sparked my curiousity and have always given me nothing but encouragement in both my more rational as well as my more hare-brained schemes. This thesis is dedicated to them.

כי אלף שנים בעיניך
כיום אתמול כי יעבר
(תהלים צ:ד)

For a thousand years in thy sight
are but as yesterday when it is past
(Psalms 90:4)

Table of Contents

List of Tables

Chapter 2

Chapter 3

Chapter 4

Appendix A

List of Figures

Chapter 2

Chapter 3

Chapter 4

Appendix A

List of Appendices

Introduction

The ^{87}Rb-^{86}Sr system is a long-lived isotope geochronometer. ^{87}Rb, the naturally occurring radioactive isotope of Rb, undergoes β-decay to stable ^{87}Sr with a half-life of approximately 50 Ga. Sr has four naturally occurring stable isotopes: ^{84}Sr, ^{86}Sr, ^{87}Sr, and ^{88}Sr. Decay of ^{87}Rb to ^{87}Sr results in variable $^{87}Sr/^{86}Sr$ in minerals with different Rb/Sr, and measurement of $^{87}Rb/^{86}Sr$ and $^{87}Sr/^{86}Sr$ allows for the determination of the age of the rock. Accurate ages depend not only on the quality of the isotopic analysis, but also on the accuracy of the ^{87}Rb decay constant, λ_{87}. Rb-Sr dates are calculated from the equation:

$$\left(\frac{^{87}\mathrm{Sr}}{^{86}\mathrm{Sr}}\right)_m = \left(\frac{^{87}\mathrm{Sr}}{^{86}\mathrm{Sr}}\right)_0 + \left(\frac{^{87}\mathrm{Rb}}{^{86}\mathrm{Sr}}\right)\left(e^{\lambda t} - 1\right) \qquad \text{(Equation 1)}$$

where $(^{87}Sr/^{86}Sr)_m$ is the measured ratio of the Sr isotopes in the sample, $(^{87}Sr/^{86}Sr)_0$ is the initial ratio of the Sr isotopes at the time of formation of the rock or mineral, $(^{87}Rb/^{86}Sr)$ is the measured ratio of ^{87}Rb to ^{86}Sr at the present time, and t is the time elapsed since crystallization. If $(^{87}Sr/^{86}Sr)_0$ is known, or can be estimated, the age of the sample can be directly calculated from Equation 1. Typically, covariations are sought between $(^{87}Sr/^{86}Sr)_m$ and $(^{87}Rb/^{86}Sr)$ in a cogenetic suite of rock or mineral samples having a natural spread in Rb/Sr. If all samples have the same age and had identical $(^{87}Sr/^{86}Sr)_0$, when plotted on a diagram of $^{87}Sr/^{86}Sr$ v. $^{87}Rb/^{86}Sr$ they will fall on a straight line, defined by equation 1, whose slope will be $(e^{\lambda t}-1)$, proportional to the time that the system has remained closed – the age of the samples (Faure and Powell, 1972; Faure, 1986).

The additional assumption that λ_{87} is accurately known has unfortunately not been the case, but this has not been for a lack of trying. Dozens of experiments have measured λ_{87} over the course of nearly a century. Three methods have been used to measure decay constants: 1) direct decay counting, 2) geochronological age comparison, and 3) ingrowth, or daughter isotope accumulation. The direct counting method is a physical method involving the detection and counting of β-particles as they decay from ^{87}Rb. Geochronological age comparisons require the parallel determination of the age of a rock by analysis with another isotope geochronometer having a well known rate of decay, such as U-Pb along with Rb-Sr analysis, ideally on the same sample. A Rb-Sr isochron is plotted, but instead of using the isochron to solve for t, the age determined by the other isotopic system is assumed to be the age of the rock, and is inserted into Equation 1, which is then solved for λ_{87}. Ingrowth involves allowing a purified sample of parent element to decay over a measured period of time, and then measuring the accumulated daughter isotope over that time. Like age comparisons, the decay time and measured quantity of accumulated decay product are used to calculate λ_{87}. Historically, nearly forty measurements have been made by direct counting and approximately another fifteen by age comparison. Only two studies have measured ^{87}Sr accumulation in a purified Rb sample (McMullen et al., 1966; Davis et al., 1977).

Measurements of λ_{87} since 1980 converge on a value between 1.396-1.402 × $10^{-11}a^{-1}$ (× $10^{-11}a^{-1}$ hereafter understood) (Minster et al., 1982; Shih et al., 1985; Amelin and Zaitsev, 2002; Rotenberg et al., 2005,2009; Kossert et al., 2003; Nebel et al., 2006a, 2006b), more than 1% lower than the provisional value of 1.42 recommended by Steiger and Jäger in 1977, resulting in some investigators using the conventional value of 1.42 (e.g. Glodny et al., 2008) and others adopting an updated value (e.g. Edmunson et al., 2009). Consequently, there is disagreement

between laboratories, and there is a greater than 1% bias in Rb-Sr ages regardless of the analytical precision. This error is too large for comparisons with U-Pb ages to be meaningful. For example, Amelin et al. (2005) have resolved the U-Pb ages of silicates from those of phosphates in primitive meteorites, and used that chronological information to constrain the cooling rate of a meteorite parent asteroid over a time scale of 12 Ma. But a 1% decay constant error for a 4560 Ma meteorite is larger than this interval.

This thesis presents the results of a new ^{87}Sr accumulation experiment to measure λ_{87} with increased precision and accuracy. Despite the convergence of the more recent measurements by other methods, an accumulation experiment is important. Direct counting and age comparisons have biases that are unique to each type of experiment. For example, direct counting requires corrections for undetected low energy decays, and historically the measurements have scattered widely. Age comparisons require assumptions about the geological history of the samples studied as well as the accuracy of the decay constant of the isotopic system used for comparison. The current agreement between different studies could be fortuitous, as apparently was the agreement between all three types of experiments leading to the adoption of 1.42 by the Subcommission on Geochronology (Steiger and Jäger, 1977). Accumulation experiments have their own set of biases, but they are more easily quantified, and are limited to the purity of the starting material and the analytical uncertainties.

I have also undertaken a combined U-Pb and Rb-Sr study of ordinary chondrites. This provided an opportunity to follow up on previous results of U-Pb studies on chondrules, chondrule silicates, and phosphates from ordinary chondrite H5 Richardton (Amelin et al., 2005) and at the same time put the newly determined ^{87}Rb decay-constant to use.

The chondritic meteorites are among the most primitive objects in our solar system. As such, they afford us the opportunity to study first-hand the materials from which the terrestrial planets formed and to understand the processes by which they developed. While a basic understanding of the early history of the chondrite parent bodies has been achieved, there remains uncertainty over many of the details of the formation processes, the structure of the bodies, their sizes, accretion intervals, and metamorphic histories (Wasson, 1972; Scott and Krot, 2007). The U-Pb study of H5 Richardton (Amelin et al., 2005) showed that the U-Pb system can resolve time differences of a few Ma in early solar system history, and can be used to put constraints on the cooling rates of meteorite parent bodies. Cooling rates can then be used to model planetesimal accretion and heating. The current study presents the findings of U-Pb and Rb-Sr analyses of thirteen additional ordinary chondrites representing a variety of classes and metamorphic grades.

This thesis is structured as follows:

Chapter 2 describes the measurement of λ_{87} by ^{87}Sr accumulation. It reviews the history of ^{87}Rb decay-constant measurements and the current state of λ_{87} followed by the description of the accumulation experiment itself and its results. A $RbClO_4$ salt was purified in 1976 (Davis, 1978). Approximately 30 years later, aliquots of this salt were spiked, dissolved, and Sr was chemically separated from Rb. Strontium isotopic ratios were measured by thermal ionization mass spectrometry (TIMS), and the measured isotopic ratios were used to calculate λ_{87}. The new result is discussed in the context of other recent, and relatively precise measurements. The manuscript was written by E. Rotenberg.

Chapter 3 describes the calibration of a ^{84}Sr-^{86}Sr double-spike used for the λ_{87} measurement experiment. Although this work was done before the

decay-constant experiment, the spike is ancillary, although crucial to, the λ_{87} measurements. Essentially a methods paper, it is important for the geochemistry community since it examines a number of issues that are common to the preparation of any tracer solution, and more broadly, any solution whose concentration must be known precisely. These issues are rarely discussed in the literature but are critical to any experiments based on gravimetry. Appendix A describes calibration of a ^{84}Sr spike used for initial measurements of λ_{87} in this study. The concentration of this spike was not determined to the same precision as the double-spike. In addition, because it is enriched only in ^{84}Sr, it was not useful in correcting for instrumental fractionation in the highly radiogenic Sr samples analyzed for the λ_{87} measurements. The manuscript was written by E. Rotenberg.

Chapter 4 describes a combined U-Pb and Rb-Sr study of ordinary chondrites. The introduction outlines the valuable contribution of long-lived chronometers to our understanding of the early solar system. Chondrules and silicate fractions, as well as phosphate fractions from some meteorites were separated from crushed samples of the meteorites. U-Pb and Rb-Sr isotopes were analyzed by TIMS, and ages were calculated for the various samples. The chronological significance of these is discussed in the context of the cooling history of the ordinary chondrite parent bodies. Rb-Sr ages provided an opportunity to apply the newly re-measured decay constant, λ_{87}, and compare them against ages determined using the U-Pb system. Some Rb-Sr dates from the literature are recalculated and discussed. Meteorite samples were prepared by and analyzed by E. Rotenberg and Y. Amelin. E. Rotenberg performed approximately 70% of the sample preparation and sample analysis. The manuscript was written by E. Rotenberg.

References

Amelin Y. and Zaitsev A.N. (2002) Precise geochronology of phoscorites and carbonatites: The critical role of U-series disequilibrium in age interpretations. *Geochim. Cosmochim. Acta* **66**, 2399-2419.

Amelin, Y., Ghosh, A., and Rotenberg, E. (2005) Unraveling the evolution of chondrite parent asteroids by precise U-Pb dating and thermal modeling. *Geochim. Cosmochim. Acta* **69**, 505-518.

Davis D.W. (1978) *Determination of the 87Rb decay constant: An Rb/Sr and Pb/Pb study of the Labrador Archean complex*. Ph.D. Thesis, Univ. Alberta.

Davis D.W., Gray J., Cumming G.L., and Baadsgaard H. (1977) Determination of the 87Rb decay constant. *Geochim. Cosmochim. Acta* **41**, 1745-1749.

Edmunson, J., Borg, L.E., Nyquist, L.E., and Asmerom, Y. (2009) A combined Sm-Nd, Rb-Sr, and U-Pb isotopic study of Mg-suite norite 78238: Further evidence for early differentiation of the Moon. *Geochim. Cosmochim. Acta* **73**, 514-527.

Faure, G. (1986) *Principles of Isotope Geology, 2nd Ed.* John Wiley & Sons, New York, Chichester, Brisbane, Toronto, Singapore, 589 p.

Faure, G. and Powell, J.L. (1972) *Strontium Isotope Geology*. Springer-Verlag, Berlin, Heidelberg, and New York, 188 p.

Glodny, J., Kühn, A., and Austrheim, H. (2008) Diffusion versus recrystallization processes in Rb-Sr geochronology: Isotopic relics in eclogite facies rocks, Western Gneiss Region, Norway. *Geochim. Cosmochim. Acta* **72**, 506-525.

Kossert K. (2003) Half-life measurements of ^{87}Rb by liquid scintillation counting. *App. Rad. and Isot.* **59**, 377-382.

McMullen C.C., Fritze K., and Tomlinson R.H. (1966) The half-life of rubidium-87. *Can. J. Phys*. **44**, 3033-3038.

Minster J-F., Birck J-L. and Allègre C.J. (1982) Absolute age of formation of chondrites studied by the ^{87}Rb-^{87}Sr method. *Nature* **300**, 414-419.

Nebel, O., Mezger, K., Scherer, E.E., and Patchett, J. (2006a) Recalibration of the Rb decay constant by age comparison against three U-Pb dated igneous rocks. *Geophys. Res. Abstracts*. **8,** 08036**.**

Nebel O., Mezger K., Scherer E.E., and Davies G.R. (2006b) Determination of the Rubidium Decay Constant by Age Comparison Against the U-Pb System, *Eos Trans. Am. Geophys. Union* 87 (52), Fall Meet. Suppl., Abstract V21A-0558

Scott, E.R.D, and Krot, A.N. (2007) Chondrites and their components. In *Treatise on Geochemistry*, K.K. Turekian and H.D. Holland eds., Elsevier. 7800 p. Vol. 1, Chapter 7.

Shih C.-Y., Nyquist L.E., Bogard D.D., Wooden J.L., Bansal B.M., and Wiesmann H. (1985) Chronology and petrogenesis of a 1.8 g lunar granitic clast: 14321,1062. *Geochim. Cosmochim. Acta* **49**, 411-426.

Steiger R.H. and Jäger E. (1977) Subcommission on geochronology: Convention in the use of decay constants in geo- and cosmochemistry. *Earth Planet. Sci. Lett*. **36**, 359-362.

Rotenberg, E., Davis, D.W., and Amelin, Y. (2005) Determination of the ^{87}Rb decay constant by ^{87}Sr accumulation. 15th Annual V.M. Goldschmidt Conference, Abstract. *Geochim. Cosmochim. Acta* **69**, A326.

Rotenberg, E., Davis, D.W., and Amelin, Y., (2009) The decay constant of ^{87}Rb. *EOS Trans. Am. Geophys. Union*, **90** (22), Jt. Assem. Suppl., Abstract GA14A-06.

Wasson, J.T. (1972) Formation of Ordinary Chondrites. *Rev. Geophys. Space Phys.* **10**, 711-759.

Chapter 2

The decay-constant of ^{87}Rb

Ethan Rotenberg, Donald W. Davis, and Yuri Amelin

1. Introduction

The natural radioactivity of rubidium was discovered in 1905 by J.J. Thomson when he observed the emission of negative corpuscles – electrons – from rubidium even in the absence of any light source. Campbell and Wood (1906) confirmed the result a year later. Since then, there have been numerous attempts by different methods to quantify the rate of β-decay of ^{87}Rb by measuring its decay-constant, λ_{87} (Table 1 and Figure 1). Faure (1986) perhaps understated the case when he wrote that "the half-life of ^{87}Rb has been measured many times with somewhat contradictory results." In 1977, the International Union of Geological Sciences (IUGS) Subcommission on Geochronology recommended the value of $1.42 \times 10^{-11} a^{-1}$ with the caveat that "[t]he recommendation represents a *convention* for the sole purpose of achieving interlaboratory standardization" (Steiger and Jäger, 1977) [emphasis in original].

Notwithstanding the IUGS recommendation, a consensus has not been reached. Many laboratories continue to use the conventional value (Glodny et al., 2008; Bosse et al., 2005). Some investigators (e.g. Borg et al., 2003; Edmunson et al., 2009) have adopted the value of $1.402 \times 10^{-11} a^{-1}$ recommended by Minster et al. (1982) and Shih et al. (1985). More than thirty years after the adoption of the convention of $1.42 \times 10^{-11} a^{-1}$, there remains a discrepancy of over one percent among the various estimates of λ_{87} currently in use.

With the increased precision of modern mass spectrometry, decay constant uncertainty can represent a significant portion of the total error in Rb-Sr age determinations. Were we dealing only with the Rb-Sr system, and if all investigators agreed on a conventional value, we could perhaps accept this uncertainty for comparisons of Rb-Sr ages with one another since it would have

a minor effect on relative ages. But increasingly, investigators are interested in comparing ages from different isotopic systems, especially U-Pb, which is now much more commonly used as a geochronometer.

Decay constant determinations fall into three categories: 1) direct decay counting – β-counting in the case of ^{87}Rb, 2) geological age comparisons – the comparison with ages determined using a better-known decay system such as U-Pb and 3) ingrowth – the accumulation and measurement of daughter isotope over a laboratory time scale (Begemann et al., 2001). In principle, decay-constants can also be calculated theoretically, but "[p]redictions for forbidden transitions in general are hampered by lack of knowledge concerning the nuclear matrix elements..." (Greuling, 1942; Konopinski and Langer, 1954). Thus far, nuclear physics has not been able to furnish us with a sufficiently accurate estimate of λ_{87}. In the years since the IUGS report, λ_{87} has been revisited by several investigators, mostly by geological age comparisons, but also by direct counting. All these studies report greater precision than the earlier studies, and are in better agreement with one another. The mounting evidence from these studies as well as the Begemann et al. (2001) critical review of earlier ones suggests that the value recommended by Steiger and Jäger is 1-2% higher than the actual value. Although the more recent studies are more precise than earlier ones, and converge around a common value, in the past both counting experiments and age comparisons have been inaccurate primarily due to their dependence on assumptions and models.

With an aim of determining λ_{87} with minimum model dependence, and to provide an independent assessment of the accuracy of these latest studies, we have used the third method: ^{87}Sr accumulation. This is the first accumulation experiment reported since 1976 and we have attained precision better than the other recent measurements by other methods. Following Davis et al. (1977) we

have counted ^{87}Sr accumulated in a $RbClO_4$ salt over approximately 30 years. Using the data from our current work combined with the other determinations since the 1977 IUGS recommendation as well as some recent revisions of earlier experiments, we propose a more accurate and precise value for λ_{87}.

2. Background and History

^{87}Rb decays to stable ^{87}Sr by:

$$^{87}_{37}\mathrm{Rb} \rightarrow ^{87}_{38}\mathrm{Sr} + \beta^- + \bar{\nu} + Q$$

where β^- is a beta-particle, $\bar{\nu}$ is an anti-neutrino, and Q is the decay energy. This decay energy is shared, as kinetic energy, between the β-particle and $\bar{\nu}$. This is a third-forbidden, non-unique, transition with a spin change, ΔI, of 3 (from $^3/_2-$ to $^9/_2+$) indicating that it is a highly improbable transition and consequently has an extremely long half-life ($T_{½}$) – nearly 50 billion years (Konopinski and Bethe, 1938; Ahrens, 1949). The endpoint energy of the transition is about 283 keV (Grau Carles and Kossert, 2007; Wapstra et al., 2003; Baum et al., 2002) but because this energy is shared between the β-particle and anti-neutrino, the energy of the β-particle can range from nearly the full decay energy to < 10 keV, with an average energy of only 44 keV (Curran et al., 1951; Lewis, 1952; MacGregor and Wiedenbeck 1952). About ~20% carry energies < 15 keV (Neumann and Huster, 1976). The low energy of the β-particle combined with the low activity of ^{87}Rb have made λ_{87} difficult to measure by laboratory methods.

2.1 Counting Experiments

Counting experiments directly detect emitted β-particles with gas or scintillation counters. But because of the extremely low energy of the β-particles this method requires corrections for particles not detected by the counter due to self-absorption in the sample or absorption by the backing of the sample, as well

as detector efficiencies, geometry, scattering, noisy scintillators and other factors (Neumann and Huster, 1976; Begemann et al., 2001; Kossert, 2003). Owing largely to the extensive corrections and extrapolations required, early reported values varied by more than 50 percent (Figure 1 and Table 1).

The first counting experiment was performed by Otto Hahn and Martin Rothenbach in 1919 with an ionization chamber. They reported a value of $1.4 \times 10^{-11} a^{-1}$. This value was given without an error and has been adjusted here for the subsequent discovery that Rb has two isotopes, only one of which is radioactive (Eklund, 1947). The advent of liquid scintillators should have improved the situation, since it meant that the Rb sample could be dissolved in the scintillator, and absorption of β-rays by the sample itself should have been eliminated. However, early liquid scintillators were noisy, requiring a great deal of extrapolation for the low energy counts (Neumann and Huster, 1976).

Neumann and Huster (1976) found that many earlier 4π proportional counter experiments produced similar measurements to their own, but that the extrapolations to low energies were not properly estimated. They found similar problems with the extrapolation procedures used for liquid scintillation experiments. Neumann and Huster's own experiments yielded $\lambda_{87} = 1.42^{+0.02}_{-0.03} \times 10^{-11} a^{-1}$, and this was one of four measurements that Steiger and Jäger used as a basis for their provisional conventional value.[1]

When Begemann et al. (2001) reviewed the state of the decay constants used for geochronology twenty-five years later, no new counting experiments had been undertaken. They note that Neumann and Huster weighted each of their data points equally in their linear regression. But Begemann et al. point out that

[1] Physicists traditionally quote half-lives ($T_{½}$), while geochronologists use decay constants ($\lambda = \frac{\ln 2}{T_{½}}$). Throughout this paper, we use decay constants, and values reported as half-lives in the literature have been converted to decay constants. Table 1 presents both.

weighting the same data points by their uncertainties, and omitting two outlying points, yields a lower value of 1.403 ± 0.009 ($\times 10^{-11}a^{-1}$ hereafter understood). Kossert (2003) has reported the sole counting experiment since 1976. In his liquid scintillation experiment, which sought to address the problems with the earlier scintillation studies discussed by Neumann and Huster, he determined $\lambda_{87} = 1.396 \pm 0.009$. Kossert used both RbCl and $RbNO_3$ for his measurements, which affords the opportunity to check for impurities and/or non-stoichiometry in the compounds. There is a systematic bias between the two Rb sources: all measurements on $RbNO_3$ yield higher values for λ_{87} than the RbCl measurements. The four $RbNO_3$ measurements have a weighted average of 1.398 ± 0.003 (MSWD = 74), and the three RbCl measurements give 1.393 ± 0.002 (MSWD = 87). Kossert attributes this variation to the different hygroscopic behaviour of the two compounds, which affected the gravimetry. In 2001, Begemann et al. were sounding what has become a familiar refrain when they "recommend[ed] that the value of λ_{87} should be re-determined with improved accuracy."

2.2 Age Comparisons

In 1937, Hahn et al. found that the Sr contained in a lepidolite with high concentration of Rb was highly enriched in ^{87}Sr. This demonstrated that ^{87}Rb is the only natural radioactive isotope of Rb and led to the suggestion that the Rb-Sr isotope system could be used for determining geological ages. That same year Hemmendinger and Smythe (1937) confirmed by a counting experiment that ^{87}Rb is the only radioactive isotope of Rb. The following year Straßmann and Walling (1938) reported the first age comparison measurement of λ_{87} giving a value of 1.1. Over a dozen age comparison studies have been undertaken since then. For the age comparison method, Rb-Sr mass spectrometric measurements of a geological

sample are used to construct an isochron: $(^{87}Sr/^{86}Sr) = (^{87}Sr/^{86}Sr)_i + (^{87}Rb/^{86}Sr)(e^{\lambda t}-1)$. The age of the same sample is measured by means of another isotopic system, most often U-Th-Pb or K-Ar. The age determined by this other system is assumed to be accurate, and is then substituted for t in the Rb isochron equation and used to solve for λ_{87}.

With the advent of isotope dilution mass spectrometry, age comparison became a much more reliable method to determine λ_{87}. The agreement between age comparison studies reported since 1950 is better than that of counting experiments over the same time. Of the five age comparisons since 1980, four have errors of less than one percent, and indicate that the Steiger and Jäger recommendation of 1.42 is too high. The fifth (Williams et al., 1982) confirms the recommended value of Steiger and Jäger within the level of precision of the experiment.

These four relatively recent age comparisons utilize samples from three distinct planetary sources: meteoritic, lunar, and terrestrial. They agree within error on a value of 1.40 (Minster et al., 1982: 1.402 ± 0.008; Shih et al., 1985: 1.402 ± 0.011; Amelin and Zaitsev, 2002: 1.396-1.404 ± 0.006; Nebel et al., 2006a: 1.399 ± 0.003; Nebel et al. 2006b: 1.398 ± 0.002). All four of these values (Table 1 and Figure 1, inset) are in excellent agreement with Kossert's liquid scintillation experiment and with Neumann and Huster's value as adjusted by Begemann et al. (2001) as well as Davis et al.'s (1977) results as reinterpreted by Begemann et al.

There are two fundamental uncertainties in age comparisons. The first is the uncertainty in the decay-constant of the isotope system that is used for comparison (e.g. ^{235}U, ^{238}U, ^{40}K). The second is the assumption that Rb-Sr and the isotopic system with which it is compared in the sample (e.g. U-Pb) have closed at the same time, and that the thermal and chemical history they have undergone

has not affected the two systems differently. Since an age comparison can only be as accurate as the reference date, it is crucial that the systems used for comparison have accurately determined decay-constants. The two U-Pb decay systems have the most accurately determined decay constants among isotopes commonly used for radiometric dating (Jaffey et al., 1971; Begemann et al., 2001). This is partly because the specific activities of the U isotopes are comparatively high. In addition these isotopes are alpha emitters, and α-particles are more easily detected than β-particles and are not emitted in a continuous spectrum, which for β-particles requires corrections for low energy decays. Therefore the most precise age comparisons have relied on the U-Pb system. Although the U decay-constants are currently the best constrained, Schoene et al. (2006) have recently determined the ratio of λ_{235} to λ_{238} more precisely and Schön et al. (2004) have called for the re-measurement of the U decay-constants.

The second assumption, that the two isotopic systems actually date the same event, will be fulfilled only in those samples that have cooled quickly and that have not subsequently been subjected to processes which may have selectively reset one of the two systems, such as aqueous alteration, recrystallization, or shock metamorphism in the case of meteorites. Zartman (1964) sums up these assumptions well in his discussion of comparisons between Rb-Sr and K-Ar ages:

> If we assume the K^{40} decay constants to be correct, the decay constant of Rb^{87} should be decreased by 3 per cent in order to bring the two dating systems into best concordance. This is equivalent to using a Rb^{87} half-life of 48.5×10^9 years [λ_{87} equivalent: 1.43], which is midway between the values of Flynn & Glendenin (1959) and Aldrich & Wetherill (1958). It is, of course, possible that the two geochronologic systems do not begin keeping time simultaneously, or that slight diffusive daughter loss occurs in one of them.

Amelin and Zaitsev (2002) discussed this question at some length, and defended the assumption that the U-Pb and Rb-Sr ages of their samples record the same event. Recognizing the possibility of slow cooling, they present values for λ_{87}

ranging from 1.396 ± 0.006 to 1.404 ± 0.007 (using a recalculated $\lambda^{232}Th = 4.934 \pm 0.015 \times 10^{-11}a^{-11}$). Thus, while any one of these age comparisons has a precision of 0.5% or better, there remains a question of accuracy owing to dependence on choosing an appropriate model for the thermal history of the sample.

2.3 ^{87}Sr accumulation

The accumulation method involves purifying a compound of the parent element (in this case $RbClO_4$), and then allowing the parent to decay for sufficient time to build up a measurable quantity of daughter isotope (^{87}Sr). The quantity of accumulated daughter (^{87}Sr) is measured by mass spectrometry, and λ_{87} is calculated from the amount of accumulated daughter (^{87}Sr) and the starting mass of parent (^{87}Rb) determined gravimetrically.

The great theoretical advantage of an accumulation experiment over age comparison or direct counting is the relative freedom from assumptions and models. In a sense ^{87}Sr accumulation is in fact an age comparison, except that the age of the sample is known exactly and its history is far better characterized than that of a natural sample. Because only a single isotopic system is involved, we need not assume that two (or more) isotopic systems exhibited comparable behaviour on a geologic timescale. It is therefore, at least in principle, a practically model-independent method to determine λ_{87} so that almost all error should be confined to the analytical error of the measurements. This method is not without its own drawbacks, however. This is perhaps best evidenced by the fact that despite all of the advantages outlined above, only two of the dozens of previous attempts to measure λ_{87} have been by ^{87}Sr accumulation. In fact, both of these studies measured ^{87}Sr accumulated in the same $RbClO_4$ salt prepared by McMullen et al. in 1956 (Brouwer et al., 1964; Thode et al., 1965; McMullen, 1966;

Davis et al., 1977; Davis, 1978), and consequently are not completely independent assessments of λ_{87}.

The primary inconvenience in performing an accumulation experiment for a long-lived isotope like ^{87}Rb is waiting many years while sufficient daughter isotope accumulates for precise measurement. Other complications of this conceptually simple experiment include purifying a Rb compound such that there is little or no ^{87}Sr initially present, as well as the chemical separation of several hundred pg of stable radiogenic daughter ^{87}Sr ($^{87}Sr^*$) from gram quantities of parent Rb without further contamination with common Sr. Ingrowth is not completely free of assumptions either: the purity, stoichiometry, and homogeneity of the salt, correction for ^{87}Sr blank and ^{87}Rb interference are all estimated or assumed, but those assumptions can be well constrained. In addition, in the case of the current work (as well as the previous accumulation experiments), a single source of Rb, $RbClO_4$ salt, was used so there is no independent check on purity or stoichiometry.

3. Experimental Procedure

3.1 Treatment of $RbClO_4$ salt

$RbClO_4$ was purified by Davis in 1976 in Edmonton, Alberta. The salt was obtained from Terochem Laboratories, Ltd. and was certified to contain less than 600 ppm of impurities, including 10 ppm Sr. It was further purified of Sr by repeated precipitation in sub-boiling distilled water. The isotopic composition of the initial salt was precisely determined before purification (Davis, 1978). Four batches of high purity $RbClO_4$: A, B, C, and D, were prepared. Batches A, B, and D were precipitated five times; batch C was precipitated six times.

The salt was stored in 500 mL Nalgene® LPE bottles for approximately 32 years, allowing a sufficient quantity of $^{87}Sr^*$ to accumulate from the decay of ^{87}Rb

for precise mass spectrometric measurement. One gram of $RbClO_4$ can be expected to produce approximately 1.8 pg of $^{87}Sr^*$ per year, or 57.6 pg per gram over 32 years. Aliquots from each of the four batches, ranging from 2.1 - 10.6 g, were taken for measurement of $^{87}Sr^*$. To ensure dryness, earlier $RbClO_4$ aliquots Sr #3-Sr#18 were heated to 195 °C in Al-foil dishes or Savillex® PFA vials in an oven. Aliquots Sr_2007-10 – Sr_2007-15 and Sr_2008-01 – Sr_2008-06 were heated to 260 °C for several hours in quartz crucibles. The final six $RbClO_4$ aliquots, Sr_2008-01 – Sr_2008-06, were heated to 350 °C for approximately 19 hours.

3.2 Gravimetry

All samples were weighed on an OHAUS Analytical *Plus*® (AP250D-O) analytical balance. Calibration and reproducibility were regularly checked using standard weights and vials were weighed repeatedly to assess reproducibility. A Mettler Toledo® U-Ionizer was placed at the door of the balance chamber, and all samples, vials, and crucibles were passed through it to minimize the effects of static charge on weighing.

3.3 Spiking and Dissolution

To avoid transferring $RbClO_4$ after weighing and risking loss of salt, Sr#3–Sr#18 were weighed in the 90 mL Savillex vials in which they were dissolved. Because of the poor reproducibility of the weights of the 90 mL vials, subsequent samples were weighed in quartz crucibles. After weighing, $RbClO_4$ salt was transferred to 90 mL Savillex® vials. Because it is difficult to ensure quantitative transfer of the salt from the crucible, the weight of the empty crucible plus any $RbClO_4$ residue was subtracted from the weight of the crucible with $RbClO_4$.

The salt was covered with Milli-Q® H_2O and spiked in the 90 mL Savillex® vials. The procedure for weighing spikes and adding to the salt vial for Sr_2007-10 – Sr_2008-06 follows the same procedure for weighing spikes for spike calibration (Chapter 3 sections 2.2.4 and 2.3). For Sr#3–Sr#18, using the ^{84}Sr spike, spikes were measured in a calibrated pipette, and also weighed.

Additional water, sufficient to dissolve $RbClO_4$, was added to the vials, which were then covered, and the salt was dissolved by heating to near boiling. Equilibration with spike was achieved via convection of the hot solution on the hotplate. For aliquots Sr#3-Sr#18 and Sr_2007-10 – Sr_2008-06, neither magnetic stirrers nor other mechanical mixing were employed. For the final set, Sr_2008-21 – Sr_2008-26, samples were heated to ~80 °C in an oven . The vials, which each contained a magnetic stirring element, were then placed on a stirring hot-plate (surface temperature 135 °C). After visual inspection indicated complete dissolution of the salt, the solution was stirred for an additional 20 minutes. No systematic difference in λ_{87} values was seen between the stirred aliquots and the others except that blanks in the stirred aliquots proved to be higher.

3.4 Chemical separation

Coarse separation of Rb and Sr was achieved via differential solubility. It was indeed on account of this property that $RbClO_4$ was originally chosen for the experiment by McMullen et al. (1966; Fritze and Kennet, 1960). $Sr(ClO_4)_2$ is always in solution due to its small quantity and high solubility (310 g/100 mL). $RbClO_4$, on the other hand, is moderately soluble in hot water, but only slightly soluble in cold water: 20g/100mL at 100 °C, 1g/100mL at 0 °C (Lide, 2005). Each solution was evaporated on a hotplate to approximately 2-3 mL. At this point,

most of the $RbClO_4$ had precipitated. At 100 °C, 3 mL of H_2O can hold just over 500 mg of $RbClO_4$ in solution. At room temperature, it can hold only 30 mg.

As the solution cooled, $RbClO_4$ precipitated further. The remaining solution was removed with a polyethylene pipette from the dissolution vial, and transferred to a 3 mL Savillex® vial. The solution was further evaporated, inducing additional precipitation of $RbClO_4$. When less than 0.5 mL of solution remained, the solution was removed with a pipette, the vial with precipitated $RbClO_4$ was rinsed out, and the solution returned to the vial. The solution was then cooled further with dry-ice to freezing. The solution was thawed, and when the frozen solution was almost completely melted, the solution was again pipetted out of the vial, and the vial was again rinsed of the final precipitate of $RbClO_4$. At this point, with less than 0.5 mL of solution at close to 0 °C, the solution should contain no more than 5 mg of $RbClO_4$. Via differential solubility, Rb was reduced by a factor of about one-thousand. However, 5 mg of $RbClO_4$ (about 2.3 mg of Rb) must still be separated from only a few hundred pg of Sr – a factor of about ten-million.

Fine separation was achieved by passing the remaining solution twice through 50 μL Teflon® micro-columns loaded with Eichrom SrSpec® solvent extraction resin. Resin was washed with MQ H_2O, then conditioned with 4N HNO_3. 7N HNO_3 was added to the sample solution to make approximately 4N HNO_3 solution and the sample was then loaded onto the column. Rb was washed out of the column with 4N HNO_3. Sr was then eluted with H_2O and collected. After the first pass, the collected Sr solution was evaporated again down to a small drop, to which 7N HNO_3 was added to again make approximately 4N HNO_3 solution. The sample was reloaded onto a new column with new resin, and the same chemistry procedure was repeated. After the second pass, 15 drops of 0.05 N H_3PO_4 were added to each sample, and then the

solution was completely evaporated on a hot-plate. Most samples dried down as dark spots, indicative of organic compounds that washed through the resin with the sample. This is typical of the SrSpec® resin. The organics were oxidized by evaporation with several drops of concentrated $HClO_4$.

3.5 Mass spectrometry

Four different loading techniques were tested for loading small Sr samples:

1. H_2O with a small amount of H_3PO_4 on oxidized Ta filaments – the standard technique.
2. Ta_2O_5 slurry on Re filaments (Lars Borg, pers. comm.)
3. Ta_2O_5 slurry on W filaments (adapted from Birck (1986), who used a Ta solution)
4. TaF on W filaments (Samson et al., 1995)

It was found that methods 2 and 4 produced much stronger emission than methods 1 and 3 for loads smaller than 1 ng. Method 2 exhibited two advantages over method 4. First, Rb burned off at a lower temperature, allowing for Sr measurement with less Rb interference. Secondly, method 2 provided longer lasting and more stable emission. Method 4 tended to yield a burst of high intensity but quickly burned off the entire sample without permitting sufficient time for precise measurement.

Samples were loaded on Re filaments with a Ta_2O_5 slurry. About 1 μL of Ta_2O_5 slurry was loaded on the filament, and evaporated with a current of about 0.5 A. When the slurry was nearly dry, the sample was loaded on top of the slurry, mixing with it. The filament was then slowly heated up until H_3PO_4 fumed – around 1.8-2 A.

All samples were measured by thermal ionization mass spectrometry (TIMS) in static-multicollector mode on the VG 354 at the Jack Satterly Geochronology Laboratory (JSGL) at the University of Toronto. Some static multicollector analyses were replicated with Daly detector measurements, either from a separate load, or by decreasing the intensity during the multicollector run, taking single-collector measurements at low intensity, and then increasing the intensity for completion of the multi-collector measurements.

3.6 Data Reduction

A linear fractionation approximation was applied to the measured ratios. Although an exponential approximation might be a more accurate model of Sr fractionation from Re filaments (Dickin, 1995), the difference is negligible compared to other sources of error. Use of linear fractionation allows an analytical solution for a mixture of sample with unknown isotopic composition (IC) and spike with known IC, which otherwise would have to be determined numerically. Linear fractionation approximations applied to SRM-987 standards run on the VG 354 at JSGL fall within the tolerance of the certified IC of SRM-987 of $^{87}Sr/^{86}Sr = 0.71034 \pm 0.00026$. 24 standards of 49-788 pg Sr, comparable in size and beam intensity to the λ_{87} measurements, averaged $^{87}Sr/^{86}Sr$ of 0.71039, with 2σ of 0.00042. Several λ_{87} measurements were solved numerically for the exponential approximation, and the results agreed with the simpler linear approximation to better than 0.02%. The linear approximation is therefore considered sufficiently accurate for the purposes of this experiment. Because the fractionation correction depends on the signal of ^{86}Sr, which was very low in the ^{84}Sr-spike measurements, these measurements have large analytical errors.

The fractionation correction was calculated by simultaneously solving the $^{88}Sr/^{86}Sr$ and $^{84}Sr/^{86}Sr$ isotope dilution equations for the fractionation factor, α, and

the spike to blank ratio (S/B – where blank, B, includes all common Sr). Nearly identical results were calculated from the equations given by Kostitsyn and Zhuravlev (1988). Once the fractionation factor, α, was determined, it was used to correct the measured isotopic ratios. Moles of $^{87}Sr^*$ were calculated from S/B, corrected $^{87}Sr/^{86}Sr$, and the weighed quantity of spike mixed with the sample. Calculated moles of $^{87}Sr^*$, moles of $RbClO_4$ (determined gravimetrically), and decay time, t, were used to calculate the decay constant, λ_{87}, by the approximation for short decay times: $\lambda_{87} \cong (^{87}Sr^*)\times(^{87}Rb)^{-1}\times t^{-1}$.

Errors were determined by two methods. In one case, values of λ_{87} were calculated from the mass spectrometer ratios on a cycle by cycle basis and a random standard error determined from the root-mean-square of the results. This was then augmented by estimates of uncertainty in weights based on replicate measurements over several years. In the second case, variations in λ_{87} were calculated for each parameter plus its estimated standard deviation and these were summed in quadrature to determine a total standard deviation for the decay constant measurement. Both approaches yielded similar uncertainties. The uncertainties quoted here are those calculated by the first approach. All errors on our decay constant determinations are quoted at twice the standard deviation.

4. Results

The results presented here represent two stages of measurement of λ_{87} by Sr accumulation. The same $RbClO_4$ salt was used in all measurements, but the early determinations used a ^{84}Sr spike, whereas a ^{84}Sr-^{86}Sr double spike was used in later determinations. The $RbClO_4$ samples have extremely low common Sr, which makes correction for fractionation by correcting to natural $^{86}Sr/^{88}Sr$ (= 0.1194) difficult. The individual measurements using the ^{84}Sr had large errors,

partly because of the fractionation correction, and partly because of weighing errors for both salt and spike. In an attempt to improve both precision and accuracy, the $RbClO_4$ analyses were repeated with several improvements. Firstly, a ^{84}Sr-^{86}Sr double-spike was prepared and precisely calibrated. The double-spike provided for much more precise and accurate correction for instrumental fractionation. Secondly, the salt was weighed in quartz crucibles with better reproducibility than those weighed in Al-foil dishes or 90 mL Savillex® vials. Finally, the spike was also weighed more accurately. For the early experiments, a pipette was used for spiking, while for the later experiments with the new spike, each spike aliquot was measured gravimetrically. The single spike measurements were done in three sets, yielding sixteen measurements. The double-spike experiments also consisted of three sets, each consisting of six aliquots. Table 2a presents $RbClO_4$ sample weights (g salt), salt batches, decay times, $^{87}Sr^*$, and λ_{87}. Isotopic ratios of λ_{87} measurements are presented in Table 2b and additional information, such as spike weights (pg Sr) and non-radiogenic Sr (blank), are presented in Table 2c. Sr_2008-04, failed to produce a measurable signal on the mass spectrometer, leaving 17 successful measurements of λ_{87} using the double-spike. Use of the double-spike greatly increased the internal precision of each individual measurement, however they scatter outside of their analytical errors.

4.1 Decay Constant values

Results of 31 measurements are shown in Figure 2 and detailed in Table 2a. $^{87}Sr^*$ ranges from 105-616 pg. Weighted averages were calculated with Isoplot/Ex 3.0 (Ludwig, 2003). An average of the measurements weighted by uncertainties and taking scatter into account scatter (Model 2 weighted average) yields 1.3991 ± 0.0010. The MSWD of 78 indicates what is obvious from

inspection of Figure 2, that the data scatter well outside of their analytical errors. The average for the measurements with the ^{84}Sr spike is 1.3971 ± 0.0018 (MSWD = 3.5), and for the measurements with double-spike is 1.3992 ± 0.0014 (MSWD = 142). The range for the double-spike measurements, 1.3958-1.4059, is smaller than the range for the ^{84}Sr-spike measurements, 1.3933-1.4166, but the fit is worse on account of the smaller errors for each individual measurement. Sr_2007-14, at 1.4059, plots 0.2% higher than the next highest double-spike measurement. This sample exhibited anomalous fractionation during mass spectrometric analysis and therefore can be excluded from the average. Sr_2008-22, which also plots higher than most of the double-spike measurements, has more than three times as much common Sr as the next highest. It is likely that this high blank contributes to inaccuracy in correcting for common Sr so this measurement should be eliminated from the average as well. The elimination of these two points reduces the average of the remaining 15 double-spike measurements only slightly, to 1.3988, and reduces the MSWD to 118. The average (Model 2) of the 29 measurements excluding those two points is 1.3988 ± 0.0009 (MSWD = 61). The exclusion of these two outliers slightly reduces the scatter, but considerable scatter in excess of the analytical errors remains. This result is puzzling considering the care taken at every step to eliminate sources of error. The various sources of error are assessed below.

The ^{84}Sr spike measurements presented here differ from the preliminary results reported in Rotenberg et al., (2004, 2005), which indicated a higher value of 1.421. This was the result of an error in the calculation of λ_{87} and was corrected in the presentation of the data at the 15th annual Goldschmidt Conference in 2005.

Primarily owing to larger errors in the individual measurements, the ^{84}Sr-spike measurements have only a little excess scatter. Reducing these errors

and the overall scatter were the primary motivations for repeating the measurements with a more carefully calibrated ^{84}Sr-^{86}Sr double spike. These efforts were very successful in reducing the errors in the individual measurements. However, the double-spike measurements scatter outside those reduced errors, resulting in the high MSWD.

Batch D is the only batch for which all measurements – both ^{84}Sr and double-spike – very nearly agree within their analytical uncertainties. Batch D also plots the lowest of all batches, at 1.3961 ± 0.0006 (MSWD = 2.6). Batch C shows the most scatter. This is primarily due to Sr_2008-03. With a value of 1.4023 ± 0.0002, it is fairly precise, but plots above the rest of the double-spike batch C measurements. Sr#4, also from Batch C, plots even higher at 1.4135 ± 0.0112 but it does not strongly affect the fit of the data due to its large analytical error. Exclusion of Sr_2008-03 from the average would result in a value of 1.3966 ± 0.0005, for Batches C and D with an MSWD of 6. Like batch D, the batch C measurements (excluding Sr_2008-03) indicate a lower value for λ_{87}. However there is no *a priori* reason to exclude this analysis. 19 lower measurements give an average of 1.3966 ± 0.0003 with MSWD of 2.8 (Figure 3). By contrast, the 10 higher measurements have an average of 1.4005 ± 0.0013 with MSWD of 58. The better agreement among the lower measurements suggests that the scatter may in part be due to a systematic bias toward higher values. The median of the measurements, which does not weight the data points, is 1.3975 ± 0.0011, and further illustrates that there are more lower measurements than higher ones. Below we discuss the various sources of error in some detail.

5. Sources of error contributing to scatter

As outlined above, although ^{87}Sr accumulation is far less assumption dependent than either counting or age comparison, there are a number of

assumptions required in addition to the sources of analytical uncertainty. The excess scatter in the data implies either that one of these sources of uncertainty has been underestimated, or that there is an additional source of uncertainty that has not been identified.

5.1 Common Sr

A leading contribution to the uncertainty in the 1977 accumulation experiment was the correction for initial ^{87}Sr present in the salt. Cryptic excess ^{87}Sr would cause the calculated decay constant to be greater than the true value. The IC of the Sr present in the salt prepared in 1956 was not measured. Consequently, Davis et al. (1977) had to assume $^{87}Sr/^{86}Sr$ of 0.709, the IC of the Sr in the reagents used in their laboratory and the average value in modern seawater, for the Sr in the salt. Because those samples contained significant initial quantities of common Sr, this resulted in a major source of bias. In the 1977 experiment, the most radiogenic sample had $^{87}Sr/^{88}Sr$ of 0.38474 (78% of the ^{87}Sr was radiogenic) with an average for all the samples of only 64% radiogenic Sr and a total range from 48-78%. Based upon their statistical evaluation, Begemann et al. (2001) suggested that a more appropriate value for $^{87}Sr/^{86}Sr$ initially in the salt would be 0.730. Applying this 3% change to the assumed $^{87}Sr/^{86}Sr$ yields a 1% reduction in λ_{87}, to 1.406 ± 0.007. Consequently, there is at least a 1% uncertainly in the 1977 accumulation experiment due solely to the value used for the common Sr correction.

This uncertainty has been greatly reduced in our current work due to the much higher percentage of radiogenic Sr. In this work all samples but two have a greater percentage of radiogenic ^{87}Sr than the *most* radiogenic sample in the 1977 experiment. The magnetic stirring elements employed for the final set of measurements appear to have contributed relatively large quantities of common

Sr to the samples in spite of acid cleaning. However, 20 of the 31 measurements have greater than 90% radiogenic ^{87}Sr. Six of the 11 with less than 90% radiogenic ^{87}Sr are from samples dissolved with the aid of the stirrers.

The range of common Sr content (Table 2c) for the measurements without stirrers (Sr#3 – Sr#18 and Sr_2007-01 – Sr_2008-06) is 73 – 486 pg, while the range for the final set, with stirrers (Sr_2008-21 – Sr_2008-26) is 523 – 764 pg (excluding the anomalously high 2754 pg for Sr_2008-25). Procedure blanks measured along with samples range from 23-61 pg, with an average of 41 pg (Table 3). The total common Sr for each measurement is the sum of the procedure blank – Sr added during processing in the course of the experiment – and Sr initially in the $RbClO_4$ salt when it was prepared and purified in 1976. There is no correlation between batch and amount of common Sr. If the average procedure blank (40 pg) is subtracted from the common Sr in each sample, we calculate the average initial Sr to be ~ 40 pg Sr/g $RbClO_4$. The samples with the lowest common Sr have approximately 25 pg Sr/g $RbClO_4$, which sets an upper limit on the quantity of initial Sr. Procedure blanks for the final set were originally processed without magnetic stirrers. Upon observation of the high blanks in those samples processed with stirrers, a procedure blank was measured with a magnetic stirrer that was not cleaned at all (in order to measure the upper limit of Sr contributed from the stirrers), and found to be 2784 pg – comparable to the anomalously high blank in Sr_2008-22. This implicates the stirrers as contributing the additional Sr to those samples in which they were used.

The current measurements, with their highly radiogenic Sr, are far less sensitive to the choice of $^{87}Sr/^{86}Sr$ for common Sr correction than the 1977 measurements were. For example, there is no coherent relationship between the assumed IC of the common Sr and the standard deviation of the average of the λ_{87} measurements, as pointed out by Begemann et al. (2001) for the Davis et al.

(1977) data set. However, the results are not completely insensitive to this parameter. For example, for Sr_2007-12 (93.54% radiogenic), varying $^{87}Sr/^{86}Sr$ widely, from 0.700-0.730 (~4%), results in a variation in λ_{87} of 0.28%. Though this variation is considerably smaller than for the 1977 experiments, it is not negligible compared to the errors. For those samples processed without magnetic stirring elements, common Sr is dominated by that contained initially in the salt. The isotopic composition of the salt before purification was measured by Davis (1978) and found to be 0.709 ± 0.001. Attempts to obtain a precise measurement after purification were unsuccessful, because of the low concentration. However, this value is unlikely to differ from the composition of the water which was similar to that in the unpurified salt (Davis, 1978). The best attempt to measure $^{87}Sr/^{86}Sr$ of Sr in the water used for dissolving $RbClO_4$ in the JSGL lab yielded 0.71006 ± 0.00062. The average of three measurements of the $^{87}Sr/^{86}Sr$ of the Sr from the magnetic stirrers is 0.71003 ± 0.00061.

Overall, there is no noticeable relationship between the ratio of radiogenic to non-radiogenic Sr and λ_{87} or degree of scatter. Variance in the least radiogenic measurements (those with magnetic stirrers) is slightly reduced when $^{87}Sr/^{86}Sr = 0.716$ is used for the common Sr correction. But there is no evidence that the Sr contributed by the stirrers or any other source has such high $^{87}Sr/^{86}Sr$.

5.2 Dryness of salt

$RbClO_4$ salt aliquots were heated prior to weighing in order to ensure dryness. The salt was purified by precipitation, and therefore might contain fluid inclusions. $RbClO_4$ is not hygroscopic so moisture should not adsorb onto the crystals. In any case, H_2O could increase the weight of the salt, and artificially decrease λ_{87}. $RbClO_4$ undergoes a phase transition from orthorhombic to cubic crystal structure at 281 °C (Raghurama et al., 1987). It melts and

decomposes to RbCl between 550-575 °C (Walker et al., 2001; Serezhkina et al., 1973; authors' unpublished experiments). The salt samples for the ^{84}Sr-spike measurements were heated to 195 °C in an oven. Subsequent experiments showed additional loss of about 0.05% when the salt was heated from 195 °C to 240 °C. The measurements run with the ^{84}Sr-spike might therefore be up to 0.05% too high. The analytical errors on these measurements are considerably higher than this, and therefore the results are not significantly affected.

The first two sets of ^{84}Sr-^{86}Sr-spiked samples were heated to 260 °C in a muffle furnace while the final set was heated to 350 °C. Step heating experiments showed that above 240 °C the salt did not lose additional weight, and weight losses for samples heated to 350 °C were similar to those heated to 240 °C. Details of heating each sample, as well as step heating experiment results are shown in Table 4a and 4b. Salt from Batch C consistently lost more weight upon heating than the other batches. Average weight loss for Batch C when heated (to 260 or 350 °C) was 0.5% versus 0.23% for the other batches and is most likely due to more fluid inclusions in this batch. When purified in 1976, Batch C was precipitated six times instead of five times for the other batches. The procedure for the extra precipitation was identical to the other five, and this is the only difference in preparation of Batch C versus the other batches. Considering the stability of the weight of the salt after heating above 240 °C and the fact that hydration would decrease measured λ_{87} values, it is unlikely that the scatter is caused by residual moisture in different aliquots.

5.3 Gravimetry

All samples and spikes were weighed on an OHAUS Analytical *Plus*® (AP250D-O) analytical balance. Repeated weighing of standards from 2006 through 2008 indicates long term overall stability and reproducibility of ± 10 μg

for a 1 g mass (± 10 ppm) and ± 200 μg for a mass of 100.000 8 g (± 2 ppm). $RbClO_4$ salt aliquots for the measurements with the ^{84}Sr-spike were weighed in Al-foil dishes or 90 mL Savillex® vials. These dishes and vials were not weighed repeatedly to assess reproducibility – one of the shortcomings of those measurements. Salt samples for the double-spike measurements were weighed in quartz crucibles while spikes were weighed in 7 mL Savillex Teflon vials. Vial and crucible weights are not as reproducible as standards, presumably owing to adsorption of water and/or static charge on the glass and plastic. Quartz crucibles for weighing were weighed empty at least a dozen times over the course of more than a year as part of various preliminary experiments. These weighings yield good constraints on the reproducibility of the weights of the empty crucibles (Table 5 and Figure 4). Six crucibles were used, four were bowl-shaped and translucent, without covers, the other two were straight-sided, with covers, and clear. The reproducibility of the weighings for five of the six crucibles is better than 20 ppm (2σ standard deviation). While the empty crucibles weigh between 9.3 and 20.5 g, the salt weighed in them typically weighs only 3 g. Relative to 3 g, the errors range from 35-165 ppm. The difference between λ_{87} calculated with low and high sample weight estimates is just 0.007%. The data scatter over about 0.5%, so gravimetry is not likely the source of the scatter.

Another possible source of error related to gravimetry is the correction applied to spike weights for evaporation during weighing. The spiking procedure is detailed in Chapter 2 (2.3.4 and 2.3.5). Of a total of 24 weighed aliquots of spike, ranging from 1.7 to 6.5 g (of spike solution), the average evaporation rate is 0.8 mg/min., with a range of 0.6-1.1 mg/min. The rate of evaporation is generally correlated to the quantity of spike, with larger quantities of spike evaporating faster, presumably because the solution surface is closer to

the opening, and therefore the walls of the vial afford less protection from the ambient atmosphere and evaporation. Evaporation for each spike aliquot was measured three times. For any individual sample, the maximum variation in this rate between the three measurements is only 0.08 mg/min. This would represent less than 0.01% contribution to the error of the *smallest* spike. There is no correlation between salt or spike quantity and the measured decay-constant value. It is therefore considered unlikely that the spiking error has been underestimated, or that errors in the spike weight are responsible for the excess scatter.

Changes in concentration of the double-spike due to diffusion through the Teflon® bottle were monitored. This was not the case for the ^{84}Sr-spike. Since the spike tends to become more concentrated over time owing to diffusion of H_2O out of the bottle (though it can also become more dilute in a humid atmosphere), we would expect to see a decrease in λ_{87} measured with the ^{84}Sr spike over time if this were a factor. This was not observed. Either changes in concentration were trivial, or other sources of error are sufficiently large to mask this effect. The double-spike increased in concentration from 0.18755 to 0.18816 ng Sr/g solution (0.33%) over one year. The measurements with the double spike were adjusted for this effect.

5.4 Loss of spike or sample

For the double-spike measurements, the weighing and spiking procedures were designed to minimize the possibility of loss of either spike or sample subsequent to weighing. Loss of spike will cause the calculated decay constant to be too large, while lost salt will make the decay constant appear too small. The spike weighing and transfer procedure is the same as that used for calibrating the spike (Chapter 3, sections 2.2.4 and 2.3). For the spike

calibrations, the reproducibility is excellent – the total range is less than 0.1%. Consequently, it is unlikely that uncertainties in the spiking procedure are responsible for the scatter in the data.

5.5 Rb Correction

Because ^{87}Rb and ^{87}Sr are isobars, the parent isotope will interfere with measurement of the daughter if chemical separation is incomplete, and a correction must be made for this interference. Correction – to the extent that it was required – was accomplished by multiplying the intensity of the mass 85 signal by 0.38576 (^{87}Rb/^{85}Rb of natural Rb) and subtracting this product from the mass 87 signal to arrive at the fraction supplied by ^{87}Sr. Rb evaporates from the filament at much lower temperature than Sr. Rb mostly evaporates before the filament even glows, at about 1 A, and by about 1.6 A there is very little Rb signal. For samples that still had significant Rb signals past 1.6 A, the filament was set at 1.8 A (~1200 °C) for about 20 minutes to burn off the remaining Rb. Sr yields a measurable signal at about 1400 °C (~2 A). Consequently, by the time Sr measurement conditions are reached, any remaining Rb should be highly fractionated. If this is indeed the case, then the IC of natural Rb might not be appropriate for the Rb correction. Since ^{87}Rb/^{85}Rb should be above the nominal value in the fractionated residue, this effect can only elevate λ_{87} measurements.

In a test with a mix of Rb and Sr standards to mimic an actual sample (albeit, with much more Sr), using a correcting ratio of ^{87}Rb/^{85}Rb = 0.38576 resulted in nearly nominal 87/86 in Sr of 0.71022. There is very little Rb in most samples, making the results fairly insensitive to the choice of Rb correction. To test the possibility that the scatter is due to too low a value for ^{87}Rb/^{85}Rb used for correcting for ^{87}Rb interference, λ_{87} was recalculated using ^{87}Rb/^{85}Rb values ranging from 0.38576 (nominal) up to 0.40006 (3.7% fractionation), which was

found to have a large effect on only two measurements: Sr_2007-11 (reduced 0.3%) and Sr_2008-24 (reduced 0.5%), and these measurements are not among those that yielded anomalously high values of λ_{87}. Four other measurements exhibited small reductions, < 0.1%. The remaining measurements are essentially indistinguishable whether corrected with 0.38576 or 0.40006. The weighted average of all the measurements is reduced by only 0.0002 (0.01%), by correcting with 0.40006, and if the two most sensitive points are excluded, the average is reduced by just 40 ppm. Samples that are least sensitive to variation in $^{87}Rb/^{85}Rb$ still exhibit the same overall scatter that is observed over the entire set of data, and there is no correlation between ^{87}Rb correction and measured λ_{87}, so the Rb correction is not likely responsible for the scatter, nor can it be considered to have a significant contribution to the overall accuracy.

5.6 The decay time, *t*

The decay time, *t*, is measured from the precipitation of the $RbClO_4$ salt in 1976 (recorded to the hour) until chemical separation of Sr (now including $^{87}Sr^*$) from Rb in preparation for mass spectrometry. After this point, no further $^{87}Sr^*$ can be added. Coarse separation is achieved via differential solubility of $RbClO_4$ and $Sr(ClO_4)_2$, followed by fine separation by solvent extraction column chemistry. The separations typically take two to three days. Since the initial coarse separation removes at least 90% of the Rb, the initial removal of supernatant solution with $Sr(ClO_4)_2$ is taken as the end-point for *t*. Every effort was made to achieve chemical separation the next day, and in all cases it was done within several days. Over the course of 32 years, one day represents 0.009% of the decay time. Thus, under- or over-estimating the time cannot be responsible for the scatter in the data.

5.7 Contamination of vials from previous experiments

The same sets of vials (90 mL for dissolution, 3 mL and 7 mL for chemical separation) were reused for each set of experiments. The vials were cleaned thoroughly between each use, and blanks were measured periodically at various stages of the cleaning cycle. Because the vials were always used for solutions of roughly the same concentrations and with the same approximate IC, very large quantities of cross-contamination would be required to influence the results, even without cleaning. With the numerous cleaning cycles between uses for different samples, cross-contamination can be discounted.

5.8 Purity/Stoichiometry/Homogeneity of salt

The salt was purified in 1977 from high purity $RbClO_4$ obtained from Terochem Laboratories, Ltd. in Edmonton, Alberta and was certified to contain less than 600 ppm of impurities. It was further purified of Sr by Davis by repeated dissolution and precipitation, decanting the supernatant solution at each step (Davis, 1978). We have undertaken no further assessments of impurities in the salt. Neither was stoichiometry assessed. We did one test, heating $RbClO_4$ to decomposition, and the difference in weight between the $RbClO_4$ and the decomposition product, RbCl, matched to within 0.3%. During the decomposition, some of the material seems to have vaporised and deposited on the outside of the crucible and on the floor of the furnace. This lost material likely accounts for most of the discrepancy between the predicted difference in weight between pure $RbClO_4$ and RbCl. Unless there are heterogeneities in the salt, impurities or non-stoichiometry would affect all measurements systematically but would not account for scatter in the data, since all $RbClO_4$ was from the same source and was treated only with ultra-clean water. Inhomogeneity in the salt could cause unexpected scatter, but this would most

likely be due to fluid inclusions, and the heating experiments demonstrated that they should not be a significant factor.

5.9 Spike Calibration

Two different spikes were used for the measurements, a ^{84}Sr-spike and a ^{84}Sr-^{86}Sr double-spike. ICs and concentrations of the spikes are shown in (Table 6). The ^{84}Sr-spike was calibrated against several solutions prepared from $SrCO_3$ SRM-987. This calibration is described in Appendix A. The calibrations were performed at the dilute working concentration of approximately 13 ng Sr/g. Because of the low concentration, addition of common Sr during handling for the calibration experiments can significantly affect the measurements. Furthermore, once calibrated, changes in the concentration were not monitored. Calibration of the ^{84}Sr-^{86}Sr double-spike is discussed in detail in Chapter 3. It was calibrated at 833 ng Sr/g, making the calibrations far less sensitive to addition of common Sr. The fair agreement between the ^{84}Sr-spike measurements and the ^{84}Sr-^{86}Sr double-spike measurements confirms that despite the concerns about the accuracy of the ^{84}Sr-spike calibration, the measured concentration is accurate.

The contributions to the uncertainty in the double-spike concentration are: weighing uncertainty in the preparation of calibrating solutions and mixtures with spike, mass spectrometer analytical uncertainty, and uncertainty in the IC of the spike. The first two components are about 0.035%, and this is simply added to the final decay constant uncertainty below. The isotopic composition of the spike appears twice in the calculation of decay-constants: 1) as it affects the calculated concentration of the spike, and 2) as it affects the correction of mass spectrometer measurements for instrumental fractionation.

Increasing the value of ^{84}Sr/^{86}Sr in the spike – within its uncertainty – results in increasing the concentration of the spike by ~ 0.18%, which results in the increase

of the decay-constant average by the same amount. However, if the spike concentration is held constant, the same increase in $^{84}Sr/^{86}Sr$ in the spike results in lowering the decay-constant average by ~ 0.1% due solely to fractionation correction. Thus the two effects of the spike IC partially cancel out, with a total contribution of ± 0.078%. The spike IC component is also included in the total uncertainty in λ_{87} below, but it does not affect the scatter of the data.

6. Discussion

6.1 Best estimate of the decay constant

Excluding the two outlying measurements, Sr_2007-14 and Sr_2008-25, and including the error in concentration of the spike, the weighted average of the current measurements is $1.3991 \pm 0.0010 \times 10^{-11} a^{-1}$ but the scatter is outside of the assigned errors, indicating the presence of an unidentified source or sources of uncertainty. An important question is whether the unknown error is systematic, forcing the result in one direction, or random.

The scatter in the λ_{87} measurements presents a quandary for determining a best value. Despite examination of every conceivable source of systematic bias that might cause excess scatter, we have not been able to determine the source. Scatter outside of the analytical errors implies that there is a source of random error that has not been taken into account. On the other hand, the skew in the data towards lower measurements implies that there is a systematic bias increasing some values but not others. If the scatter is systematic, it is appropriate to exclude the higher data points, and to use non-parametric statistics that do not require assumptions about the shape of the distribution, but if the scatter is random, then all measurements should be included. Because this involves choosing between two scenarios only one of which accurately

represents the actual value, there is no truly satisfactory way to decide on a best value, and a compromise must be made.

An effort was made to conservatively estimate both the value of λ_{87} and the uncertainty attached to the value. In order to allow for the possibility that the scatter is indeed random we have increased the error of each of the data points by a fixed amount incrementally until the MSWD approaches unity. This additional error is added in quadrature as an absolute error rather than a relative error because an absolute error will affect the more precise points more than the less precise ones. Because the individual errors are increased, the total error of the average is decreased, and it is therefore multiplied by a Student *t*-factor of 2.045 for 95% confidence with 29 degrees of freedom. This yields a value of 1.3979 ± 0.0023 (0.165%) (MSWD = 1.4). For the double-spike measurements alone, the result is the same, with MSWD = 0.93. The uncertainty fully encompasses the average of the 19 lower measurements, 1.3966 ± 0.0003 (MSWD = 2.8).

MacMahon et al. (2004) discuss how best to assess discrepant data, specifically in the case of the decay-constants of ^{90}Sr and ^{137}Cs. The cases they deal with differ in that the discrepant data are from different experiments by different investigators rather than multiple repetitions of the same experiment. The scatter in ^{137}Cs decay-constant measurements appears similar to the scatter in our own data. Among other methods, they note that the median is insensitive to outliers and is a robust estimator of discrepant data. The problem is assigning an error to a median. The median λ_{87} calculated by Isoplot (Ludwig, 2003) is 1.3975 ± 0.0011. This is close to the estimate we have calculated, and our larger errors ensure accuracy, at the cost of precision. Adding to this the uncertainty in spike ^{84}Sr/^{86}Sr (0.078%) and concentration (0.035%) gives a final preferred value of 1.3979 ± 0.0026.

6.2 λ_{87} in the context of the other recent measurements

The current result is shown with other λ_{87} measurements reported since 1977 in Figure (1 inset). The good agreement between the measurements effectively satisfies the challenge put forth by Neumann and Huster (1976) that "[t]he determination of a reliable, physically founded value of the ^{87}Rb half-life requires a great number of independent measurements in order to eliminate systematic errors. Full agreement between the different measuring methods should be aimed at."

Amelin and Zaitsev (2002) offer estimates of λ_{87} ranging from 1.396, assuming rapid cooling, up to 1.404, accounting for the possibility of slow cooling. Although the rate of cooling does not affect the precision of the calculation, it does affect the accuracy. With the exception of Williams et al. (1982), all of the measurements since 1977 agree within their reported errors. Four of these are geochronologic age comparisons. Three of them (Minster et al., 1982; Amelin and Zaitsev, 2002; Nebel et al., 2006a, 2006b) compare Rb-Sr with the U-Th-Pb system, while two (Williams et al., 1982; Shih et al., 1985) compare Rb-Sr with the K-Ar system. The age comparisons span a wide range of planetary materials, as well as a wide span of ages. Nebel et al. examined Rb-Sr in three U-Pb dated rocks. Williams et al. (1982) present a table of previously determined Rb-Sr and K-Ar ages that agree with $\lambda_{87} = 1.42$. They suggest that if there is a systematic bias between the two isotopic systems, it is less than ± 0.3%. Williams et al.'s samples span an age range of 98 Ma to 445 Ma. Except for one relatively imprecise result, these are Rb-Sr model ages, not isochrons, which remain subject to assumptions about the initial Sr IC, as well as the cooling history. In addition, the current value of the ^{40}K decay constant has been found to be inconsistent with that of the ^{238}U decay constant in recent precise studies where ^{40}Ar-^{39}Ar ages tend to be systematically younger than U-Pb ages by about

1% (e.g. Pálfy et al., 2007). The current work is in good agreement with the counting experiment by Kossert (2003), which determined a value of 1.396 ± 0.009.

The state of knowledge of λ_{87} can now be said to be very good. Nearly all laboratory and U-Pb age comparison determinations after 1977 agree within error and indicate that the IUGS recommended value of 1.42 is too high. Two of these experiments have the highest precision of any done thus far – close to 0.2%. At this time it seems appropriate to recommend an updated value to the isotope geology community. Holden (1990) and others (Schiller and Eberhardt, 1991; Pommé et al., 2008) have cautioned against simply taking weighted averages of results of experiments of fundamentally different types. Counting experiments, geological age comparisons, and ingrowth measurements have their own independent systematic errors. Pommé et al. noted that "Half-life measurements are mostly performed at a limited number of laboratories. This degree of specialization, however, is no guarantee for quality. Even the most experienced researchers seem to underestimate the uncertainty and do not provide to the scientific community the information that is required for traceability." This statement was written specifically with regard to counting experiments, but it applies to other methods as well. The excess scatter in our data lead to the conclusion that we have underestimated at least one source of uncertainty. We have attempted to minimize systematic error as discussed above and avoid at least the second aspect of their criticism by providing, to the best of our ability, the identified sources of uncertainty and our estimates of their magnitude. Kossert (2003) and Amelin and Zaitsev (2002) also provide detailed discussion of their sources of error.

Despite the current agreement of results from different methods, we argue that the value chosen for the decay constant should be based on the best

laboratory measurement. Any determination based on comparison with other systems will inevitably be subject not only to uncertainty in other decay constants (^{238}U, ^{235}U and ^{40}K in this case) but also to uncertainty over differing responses of the systems to metamorphic and hydrothermal histories of the samples. Because of the low energy of beta emission from ^{87}Rb, there will always remain uncertainty over the necessary corrections in counting experiments. Despite their practical difficulties, only accumulation experiments can, in principle, provide unbiased determinations. We suggest that our 'best' estimate of $1.398 \pm 0.003 \times 10^{-11} a^{-1}$ be adopted as the accepted value of λ_{87} until a more accurate determination can be made. The agreement within error among all recent determinations provides assurance that this value is accurate but averaging all of them will not increase the accuracy because of the uncertainties described above.

Sufficient $RbClO_4$ remains from all four batches that future sets of measurements could be taken. It is recommended that these be performed after intervals of about a decade. The amount of salt per sample used in the present study was about a factor of ten less than in the Davis et al. (1977) study. As methods improve, this may continue to decrease. Measurements of radiogenic ingrowth after different intervals might reduce some possible sources of systematic error such as initial $^{87}Sr/^{86}Sr$.

7. Accumulation experiments for other decay-constants

Uncertainty has surrounded λ_{87} for nearly a century, and we can now finally say that it is one of the best constrained decay constants in common use for geochronology. However there are uncertainties in other decay constants and ingrowth might be an underutilized method for re-determination and cross-checks of other methods. It may be applied to other decay-constants that are still

controversial, e.g. ^{176}Lu, ^{187}Re (Lindner et al. 1989, GCA), ^{40}K, and ^{138}La. Recently, Schön et al. (2004) and Schoene et al. (2006) have questioned whether one or both of the U decay constants should be revised, and an ingrowth experiment involving He accumulation from the first decays may be appropriate here as well. Each of these experiments will surely have its individual difficulties to overcome. We have tried to emphasize in this report and in our description of the spike calibration (Chapter 2) how even minor details can become major obstacles. However, accumulation of daughter isotope is potentially the most precise and accurate method to measure decay constants and should be considered for these other isotopes.

It is important to note the importance of agreement between all three methods. In discussion of Huster's 1956 counting experiment, Inghram commented:

> I bring up this argument for the same old reason. We go back to the half-life of U^{235} which Nier did in 1939 and which the counting people didn't believe for 8 years. Finally they did a careful counting experiment and now the value agrees within 1% of Nier's figure. So I don't think you can completely neglect this geological evidence (Huster, 1956).

The situation with λ_{87} was similar: for many years, Aldrich et al.'s value of 1.39 was used, until biased counting and ingrowth evidence indicated that the value was 1.42 – and this value was ultimately accepted provisionally by the geochronology community. But in the ensuing years, increasing *geological* evidence indicated that Aldrich et al.'s value was closer to the actual value than the provisional recommendation was. The story of λ_{87} measurements demonstrates that two methods are not necessarily sufficient and that it is possible even for all three methods to accord, and yet be inaccurate. For the present time, all three methods converge on a λ_{87} value near $1.398 \times 10^{-11} a^{-1}$. We have shown that even when all sources of uncertainty cannot be accounted for, ingrowth is capable of precision better than the best counting experiments and

geological age comparisons. Accuracy is ensured by the limited assumptions required. Decay constants for geochronology are rarely measured, but they are relied upon by the geochronology community. In order for the community to rely on the accuracy of the decay constants, the utmost care must be taken in all measurements to eliminate uncertainties, and all known sources of uncertainty must be reported.

8. References

Afanass'yev G.D., Brandt S.B. Bagdassaryan G.P. Gorokhov I.M., Dunayev V.A., Zykov S.I., Rubenstein M.M. (1970) Summarized Analyses of Standards. *Eclogae geol. Helv.* **63**, 9-14.

Afanass'yev G.D., Zykov S.I., Gorokov I.M., and Shanin L.L. (1974) Correlativity of geochronometric ages yielded by coexisting minerals with different 40K, 87Rb and some other radioactive element decay constants. *International Meeting for Geochronology, Cosmochronology and Isotope Geology, Paris.* (abstract) .

Ahrens, L. (1949) Measuring geologic time by the strontium method. *Geol. Soc. Am. Bull.* **60**, 217-266.

Aldrich L.T., Wetherill G.W., Tilton G.R., and Davis G.L. (1956) Half-life of Rb^{87}. *Phys. Rev.* **103**, 1045-1047.

Amelin Y. and Zaitsev A.N. (2002) Precise geochronology of phoscorites and carbonatites: The critical role of U-series disequilibrium in age interpretations. *Geochim. Cosmochim. Acta* **66**, 2399-2419.

Baum E.M., Knox H.D., and Miller T.R. (2002) *Chart of the Nuclides Sixteenth ed.*, KAPL, Inc., Schenectady.

Beard G.B. and Kelly W.H. (1961) "Self-scintillation" study of the beta decay of Rb^{87}. *Nuclear Physics* **28**, 570-577.

Begemann F., Ludwig K.R., Lugmair G.W., Min K., Nyquist L.E., Patchett P.J., Renne P.R., C.-Y. Shih, Villa I.M., and Walker R.J. (2001) Call for an improved set of decay constants for geochronological use. *Geochim. Cosmochim. Acta* **65**, 111-121.

Birck, Jean Louis. (1986) Precision K-Rb-Sr isotopic analysis: Application to Rb-Sr chronology. *Chem. Geol.* **56**, 73-83.

Borg, L.E., Nyquist, L.E., Wiseman, H., Shih, C.-Y., and Reese, Y. (2003) The age of Dar al Gani 476 and the differentiation history of the martian meteorites inferred from their radiogenic isotopic systematics. *Geochim. Cosmochim. Acta* **67**, 3519-3536.

Brouwer W., Tomlinson R.H., McMullen, C.C., and Fritze, K. (1964) A mass spectrometric determination of the half-life of Rb^{87}. *Physics in Canada* **20**, 44-45.

Brinkmann G.A., Aten Jr. A.H.W., and Veenboer J. Th. (1965) Natural radioactivity of K-40, Rb-87 and Lu-176. *Physica* **31**, 1305-1319.

Campbell, N.R. and Wood, A. (1906) The radioactivity of the alkali metals. *Proc. Camb. Phil. Soc.* **14**, 15-21.

Curran S.C., Dixon D., and Wilson H.W. (1951) The natural radioactivity of rubidium. *Phys. Rev.* **84**, 151-152.

Curran S.C., Dixon D., and Wilson H.W. (1952) The natural radioactivity of rubidium. *Phil. Mag.* **43**,82-92.

Davis D.W. (1978) *Determination of the ^{87}Rb decay constant: An Rb/Sr and Pb/Pb study of the Labrador Archean complex*. Ph.D. Thesis, Univ. Alberta.

Davis D.W., Gray J., Cumming G.L., and Baadsgaard H. (1977) Determination of the ^{87}Rb decay constant. *Geochim. Cosmochim. Acta* **41**, 1745-1749.

Dickin, A.P. (1995) *Radiogenic Isotope Geology*. Cambridge University Press: Cambridge. 490 pp.

Edmunson, J., Borg, L.E., Nyquist, L.E., and Asmerom, Y. (2009) A combined Sm-Nd, Rb-Sr, and U-Pb isotopic study of Mg-suite norite 78238: Further evidence for early differentiation of the Moon. *Geochim. Cosmochim. Acta* **73**, 514-527.

Egelkraut K. and Leutz H. (1961) β-spektrum und halbwertszeit des Rb^{87}. *Z. Phys.* **161**, 13-19.

Eklund S. (1947) The half-life period of ^{87}Rb. *Arkiv Mat., Astronom. Fysik (A)* [Full title: *Arkiv för Matematik, Astronomi och Fysik*] **33a**, 60.

Faure, G. (1986) *Principles of Isotope Geology, 2nd Ed.* John Wiley & Sons, New York, Chichester, Brisbane, Toronto, Singapore, 589 p.

Flinta J. and Eklund S. (1954) On the radioactivity of Rb87. *Ark. Fys*. [full title: *Arkiv för Fysik*] **7**, 401.

Flynn K.F. and Glendenin L.E. (1959) Half-life and beta spectrum of Rb^{87}. *Phys. Rev.* **116**, 744-748.

Fritze K. and Kennet T.J. (1960) The Identification and Half Lives of Fission-Product Rb^{92} and Rb^{93}. *Can. J. Phys.* **38**, 1614-1622.

Fritze K. and Straßmann F. (1956) Indirekte bestimmung der halbwertszeit des rubidiums. *Z. Naturforsch.* **11a**, 277.

Geese-Bähnisch I. (1955) Zum b-zerfall des rubidiums 87: Nachprüfung des zerfallsschemas und neubestimmung der halbwertszeit. *Z. Phys*. **142**, 565-584.

Geese-Bähnisch I. and Huster E. (1954) Neubestimmung der halbwertszeit des 87Rb. *Naturwissenschaften* **41**, 495-496.

Geese-Bähnisch I., Huster E., and Walcher, W. (1952) Zu halbertszeit und zerfallsschema des Rb87. *Naturwissenschaften* **39**, 379-380.

Glodny, J., Kühn, A., and Austrheim, H. (2008) Diffusion versus recrystallization processes in Rb-Sr geochronology: Isotopic relics in eclogite facies rocks, Western Gneiss Region, Norway. *Geochim. Cosmochim. Acta* **72**, 506-525.

Glendenin L.E. (1959) Present status of the decay constants. *Ann. New York Acad. Sci.* **91**,166-179.

Grau Carles, A., and Kossert, K. (2007) Measurement of the shape-factor functions of the long-lived radionuclides ^{87}Rb, ^{40}K and ^{10}Be. *Nucl. Instr. and Meth. A* **572**, 760-767.

Greuling, E. (1942) Theoretical Half-Lives of Forbidden β-Transitions. *Phys. Rev.* **61**, 568-577.

Hahn O. and Rothenbach M. (1919) Über die radioaktivität des rubidiums. *Physikalische Zeitschrift* **20**, 194-202.

Hahn O., Straßmann F., and Walling E. (1937) Herstellung wägbarer mengen des strontiumisotops 87 als umwandlungsproduckt des rubidiums aus einem kanadischen glimmer. *Naturwissenschaften* **25**, 189.

Haxel O. and Houtermans F.G. (1948) Gleichzeitige emission von zwei elektronen beim radioaktiven zerfall des rubidium 87. *Z. Phys*. **124**, 705-713.

Haxel O., Houtermans F.G., and Kemmerich M. (1948) On the half-life of Rb^{87}. *Phys. Rev*. **74**, 1886-1887.

Hemmendinger, A., and Smythe, W.R. (1937) The radioactive isotope of rubidium. *Phys. Rev.* **51,** 1052-1053.

Holden, N. (1990) Total half-lives for selected nuclides. *Pure App. Chem.* **62**, 941-958.

Huster, E. (1956) A redetermination of the half-life of ^{87}Rb. *Nuclear Processes in Geologic Settings*, *Proceedings of the Second Conference*. Nuclear Science Series Report Number 19. National Academy of Sciences – National Research Council and National Science Foundation, Washington, D.C.

Jaffey, A.H., Flynn, K.F., Glendenin, L.E., Bentley, W.C., and Essling, A.M. (1971) Precision measurement of half-lives and specific activities of ^{235}U and ^{238}U. *Phys. Rev. C* **4,** 1889-1906

Kemmerich M. (1949) Die halbwertszeit des rubidiums. *Z. Phys*. **126**, 399-409.

Konopinski, E.J. and Bethe, H.A. (1938) The Mean Life of Rubidium 87. *Phys. Rev.* **53**, 679 (abstract).

Kossert K. (2003) Half-life measurements of ^{87}Rb by liquid scintillation counting. *App. Rad. and Isot.* **59**, 377-382.

Kostitsyn Yu.S. and Zhuravlev A.Z. (1988) Analysis of erros in and methods of optimizing the method of isotope dilution. *Geochem. Int.* **25**, 100-113. (trans. from Russian, Geokhimiya, No. 7, pp. 1024-1036, 1987).

Kovách A. (1964) A re-determiniation of the half-life of rubidium-87. *Acta Phys. (Hung.)* **17**, 341-351.

Kulp J.L., Engels J. (1963) Discordances in K-Ar and Rb-Sr isotopic ages. *Radioactive Dating; Proceedings of the symposium on radioactive dating held by the IAEA* 219-238.

Leutz H., Wenninger H., and Ziegler K. (1962) Die Halbwertszeit des Rb^{87}. *Z. Phys*. **169**, 409-416.

Lewis G.M. (1952) The natural radioactivity of rubidium. *Phil. Mag.* **43**, 1070-1074.

Libby W.F. (1957) Simple absolute measurement technique for beta radioactivity. *Anal. Chem*. **29**, 1566-1570.

Lide, David R. ed., (2005) *CRC Handbook of Chemistry and Physics*, *Internet Version 2005*, <http://www.hbcpnetbase.com>, CRC Press, Boca Raton, FL.

Lindner, M., Leich, D.A., Russ, G.P., Bazan, J.M., and Borg, R.J. (1989) Direct determination of the half-life of ^{187}Re. *Geochim. Cosmochim. Acta* **53**, 1597-1606.

Ludwig K. R. (2003) Isoplot/Ex version 3.00, a geochronological toolkit for Microsoft Excel. Berkeley Geochronology Center Special Publication #4.

MacGregor M.H. and Wiedenbeck M.L. (1952) The decay of rubidium 87. *Phys. Rev*. **86**, 420-421.

MacGregor M.H. and Wiedenbeck M.L. (1953) The decay of rubidium 87. *Proceedings of the Conference on Nuclear Processes in Geologic Settings* 1 (abstract).

MacGregor M.H. and Wiedenbeck M.L. (1954) The third forbidden beta spectrum of rubidium-87. *Phys. Rev*. **94**, 138-140.

MacMahon, D., Pearce, A., Harris, P. (2004) Convergence of techniques for the evaluation of discrepant data. *Appl. Radiat. Isot.* **60**, 275-281.

McMullen C.C., Fritze K., and Tomlinson R.H. (1966) The half-life of rubidium-87. *Can. J. Phys*. **44**, 3033-3038.

McNair A. and Wilson H.W. (1961) The half-life of rubidium-87. *Phil. Mag.* **6**, 563-572 .

Minster J-F., Birck J-L. and Allègre C.J. (1982) Absolute age of formation of chondrites studied by the ^{87}Rb-^{87}Sr method. *Nature* **300**, 414-419.

Mühlhoff W. (1930) Aktivität von kalium und rubidium gemessen mit dem elektronenzählrohr. *Annalen der Physik* **7**, 205-224.

Nebel, O., Mezger, K., Scherer, E.E., and Patchett, J. (2006a) Recalibration of the Rb decay constant by age comparison against three U-Pb dated igneous rocks. *Geophys. Res. Abstracts*. **8,** 08036**.**

Nebel O., Mezger K., Scherer E.E., and Davies G.R. (2006b) Determination of the Rubidium Decay Constant by Age Comparison Against the U-Pb System, *Eos Trans. AGU 87* (52), Fall Meet. Suppl., Abstract V21A-0558

Neumann W. and Huster E. (1972) Neubestimmung der Halbwertszeit des ^{87}Rubidiums durch Vergleich von Messungen an den getrennten Isotopen ^{87}Rb und ^{85}Rb. *Z. Naturforsch.* **27a**, 862.

Neumann W. and Huster E. (1974) The half-life of ^{87}Rb measured as a difference between the isotopes ^{87}Rb and ^{85}Rb. *Z. Phys*. **270**, 121-127.

Neumann W. and Huster E. (1976) Discussion of the ^{87}Rb half-life determined by absolute counting. *Earth Planet. Sci. Lett*. **33**, 277-288.

Orbán G. (1931) . Untersuchungen über die Radioaktivität der Alkalimetalle mit der Nebelstrahlmethode. *Sitzungsberichte - Akademie der Wissenschaften in Wien, Mathematisch-Naturwissenschaftliche Klasse. Abteilung IIa: Mathematik, Astronomie, Physik, Meteorologie und Mechanik.* **140**, 121-141.

Ovchinnikova G.V. (Also Ovtshinnikova or Ovchinnikeva) (1960) Determination of the beta-decay constant of Rb87 by a geochemical method. *Geokhemia* [*Geochemistry A Translation of Geokhimiya*] **5**, 466 [**5**, 392 in Russian].

Pálfy, J., Mundil, R., Renne, P.R., Bernor,R.L., Kordos, L, and Gasparik, M. (2007) U–Pb and ^{40}Ar/^{39}Ar dating of the Miocene fossil track site at Ipolytarnóc (Hungary) and its implications. *Earth Planet. Sci. Lett.* **258**, 160-174.

Pommé, S., Camps, J., Van Ammel, R., and Paepen, J. (2008) Protocol for uncertainty assessment of half-lives. *Journal of Radioanalytical and Nuclear Chemistry*, **276**, 335-339.

Raghurama G., Al-Dhahir TA, and Bhat HL. (1987) Optical studies on the orthorhombic-cubic transitions for $KClO_4$, $RbClO_4$ and $CsClO_4$. *J. Phys. C: Solid State Phys.* **20**, 4505-4511.

Rausch W. and Schmidt W. (1960) Neubestimmung der halbwertszeit des ^{87}Rb. *Physikalische Verhandlungen* **11**, 66.

Rotenberg E., Davis D.W., and Amelin Y. (2004) Determination of the ^{87}Rb decay constant by ^{87}Sr accumulation. *32nd Int. Geol. Congr*., Abs. Vol., pt. 1,abs. 172-5, p. 811.

Rotenberg, E., Davis, D.W., and Amelin, Y. (2005) Determination of the ^{87}Rb decay constant by ^{87}Sr accumulation. 15th Annual V.M. Goldschmidt Conference, Abstract. *Geochim. Cosmochim. Acta* **69**, A326.

Rotenberg, E., Davis, D.W., and Amelin, Y., (2009) The decay constant of ^{87}Rb. *EOS Trans. Am. Geophys. Union*, **90** (22), Jt. Assem. Suppl., Abstract GA14A-06.

Samson S.D., Coler D.G., and Speer, J.A. (1995) Geochemical and Nd-Sr-Pb isotopic composition of Alleghanian granites of the sourther Appalachians: Origin, tectonic setting, and source characterization. *Earth Planet. Sci. Lett.* **134**, 359-376.

Schiller, S.B. and Eberhardt, K.R. (1991) Combining data from independent chemical analysis methods. *Spectrochimica Acta* **46B**, 1607-1613.

Schoene, B., Crowley, J.L., Condon, D.J., Schmitz, M.D., and Bowring, S.A. (2006) Reassessing the uranium decay constants for geochronology using ID-TIMS U-Pb data. *Geochim. Cosmochim. Acta* **70**, 426-445.

Schön, R., Winkler, G, and Kutschera, W. (2004) A critical review of experimental data for the half-lives of the uranium isotopes ^{238}U and ^{235}U. *Appl. Radiat. Isot.* **60**, 263-273.

Sen-Chowdhury, P.K. (also Chowdhury, Chaudhury) (1942) Radio-activity of Rubidium. *Proceedings of the National Institute of Sciences of India* [*Proceedings of the Indian National Science Academy*] **8**, 45.

Serezhkina, L.B., Grigorovich, Z.I., Serezhkin, V.N., Tamm, N.S., and Novoselova, A.V. (1973) Some properties of cesium and rubidium perchloratoberyllates. *Russian Chem. Bull.* **22**, 433-434. (Translated from Izvestiya Akademii Nauk SSSR, Seriya Khimicheskaya, **2**, 451-452, 1973).

Shih C.-Y., Nyquist L.E., Bogard D.D., Wooden J.L., Bansal B.M., and Wiesmann H. (1985) Chronology and petrogenesis of a 1.8 g lunar granitic clast: 14321,1062. *Geochim. Cosmochim. Acta* **49**, 411-426.

Steiger R.H. and Jäger E. (1977) Subcommission on geochronology: Convention in the use of decay constants in geo- and cosmochemistry. *Earth Planet. Sci. Lett*. **36**, 359-362.

Straßmann F. und Walling E. (1938) Die abscheidung des reinen Strontium-Isotops 87 aus einem alten rubidiumhaltigen Lepidolith und die Halbsertszeit des Rubidiums. *Berichte der Deutschen Chemischen Gesellschaft* **71**, 1B, 1.

Thode H.G, McMullen C.C., Pleva J., Heyland G., and Tracy B. (1965) Mass Spectrometric Studies. *McMaster Nuclear Reactor – Reactor Research Report*. B26-B28.

Thomson J.J (1905) On the emission of negative corpuscles by the alkali metals. *Phil. Mag.* **10**,584-591.

Walker, D., Hughes, G., Cranswick, M.D.L., Clark, S.M., and Buhre, S. Synthesis and thermal decomposition of tetragonal $RbClO_4$ and volume of fluid O_2 from 2 to 9 GPa, *Geochem. Geophys. Geosystems* **2**, Paper number: 2001GC000154.

Wetherill G.W., Aldrich L.T., Tilton G.R., and Davis G.L. (1956) Half-life of Rb^{87}. *Bull. Am. Phys. Soc.* **1**, 31.

Wapstra, A.H., Audi, G., and Thibault, C. (2003) The AME2003 atomic mass evaluation (I). Evaluation of input data, adjustment procedures. *Nucl. Phys. A* **729**, 129-336.

Williams I.S., Tetley N.W., Compston W., and McDougall I. (1982) A comparison of K-Ar and Rb-Sr ages of rapidly cooled igneous rocks: two points in the Palaeozoic time scale re-evaluated. *J. geol. Soc. London* **139**, 557-568.

Zartman R.E. (1964) A geochronologic study of the Lone Grove pluton from the Llano Uplift, Texas. *J. Petrol.* **5**, 359-408.

Table 1. Decay Constant Measurements

		year	$T_{½}$ ($\times 10^{10}$ a)		λ ($\times 10^{-11}$ a^{-1})	
Direct Counting						
Gas Counters	Hahn and Rothenbach	1919	**5** [2]		1.4	
	Holmes and Lawson	1926	**10** [7]		0.07	
	Mühlhoff	1930	**12** [2]		0.58	
	Orbán	1931	**4.5**		1.5	
	Sen-Chowdhury	1942	**7.459**		0.929	
	Saha, Ajit Kumar	1946	**7.45**		0.9	
	Eklund	1947	**5.8**	**± 1.0**	1.2	± 0.2
	Haxel and Houtermans	1948	**6.9** [3]	**± 0.7**	1.00	± 0.1
	Haxel et al.	1948	**6.0**	**± 0.6**	1.16	± 0.1
	Kemmerich (PhD Dissertation)	1948	6	± 0.6	1.16	± 0.1
	Kemmerich	1949	**6.0** [3]	**± 0.6**	1.16	± 0.1
	Curran et al.	1951	**6.15**	**± 0.3**	1.13	± 0.1
	Curran et al.	1952	**6.15**		1.13	
	Geese-Bähnisch et al.	1952	**6.0**		1.16	
	MacGregor and Wiedenbeck	1952	**6.29**	**± 0.3**	1.10	± 0.1
	MacGregor and Wiedenbeck	1953	**6.4**	**± 0.3**	1.08	± 0.1
	MacGregor and Wiedenbeck	1954	**6.2**	**± 0.3**	1.12	± 0.1
	Flinta and Eklund	1954	**6.1**	**± 0.2**	1.14	± 0.04
	Geese-Bähnisch and Huster	1954	**4.3**	**+0.3 -0.2**	1.61	+0.11 -0.06
	MacGregor and Wiedenbeck	1954	**6.2**	**± 0.3**	1.12	± 0.1
	Geese-Bähnisch	1955	**4.3**	**+0.3 -0.2**	1.61	+0.11 -0.06
	Huster	1956	**4.3**	**+0.3 -0.2**	1.61	+0.11 -0.06
	Libby	1957	**5.07**	**± 0.2**	1.37	± 0.05
	Rausch and Huster		**4.99** [8]		1.39	
	Rausch and Schmidt	1960	**4.72** [4]	**± 0.2**	1.47	± 0.02
	McNair and Wilson	1961	**5.25**	**± 0.2**	1.32	± 0.03
	Neumann and Huster	1972	**4.88** [5]	**± 0.10**	1.42	± 0.03
	Neumann and Huster	1974	**4.88** [5]	**+0.06 -0.10**	1.42	+0.02 -0.03
Liquid Scintillators	Flynn and Glendenin	1959	**4.70**	**± 0.10**	1.47	± 0.03
	Glendenin	1959	**4.70**	**± 0.05**	1.47	± 0.02
	Kovách	1964	**4.77**	**± 0.10**	1.45	± 0.03
	Brinkmann et al.	1965	**5.22**	**± 0.15**	1.33	± 0.04
	Kossert	2003	**4.967**	**± 0.032**	1.396	± 0.006
Solid Scintillators	Lewis	1952	**5.90**	**± 0.3**	1.17	± 0.1
	Beard and Kelly	1961	**5.53**	**± 0.10**	1.25	± 0.02
	Egelkraut and Leutz	1961	**5.82**	**± 0.1**	1.19	± 0.02
	Leutz et al.	1962	**5.80**	**± 0.12**	1.20	± 0.02
Age Comparisons						
K-Ar	Fritze and Straßmann	1956	**4.6**	**± 0.5**	1.51	± 0.15
	Jamieson and Schreiner	1957			**1.26**[11]	**± 0.04**
	Kulp		**4.8** [9]		1.44	
	Kulp and Engels	1963	**4.70**		1.47	
	Zartman	1964	**4.85**		1.43	
	Afanass'yev et al.	1970	4.99		**1.39**	
	Afanass'yev et al.	1974	4.88		**1.42**	
	Williams et al.	1982	4.88		**1.42**	
U-Pb	Hahn et al.	1937	6.3		1.1	
	Straßmann und Walling	1938	6.3		1.1	
	Aldrich et al.	1956	**5.0**	**± 0.2**	1.39	± 0.06
	Wetherill et al.	1956	**5.0**	**± 0.2**	1.39	± 0.06
	Ovchinnikova	1960	5.02	± 0.2	**1.38**	**± 0.05**
	Minster et al.	1982	4.944	± 0.028	**1.402**	**± 0.008**
	Shih et al.	1985	4.944	± 0.039	**1.402**	**± 0.011**
	Amelin and Zaitsev[10]	2002	4.965	± 0.021	**1.400**	**± 0.010**
	Nebel et al.	2006a	4.955	± 0.011	**1.399**	**± 0.003**
	Nebel et al.	2006b	4.958	± 0.011	**1.398**	**± 0.003**
^{87}Sr* Accumulation						
	Thode et al.	1965	**4.60**	**± 0.06**	1.51	± 0.02
	McMullen et al.	1966	**4.72**	**± 0.04**	1.47	± 0.01
	Davis et al.	1977	4.885	± 0.041	**1.419**	**± 0.012**
	Davis	1978	4.885	± 0.041	**1.419**	**± 0.012**
	Rotenberg et al. (abstract)	2004	4.916	±0.024	**1.410**	**±0.007**
	Rotenberg et al. (abstract)	2005	4.9596	± 0.0078	**1.3976** [6]	**± 0.0022**
	Rotenberg et al. (abstract)	2009	4.9578	± 0.0032	**1.3981**	**± 0.0009**
	Current work	2009	4.9585	± 0.0092	**1.3979**	**± 0.0026**

Table 1. Decay Constant Measurements (notes)

[(1)] a number of these values are quoted differently by later authors. Occassionally they explain that they have made corrections or recalculated the values. Other times they do not. Except where corrected for ^{87}Rb, values are quoted as published. Both decay constants, λ, and half-lives, $T_{½}$, are given. Numbers in bold are the published value, while the corresponding value is calculated from the published value. It should also be noted that not all of these values represent new and independent determinations. Some authors published several values as the work progressed. Some age comparisons simply state that when such decay constant is used, ages agree well.

[(2)] corrected from published value after the discovery of isotopes

[(3)] corrected by Brinkman *et al.* (1965) for "wrong decay scheme" to 4.6 ± 0.5 and 4.0 ± 0.4 respectively

[(4)] Neumann and Huster (1974) correct to 4.6 for KCl content of RbCl

[(5)] Begemann *et al.* (2001) taking a weighted average and omitting two data points recalculate a value of 1.403 ± 0.009

[(6)] This is the value presented at the Goldschmidt Conference (2005), adjusted from the value of 1.421 ± 0.001 published in the conference abstracts

[(7)] This determination is based on analysis of published data. It probably should be corrected for the fact that only ^{87}Rb is radioactive, which would yield T½ = 3.86 (λ_{87} = 1.80)

[(8)] Private communication to Aldrich, Wetherill, Davis, and Tilton (1958)

[(9)] Personal communication to Flynn and Glendenin (1959)

[(10)] Average of values for rapid cooling and slow cooling in samples analyzed

[(11)] Value that yields best agreement with U/Pb, however, the authors caution that: "[t]he value of adjusting a decay constant by cross-comparisons of ages determined by diffeernt decay schemes seems to be doubtful until a statistical determination of all variations including sample variations has been made using both decay schemes."

Table 2a - λ_{87} measurements

Sample	Batch	Precipitation Date	Separation Date	t (y)	$^{87}Sr^*$ (pmol)	2σ	$RbClO_4$ (g)	2σ	^{87}Rb (mol)	λ_{87} ($\times 10^{-11} a^{-1}$)	2σ
Sr #3	**C**	1976-09-09 15:00	2003-12-18	27.270	1.226 40	± 0.003 42	2.126 25	± 0.032 72	0.003 20	**1.404 4**	**± 0.003 5**
Sr #4	**C**	1976-09-09 15:00	2003-12-18	27.270	2.231 46	± 0.037 12	3.835 52	± 0.032 72	0.005 78	**1.416 6**	**± 0.011 2**
Sr #5	**D**	1976-09-21 14:00	2004-01-21	27.330	1.755 09	± 0.011 70	3.048 49	± 0.071 95	0.004 59	**1.398 7**	**± 0.010 4**
Sr #6	**D**	1976-09-21 14:00	2004-01-21	27.330	1.933 00	± 0.008 93	3.357 06	± 0.071 96	0.005 06	**1.398 9**	**± 0.011 8**
Sr #9	**B**	1976-09-04 12:00	2004-02-17	27.455	2.385 62	± 0.009 74	4.141 00	± 0.050 84	0.006 24	**1.393 3**	**± 0.007 3**
Sr #10	**B**	1976-09-04 12:00	2004-02-17	27.455	2.966 49	± 0.003 54	5.119 21	± 0.093 46	0.007 71	**1.401 4**	**± 0.004 1**
Sr #11	**C**	1976-09-09 15:00	2004-02-17	27.441	2.563 60	± 0.004 34	4.435 02	± 0.058 43	0.006 68	**1.398 6**	**± 0.005 7**
Sr #12	**D**	1976-09-21 14:00	2004-02-17	27.408	2.475 73	± 0.003 86	4.303 31	± 0.052 22	0.006 48	**1.393 7**	**± 0.004 6**
Sr #13	**A**	1976-08-27 23:00	2004-03-29	27.589	2.661 26	± 0.002 30	4.587 74	± 0.013 31	0.006 91	**1.396 1**	**± 0.017 7**
Sr #14	**A**	1976-08-27 23:00	2004-03-29	27.589	1.795 62	± 0.008 18	3.092 69	± 0.036 58	0.004 66	**1.397 3**	**± 0.013 8**
Sr #15	**B**	1976-09-04 12:00	2004-03-29	27.567	1.262 95	± 0.006 06	2.175 02	± 0.020 24	0.003 28	**1.398 6**	**± 0.013 3**
Sr #16	**B**	1976-09-04 12:00	2004-03-29	27.567	2.064 53	± 0.000 70	3.560 07	± 0.013 29	0.005 36	**1.396 8**	**± 0.001 2**
Sr #17	**C**	1976-09-09 15:00	2004-03-29	27.551	1.204 85	± 0.000 74	2.082 61	± 0.013 29	0.003 14	**1.394 3**	**± 0.002 5**
Sr #18	**D**	1976-09-21 14:00	2004-03-29	27.521	1.704 37	± 0.001 64	2.950 88	± 0.013 30	0.004 44	**1.393 5**	**± 0.004 5**
Sr_2007-10	**A**	1976-08-27 23:00	2007-12-25	31.326	4.297 14	± 0.000 12	6.505 47	± 0.000 10	0.009 80	**1.400 0**	**± 0.000 4**
Sr_2007-11	**B**	1976-09-04 12:00	2007-12-25	31.305	4.306 52	± 0.000 27	6.533 08	± 0.000 13	0.009 84	**1.398 2**	**± 0.000 8**
Sr_2007-12	**C**	1976-09-09 15:00	2007-12-25	31.291	5.642 68	± 0.000 08	8.570 54	± 0.000 09	0.012 91	**1.397 1**	**± 0.000 3**
Sr_2007-13	**D**	1976-09-21 14:00	2007-12-25	31.258	1.920 92	± 0.000 23	2.922 44	± 0.000 11	0.004 40	**1.396 2**	**± 0.000 7**
Sr_2007-14	**A**	1976-08-27 23:00	2007-12-25	31.326	2.721 64	± 0.000 05	4.103 17	± 0.000 04	0.006 18	**1.405 9**	**± 0.000 6**
Sr_2007-15	**B**	1976-09-04 12:00	2007-12-25	31.305	2.430 95	± 0.001 54	3.681 11	± 0.000 05	0.005 54	**1.400 7**	**± 0.002 2**
Sr_2008-01	**A**	1976-08-27 23:00	2008-05-02	31.680	3.745 04	± 0.000 06	5.613 43	± 0.000 05	0.008 45	**1.398 3**	**± 0.000 4**
Sr_2008-02	**B**	1976-09-04 12:00	2008-05-02	31.658	2.634 71	± 0.000 11	3.959 03	± 0.000 35	0.005 96	**1.395 8**	**± 0.000 8**
Sr_2008-03	**C**	1976-09-09 15:00	2008-05-02	31.644	7.087 89	± 0.000 05	10.605 96	± 0.000 10	0.015 97	**1.402 3**	**± 0.000 2**
Sr_2008-05	**C**	1976-09-09 15:00	2008-05-02	31.644	3.227 54	± 0.000 09	4.851 99	± 0.000 04	0.007 31	**1.395 8**	**± 0.000 4**
Sr_2008-06	**D**	1976-09-21 14:00	2008-05-02	31.611	2.703 05	± 0.000 10	4.064 33	± 0.000 04	0.006 12	**1.396 9**	**± 0.000 4**
Sr_2008-21	**D**	1976-09-21 14:00	2008-11-14	32.148	1.544 86	± 0.000 18	2.285 85	± 0.000 10	0.003 44	**1.395 9**	**± 0.000 7**
Sr_2008-22	**C**	1976-09-09 15:00	2008-11-14	32.181	2.740 23	± 0.000 18	4.033 08	± 0.000 11	0.006 07	**1.401 9**	**± 0.000 8**
Sr_2008-23	**C**	1976-09-09 15:00	2008-11-14	32.181	1.441 78	± 0.000 15	2.130 32	± 0.000 11	0.003 21	**1.396 4**	**± 0.000 9**
Sr_2008-24	**B**	1976-09-04 12:00	2008-11-16	32.200	2.509 65	± 0.000 69	3.702 98	± 0.000 10	0.005 58	**1.397 5**	**± 0.001 1**
Sr_2008-25	**B**	1976-09-04 12:00	2008-11-16	32.200	2.653 28	± 0.000 06	3.912 66	± 0.000 07	0.005 89	**1.398 3**	**± 0.000 5**
Sr_2008-26	**A**	1976-08-27 23:00	2008-11-16	32.222	1.969 85	± 0.000 40	2.900 27	± 0.000 18	0.004 37	**1.399 6**	**± 0.000 8**

Table 2b - Isotopic ratios of λ_{87} measurements

Sample	Batch	$^{86}Sr/^{88}Sr$[a]	2σ	$^{87}Sr/^{86}Sr$[a]	2σ	$^{84}Sr/^{86}Sr$[a]	2σ	$^{87}Sr/^{88}Sr$[a]	S/B[b]	2σ
Sr #3	**C**	0.124 80	± 0.000 24	6.242 23	± 0.009 56	79.536	± 0.153	0.779 00	8.232 44	± 0.016 62
Sr #4	**C**	0.131 01	± 0.000 12	21.310 24	± 0.019 85	162.456	± 1.480	2.791 92	17.797 62	± 0.188 56
Sr #5	**D**	0.132 99	± 0.000 12	19.444 02	± 0.047 20	187.892	± 1.446	2.585 93	20.863 38	± 0.182 79
Sr #6	**D**	0.132 93	± 0.000 08	21.251 99	± 0.020 71	187.148	± 1.057	2.824 99	20.761 73	± 0.131 12
Sr #9	**B**	0.123 59	± 0.000 02	9.155 72	± 0.009 80	62.424	± 0.307	1.131 57	6.389 18	± 0.032 09
Sr #10	**B**	0.123 91	± 0.000 01	12.001 04	± 0.009 33	66.992	± 0.102	1.487 07	6.879 72	± 0.010 86
Sr #11	**C**	0.121 56	± 0.000 00	5.466 99	± 0.007 62	32.739	± 0.073	0.664 57	3.289 80	± 0.007 52
Sr #12	**D**	0.121 93	± 0.000 01	6.084 06	± 0.003 01	38.245	± 0.080	0.741 85	3.856 43	± 0.008 14
Sr #13	**A**	0.122 36	± 0.000 02	7.459 18	± 0.043 54	44.531	± 0.289	0.912 71	4.509 71	± 0.029 96
Sr #14	**A**	0.124 64	± 0.000 03	8.576 31	± 0.034 74	77.306	± 0.450	1.068 93	7.990 06	± 0.048 78
Sr #15	**B**	0.126 71	± 0.000 06	8.305 01	± 0.042 58	106.035	± 0.855	1.052 29	11.160 62	± 0.096 63
Sr #16	**B**	0.125 23	± 0.000 00	10.728 63	± 0.001 60	85.601	± 0.040	1.343 53	8.894 47	± 0.004 34
Sr #17	**C**	0.124 00	± 0.000 00	5.368 17	± 0.003 62	68.301	± 0.067	0.665 67	7.020 04	± 0.007 19
Sr #18	**D**	0.124 13	± 0.000 01	7.480 69	± 0.012 32	70.075	± 0.140	0.928 57	7.210 47	± 0.015 12
Sr_2007-10	**A**	2.325 92	± 0.000 35	0.836 06	± 0.000 09	0.889 83	± 0.000 01	1.944 61	3.778 35	± 0.000 63
Sr_2007-11	**B**	3.128 10	± 0.001 43	0.862 93	± 0.000 22	0.901 46	± 0.000 09	2.699 34	5.251 52	± 0.002 68
Sr_2007-12	**C**	1.384 07	± 0.000 22	0.932 49	± 0.000 07	0.859 18	± 0.000 04	1.290 63	2.118 41	± 0.000 38
Sr_2007-13	**D**	2.901 06	± 0.000 61	0.747 37	± 0.000 16	0.898 77	± 0.000 02	2.168 17	4.828 82	± 0.001 13
Sr_2007-14	**A**	2.485 91	± 0.003 66	0.920 31	± 0.000 07	0.892 73	± 0.000 06	2.287 81	4.067 67	± 0.006 65
Sr_2007-15	**B**	1.732 42	± 0.000 80	0.848 83	± 0.001 22	0.874 39	± 0.000 09	1.470 53	2.723 95	± 0.001 40
Sr_2008-01	**A**	2.477 09	± 0.000 49	0.880 67	± 0.000 05	0.892 58	± 0.000 02	2.181 49	4.051 82	± 0.000 89
Sr_2008-02	**B**	3.108 14	± 0.001 65	0.836 46	± 0.000 09	0.901 21	± 0.000 03	2.599 85	5.213 90	± 0.003 09
Sr_2008-03	**C**	2.005 10	± 0.000 33	0.965 55	± 0.000 05	0.882 63	± 0.000 02	1.936 03	3.204 55	± 0.000 59
Sr_2008-05	**C**	2.138 01	± 0.000 40	0.807 26	± 0.000 06	0.885 90	± 0.000 02	1.725 93	3.441 13	± 0.000 71
Sr_2008-06	**D**	4.181 30	± 0.000 52	0.639 22	± 0.000 06	0.909 85	± 0.000 02	2.672 78	7.273 97	± 0.001 03
Sr_2008-21	**D**	0.655 24	± 0.000 23	0.609 02	± 0.000 09	0.774 92	± 0.000 03	0.398 96	0.882 71	± 0.000 39
Sr_2008-22	**C**	0.297 48	± 0.000 06	0.676 59	± 0.000 07	0.582 49	± 0.000 07	0.201 19	0.291 04	± 0.000 11
Sr_2008-23	**C**	0.505 23	± 0.000 11	0.718 06	± 0.000 08	0.727 42	± 0.000 05	0.362 71	0.633 45	± 0.000 19
Sr_2008-24	**B**	0.577 24	± 0.000 48	0.750 93	± 0.000 40	0.753 30	± 0.000 15	0.433 48	0.752 90	± 0.000 79
Sr_2008-25	**B**	0.719 62	± 0.000 08	0.700 06	± 0.000 04	0.789 25	± 0.000 02	0.503 67	0.990 20	± 0.000 14
Sr_2008-26	**A**	0.581 48	± 0.000 28	0.667 68	± 0.000 21	0.754 64	± 0.000 09	0.388 12	0.759 94	± 0.000 46

[a] **corrected for fractionation**

[b] **atomic ratio of Sr from spike (S) to non-radiogenic "blank" Sr (B)**

Table 2c - Spike aliquots, radiogenic $^{87}Sr^*$ and non-radiogenic Sr

Sample	Batch	Spike	Spike (g)	2σ	Concentration (ng Sr/g)	Spike Sr (pg)	Blank Sr (pg)	Blank ^{87}Sr (pg)	$^{87}Sr^*$ (pg)	% radiogenic $^{87}Sr^c$
Sr #3	**C**	^{84}Sr	0.113 45	± 0.000 04	13.256	1503.85	186.9	13.0	106.59	89 %
Sr #4	**C**	^{84}Sr	0.113 46	± 0.000 04	13.256	1503.98	86.5	6.0	193.93	97 %
Sr #5	**D**	^{84}Sr	0.113 48	± 0.000 08	13.256	1504.29	73.8	5.1	152.53	97 %
Sr #6	**D**	^{84}Sr	0.113 46	± 0.000 08	13.256	1504.03	74.1	5.2	167.99	97 %
Sr #9	**B**	^{84}Sr	0.113 56	± 0.000 06	13.256	1505.35	241.1	16.8	207.33	92 %
Sr #10	**B**	^{84}Sr	0.113 46	± 0.000 11	13.256	1504.07	223.7	15.6	257.81	94 %
Sr #11	**C**	^{84}Sr	0.113 53	± 0.000 07	13.256	1504.95	468.0	32.7	222.80	87 %
Sr #12	**D**	^{84}Sr	0.113 48	± 0.000 06	13.256	1504.25	399.1	27.9	215.16	89 %
Sr #13	**A**	^{84}Sr	0.113 56	± 0.000 02	13.256	1505.40	341.5	23.8	231.29	91 %
Sr #14	**A**	^{84}Sr	0.113 64	± 0.000 04	13.256	1506.39	192.9	13.5	156.05	92 %
Sr #15	**B**	^{84}Sr	0.113 55	± 0.000 02	13.256	1505.20	138.0	9.6	109.76	92 %
Sr #16	**B**	^{84}Sr	0.113 69	± 0.000 02	13.256	1507.12	173.4	12.1	179.43	94 %
Sr #17	**C**	^{84}Sr	0.113 66	± 0.000 02	13.256	1506.72	219.6	15.3	104.71	87 %
Sr #18	**D**	^{84}Sr	0.113 57	± 0.000 02	13.256	1505.53	213.6	14.9	148.13	91 %
Sr_2007-10	**A**	^{84}Sr-^{86}Sr	4.594 41	± 0.000 02	0.187 71	862.42	235.3	16.4	373.46	96 %
Sr_2007-11	**B**	^{84}Sr-^{86}Sr	4.464 74	± 0.000 44	0.187 71	838.09	164.5	11.5	374.28	97 %
Sr_2007-12	**C**	^{84}Sr-^{86}Sr	5.326 68	± 0.000 02	0.187 71	999.88	486.6	34.0	490.40	94 %
Sr_2007-13	**D**	^{84}Sr-^{86}Sr	2.314 23	± 0.000 05	0.187 71	434.41	92.7	6.5	166.94	96 %
Sr_2007-14	**A**	^{84}Sr-^{86}Sr	2.632 19	± 0.000 04	0.187 71	494.09	125.2	8.7	236.53	96 %
Sr_2007-15	**B**	^{84}Sr-^{86}Sr	2.549 49	± 0.000 04	0.187 71	478.57	181.0	12.6	211.27	94 %
Sr_2008-01	**A**	^{84}Sr-^{86}Sr	3.790 74	± 0.000 26	0.187 83	712.01	181.2	12.6	325.48	96 %
Sr_2008-02	**B**	^{84}Sr-^{86}Sr	2.819 97	± 0.000 57	0.187 83	529.69	104.7	7.3	228.98	97 %
Sr_2008-03	**C**	^{84}Sr-^{86}Sr	6.493 22	± 0.000 15	0.187 83	1219.65	392.4	27.4	616.00	96 %
Sr_2008-05	**C**	^{84}Sr-^{86}Sr	3.576 57	± 0.000 28	0.187 84	671.82	201.3	14.0	280.50	95 %
Sr_2008-06	**D**	^{84}Sr-^{86}Sr	3.833 10	± 0.000 26	0.187 83	719.99	102.1	7.1	234.92	97 %
Sr_2008-21	**D**	^{84}Sr-^{86}Sr	2.266 17	± 0.000 48	0.197 53	447.63	522.8	36.5	134.26	79 %
Sr_2008-22	**C**	^{84}Sr-^{86}Sr	3.599 42	± 0.000 55	0.197 51	710.94	2518.3	175.8	238.15	58 %
Sr_2008-23	**C**	^{84}Sr-^{86}Sr	1.716 96	± 0.000 63	0.197 52	339.14	551.9	38.5	125.30	76 %
Sr_2008-24	**B**	^{84}Sr-^{86}Sr	2.825 77	± 0.000 38	0.197 52	558.14	764.3	53.3	218.11	80 %
Sr_2008-25	**B**	^{84}Sr-^{86}Sr	3.262 34	± 0.000 33	0.197 53	644.41	670.9	46.8	230.59	83 %
Sr_2008-26	**A**	^{84}Sr-^{86}Sr	2.576 70	± 0.000 42	0.197 52	508.95	690.5	48.2	171.20	78 %

[c] the percentage of ^{87}Sr that is from radioactive decay of ^{87}Rb in the $RbClO_4$ salt

Table 3 - Procedure Blanks

	pg Sr	pg ^{87}Sr
Blank #4	42.98	3.00
Blank #5	43.05	3.00
Blank K3	35.88	2.50
Sr_2007-16	22.94	1.60
Sr_2007-17	44.23	3.09
Sr_2008-17	37.89	2.64
Sr_2007-18	55.10	3.85
Sr_2007-27	22.77	1.59
Sr_2007-28	61.22	4.27
Average	**40.67**	**2.84**

Table 4a - Change in weight of $RbClO_4$ salt after heating (drying)

Batch	Sample	Change in weight after heating (g)	%age	Temperature (°C)	Time	Second Stage Heating after heating (g)	%age	Temperature (°C)	Time
C	**Sr #3**	0.015 89	0.747	200					
C	**Sr #4**	0.023 35	0.609	200					
D	**Sr #5**	0.008 23	0.270	170					
D	**Sr #6**	0.007 83	0.233	200					
A	**Sr_2007-01**	0.005 71	0.167	195	(1½ hrs)	0.001 18	0.034	262	(1½ hrs)
B	**Sr_2007-02**	0.026 13	0.214	195	(1½ hrs)	0.007 67	0.062	262	(1½ hrs)
C	**Sr_2007-03**	0.029 68	0.546	195	(1½ hrs)	0.003 12	0.057	262	(1½ hrs)
D	**Sr_2007-04**	0.005 98	0.147	195	(1½ hrs)	0.002 15	0.053	262	(1½ hrs)
C	**Sr_2007-05**	0.008 56	0.156	195	(1½ hrs)	0.002 90	0.053	262	(1½ hrs)
D	**Sr_2007-06**	0.006 58	0.163	195	(1½ hrs)	0.001 52	0.039	262	(1½ hrs)
A	**Sr_2007-10**	0.013 63	0.210	260	(4 hrs)				
B	**Sr_2007-11**	0.012 60	0.193	260	(4 hrs)				
C	**Sr_2007-12**	0.051 98	0.606	260	(4 hrs)				
D	**Sr_2007-13**	0.007 76	0.265	260	(4 hrs)				
A	**Sr_2007-14**	0.007 93	0.193	260	(4 hrs)				
B	**Sr_2007-15**	0.005 91	0.160	260	(4 hrs)				
A	**Sr_2008-01**	0.012 02	0.214	260	(3 hrs)				
B	**Sr_2008-02**	0.010 17	0.257	260	(3 hrs)				
C	**Sr_2008-03**	0.058 35	0.550	260	(3 hrs)				
C	**Sr_2008-05**	0.025 09	0.517	260	(3 hrs)				
D	**Sr_2008-06**	0.009 12	0.224	260	(3 hrs)				
D	**Sr_2008-21**	0.005 70	0.249	350	(19 hrs)				
C	**Sr_2008-23**	0.011 71	0.550	350	(19 hrs)				
B	**Sr_2008-24**	0.011 34	0.306	350	(19 hrs)				
B	**Sr_2008-25**	0.012 50	0.319	350	(19 hrs)				
A	**Sr_2008-26**	0.005 49	0.189	350	(19 hrs)				
Batch A average			**0.195**						
Batch B average			**0.242**						
Batch C average			**0.535**						
Batch D average			**0.222**						

Table 4a - Change in weight of $RbClO_4$ salt after heating (drying)

Table 4b - Results of Step Heating Experiment - 3.84906 g of $RbClO_4$ salt Batch B

Temperature (°C)	Weight difference (g)	(ppm)	difference (%)
100	0.001 32	343	0.034 29 %
150	0.001 89	491	0.049 10 %
195	0.002 67	694	0.069 37 %
220	0.000 46	120	0.011 95 %
240	0.000 20	52	0.005 20 %
260	0.000 53	138	0.013 77 %
280	0.000 02	5	0.000 52 %
310	-0.000 04	-10	-0.001 04 %
330	0.000 04	10	0.001 04 %
350	0.000 03	8	0.000 78 %
370	-0.000 02	-5	-0.000 52 %
390	0.000 00	0	0.000 00 %
410	0.000 01	3	0.000 26 %
430	0.000 01	3	0.000 26 %
450	0.000 40	104	0.010 39 %
470	0.000 12	31	0.003 12 %
500	0.000 60	156	0.015 59 %
550*	1.343 94	34.916 %	34.916 05 %

* When heated to 550 °C, the salt decomposed to RbCl. The loss in weight was 34.916%. The stoichimetric difference between $RbClO_4$ and RbCl is 34.608%. The 0.308% difference is likely due mostly to the loss of a small amount of salt when vaporised and recrystallized on the exterior of the crucible.

Table 5 - Weights of empty SiO_2 crucibles for weighing $RbClO_4$

Crucible	Weight (g)	2σ (ppm)
White Translucent 1	20.169 56	164.79
White Translucent 2	20.505 92	43.74
White Translucent 3	19.965 47	57.37
White Translucent 4	19.467 94	34.87
Transparent 1	9.377 22	50.42
Transparent 2	11.658 15	54.69

Table 6 - Isotopic composition and concentration of spikes

Isotopic composition and concentration of spikes

^{84}Sr spike[a]	
$^{84}Sr/^{86}Sr$	1697.8
$^{87}Sr/^{86}Sr$	0.166 38
$^{88}Sr/^{86}Sr$	0.655 35
Corresponding Isotopic Abundances	
^{84}Sr	0.998 92
^{86}Sr	0.000 59 ± 0.000 01
^{87}Sr	0.000 10 ± 0.000 01
^{88}Sr	0.000 39 ± 0.000 01
Concentration	
13.256 ± 0.023 ng Sr/g	

^{84}Sr-^{86}Sr double spike	
$^{84}Sr/^{86}Sr$	0.932 55 ± 0.000 40
$^{87}Sr/^{86}Sr$	0.010 31 ± 0.000 01
$^{88}Sr/^{86}Sr$	0.022 40 ± 0.000 01
Corresponding Isotopic Abundances	
^{84}Sr	0.474 51 ± 0.000 04
^{86}Sr	0.508 83 ± 0.000 04
^{87}Sr	0.005 256 ± 0.000 001
^{88}Sr	0.011 399 ± 0.000 003
Calibrated Concentration	
832.99 ± 0.29 ng Sr/g	
Diluted Working Concentration[b]	
0.187 67 ± 0.000 10 ng Sr/g	
0.197 50 ± 0.000 11 ng Sr/g	

[a] Certificate of Analysis of NBS-988

[b] Additional dilute spike was required and rediluted accounting for two different spike concentrations. Spike weight was tracked which accounts for the slight differences in spike concentration in Table 2c.

Figure 1 - Historical Measurements of λ_{87}

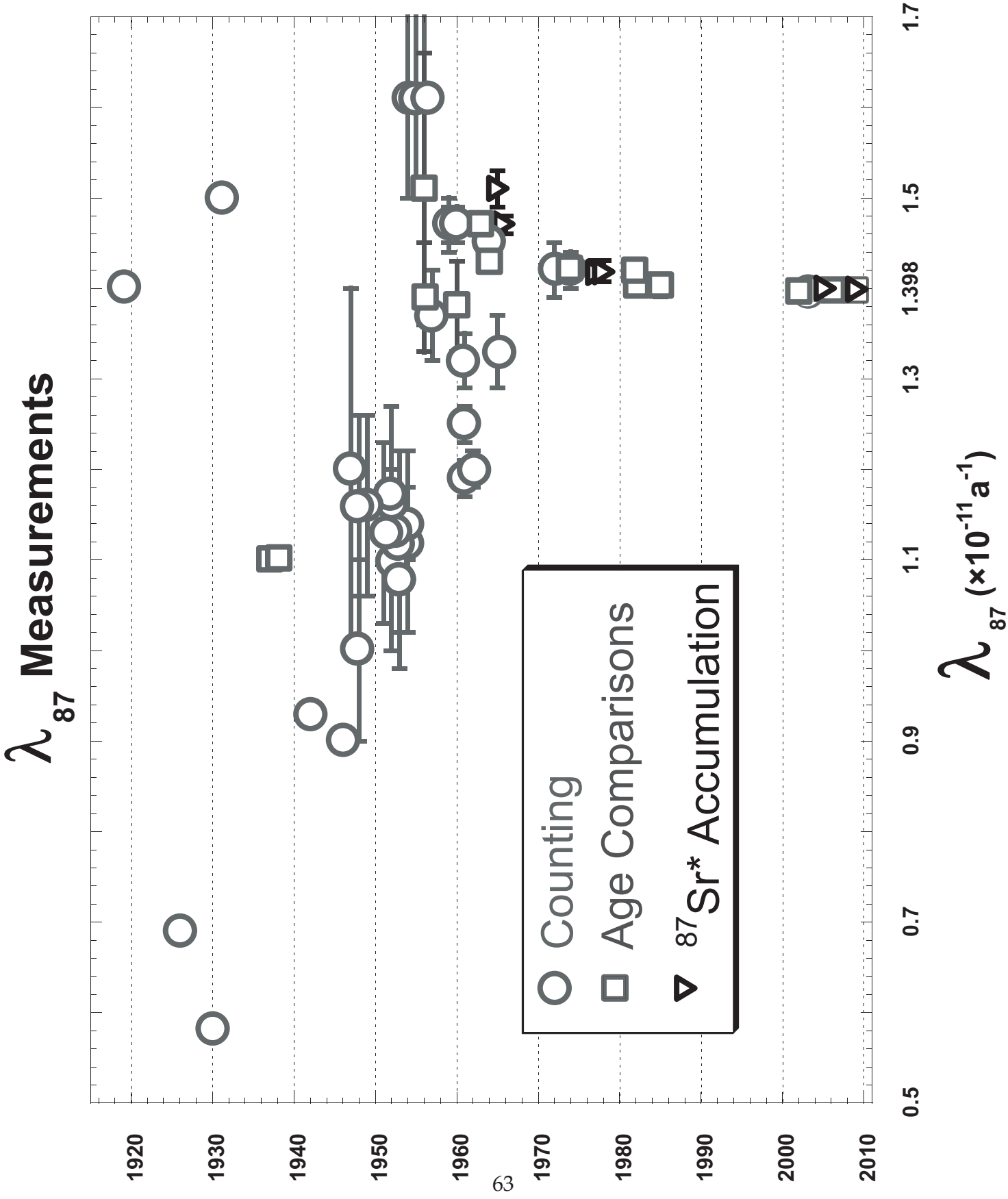

Figure 1 (inset) - Historical Measurements of λ_{87}

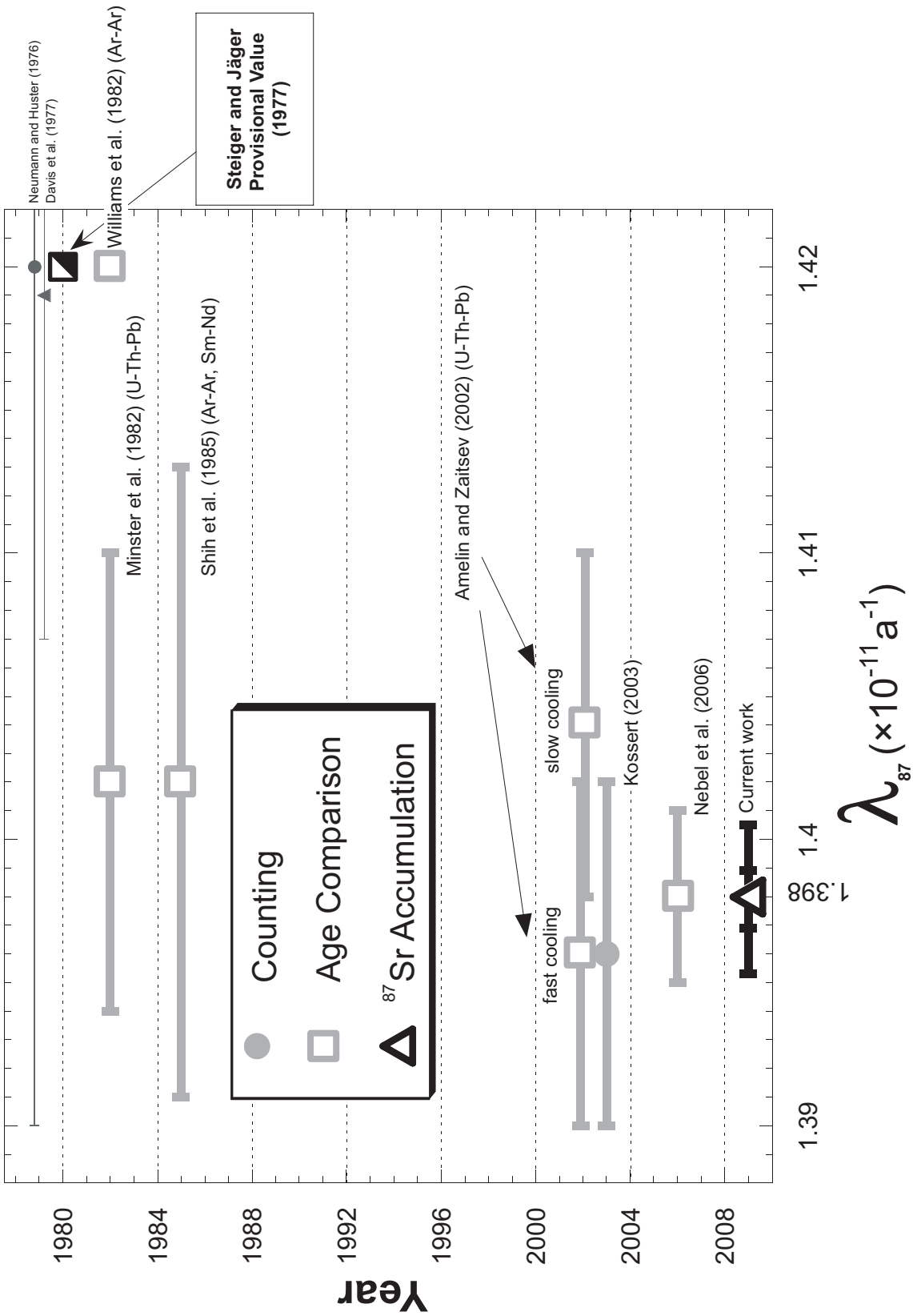

Figure 2 - λ_{87} measurements

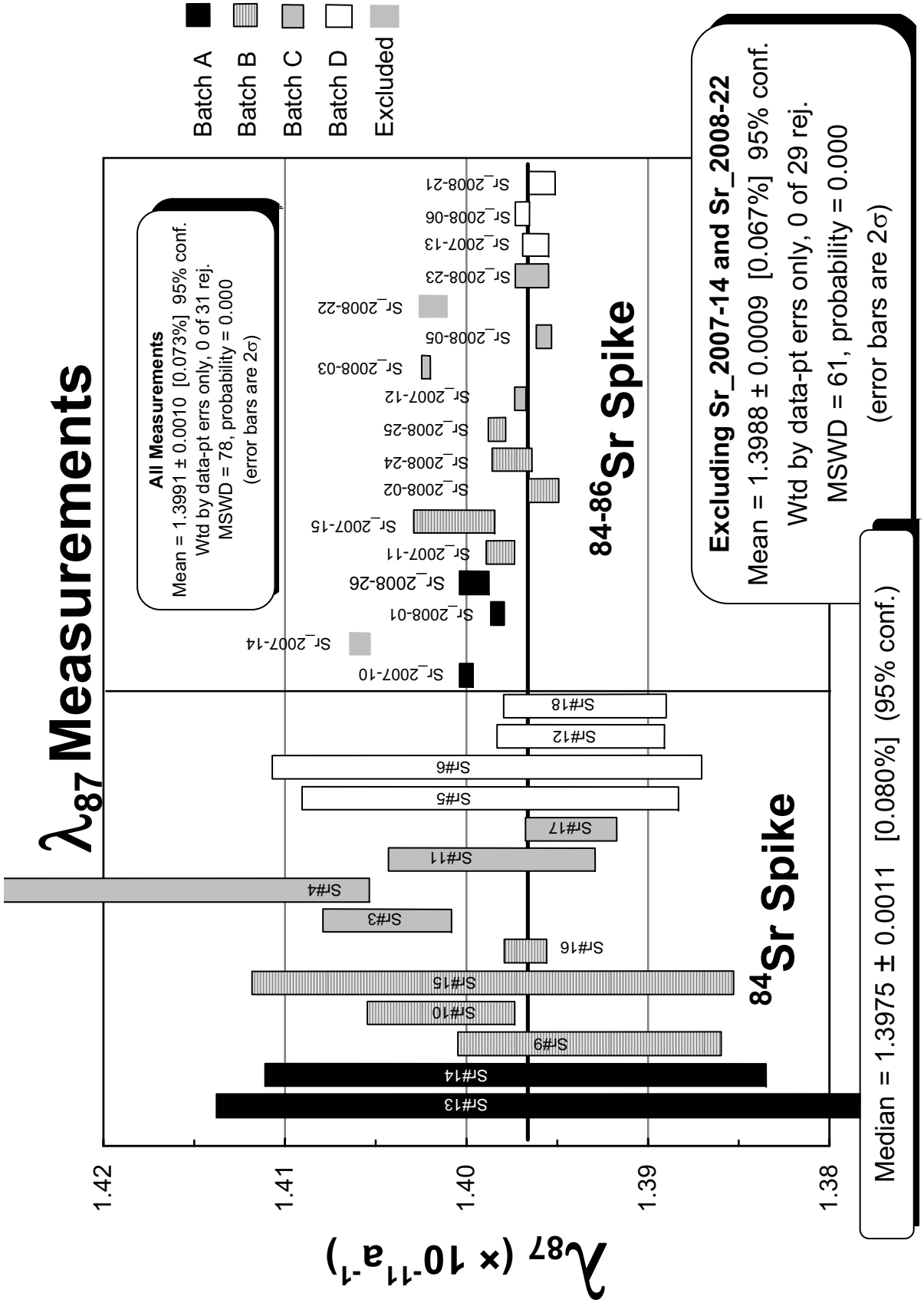

Figure 3 - Low λ_{87} measurements that agree

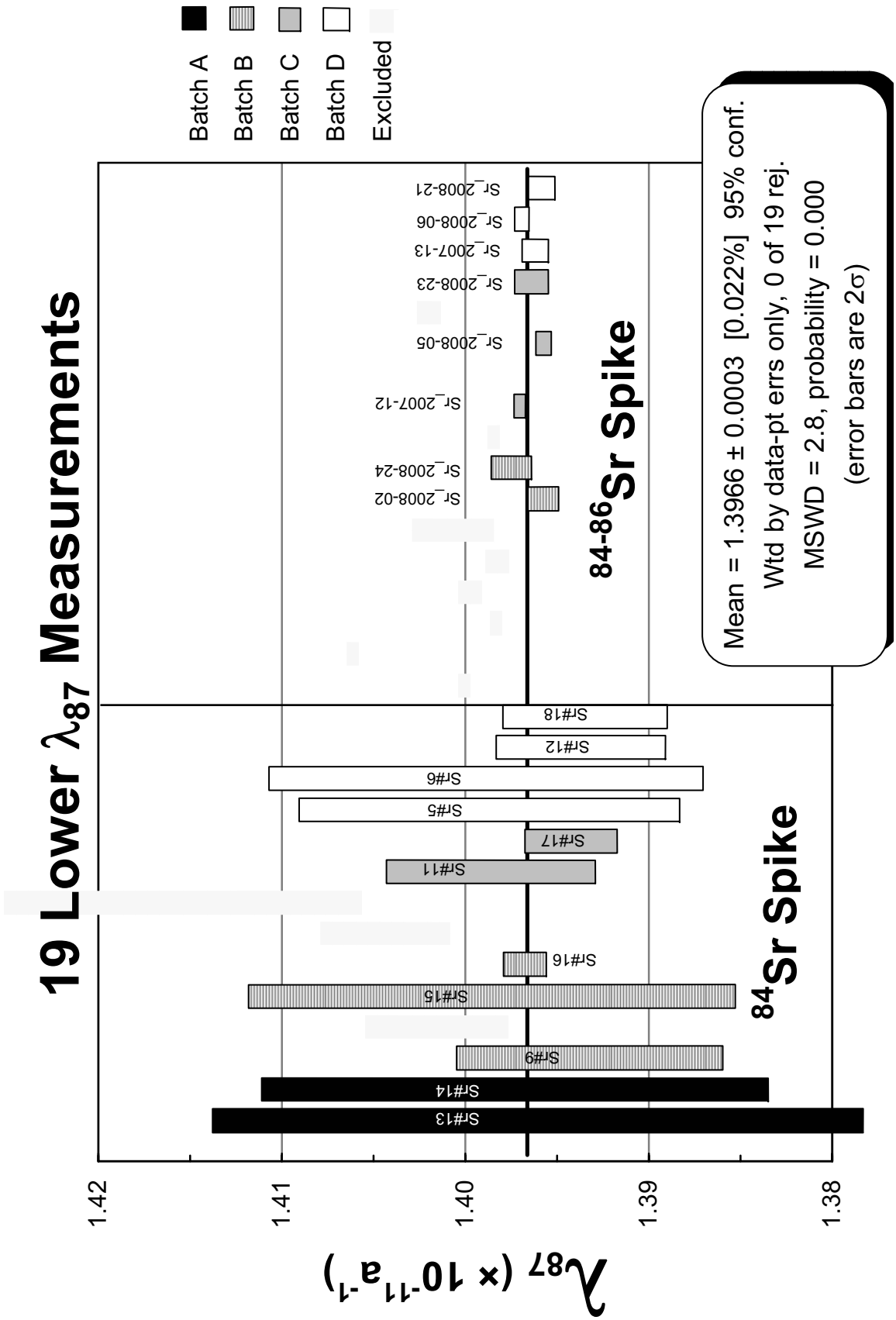

Figure 4 - Reproducibility of weighing quartz crucibles

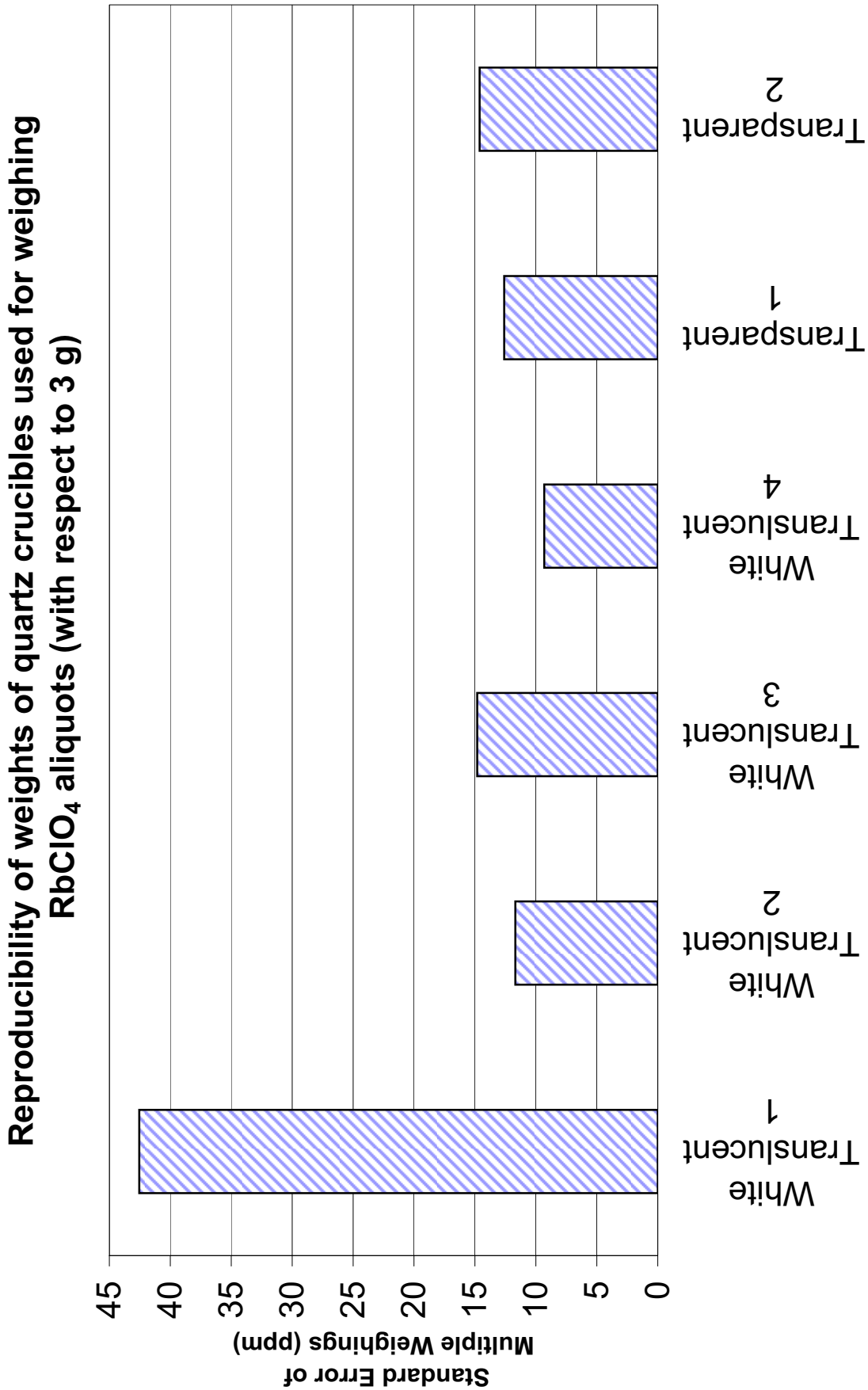

Chapter 3

Preparation and calibration of a strontium double-spike for high precision isotopic composition and concentration measurements

Ethan Rotenberg, Donald W. Davis, and Yuri Amelin

1. Introduction

Measurements of isotopic ratios of strontium in geologic samples are routinely corrected for instrumental mass fractionation by normalizing to natural $^{86}Sr/^{88}Sr$. ^{86}Sr and ^{88}Sr are both stable and non-radiogenic, and therefore their ratios in nature are considered to be invariant (Long, 1966), with $^{86}Sr/^{88}Sr = 0.1194$ (Steiger and Jäger, 1977). For highly radiogenic samples containing little or no non-radiogenic Sr, this normalization procedure is not possible due to weak ^{86}Sr and ^{88}Sr signals which result in imprecise normalized ratios. In these cases, a double-spike is appropriate.

A ^{84}Sr-^{86}Sr double-spike was prepared in conjunction with an experiment to re-determine the decay-constant of ^{87}Rb (λ_{87}). λ_{87} was determined by measuring the amount of radiogenic ^{87}Sr ($^{87}Sr^*$) accumulated in a $RbClO_4$ salt. For the decay-constant measurements, it was not sufficient to determine only isotopic ratios, but also the absolute molar abundance of $^{87}Sr^*$ accumulated due to decay of ^{87}Rb in the salt over the course of the experiment (~32 years). It was therefore necessary to prepare a spike with precisely determined Sr concentration as well as isotopic composition.

The decay-constant measurements were first attempted with a spike enriched only in ^{84}Sr. With low common Sr, and consequently a very weak ^{86}Sr signal (typically < 10^{-13} A), it was not possible to precisely correct for instrumental fractionation by normalizing to the nominal $^{86}Sr/^{88}Sr$ value of 0.1194. To overcome this problem, a double-spike enriched in both ^{84}Sr and ^{86}Sr was prepared. ^{87}Sr is the isotope of interest for the decay-constant measurements, and therefore should not be masked with additional ^{87}Sr in a tracer. ^{88}Sr is the most abundant isotope of natural Sr (82.58 %), and is therefore most useful for

monitoring common Sr in the samples: either initially contained in the salt, or added during processing of the samples, and correcting for ^{87}Sr blank. Thus the other two natural isotopes of Sr, ^{84}Sr and ^{86}Sr, remain available for the tracer. With a double-spike yielding strong signals on these two usually weak peaks, it was possible to correct for instrumental fractionation with far greater precision than in earlier experiments.

The concentrated double-spike was prepared from nearly pure ^{84}Sr, SRM-988, and from somewhat less pure, commercially available ^{86}Sr. The isotopic composition of this spike was determined by thermal ionisation mass spectrometry (TIMS). Calibrating solutions were prepared from $SrCl_2$ and Sr-metal. The spike was mixed with the calibrating solutions in measured quantities, and the isotopic ratios of the mixtures were measured by TIMS. Finally, the concentration of Sr in the double-spike was calculated from the measured isotopic ratios and quantities of each solution in the mixtures.

2. Procedure

2.1 Preparation of the Tracer Solution

The double-spike was prepared by mixing high-purity ^{84}Sr from a sealed ampoule of SRM-988 with somewhat lower purity ^{86}Sr obtained from Cambridge Isotope Laboratories. ^{84}Sr was in a dilute HNO_3 solution , while ^{86}Sr was obtained as a carbonate. The NBS Certificate of Analysis gives the atom fraction of ^{84}Sr as 99.892% (NBS, 1973). The Certificate of Analysis for $^{86}SrCO_3$ gives the isotopic enrichment as 96.89% (CIL, 2006). The two isotopes were mixed to a roughly 1:1 ratio in a dilute HNO_3 solution.

2.2.0 Preparation of the Sr calibrating solutions

For determination of the concentration of the spike, four solutions were prepared from Sr with natural isotopic compositions (IC). The utmost care was

taken to prepare these solutions with precisely known concentration. Two solutions were prepared from Sr-metal, and two were prepared from $SrCl_2$. Both the chloride and the metal were procured from Alfa Aesar® in sealed ampoules under Ar in approximately 5 g quantities. Solutions were prepared from Sr from two different sources, metal and salt, in order to check for lack of stoichiometry in the salt or impurities in either the salt or metal. SRM-987 $SrCO_3$ was not used because of concerns from calibrating an earlier spike (see Appendix A) where the various calibrations using solutions prepared from that salt did not agree.

2.2.1 Sr-metal and $SrCl_2$ weighing procedure

Sr-metal is available either as large chunks (~2 g) or as small distilled dendritic pieces. Although the appearance of the Sr-metal in the sealed ampoule was shiny and metallic, it was clearly discernable that some were dark goldish in color while others were more silvery. It was assumed that the darker color was tarnish. An appreciable quantity of tarnish will increase the weight of the metal and yield an apparent Sr concentration higher than the actual concentration. Consequently, for the first solution we used a single piece of metal because to the degree that there was surface tarnish, the ratio of surface-area to volume would be smaller, and therefore the effect would be less pronounced than with small pieces. In addition, it is easier to ensure quantitative transfer of a single piece of Sr than of many small pieces. The second metal solution was prepared from small pieces.

Because Sr-metal is highly reactive and $SrCl_2$ is hygroscopic, careful handling of materials was required before and during weighing and dissolution, as exposure to air or atmospheric moisture rapidly increases the weight. Sr-metal (solutions JSGL 3.0 and JSGL 5.0) and the $SrCl_2$ for one solution (JSGL 2.0) were weighed inside a glove-bag filled with dry N_2. $SrCl_2$ for the fourth

solution (JSGL 6.0) was weighed inside the sealed glass ampoule – under Ar – in which it was received from Alfa Aesar®. The entire contents were transferred into the dissolution bottle, and the empty ampoule (with any $SrCl_2$ residue) was weighed. The empty ampoule weight was subtracted from the weight of the full ampoule to determine the net weight of $SrCl_2$.

Owing to the N_2 atmosphere in the glove-bag, it might be considered that strontium-nitride might form. This is unlikely, however, since Sr_3N_2 does not form below 380 °C (Lide, 2008).

2.2.2 Assessment of the rate of reactivity of Sr-metal and $SrCl_2$

Because we were unable to completely eliminate air from the nitrogen filled plastic bag, it was necessary to assess the rate of reactivity of the Sr-metal and $SrCl_2$. Formation of SrO or $Sr(OH)_2$ will increase the weight of the metal, leading to an erroneously high concentration of Sr in the solutions, unless this reaction is taken into account. $SrCl_2$ also increases in weight, presumably by hydration from residual water-vapor inside the glove-bag. In order to assess the reactivity of Sr-metal in the primarily N_2 atmosphere, test samples of Sr-metal were weighed in 7 mL Savillex® vials with the cover tightly closed. The vial was then opened in the N_2 atmosphere and placed on the balance, leaving the door to the weighing chamber open, and noting the increase in weight at one minute intervals. This was repeated for several minutes in order to satisfactorily determine the rate of reaction of Sr with the residual O_2 in the glove bag.

The same procedure was followed for the Sr samples actually used to prepare the solutions. The glass ampoule was opened, and the Sr or $SrCl_2$ was transferred to the Savillex® weighing vial. The time between the breaking of the seal of the ampoule and the closing of the vial was noted. Then the vial was weighed. To assess the increase in weight in the time between the breaking of

the sealed ampoule and the time that the cover of the vial was tightly closed, the vial was re-opened, and the rate of reaction (weight gain) was measured. This reaction rate was then used to correct for the brief time that the Sr-metal or $SrCl_2$ had been exposed to the atmosphere.

2.2.3 Sr-metal/$SrCl_2$ Dissolution

Dissolution of $SrCl_2$ is easily accomplished. The compound is highly soluble and not particularly reactive. $SrCl_2$ was decanted from the Savillex® vial in which it was weighed into a weighed 125 mL Nalgene FEP Teflon® bottle. Ultrapure Milli-Q® water (hereafter MQ, water, or H_2O) and about 20 mL of 7N HNO_3 were added to the first solution, JSGL 2.0; water and about 10 mL of 6N HCl were added to the second solution, JSGL 6.0.

Dissolution of Sr-metal, on the other hand, is not straightforward. Sr-metal readily reacts with water to form soluble $Sr(OH)_2$. This reaction was desirable, but the rate of reaction had to be controlled in order to ensure that no Sr escaped the bottle as a result of vigorous reaction. In an initial experiment, drops of water were added very slowly to the Sr-metal. However, the reaction was sufficiently violent that Sr likely escaped from the bottle with bursts of evolved H_2 and steam. For the first Sr-metal solution, JSGL 3.0, an Al-foil collar was placed around and above the neck of the bottle. The smallest possible drops of H_2O were added slowly to the bottle and reacted with the Sr. The Al-foil collar was designed catch and display any deposition of material escaping the bottle. The foil collar was weighed before and after the reaction and found to be about 180 μg heavier after the reaction, with no visible residue on the foil.

For the second Sr-metal solution, JSGL 5.0, a more sophisticated approach was taken. Two small weighed polystyrene vials, filled with a few mL of H_2O, were carefully lowered into the dissolution bottles beside the Sr metal. The

bottles were loosely covered – to prevent the build-up of evolved H_2 gas – and Sr-metal was allowed to react for approximately one week with the water-vapor in the bottle. The Sr-metal slowly reacted into a flocculent white substance – $Sr(OH)_2$. Despite the precautions taken, when water was ultimately slowly added to what was presumed to be completely reacted $Sr(OH)_2$, additional gases were evolved, and there was some fizzing. However, judging from the tiny size of the droplets on the sides of the bottle, and the fact that these droplets were observed only in the lower portion of the bottle, it is unlikely that a significant quantity of Sr escaped the bottle.

In order to ensure complete transfer of both the metal and the chloride from the Savillex® vials in which they were weighed, following the transfer the vial was rinsed five times with H_2O, and each rinse was decanted into the dissolution bottle. In the case of the metal, obviously this could not be done until the metal in both the bottle and the vial had completely reacted.

2.2.4 Dilution

The master solutions were highly concentrated owing to practical requirements: sufficient metal or salt had to be used to weigh precisely, and the capacity of the analytical balance of 210 g limited the quantity of any single solution. Working concentrations for the spike calibration experiment were approximately 500 ng/g, requiring dilution of five orders of magnitude. Dilutions were performed in four steps. About 5 mL of solution were poured from the 125 mL bottle into a 7 mL vial for weighing. After weighing, the solution was poured into another 125 mL bottle. To ensure complete transfer, the vial was rinsed five times with water, and these rinses were poured into the new bottle. The solution was then diluted with approximately 100 mL of water and a few mL of acid. The new solution was weighed, and the procedure was

repeated four times. All dilutions and concentrations were measured by weight, not by volume.

It was noted that for small quantities of solution, the evaporation from the open vial during the dilution procedure might be sufficient to significantly affect the concentration of the solution. To account for this, the weighing procedure prescribed that the vial be left open for 2 minutes (in earlier experiments for just one minute) immediately after the concentrated solution was poured from a bottle to a vial. The vial was then capped and weighed. After weighing, the vial was opened again for two minutes, capped, and re-weighed. This was repeated two more times to determine the average evaporation over two minutes. This measured average weight loss was added to the original measured weight of the vial to account for the evaporation during the first two minutes that it was left open.

2.3 Mixing procedure Spike and Standard

For measuring the concentration of the spike, spike and calibrating solutions were mixed together to create mixtures with ^{84}Sr:^{86}Sr:^{88}Sr roughly 1:1:1. The weighing and mixing procedure followed the same protocol as the weighing and dilution of Sr solutions. To ensure homogeneity, bottles of spike and calibrating solution were swirled for one minute prior to decanting into Savillex® vials for weighing. Several grams of calibrating solution were weighed in a clean, empty, 7 mL Savillex® vial. Since the spike for all mixtures was the same, all spike aliquots were weighed in the same 7 mL Savillex® vial, H5, and transferred to the vial containing Sr calibrating solution.

Because the solutions were mixed in a 7 mL vial, it was not possible to rinse the spike vial several times in order to ensure complete transfer of spike, as this would have overflowed the vial. Instead, the spike vial was inspected

visually to ensure that no drops of spike remained – especially on the lip of the vial where there was a noted tendency for a tiny drop to adhere after decanting. The vial was then rinsed with a small quantity of water, which was decanted into the vial containing the calibrating solution. Three mixtures were prepared from each calibrating solution, except JSGL 6.4 ($SrCl_2$) from which only two mixtures were prepared, resulting in eleven measurements of the concentration of the spike. Spike and calibrating solutions were equilibrated by heating on a hot-plate prior to evaporation of samples with H_3PO_4 in preparation for loading on filaments.

2.4 Gravimetry

All weighing of Sr, $SrCl_2$, bottles, vials, and solutions was performed on an OHAUS Analytical *Plus*® (AP250D-O) analytical balance with a capacity of 210 g. The resolution on this balance is 10 μg up to 52 g, and 100 μg above 52 g. Reproducibility was checked regularly with standard masses and periodically against NBS Class "S" Calibration weights. A Mettler-Toledo U-Ionizer was placed just outside the weighing chamber to discharge static buildup on vials, bottles, and samples.

2.5 Mass Spectrometry

The isotopic compositions (IC) of the spike and the calibrating solutions were measured by TIMS, as were the isotopic ratios in the mixtures of spike and calibrating solution used to determine the concentration of the spike. Most of the mass spectrometry was carried out at the Jack Satterly Geochronology Laboratory (JSGL) at the University of Toronto, equipped with a VG 354. Some replicate mass spectrometer measurements were performed on the Triton at the Geological Survey of Canada Geochronology Laboratory in Ottawa. Mass

spectrometry procedures were the same as for λ_{87} measurements (Chapter 2, section 3.5)

3. Results and discussion

3.1.0 Determining the Isotopic Composition (IC) of the Tracer Solution

For mass spectrometric measurements of natural Sr, $^{86}Sr/^{88}Sr$ (=0.1194) is typically used as a normalizing ratio to correct for instrumental fractionation. However, this is not possible for analyses of isotopically enriched Sr that does not have natural abundances of the non-radiogenic isotopes. There are a number of approaches to correcting for fractionation in the absence of stable, non-radiogenic isotope pairs: a) total sample evaporation, b) gravimetric determination, c) external correction, and d) vector analytical calculation from analyses of spike, standard, and mixtures of the two (Galer, 1999). Gravimetric determination requires weighable quantities of enriched Sr with known IC, which were not available, and therefore this method was not considered.

3.1.1 Total Sample Evaporation

For the total sample evaporation (TSE) method, the sample is heated and measurement of ratios begins as soon as a signal is acquired. Signals are measured continuously until the sample is exhausted. Light isotopes are enriched due to preferential evaporation at the beginning of the run and become depleted by the end of the run. Integrating over the course of the entire run counts the signals from the entire sample, and therefore is insensitive to the particular fractionation at any given time during the run. However, in order for this method to be accurate, the entire sample must be counted, and the ionization efficiency must remain constant throughout the run (Richter and Goldberg, 2003).

Several attempts were made to measure Sr standards (SRM-987) under total sample evaporation conditions, but these measurements yielded isotopic ratios of approximately $^{84}Sr/^{86}Sr = 0.05634$, $^{87}Sr/^{86}Sr = 0.71116$, and $^{86}Sr/^{88}Sr = 0.11909$. These ratios are all fractionated from the certified values by about 0.1%/amu. This may have been due to the loading method or program used for the mass spectrometric measurements. It may also have been due to variable ionization efficiency during the run. The temperature of the filament increases throughout the run, which will affect ionization efficiency. Had a double filament arrangement been used, it is possible that the results would have been more accurate. Because this method was only attempted as a test after obtaining good results with the other methods, no further TSE experiments were attempted.

3.1.2 External Correction/Normalization

Another approach to fractionation correction in the absence of a normalizing ratio is to assume that the fractionation (on a given machine, with a given loading method, and a given sample size) will be the same for the unknown sample as it is for a standard. Samples and standards for this experiment were run on single Re filaments with a Ta_2O_5 slurry. This unusual loading method was used because it is was determined to be the best method for running sub-nanogram loads of Sr for the λ_{87} experiment, and consequently the same method was used for all measurements pertaining to that experiment (Chapter 1, 3.5). Thirteen Sr standards (SRM-987) run on the Jack Satterly Geochronology Laboratory VG 354 have $^{86}Sr/^{88}Sr$ for the first block equal to 0.120 60 ± 0.000 12 (2σ standard deviation), or a fractionation factor (α) of 0.005 ± 0.0005/amu (one-half of one-percent fractionation per amu). Four measurements of the IC of the spike were made by this method (Table 1-2).

These measurements yields average ratios in the spike of:

$^{88}Sr/^{86}Sr$ 0.022 40 ± 0.000 03

$^{87}Sr/^{86}Sr$ 0.010 32 ± 0.000 01

$^{84}Sr/^{86}Sr$ 0.933 45 ± 0.000 99

which correspond to isotopic abundances:

^{84}Sr: 0.474 76 ± 0.000 27

^{86}Sr: 0.508 60 ± 0.000 25

^{87}Sr: 0.005 25 ± 0.000 01

^{88}Sr: 0.011 39 ± 0.000 02

This method relies on the assumption that the spike fractionates in the same manner that the standards do, and this is a reasonable assumption, especially given enough standard runs, and similar sample sizes and loading methods. However, it ultimately relies on an assumption that cannot be tested.

3.1.3 Mixing aliquots of known and unknown isotopic composition

Finally, the unknown IC of a sample (i.e. our spike) can be calculated free of fractionation effects by vector analysis of uncorrected mass spectrometer measurements of the unknown, a mixture of the unknown with a standard of known – and different –composition, and the known IC of that standard (Russell, 1971). As explained by Galer (1999), when the measured ratios are plotted in a vectorial 3-space where the axes are the three independent ratios of Sr (e.g. $^{84,87,88}Sr/^{86}Sr$), two intersecting planes can be constructed, one containing the three points: 1) true standard composition, 2) measured spike composition, and 3) true spike composition, the other containing the points: 1) true standard composition, 2) measured mixture composition, and 3) true mixture composition. The measured ratios will be biased by fractionation, but the directions of the fractionation vectors are determined from the positions of the points and the

respective isotope fractionation vectors are constrained to lie on the same planes for the unknown and mixture. The intersection of the two planes defines the mixing line between unknown, mixture, and standard. The true standard composition, and the measured ratios of the pure spike and mixtures are known, the true mixture and spike compositions, are unknown. The problem can be readily solved using matrix functions in Microsoft Excel® following the method of Galer (1999).

Two different mixtures of double-spike and SRM-987 were prepared. Replicate measurements were carried out on the same sets of solutions on the VG 354® at JSGL and on the Triton® at the Geological Survey of Canada. Calculations are made from combinations of measured ratios from the spike and mixture analyses, along with the true, known ratios in the standard. Because measured ratios are used, the ratios can be chosen from anywhere within the run. The IC of the spike was calculated from eleven such combinations of measured ratios. Block ratios (Table 3) were used rather than single cycle ratios and yield average values of:

$^{88}Sr/^{86}Sr$ 0.022 40 ± 0.000 01

$^{87}Sr/^{86}Sr$ 0.010 33 ± 0.000 01

$^{84}Sr/^{86}Sr$ 0.932 55 ± 0.000 40

which correspond to isotopic abundances:

^{84}Sr 0.474 51 ± 0.000 04

^{86}Sr 0.508 83 ± 0.000 04

^{87}Sr 0.005 26 ± 0.000 01

^{88}Sr 0.011 40 ± 0.000 01

3.2.0 Tracer Concentration Calibration

The tracer concentration was calibrated against four Sr solutions, two prepared from Sr-metal, and two from $SrCl_2$. Sr-metal and $SrCl_2$ were obtained from Alfa Aesar® in sealed ampoules under Ar. The metal is certified 99.95% pure, and the "ultra dry" chloride 99.995% pure. No independent attempt was made to verify the purity of the Sr. The advantage of the metal is that there is no danger of non-stoichiometry; the drawback is the highly reactive nature of Sr which makes it difficult to work with. Two different sources of Sr – metal and $SrCl_2$ – were used so that the two could act as checks on one another to test if either was impure or non-stoichiometric.

3.2.1 Reactivity of Sr-metal and $SrCl_2$

Sr-metal is highly reactive, and $SrCl_2$ is hygroscopic. Although we weighed them in a glove-bag filled with dry N_2, we weren't able to eliminate all air from the bag. We therefore measured the rate of reaction (rate of weight gain) of both the metal and the chloride in order correct for the weight increase due to reaction with air. Results are shown in Table 4.

For most tests and samples, the sample weight was found to increase due to reaction at a rate of less than 30 μg/min. Depending on the sample weight, this corresponds to between 3.5 to 8.5 ppm per minute. For two test samples that were much smaller than the actual quantities used to prepare Sr solutions (1 g and 0.2 g), the relative increase was greater – 23 and 97 ppm respectively – though the absolute rate of increase in weight of samples was average. Two of the largest samples, each nearly 5 g, increased in relative weight by about 7 ppm, within the normal range.

Although it was expected that a single piece of Sr-metal would react more slowly than the small pieces, the large single piece actually reacted more quickly

than any other sample. It gained 118 μg/min, corresponding to 61 ppm per minute. The faster reaction rate may have been the result of more O_2 in the glove-bag, which was difficult to control reliably.

$SrCl_2$ also gained weight – presumably through hydration – but more slowly than Sr-metal, gaining only 9 μg/min, corresponding to just 1.7 ppm per minute. Only one test was conducted with $SrCl_2$ and that sample was larger than any Sr-metal sample. $SrCl_2$, was in the form of small spheres, and likely had a much larger surface area than any of the Sr-metal samples.

For the weighing of the single piece of Sr metal for JSGL 3.0, the time between opening the sealed ampoule and closing the Savillex® vial with Sr was between 60-90 s. The small pieces used for JSGL 5.0 increased in weight at a rate of only 30 μg/min, and the sample was exposed to the glove-bag atmosphere for 55 s. Because the time of exposure was noted, the uncertainty in weight due to reaction is small, and can be reasonably estimated to within 60 μg (30 ppm) for the single metal chunk, and only 10 ppm for the small pieces.

Vial OS4 with $SrCl_2$ (for JSGL 2.0) was weighed twice with the cover on, the first time weighing in at 21.480 90 g, and the second time 21.480 95 g. The cover was then removed in order to test the rate of reaction upon exposure to the N_2 atmosphere. With the cover off, the vial initially weighed only 21.480 69 g. The average empty weight of vial OS4 is 16.411 99 ± 0.000 08 g (2σ = 0.000 24), so the 260 μg discrepancy between one weighing and another is within the normal range for this vial. $SrCl_2$ gained weight at a rate of only 10 μg/min, and the sample was exposed to atmosphere for just 25 s. The second $SrCl_2$ sample, JSGL 6.0, was weighed in the sealed ampoule under Ar, and therefore did not require measurement of the rate of reaction.

3.2.2 Diffusive loss: Teflon® is permeable

Teflon® vials (PFA) and bottles (FEP) were used because they can be tightly sealed and are non-wetting, so it is relatively easy to transfer liquids quantitatively. For dilution and aliquoting, attempts were made to transfer using polyethylene pipettes instead of pouring, but it was found that small droplets remain in the pipette tip, or adhere to the outside of the pipette. To ensure that the entire quantity of liquid was transferred at every step – and only that quantity – pouring was a preferable method of transfer. This precluded the possibility of storing solutions in glass volumetric flasks from which liquid can be removed only by pipette. However, storage in Teflon® bottles introduced a new problem: the permeability of Teflon®. It was pointed out nearly 50 years ago (Hamilton, 1962; Keith, 1962; and Harley et al., 1963) that polythene (polyethylene) bottles are permeable, to the extent of approximately 2% loss of solution per year. Similarly, Moore et al. (1982) were careful to withdraw all aliquots of solutions for their SRM-987 calibrating experiment over a short period of time to ensure that there would be little change in concentration between aliquots.

It was found that solutions stored in Teflon® bottles lose weight over time (Table 5) – often measurable over an interval of just several days – though at a much slower rate than polyethylene. Furthermore, one bottle stored in a humid atmosphere actually gained weight. This was noted by Hamilton (1962) as well.

Most bottles lost weight at a rate of between 200-500 μg/day, which amounts to about 0.08-0.18% per year (calculated on the basis of the net solution in each bottle). There was a wide variation in weight loss between bottles. One bottle lost weight at the very low rate of only 11 μg per day, while another lost weight much faster than the others, 786 μg/day – 0.3% per year. The bottles are all essentially identical, contain roughly the same quantity of solution, and were

stored under the same conditions, so it is not clear why there should be such a large range of permeability. In order to take the permeability of the bottles into account, the bottles were weighed periodically to monitor weight loss (or gain), and always weighed both immediately before and immediately after each time solution was removed from a bottle. The concentration of each solution was then adjusted accordingly.

Evaporation was also considered when solutions were removed from their storage bottles for weighing. The procedure used for a) diluting the standard and spike solutions, b) weighing out the solutions for mixing spike and standard, and c) weighing out spike used for the ^{87}Rb decay-constant experiment (Chapter 2: 3.3 and 5.3), all involved uncapping the spike or standard bottle, pouring several mL into a 7 mL Savillex® vial, then capping the vial and the bottle, and weighing the vial. However, this required the vial (and the bottle) to be opened for at least several seconds during which solution evaporates. Since the calibration of the spike depends upon the precise weight of standard and spike mixed together, it is crucial to consider the extent of this evaporation.

To determine the rate at which solution evaporates from an open Savillex® vial, vials with water were weighed, closed, then opened for one or two minutes, closed again, and reweighed. It was observed that for approximately 2 mL in a 7 mL Savillex® vial, evaporation proceeds at approximately 1.3 mg/min.

The weighing procedure was adjusted to take this evaporation into account. After spike or standard was poured into a vial for weighing, the vial was left open for exactly two minutes. It was then capped and weighed. The vial was again opened for two minutes, closed, and reweighed. This was repeated three times to assess the reproducibility of the rate of evaporation. The measured rate of evaporation was used to correct for the first two minutes that the vial was left open. Table 6 presents the measurements of evaporation from

open 7 mL vials. There appears to be slightly faster evaporation when the vials contain more liquid. Vials containing less than 3 mL of solution experienced average evaporation at a rate of 1.42 mg/min compared with 1.74 mg/min for those with more than 3 mL. This is likely due to the surface of the liquid being closer to the lip, and therefore faster removal of water vapor over the walls of the vial.

A final factor related to evaporation that can affect the weight of the solution stored in 125 mL bottles is the water vapor above the solution, at least some which is likely to escape when the bottle is opened. However, this is a very small effect. The vapor pressure of water at room temperature (20 °C) is 17.5 mm Hg, corresponding to a saturated vapor density of 17.3 g/m^3 (Dean, 1999). For the space above the solution in and a 125 mL bottle containing ~70 mL (0.00007 m^3), this amount to just 1.21 mg. Because this is a very small amount (for a bottle with 70 mL, it is < 20 ppm), this contribution was ignored.

Evaporation from open bottles was also measured, and found to be approximately 30 μg/min. These bottles are typically open for much less than a minute and for a bottle containing as little as 25 g of solution, this amounts to only 0.001%, and was therefore regarded as negligible as well.

3.2.4 Spike and calibration solutions should be sufficiently concentrated so that blank is negligible

The spike is calibrated at a concentration of about 500 ng total Sr/g solution. Although the working concentration of the spike for the ^{87}Rb decay-constant experiment is just ~0.19 ng/g, it must be calibrated at a higher concentration. Earlier attempts at calibrating the spike were performed with the spike at working concentration, but the reproducibility was poor. Because the spike and calibrating solutions were so dilute, small amounts of Sr blank added to the mixtures during handling were sufficient to severely disturb the ratio of

spike to standard. If there are only 300-400 pg of Sr in the standard solution to begin with, then just a few pg of added Sr blank can upset the calibration by one percent or more. When working with 1 μg of Sr, the addition of even 100 pg represents only 0.01%.

The danger of calibrating a more concentrated spike and then diluting it is that the accuracy of measurements made using that spike depend on the accuracy of the final spike dilution. The only way to cross-check at this stage would be by running large aliquots of the diluted spike, but this is impractical, and would require using a large quantity of the dilute spike. Many dilutions were performed on the concentrated standards prior to calibration using the same procedure, and the results agree very well. We therefore have high confidence in the dilution procedure.

3.2.5 Reproducibility of weights of vials and bottles

All weighing was performed on an OHAUS Analytical *Plus*® (AP250D-O) analytical balance. Reproducibility from 2006 through 2008 was ± 10 μg for a 1 g mass (± 10 ppm) and ± 200 μg for a mass of 100.000 8 g (± 2 ppm). Accuracy was assessed by periodic weighing of NBS "S" Class calibration weights, and the balance is within the tolerance for these standards.

All Sr-metal, $SrCl_2$, and solutions are weighed in Teflon® containers – 7 mL Savillex® PFA vials or Nalgene® 125 mL FEP Teflon® bottles. Weights of plastic vessels are not as reproducible as the stainless steel standards, presumably on account of static charge and/or adsorption of water. The vials weigh between 15.9-16.7 g, and have weighing errors ranging from 2.3-7.2 ppm (with one anomalously high error of 15 ppm). Weighing errors are computed from multiple weighings of the empty vials and bottles. Typically, approximately 3 g of solution are weighed in a vial, and it is therefore more

instructive to consider the error relative to the 3 g net solution rather than relative to the larger empty weight of the vial. This results in an increase of the range of errors: 12 to 38 ppm. Weights of vials and errors are presented in Table 7a and Figure 1a. The vial used for weighing out spike aliquots for spike calibrations, H5, gave better than average reproducibility: 18 ppm (calculated relative to 3 g solution). The vials used for dilutions all gave average errors of about 25 ppm relative to 3 g solution.

The weights of 125 mL bottles (Table 7b and Figure 1b) are slightly more reproducible despite the much larger ratio of surface-area to mass, which might have resulted in increased static charge and/or adsorption of water. Empty bottles and vials were stored in a desiccator with silica-gel for the duration of the weighing experiments to limit the influence of fluctuations in humidity on the measured weights. The empty bottle weights range from 39.177 – 43.973 g, and the reproducibility ranges from 1.3 – 26.7 ppm. Unlike the 7 mL vials, the bottles typically contain considerably more than their own weight in solution: consequently the errors relative to 100 g of solution are only 0.5 – 11 ppm.

The same three bottles (JSGL 3.1, JGSL 3.2, and JSGL 3.3) and four vials (I4, G2, I2, and I1) were used for the intermediate stages of dilution of all the standard solutions, keeping concentrations similar for the same containers during different dilutions. Consequently, with only moderate cleaning between different solutions, there was no risk of meaningful contamination. Two of the bottles used for these intermediate stage dilutions of standard solutions are the bottles with the largest errors, 9.9 and 11.4 ppm (with respect to 100 g), JSGL 3.3 and JSGL 3.2 respectively. Only five of the fourteen bottles used over the course of the experiment (one for each of four concentrated solutions; one for each dilute solution; three for dilutions of standard solutions; and three for the

concentrated spike and its dilution) have errors in excess of 10 ppm (in other words, reproducibility is typically better than 1 mg.

3.2.6 Isotopic composition of standard solutions

Three of the four natural isotopes of Sr, ^{84}Sr, ^{84}Sr, and ^{88}Sr, are stable and non-radiogenic; consequently, $^{84}Sr/^{86}Sr$ and $^{88}Sr/^{86}Sr$ are presumed to be invariant in natural Sr (Long, 1966). However, ^{87}Sr is radiogenic, and therefore variable, and must be measured in the calibrating solutions in order to accurately calculate the atomic weight of Sr in each calibrating solution. Results of these measurements are shown in Table 8. (the errors shown are internal errors from a few measurements). These ICs were used when calculating the concentration of the spike from respective mixtures of spike and standard calibrating solutions.

3.2.7 Concentration of Sr-metal/$SrCl_2$ calibrating solutions

The concentrations of the four concentrated solutions as well as the dilute calibrating solutions are shown in Table 9. The concentrations of the dilute solutions are given at the time of dilution.

3.2.8 Mixtures of spike and calibrating solutions and concentration of the spike

The weights of spike and calibrating solutions in each mixture are show in Table 10. Results of the spike calibrations are shown in Table 11 and Figures 2a and 2b. Spike concentration measurements are presented in units of ng Sr/g solution.

Measurements of three mixtures of JSGL 2.4 ($SrCl_2$) and spike yield an average concentration of 832.32 ± 0.12 (MSWD = 0.34). Measurements of three mixtures of JSGL 3.4 (Sr-metal) and spike yield an average concentration of 832.91 ± 0.10 (MSWD = 0.89). Measurements of three mixtures of JSGL 5.4 (Sr-metal) and spike yield an average concentration of 833.99 ± 0.17

(MSWD = 1.2). And measurements of two mixtures of JSGL 6.4 ($SrCl_2$) and spike yield an average concentration of 833.12 ± 0.13 (MSWD = 0.60).

Measurements of the concentration of the spike against the three solutions: JSGL 3.4, 5.4, and 6.4 agree within their errors. JSGL 2.4 yields a spike concentration that is lower by nearly 0.1%. This discrepancy is not due to a single outlying measurement of JSGL 2.4. Rather, as is evident from Figures 3a, all three measurements of JSGL 2.4 are internally consistent, but disagree with the measurements based on the other solutions. This indicates almost certainly that it accurately reflects the actual concentration of JSGL 2.4. If this is the case, and in light of the agreement among the three other solutions, it is most likely that there was a bias in the preparation of JSGL 2.4 whose actual concentration is therefore not quite that which was calculated from weighing and dilution.

4. Discussion

4.1.0 What accounts for the discrepancy between JSGL 2.4 and the other three calibrating solutions?

Because the measurements of JSGL 2.4 are internally consistent, the source of the discrepancy must almost certainly be in the preparation or dilution of the standard solution, and not in the mixing with spike or mass spectrometry. Careful review of all records of the weighing of salt, and all dilutions revealed no transcription or typographical errors. Furthermore, since the concentration of the spike measured against this solution is more dilute than the measurements against the other three solutions, the bias must be one that increases the apparent concentration of JSGL 2.4. This limits the possible sources of error.

1. Weighing error of the original salt?

   The $SrCl_2$ for solution JSGL 2.0 weighed 5.069 04 g (2.801 77 g Sr). A weighing error of approximately 5 mg is required for a 0.1% discrepancy. Weighing is consistently much, much more precise than that. As noted above, there is a discrepancy of about 260 μg between the weight of the vial in which the $SrCl_2$ was weighed with the cover on and the weight of the vial with the cover off. However, this discrepancy is small compared with the 5 mg necessary to produce the 0.1% discrepancy between JSGL 2.4 and the other three solutions. OS4, the vial in which the salt was weighed, fell over on its side, with the cover on, during the weighing procedure. The cap was examined carefully and contained no visible salt. 5 mg of strontium chloride would be easily visible. Furthermore, had salt been *lost* in the cap, it would have made the spike seem *more concentrated* when measured against JSGL 2.4, rather than *more dilute*. Therefore, the source of discrepancy cannot be loss of $SrCl_2$ salt during preparation. It further seems highly unlikely that the weight of $SrCl_2$ was under-estimated by 5 mg. It is therefore unlikely that the discrepancy is a result of the preparation of the master solution, JSGL 2.0, from the salt.

2. Weighing error during dilution?

   All weights for the dilution were double-checked and there are no transcription errors or miscalculations. The good agreement of the other three solutions indicates that the dilution method is reliable, so it is unlikely that the source of the error is in the dilution either.

3. Unaccounted for diffusive loss of JSGL 2.4?

   If one of the JSGL 2.x series of solutions had lost solution by diffusion without being properly monitored, it would make the spike appear to be less

concentrated. Increase in concentration due to diffusive loss from the bottle JSGL 2.0 between 2006-03-03 and dilution on 2007-07-18 amounted to approximately 0.2% – the right order of magnitude. This loss was tracked from the dissolution of the salt through to spike calibration, and accounted for at the time of dilution.

4. Calculation error.

   Concentration and dilution calculations for JSGL 2.x are the same as for the other calibrating solutions.

5. Incorrect $^{87}Sr/^{86}Sr$ for calibrating solution

   A 1% variation in $^{87}Sr/^{86}Sr$ in solution JSGL 2.4 is required to result in a discrepancy of the magnitude observed between JSGL 2.4 and the other solutions. $^{87}Sr/^{86}Sr$ in each calibrating solution was measured, and an error of 1% is unlikely.

6. Mixing of spike and calibrating solution

   The source of the discrepancy is not likely to be the mixing. Because each calibrating solution yields internally consistent results, it is highly unlikely that there was an error affecting the mixing of only one solution, and that the error biased all three measurements in the same direction and by the same amount.

4.1.2 Concentration of the spike:

A number of explanations have been considered to account for the discrepancy between JSGL 2.4 and the other three solutions, but none satisfactorily explain the discrepancy. The discrepancy is < 0.1%. If the JSGL 2.4

measurements are included, the concentration of the spike comes out to 832.82 ± 0.55 (MSWD = 31). The preferred concentration, excluding JSGL 2.0 is 832.99 ± 0.29 (MSWD = 3.6). The error includes weighing and mass spectrometry uncertainties, but does not include the uncertainty in the isotopic composition of the spike. The uncertainty in spike IC increases the total uncertainty by a further 0.08%, yielding a final value of 832.99 ± 0.94 ng Sr/g.

5. Conclusions

There are a number of important considerations when calibrating a spike. What is the spike calibrated against? The calibration is only as good as the materials against which it is calibrated. Is the calibrating material pure and stoichiometric and how can that be tested? Is it possible to analyze the material itself? A spike should be calibrated against more than one compound whenever possible – unless very reliable materials are available. Is the compound reactive or hygroscopic? If so, steps must be taken to ensure that reactions with water or atmosphere that might cause the weight to change are accounted for when weighing the compound. A vigourous reaction might also cause loss of material.

How are solutions stored, both during and after calibration? There is no purpose in carefully calibrating a solution if several weeks after the calibration the concentration will change without being noted. Plastic containers are permeable. Glass volumetric flasks should be less permeable, but they have drawbacks if the solution needs to be diluted or used regularly. Our solution is to weigh bottles before and after use and this works. There are probably other solutions for this issue, but no matter how it is done, the permeability of containers is something that must be considered. Since it is common for solutions to sit around a lab for months, and even years, this becomes an important consideration if precise concentration is required. The weights of

bottles containing solutions used for precise concentration determinations should be tracked.

How are solutions transferred – in preparation, dilution, and use? After all, calibration solutions and spikes typically are prepared in order to be *used*, not simply to be calibrated and then sit on a shelf. This means that solution bottles must be opened, and solution must be removed. The method must ensure 100% transfer, and allow for accounting of remaining material. This makes pipettes a risky business as small droplets can remain either in the pipette, or adhere to the exterior of the pipette.

For Sr, because there are three stable, non-radiogenic isotopes, measuring the IC of the calibrating solutions can be achieved with good precision using natural $^{86}Sr/^{88}Sr$ to correct for mass fractionation. Measuring the IC of the spike required precise measurement of pure spike along with mixtures of standard and spike. This must be done for other elements that do not have invariant isotope pairs (e.g. Pb).

Where gravimetry is concerned: all containers and vessels must be weighed and re-weighed so that a reasonable estimate of the reproducibility is attained. If static charge is an issue, an appropriate neutralizer should be used. In general, it is probably more reliable to weigh spikes and other solutions rather than to rely on volume. Spike calibration must be performed at appropriately high concentrations to prevent blank contamination from influencing the calibration.

We have included many details in the procedural section because preparation of solutions of known concentration is a common procedure in geochemistry and other fields. It is important that different laboratories be aware of how their colleagues prepare calibrating solutions. We also hope that if

other laboratories have better procedures, they will publish them so that they are available to the community.

6. References

CIL (Cambridge Isotope Laboratories, Inc.) (2006) Certificate of Analysis: Strontium-86 Carbonate.

Dean, J.A. (ed.) (1999) *Lange's Handbook of Chemistry*, McGraw-Hill, Inc., New York.

Galer, S.J.G. (1999) Optimal double and triple spiking for high precision lead isotopic measurement. *Chem. Geol.* **157**, 255-274.

Hamilton (1962) Storage of Standard Solutions in Polythene Bottles. *Nature* **193**, 200.

Harley J.H., Hallden N.A., and Fisenne I.M. (1963) Storage of Standardized Radioactive Solutions. *Nature* **197**, 1230.

Keith, R.L.G. (1962) Storage of Standardized Radioactive Solutions. *Nature* **196**, 500.

Lide, David R. ed., (2008) *CRC Handbook of Chemistry and Physics*, *Internet Version 2008*, <http://www.hbcpnetbase.com>, CRC Press, Boca Raton, FL.

Long, L.E. (1966) Isotope dilution analysis of common and radiogenic strontium using ^{84}Sr-enriched spike. *Earth Planet. Sci. Lett.* **1**, 289-292.

Moore, L.J., Murphy, T.J., Barnes, I.L., and Paulsen, P.J. (1982) Absolute Isotopic Abundance Ratios and Atomic Weight of a Reference Sample of Strontium. *J. Res. National Bureau of Standards* **87,** 1-8.

NBS (National Bureau of Standards) (1973) Certificate of Analysis Standard Reference Material 988. Strontium-84 Spike Assay and Isotopic Solution Standard.

Richter, S. and Goldberg, S.A. (2003) Improved techniques for high accuracy isotope ratio measurements of nuclear materials using thermal ionization mass spectrometry. *Int. J. Mass Spectrom.* **229,** 181-197.

Russell, R.D. (1971) The systematics of double spiking. *J. Geophys. Res.* **76,** 4949-4955.

Steiger R.H. and Jäger E. (1977) Subcommission on geochronology: Convention in the use of decay constants in geo- and cosmochemistry. *Earth Planet. Sci. Lett*. **36**, 359-362.

Table 1 - Measured $^{86}Sr/^{88}Sr$ of standards (SRM-987)

Data File	Date	Size (pg)	First Block $^{86}Sr/^{88}Sr$
DY08-1AA.DAT	2006-11-07	1000	0.120 56
DY07-256.DAT	2006-11-17	40000	0.120 58
DY02-252.DAT	2006-11-16	4000	0.120 58
DY05-2BA.DAT	2006-11-27	400	0.120 54
DY08-35B.DAT	2006-12-07	400	0.120 63
DY05-7BA.DAT	2007-02-18	400	0.120 69
DY10-7BD.DAT	2007-02-19	400	0.120 57
DY01-23C.DAT	2007-07-03	400	0.120 58
DY01-A46.DAT	2007-11-12	400	0.120 56
DY09-E62.DAT	2008-01-03	400	0.120 52
DY01-269.DAT	2008-03-05		0.120 71
DY14-7F5.DAT	2008-05-21	80	0.120 67
DY14-7F6.DAT	2008-05-21	80	0.120 64
Average			**0.120 60**
2σ			**0.000 12**
standard error			**0.000 03**
Average fractionation/amu:			**0.504 ± 0.051%**

Table 2 - ^{84}Sr-^{86}Sr double-spike isotopic composition based on external normalization

Data File	Date	Load Size (ng)	First Block Measured Ratios $^{88}Sr/^{86}Sr$	$^{87}Sr/^{86}Sr$	$^{84}Sr/^{86}Sr$	Normalized Ratios (0.005% fractionation/amu) $^{88}Sr/^{86}Sr$	$^{87}Sr/^{86}Sr$	$^{84}Sr/^{86}Sr$	Isotopic Abundances ^{84}Sr	^{86}Sr	^{87}Sr	^{88}Sr
DY09-7BF, 7C0	2007-02-19	3	0.022 18 ± 0.000 02	0.010 28 ± 0.000 01	0.942 78 ± 0.000 03	0.022 40	0.010 33	0.933 44	0.474 75	0.508 60	0.005 25	0.011 39
DY06-2B1	2006-11-26	20	0.022 15 ± 0.000 00	0.010 28 ± 0.000 00	0.943 14 ± 0.000 00	0.022 37	0.010 33	0.933 80	0.474 85	0.508 52	0.005 25	0.011 38
DY16-2A0, 2A1, 2A2	2006-11-23	2	0.022 17 ± 0.000 00	0.010 25 ± 0.000 00	0.942 41 ± 0.000 00	0.022 39	0.010 30	0.933 08	0.474 66	0.508 71	0.005 24	0.011 39
DY02-449	2006-12-26	1	0.022 21 ± 0.000 005	0.010 27 ± 0.000 01	0.942 82 ± 0.000 08	0.022 43	0.010 32	0.933 49	0.474 76	0.508 58	0.005 25	0.011 41
average						**0.022 40**	**0.010 32**	**0.933 45**	**0.474 76**	**0.508 60**	**0.005 25**	**0.011 39**
standard error						0.000 03	0.000 01	0.000 30	0.000 08	0.000 08	0.000 01	0.000 01
Including uncertainty in fractionation/amu of the standard measurements						**0.000 03**	**0.000 01**	**0.000 99**	**0.000 27**	**0.000 25**	**0.000 01**	**0.000 02**

Table 2 - Double-spike isotopic composition based on external normalization

Table 3 - ^{84}Sr-^{86}Sr double-spike isotopic composition from measured ratios of pure spike and spike-standard mixtures

Table 3 - ^{84}Sr-^{86}Sr double-spike isotopic composition calculated from measured ratios of pure spike and spike-standard mixtures

		Measured Ratios												Corrected Spike Ratios		
		Spike				Mixture										
Calculation	Instrument	$^{84}Sr/^{86}Sr$	2σ %	$^{87}Sr/^{86}Sr$	2σ %	$^{88}Sr/^{86}Sr$	2σ %	$^{84}Sr/^{86}Sr$	2σ %	$^{87}Sr/^{86}Sr$	2σ %	$^{88}Sr/^{86}Sr$	2σ %	$^{84}Sr/^{86}Sr$	2σ	$^{87}Sr/^{86}Sr$	2σ	$^{88}Sr/^{86}Sr$	2σ
1	VG-354	0.941 99	0.012	0.010 27	0.155	0.022 17	0.073	0.845 54	0.015	0.083 20	0.017	0.890 03	0.015	0.932 15	± 0.000 25	0.022 41	± 0.000 01	0.010 33	± 0.000 01
2	VG-354	0.941 30	0.012	0.010 28	0.155	0.022 19	0.073	0.845 54	0.015	0.083 20	0.017	0.890 03	0.015	0.932 16	± 0.000 25	0.022 41	± 0.000 01	0.010 33	± 0.000 01
3	VG-354	0.930 73	0.004	0.010 34	0.005	0.022 46	0.005	0.842 42	0.018	0.083 38	0.014	0.893 65	0.019	0.932 16	± 0.000 25	0.022 42	± 0.000 01	0.010 33	± 0.000 00
4	VG-354	0.922 86	0.001	0.010 38	0.001	0.022 64	0.001	0.845 54	0.015	0.083 20	0.017	0.890 03	0.015	0.932 26	± 0.000 23	0.022 41	± 0.000 01	0.010 33	± 0.000 00
5	VG-354	0.922 86	0.001	0.010 38	0.001	0.022 64	0.001	0.647 85	0.148	0.235 16	0.076	2.714 36	0.146	0.932 19	± 0.001 37	0.022 41	± 0.000 03	0.010 33	± 0.000 01
6	VG-354	0.922 86	0.001	0.010 38	0.001	0.022 64	0.001	0.658 22	0.106	0.233 31	0.068	2.672 61	0.129	0.932 64	± 0.001 21	0.022 40	± 0.000 03	0.010 33	± 0.000 01
7	VG-354	0.922 86	0.001	0.010 38	0.001	0.022 64	0.001	0.357 76	0.040	0.469 98	0.023	5.500 52	0.042	0.933 18	± 0.000 28	0.022 39	± 0.000 01	0.010 33	± 0.000 00
8	VG-354	0.922 86	0.001	0.010 38	0.001	0.022 64	0.001	0.359 41	0.039	0.468 90	0.021	5.476 33	0.034	0.933 20	± 0.000 26	0.022 39	± 0.000 01	0.010 33	± 0.000 00
9	Triton	0.942 19	0.006	0.010 27	0.008	0.022 18	0.012	0.360 28	0.008	0.468 22	0.005	5.462 70	0.006	0.932 82	± 0.000 38	0.022 40	± 0.000 20	0.010 32	± 0.000 02
10	Triton	0.942 19	0.006	0.010 27	0.008	0.022 18	0.012	0.659 26	0.020	0.233 04	0.008	2.667 89	0.019	0.932 75	± 0.000 20	0.022 40	± 0.000 00	0.010 32	± 0.000 02
11	Triton	0.935 79	0.007	0.010 31	0.013	0.022 32	0.010	0.655 29	0.034	0.233 73	0.016	2.683 66	0.033	0.932 68	± 0.000 33	0.022 40	± 0.000 03	0.010 32	± 0.000 02
12	Triton	0.931 55	0.008	0.010 33	0.011	0.022 42	0.009	0.643 71	0.052	0.235 79	0.024	2.730 92	0.049	0.932 15	± 0.000 48	0.022 41	± 0.000 03	0.010 33	± 0.000 02
13	Triton	0.939 57	0.011	0.010 29	0.008	0.022 23	0.014	0.354 77	0.013	0.471 78	0.007	5.545 16	0.013	0.932 55	± 0.000 14	0.022 40	± 0.000 02	0.010 32	± 0.000 02
												Weighted Mean		**0.932 55**		**0.022 40**		**0.010 33**	

Table 4 - Rate of weight gain of Sr metal and $SrCl_2$ due to reaction with atmosphere

	mg/min	ppm/min	sample weight
Tests	0.012	3.495	3.576 58
Tests	0.017	4.660	3.576 78
Tests	0.032	6.914	4.700 44
Tests	0.020	5.611	3.564 41
Tests	0.024	96.798	0.247 94
Tests	0.023	23.096	1.010 29
JSGL 1.0 - small pieces	0.036	7.163	4.963 55
JSGL 3.0 - single chunk	0.118	61.479	1.915 75
JSGL 4.0 - small pieces	0.014	3.858	3.628 67
JSGL 4.0 - small pieces	0.019	4.804	3.955 18
JSGL 4.0 - small pieces	0.030	8.535	4.170 64
JSGL 5.0 - small pieces	0.025	8.535	2.928 98
JSGL 2.0 - $SrCl_2$	0.009	1.726	5.068 73

Table 5 - Diffusive loss from 125 mL Savillex® FEP Teflon® Bottles

Bottle	days	Average rate of diffusive loss (µg/day)	percentage per year	empty bottle	gross: bottle + solution	net solution
Old Dilute Spike	134	11	0.005 %	40.745 0	115.844 2	75.099 2
JSGL 2.0	308	373	0.153 %	40.381 6	129.442 3	89.060 7
JSGL 2.4	306	363	0.113 %	41.096 4	158.667 9	117.571 5
JSGL 3.0	464	243	0.077 %	41.671 9	156.838 3	115.166 4
JSGL 3.4	323	381	0.139 %	40.796 6	141.016 3	100.219 7
JSGL 5.0	392	786	0.283 %	40.855 5	142.317 7	101.462 2
JSGL _.16	334	462	0.175 %	40.379 5	136.999 2	96.619 7
JSGL _.14	417	208	0.078 %	40.422 2	137.943 2	97.521 0

Table 6 Evaporation from 7 mL vials

Vial	Experiment	Solution	Time open (min.)	Net Weight of Solution	Rate of evaporation (mg/min)	Rate of evaporation (ppm/min)
H5	Spike calibration	Spike	1	2.035 89	1.057	519.0
H5	Spike calibration	Spike	1	2.282 10	1.172	513.4
H5	Spike calibration	Spike	1	2.101 02	1.200	571.2
H5	Spike calibration	Spike	1	2.772 28	1.318	475.5
H5	Spike calibration	Spike	1	1.923 54	1.237	642.9
H5	Spike calibration	Spike	1	2.124 52	1.272	598.6
H5	Spike calibration	Spike	1	1.892 28	1.408	744.3
H5	Spike calibration	Spike	1	1.955 47	1.567	801.2
H5	Spike calibration	Spike	1	2.663 35	1.475	553.8
H5	Spike calibration	Spike	2	2.338 37	1.618	692.1
H5	Spike calibration	Spike	2	2.606 28	1.857	712.6
G1	Spike calibration	JSGL 2.4	1	2.468 36	1.063	430.8
OS3	Spike calibration	JSGL 2.4	1	1.975 18	1.170	592.3
RE1	Spike calibration	JSGL 2.4	1	2.527 67	1.290	510.4
E6	Spike calibration	JSGL 3.4	1	2.324 62	1.220	524.8
K1	Spike calibration	JSGL 3.4	1	2.757 30	1.290	467.8
PB4	Spike calibration	JSGL 3.4	1	2.767 01	1.210	437.3
K2	Spike calibration	JSGL 5.4	1	2.627 74	1.438	547.4
K5	Spike calibration	JSGL 5.4	1	2.304 90	1.470	637.8
RE4	Spike calibration	JSGL 5.4	1	2.890 84	1.387	479.7
E2	Spike calibration	JSGL 6.4	2	2.388 65	1.797	752.2
E5	Spike calibration	JSGL 6.4	2	2.882 20	1.907	661.5
PB3	Spike calibration	JSGL 6.4	2	2.334 45	1.390	595.4
PB2	λ_{87}	Spike	2	4.594 41	2.097	456.4
PB2	λ_{87}	Spike	2	4.464 74	1.995	446.8
PB2	λ_{87}	Spike	2	5.326 68	2.185	410.2
PB2	λ_{87}	Spike	2	2.314 23	1.682	727.0
PB2	λ_{87}	Spike	2	2.632 19	1.623	616.7
PB2	λ_{87}	Spike	2	2.549 49	1.590	623.7
PB2	λ_{87} - Blank	Spike	2	3.171 46	1.700	536.0
PB2	λ_{87} - Blank	Spike	2	2.525 95	1.673	662.5
PB2	λ_{87}	Spike	2	3.790 74	1.377	363.2
PB2	λ_{87}	Spike	2	2.819 97	1.277	452.7
PB2	λ_{87}	Spike	2	6.493 22	1.817	279.8
PB2	λ_{87}	Spike	2	4.548 41	1.672	367.5
PB2	λ_{87}	Spike	2	3.576 57	1.627	454.8
PB2	λ_{87}	Spike	2	3.833 10	1.575	410.9
PB2	λ_{87} - Blank	Spike	2	3.580 26	1.577	440.4
PB2	λ_{87} - Blank	Spike	2	3.320 11	1.467	442.0
PB2	λ_{87}	Spike	2	2.266 17	1.478	652.3
PB2	λ_{87}	Spike	2	3.599 42	1.645	457.0
PB2	λ_{87}	Spike	2	1.716 96	1.352	787.2
PB2	λ_{87}	Spike	2	2.825 77	1.575	557.4
PB2	λ_{87}	Spike	2	3.262 34	1.690	518.0
PB2	λ_{87}	Spike	2	2.576 70	1.537	596.4
PB2	λ_{87} - Blank	Spike	2	2.935 76	1.223	416.7
PB2	λ_{87} - Blank	Spike	2	3.518 68	1.395	396.5
Average					**1.503**	**543.3**

Evaporation rates are based on three measurements for each vial. This table only presents the evaporation rate. It does not include each individual measurement.

Table 7a - Weights of empty 7 mL Savillex® vials used for weighing weighing spike and standard solutions

Vial	Weight	Std. Error	ppm	n	2σ	Error relative to 3 g (ppm)
OS4	16.411 99	± 0.000 08	4.7	10	0.000 24	25.8
AR3	16.706 02	± 0.000 08	4.7	4	0.000 16	26.0
AR4	16.412 48	± 0.000 04	2.3	9	0.000 11	12.4
E2	16.081 55	± 0.000 07	4.3	15	0.000 27	23.2
E6	16.038 48	± 0.000 08	5.0	12	0.000 28	26.8
G1	16.127 26	± 0.000 11	6.9	12	0.000 38	36.9
H5[(a)]	16.148 29	± 0.000 05	3.4	14	0.000 20	18.1
K1	16.007 77	± 0.000 09	5.4	13	0.000 31	28.6
K2	15.932 80	± 0.000 06	3.9	14	0.000 23	20.8
K5	16.006 13	± 0.000 05	3.3	14	0.000 20	17.7
OS3	16.205 92	± 0.000 06	3.6	10	0.000 19	19.7
PB2[(b)]	16.229 26	± 0.000 24	14.9	19	0.001 05	80.4
PB4	16.430 11	± 0.000 07	4.3	12	0.000 24	23.3
PB6	16.398 35	± 0.000 04	2.5	12	0.000 14	13.9
RE1	16.455 84	± 0.000 06	3.6	12	0.000 20	19.6
RE4	16.375 32	± 0.000 06	3.6	11	0.000 19	19.4
PB3	16.383 45	± 0.000 06	3.5	8	0.000 16	18.9
H6	15.986 14	± 0.000 05	3.3	11	0.000 18	17.7
K4[(c)]	15.956 73	± 0.000 11	7.2	14	0.000 43	38.2
AR5	16.456 46	± 0.000 05	2.8	23	0.000 22	15.2
I4[(d)]	16.164 89	± 0.000 08	4.8	19	0.000 34	25.7
G2[(e)]	16.155 72	± 0.000 09	5.4	14	0.000 33	29.3
I2[(f)]	16.065 09	± 0.000 09	5.7	15	0.000 36	30.7
I1[(g)]	16.127 57	± 0.000 10	6.2	14	0.000 38	33.5
maximum	16.706 02		14.9		0.001 05	80.4
minimum	15.932 80		2.3		0.000 11	12.4
average	16.225 99				0.000 27	25.9

[(a)] Spike aliquots for spike calibration

[(b)] Spike aliquots for λ_{87} measurements

[(c)] Spike aliquots for λ_{87} measurements

[(d)] First dilution vial for Sr calibrating solutions

[(e)] Second dilution vial for Sr calibrating solutions

[(f)] Third dilution vial for Sr calibrating solutions

[(g)] Fourth dilution vial for Sr calibrating solutions

Table 7b - Weights of Empty 125 mL Nalgene® FEP Teflon® bottles

Original Designation	Bottle	Weight	Std. Error	ppm	n	2σ	Error Relative to 100 g (ppm)
JSGL _.1	JSGL 3.1 - First Dilution	41.020 13	± 0.000 46	11.3	22	0.002 17	4.6
JSGL _.2	JSGL 3.2 - Second Dilution	42.624 26	± 0.001 14	26.8	22	0.005 37	11.4
JSGL _.3	JSGL 3.3 - Third Dilution	41.480 17	± 0.000 99	23.8	23	0.004 73	9.9
JSGL _.4	JSGL 3.4	40.796 64	± 0.000 39	9.7	12	0.001 37	3.9
JSGL _.6	JSGL 2.0	40.381 55	± 0.000 13	3.2	11	0.000 43	1.3
JSGL _.7	JSGL 5.0	40.855 47	± 0.000 20	4.9	25	0.000 99	2.0
Test Bottle	JSGL 3.0	41.671 90	± 0.000 84	20.1	21	0.003 84	8.4
JSGL _.9	JSGL 2.4	41.096 39	± 0.000 24	5.8	7	0.000 63	2.4
JSGL _.11	JSGL 5.4	43.973 15	± 0.000 59	13.4	12	0.002 04	5.9
	JSGL 6.4	39.177 48	± 0.000 24	6.1	10	0.000 76	2.4
JSGL _.13	JSGL 6.0	40.417 36	± 0.000 08	1.9	13	0.000 28	0.8
JSGL _.14	Intermediate Double-Spike	40.422 16	± 0.000 06	1.4	16	0.000 23	0.6
JSGL _.15	Dilute Double-Spike	40.744 97	± 0.000 19	4.8	23	0.000 93	1.9
JSGL _.16	Concentrated Double-spike (Calibrated)	40.379 51	± 0.000 19	4.6	4	0.000 37	1.9
	maximum	43.973 15				0.005 37	11.4
	minimum	39.177 48				0.000 23	0.6
	average	41.182 30				0.001 69	

Table 8 - Isotopic composition ($^{87}Sr/^{86}Sr$) of Sr in calibrating solutions

Table 8 - Isotopic composition ($^{87}Sr/^{86}Sr$) of Sr in calibrating solutions

		Stock #	Lot #	$^{87}Sr/^{86}Sr$	
JSGL 2.4	**$SrCl_2$**	35719	A22M25	0.708 09 ± 0.000 01	Two measurements of 5 ng samples
JSGL 3.4	**Sr-metal**	40334	G29M30	0.708 47 ± 0.000 01	One measurement of 100 ng sample
JSGL 5.2	**Sr-metal**	38624	E21P27	0.708 63 ± 0.000 05	Three measurements
JSGL 6.2	**$SrCl_2$**	35719	H17R004	0.708 10 ± 0.000 01	One measurement

Salts and Metals were procured from Alfa Aesar®

Table 9 - Preparation and Dilution of ^{84}Sr-^{86}Sr Double Spike Calibrating Solutions

Master Solution

Solution	Salt/Metal Weight	Sr Weight	Empty Bottle	2σ	Solution	Concentration (ng Sr/g solution)	2σ	Concentration at time of calibration[a]
JSGL 2.0 ($SrCl_2$)	5.068 94	2.801 71	40.381 55	± 0.000 12	119.441 2	23,456,821	± 375	23,495,639
JSGL 3.0 (Metal)	1.914 55	1.914 55	41.671 13	± 0.000 07	124.654 2	15,358,871	± 487	15,382,782
JSGL 5.0 (Metal)	2.926 25	2.926 25	40.855 47	± 0.000 20	104.454 7	28,014,572	± 489	28,041,226
JSGL 6.0 ($SrCl_2$)	5.066 03	2.800 05	40.417 36	± 0.000 08	85.786 0	32,639,889	± 774	

First Dilution

	Solution Diluted	Empty Bottle	2σ	Solution	Concentration (ng Sr/g solution)	2σ
JSGL 2.1	5.614 82	41.020 13	± 0.000 46	84.922 8	1,553,455	± 97.3
JSGL 3.1	5.418 92	41.020 13	± 0.000 46	71.765 6	1,161,533	± 83.4
JSGL 5.1	3.603 54	41.020 13	± 0.000 46	64.546 4	1,565,501	± 153.4
JSGL 6.1	4.918 81	41.020 13	± 0.000 46	73.011 4	2,198,965	± 86.7

Second Dilution

	Solution Diluted	Empty Bottle	2σ	Solution	Concentration (ng Sr/g solution)	2σ
JSGL 2.2	4.798 08	42.624 26	± 0.005 49	69.335 8	107,500	± 15.053 06
JSGL 3.2	5.106 71	42.624 26	± 0.005 49	64.728 3	91,639	± 9.268 58
JSGL 5.2	5.071 47	42.624 26	± 0.005 49	61.598 9	128,888	± 15.684 86
JSGL 6.2	4.699 55	42.624 26	± 0.005 49	68.355 0	151,183	± 10.530 83

Third Dilution

	Solution Diluted	Empty Bottle	2σ	Solution	Concentration (ng Sr/g solution)	2σ
JSGL 2.3	5.247 27	41.480 17	± 0.000 99	65.222 8	8,649	± 1.48
JSGL 3.3	6.291 26	41.480 17	± 0.000 99	80.851 8	7,131	± 0.84
JSGL 5.3	4.479 44	41.480 17	± 0.000 99	65.903 0	8,761	± 1.30
JSGL 6.3	5.727 75	41.480 17	± 0.000 99	86.793 7	9,977	± 0.76

Fourth Dilution

	Solution Diluted	Empty Bottle	2σ	Solution	Concentration (ng Sr/g solution)[a]	2σ	Concentration (nmol Sr/g solution)[a]
JSGL 2.4	5.188 76	41.096 39	± 0.000 24	79.382 5	565.303	± 0.113	6.452
JSGL 3.4	5.102 63	40.796 64	± 0.000 39	71.086 0	511.842	± 0.072	5.842
JSGL 5.4	5.668 20	43.973 15	± 0.000 59	106.138 4	467.848	± 0.071	5.340
JSGL 6.4	5.568 07	39.177 48	± 0.000 24	64.942 6	855.410	± 0.069	9.763

All weights in g, concentrations in ng Sr/g solution.

[a] The concentration of the final dilute solution changes as a result of the permeability of the Teflon® bottles in which they were stored. Bottles were weighed before and after aliquoting, and concentrations are adjusted for the diffusive loss.

Table 10 - Mixtures of ^{84}Sr-^{86}Sr double-spike and calibration solutions for spike calibration

	Standard			Spike	
Mixture	**Vial**	**Solution**	**Quantity (g)**	**Vial**	**Quantity (g)**
1	G1	JSGL 2.4 - $SrCl_2$	2.468 36 ± 0.000 40	H5	2.035 89 ± 0.000 21
2	OS3	JSGL 2.4 - $SrCl_2$	1.975 18 ± 0.000 20	H5	2.282 10 ± 0.000 21
3	RE1	JSGL 2.4 - $SrCl_2$	2.527 67 ± 0.000 21	H5	2.101 02 ± 0.000 21
4	E6	JSGL 3.4 - Sr-metal	2.324 62 ± 0.000 29	H5	2.772 28 ± 0.000 21
5	K1	JSGL 3.4 - Sr-metal	2.757 30 ± 0.000 32	H5	1.923 54 ± 0.000 21
6	PB4	JSGL 3.4 - Sr-metal	2.767 01 ± 0.000 25	H5	2.124 52 ± 0.000 22
7	K2	JSGL 5.4 - Sr-metal	2.627 74 ± 0.000 24	H5	1.892 28 ± 0.000 21
8	K5	JSGL 5.4 - Sr-metal	2.304 90 ± 0.000 21	H5	1.955 47 ± 0.000 21
9	RE4	JSGL 5.4 - Sr-metal	2.890 84 ± 0.000 20	H5	2.663 35 ± 0.000 23
10	E2	JSGL 6.4 - $SrCl_2$	2.388 65 ± 0.000 28	H5	2.338 37 ± 0.000 21
11	E5	JSGL 6.4 - $SrCl_2$	2.882 20 ± 0.000 38	H5	2.606 28 ± 0.000 68

Solution quantities are corrected for evaporation from vials during the mixing procedure

Table 11 - Measurements of concentration of ^{84}Sr-^{86}Sr double-spike

	Calibration Solution	Calibrating solution (g)	2σ	S/B[a]	2σ	Spike (g)	2σ	Concentration of Spike (ng Sr/g)	Calculated Concentration of Spike: Adjusted for permeability (ng Sr/g)[b]	Adjusted for permeability (ng Sr/g)[c]	Adjusted for permeability (ng Sr/g)[d]	2σ
$SrCl_2$	**JSGL 2.4**	2.468 36	± 0.000 40	1.251 08	± 0.000 09	2.035 89	± 0.000 21	831.766	831.930	831.949	**832.376**	**± 0.237**
$SrCl_2$	**JSGL 2.4**	1.975 18	± 0.000 20	1.752 50	± 0.000 14	2.282 10	± 0.000 21	831.755	831.920	831.939	**832.365**	**± 0.212**
$SrCl_2$	**JSGL 2.4**	2.527 67	± 0.000 21	1.260 64	± 0.000 01	2.101 02	± 0.000 21	831.656	831.820	831.839	**832.266**	**± 0.199**
Metal	**JSGL 3.4**	2.324 62	± 0.000 29	1.999 43	± 0.000 13	2.772 28	± 0.000 21	832.381	832.546	832.565	**832.992**	**± 0.177**
Metal	**JSGL 3.4**	2.757 30	± 0.000 32	1.169 36	± 0.000 03	1.923 54	± 0.000 21	832.214	832.378	832.397	**832.824**	**± 0.178**
Metal	**JSGL 3.4**	2.767 01	± 0.000 25	1.287 14	± 0.000 11	2.124 52	± 0.000 22	832.289	832.453	832.472	**832.899**	**± 0.178**
Metal	**JSGL 5.4**	2.627 74	± 0.000 24	1.320 62	± 0.000 56	1.892 28	± 0.000 21	832.268	*832.268*	832.287	**832.714**	**± 0.396**
Metal	**JSGL 5.4**	2.304 90	± 0.000 21	1.556 49	± 0.000 52	1.955 47	± 0.000 21	832.593	*832.593*	832.612	**833.039**	**± 0.326**
Metal	**JSGL 5.4**	2.890 84	± 0.000 20	1.690 27	± 0.000 34	2.663 35	± 0.000 23	832.605	*832.605*	*832.605*	**833.051**	**± 0.227**
$SrCl_2$	**JSGL 6.4**	2.388 65	± 0.000 28	0.982 94	± 0.000 04	2.338 37	± 0.000 21	833.150	*833.150*	*833.150*	**833.150**	**± 0.144**
$SrCl_2$	**JSGL 6.4**	2.882 20	± 0.000 38	0.907 83	± 0.000 04	2.606 28	± 0.000 68	833.036	*833.036*	*833.036*	**833.036**	**± 0.256**

[a] Measured atomic ratio of spike Sr (S) to calibrating solution Sr (B)

[b] Adjusted by 197 ppm for permeability of spike between JSGL 2.4-3.4 mixing and JSGL 5.4

[c] Adjusted by 23 ppm for permeability of spike between JSGL 5.4 mixings

[d] Adjusted by 536 ppm for permeability of spike between JSGL 5.4 mixings and JSGL 6.4 mixings

Values that are not adjusted at a particular stage are shown in italics

Figure 1a - Reproducibility of weights of empty 7 mL Savillex® vials

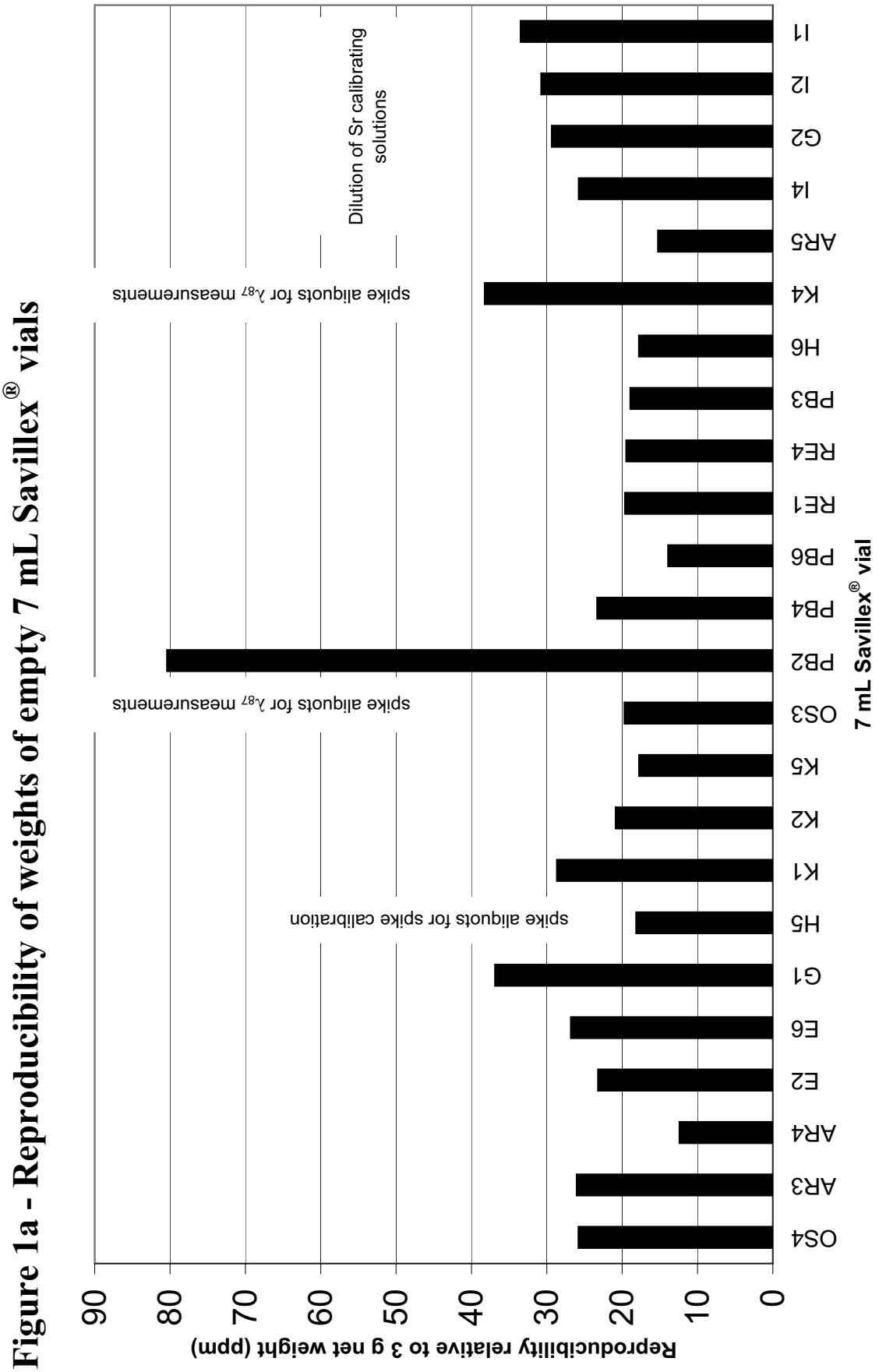

Figure 1b - Reproducibility of weights of 125 mL FEP bottles

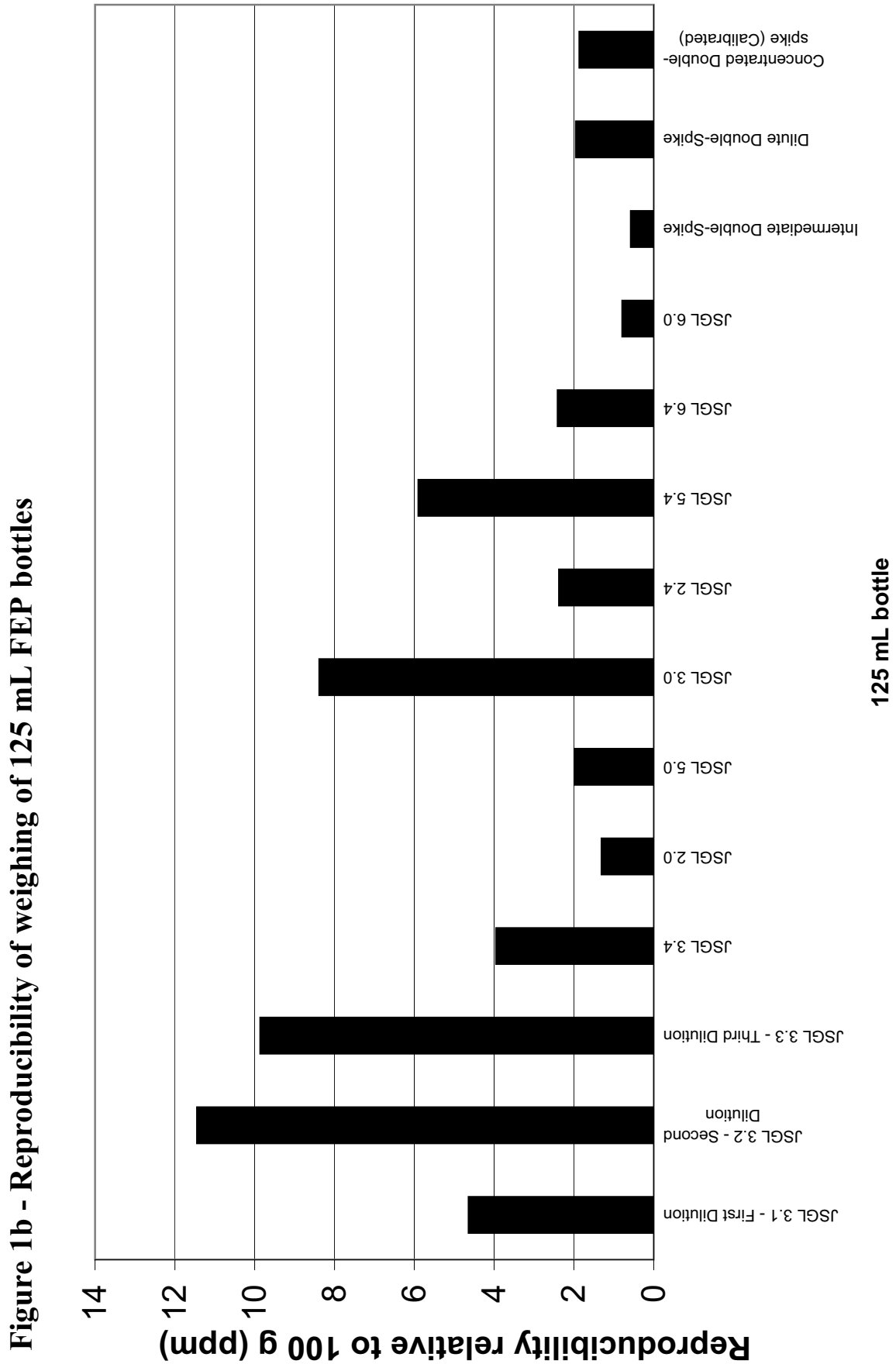

Figure 2a - Concentration of ^{84}Sr-^{86}Sr double-spike - Individual measaurements

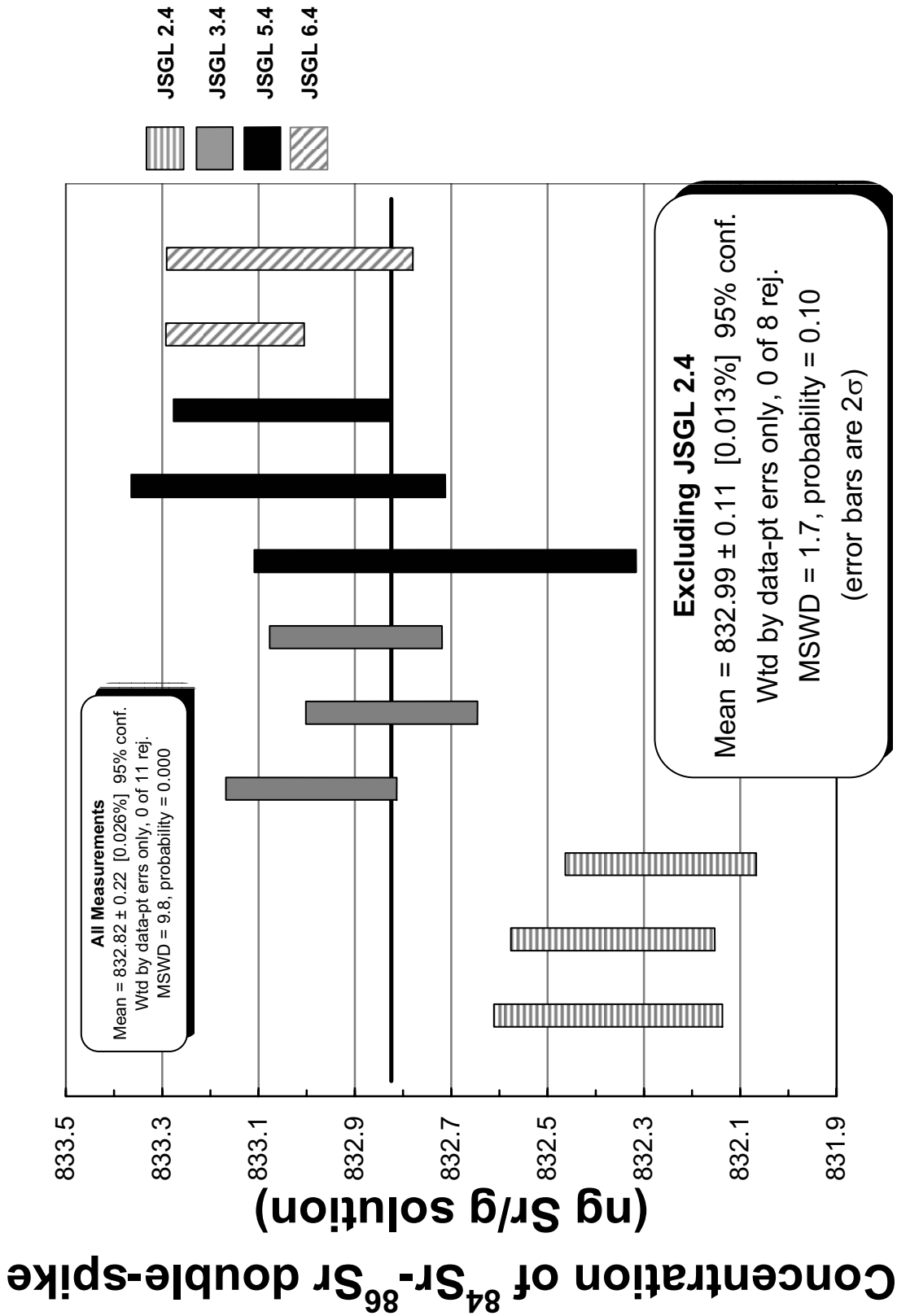

Figure 2b - Concentration of ^{84}Sr-^{86}Sr double-spike - Average measurements with each calibrating solution

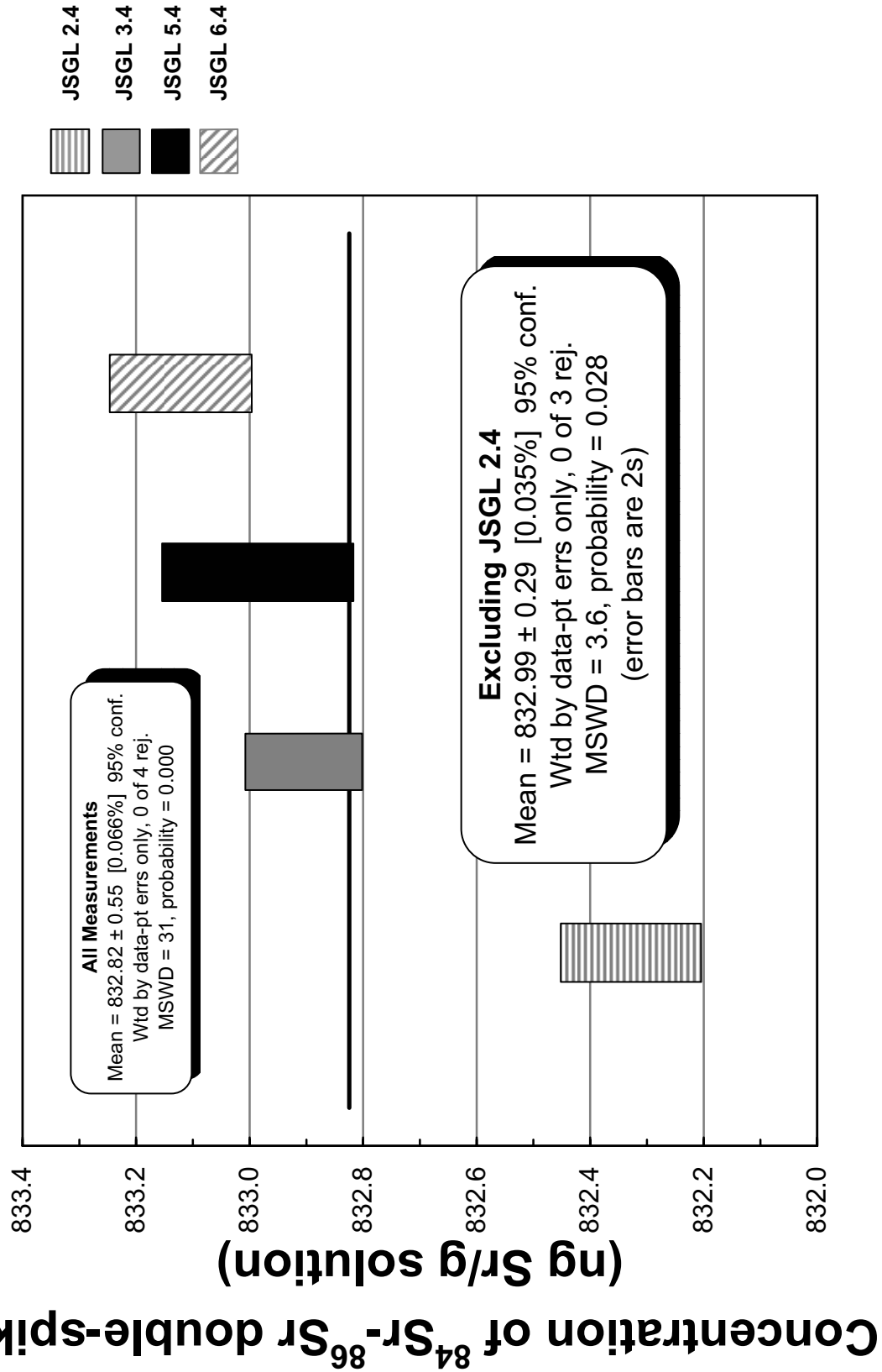

Chapter 4

A combined U-Pb, Rb-Sr chronology of ordinary chondrites

Ethan Rotenberg, Yuri Amelin, and Donald W. Davis

1. Introduction

The chondritic meteorites are among the most primitive objects in our solar system. As such, they afford us the opportunity to study first-hand the materials from which the terrestrial planets formed and to understand the processes by which they developed. While a basic understanding of the early history of the chondrite parent bodies has been achieved, there remains uncertainty over many of the details of the formation processes, the structure of the bodies, their sizes, accretion intervals, and metamorphic histories (Wasson, 1972; Chambers, 2003).

Early ordinary chondrite history had several stages (McSween, 1999). First was the formation of the chondrules themselves. Chondrules are the approximately millimeter sized igneous spherules found in primitive meteorites, which apparently originated as melt droplets prior to their inclusion in chondritic meteorite parent bodies (Hewins, 1997). The chondrules were subsequently agglomerated together within a matrix material and eventually accreted into planetesimal sized bodies. Within these parent bodies, the chondrites underwent varying degrees of thermal metamorphism. Heat for this thermal metamorphism may have come from one or more sources, though a great deal of thinking surrounds the decay of short-lived (and now extinct) ^{26}Al or ^{60}Fe (Urey, 1955; Goswami and Vanhala, 2000). Based upon these varying levels of thermal metamorphism, chondrites have been classified into four petrologic types, ranging from nearly unaltered, type 3, through types 4 and 5, to almost completely equilibrated, type 6 (Van Schmus and Wood, 1967; types 1-2 correspond to variable degrees of aqueous alteration seen in carbonaceous

chondrites). The parent bodies were subsequently fragmented by impacts, and some of those fragments eventually reached Earth.

Based on petrologic type, the ordinary chondrites are divided into two groups: unequilibrated and equilibrated. The unequilibrated ordinary chondrites (UOC) consist of petrologic type 3, while the equilibrated ordinary chondrites (EOC) consist of types 4-6. UOCs have heterogeneous textures and chemistry. Specifically, olivines have variable compositions, are often zoned, and can contain inclusions, and pyroxenes have variable Ca contents. Texturally, chondrule boundaries are very well defined, and matrix material is fine grained. UOCs are classified as 3.0-3.9 based on volatile content and degree of metamorphism (Anders and Zadnik, 1985a,b). EOCs show evidence of chemical and textural equilibration. Grains of a given mineral have essentially the same composition, and the compositions of grains of different minerals are consistent with chemical equilibration between the various minerals at high temperatures. Equilibration is further characterized by intergrowth of crystals, blurred chondrule boundaries, homogeneous mineral composition, and more coarse grained matrix material (Dodd, 1969; Dodd, 1986; Sears, 1978; Wasson,1985; Brearly and Jones, 1998).

The EOCs are interesting because they chronicle the early thermal history of their parent bodies. From their ages and thermal histories, parent body size, structure, and heating mechanisms can be deduced (Bennet and McSween, 1996). Dating of minerals from the same meteorite with different closure temperatures can yield cooling rates for the parent bodies as was accomplished for H5 Richardton (Amelin et al., 2005) and H6 Estacado (Blinova, et al., 2007).

It has been suggested that the increasing degree of thermal alteration from types 4 to 6 was the result of increasingly deeper burial within a parent asteroid that was internally heated by decay of ^{26}Al or other short-lived isotopes.

Temperature increased towards the interior, and the interior remained hot for longer causing increased thermal metamorphism with increased depth. This is commonly known as the onion-shell model and predicts younger ages with increasing petrologic type for meteorites from the same parent body (Miyamoto et al., 1981). Some cosmochronometric and other evidence supports this model, at least for some classes of meteorites (e.g. Göpel et al., 1994; Trieloff et al., 2003).

The ordinary chondrites are divided into three classes based on chemical composition. The H group has highest total Fe and a higher proportion of metallic Fe. The L group has less total Fe and a much smaller proportion of that is metallic Fe. Finally the LL group has even lower total and metallic Fe. Some meteorites are intermediate between L and LL and are sometimes classified as L/LL (Rubin, 1990). These differences have generally been taken to support the widely accepted assumption that the three classes of ordinary chondrites originated in separate parent bodies (Wood, 2005; Van Schmus and Wood, 1967; Wasson, 1972; Urey and Craig, 1953). The possibility therefore exists that the H, L, and LL groups had different histories and no single simple pattern will fit all three groups. H may well have ages that are correlated with petrologic types – in accordance with a relatively simple onion-shell model – while LL do not, as is indicated by U-Pb analyses by Göpel et al. (1994).

Chondrules are primary components of chondrites. Phosphates are secondary minerals in EOCs. They are thought to have grown during thermal metamorphism from phosphorus originally in solid solution with metal (Perron et al., 1992). Chondrule ages may not always reflect the formation of the chondrule itself, but rather the cooling of the chondrule after reheating during thermal metamorphism. In such cases and where closure temperatures are known and the difference between silicate and phosphate ages can be

determined, cooling rates can be calculated. The cooling rate can then be used to place constraints on planetesimal sizes and heating mechanisms.

Cooling rate detemination based on U-Pb dating has been accomplished successfully for H5 Richardton (Amelin et al., 2005), which provided the impetus for the current study on additional EOCs. The same chondrules, silicate fractions, and phosphate fractions analyzed for U-Pb were analyzed for Rb-Sr in an effort to compare the behaviour of the two systems and to put further constraints on the cooling histories of the ordinary chondrite parent bodies. Several previous studies (e.g. Evensen et al., 1979) have analyzed Rb-Sr in chondrules and produced isochrons with precision of about ±30 Ma. This study also affords an opportunity for the application of the re-determined of the ^{87}Rb decay-constant (λ_{87}) (Chapter 1). In this context, some meteorite Rb-Sr ages from the literature are recalculated and the results are discussed. Thirteen meteorites representing all three chemical classes have been studied and the results of these studies are presented here.

2. Samples

Thirteen ordinary chondrites were analyzed: H4 Ankober, H5 Orlovka, H6 Kidairat, L4 Saratov, L5 Elenovka, L6 Barwell, L6 Kunashak, L6 Pervomaisky, L/LL3 Unnamed Antarctic, L/LL4 Bjurböle, L/LL6 Holbrook, LL3.1 Krymka, and LL5 Tuxtuac. These meteorites were chosen based on availability and represent most classes and types of EOCs. Meteorites are summarized in Table 1.

3. Sample preparation

Meteorites were wrapped in plastic and broken into small pieces with a hammer, then crushed by hand in an alumina mortar. The crushed samples were sorted by grain size. Fractions were picked by hand under binocular microscope from heavy liquid (bromoform and methylene iodide) and magnetic

(Frantz) separations, or from coarse fractions of silicate minerals after crushing. Whole chondrules or chondrule fragments were picked from these coarse fractions. Detailed sample descriptions are given in Table 2. Samples were cleaned in ethanol in an ultrasonic bath in an attempt to separate adhering matrix minerals. Chondrules and silicate fractions were cleaned in warm 6N HCl and 7N HNO_3. Phosphates were cleaned in cold ethanol and acetone. Details of cleaning for each sample can be found in Appendix B.

Samples were spiked with ^{235}U-^{230}Th-^{205}Pb, ^{149}Sm-^{150}Nd, and ^{85}Rb-^{84}Sr tracer solutions. Samples were dissolved in HF and HNO_3 in 3 mL Savillex® PFA vials. U and Pb were separated by anion exchange column chemistry using HCl-HBr-HNO_3. Rb and Sr were separated from the eluate by cation exchange chemistry with HCl. U and Pb were loaded on single Re filaments with SiO_2 emitter. Rb was loaded on single Re filaments with SiO_2 and Sr was loaded on Ta filaments with H_3PO_4. U and Pb were measured in single collector mode using a Daly detector in pulse counting mode on a VG-354® at the Jack Satterly Geochronology Laboratory at the Royal Ontario Museum (now located at the University of Toronto). The mass discrimination correction for this detector is constant at 0.07%/AMU. Rb was also measured in single collector mode. Sr was measured in dynamic multicollector mode. Thermal mass discrimination corrections are 0.10% /AMU. Dead time of the Daly system (about 20 nsec) and multi-collector Faraday cup efficiencies were monitored using the SRM-982 Pb standard. Faraday amplifier gains were monitored daily using a constant current source. Average procedure blanks are 3.8 pg Pb, 1.3 pg Rb, and 10.4 pg Sr.

4.0 U-Pb results

Age information is presented in three ways: U-Pb concordia plots, Pb-Pb isochron plots, and Pb-Pb model dates. U-Pb concordia plots and Pb-Pb

isochrons require the assumption that the samples (chondrules, mineral fractions etc.) formed at the same time. They also require multiple samples in order to determine a best-fit a line. Both calculations assume that all samples have the same initial common Pb but the Pb-Pb isochron requires no assumptions as to the isotopic composition of that initial common Pb. U-Pb concordia plots radiogenic Pb over U ratios ($^{206}Pb^*/^{238}U$ v. $^{207}Pb^*/^{235}U$ for the Wetherill plot), and therefore require subtraction of the common Pb component from the total Pb in the sample. This requires an assumption about the isotopic composition of the initial common Pb.

Pb-Pb model dates also require an assumed initial common Pb composition, and are therefore sensitive to addition of Pb from weathering or from laboratory processing. They can be calculated for individual samples, and do not require a group of samples with the same age. Pb-Pb model dates and isochrons do not require U information, and therefore are insensitive to recent U mobility (such as from leaching).

The assumed initial composition of common Pb in the meteorites is that of troilite in the Cañon Diablo (CDT) meteorite: $^{206}Pb/^{204}Pb = 9.307$; $^{207}Pb/^{204}Pb = 10.294$; $^{208}Pb/^{204}Pb = 29.476$ (Tatsumoto et al., 1973). Troilite contains Pb but very little U or Th, and therefore the isotopic composition of meteoritic troilite, assuming no terrestrial contamination, is the composition of the common Pb incorporated into the troilite when it crystallized (Faure, 1986). This primitive Pb composition is assumed to be the composition of the common Pb in the meteorites for which these model dates are calculated, and primordial Pb is assumed to be the only Pb component other than radiogenic Pb (Amelin et al., 2005; Bouvier et al., 2007). Because the model dates assume that there is no other common Pb component, it is important to remove terrestrial contamination as much as possible by leaching samples to remove any surface or interstitial Pb.

This also highlights the importance of the Pb-Pb isochrons, which are insensitive to recent Pb loss or migration due to terrestrial contamination or laboratory handling. Agreement between dates calculated by all three methods supports the assumptions of closed systems, primordial Pb as the initial Pb, and that the dates accurately reflect the ages of the samples. U-Pb concordia and Pb-Pb isochron regressions were plotted with Isoplot/Ex 3.0 (Ludwig, 2003). Pb-Pb model dates were calculated with PbDat v. 1.24 (Ludwig, 1993).

U-Pb data for the meteorites are presented in Table 3. U-Pb concordia dates, Pb-Pb isochron dates, and Pb-Pb model dates are presented in Tables 4 and 5, and Pb data are summarized in Figures 1a-1d. Pb-Pb model dates are calculated by subtracting primordial Pb (Canyon Diablo Troilite (CDT), Tatsumoto et al., 1973) from measured Pb ratios. L5 Elenovka includes analyses of chondrules, pyroxene fractions, and phosphates. There are three phosphate analyses for LL3 Krymka and H5 Orlovka, two for LL/L4 Bjurböle and one for L4 Saratov. For the other meteorites, only chondrules and in some cases silicate fractions were analyzed.

4.1 U and Pb abundances and abundance of radiogenic Pb

Uranium concentrations range from 1 ppb to 3.4 ppm. Chondrules and silicates range from 1 ppb to 1 ppm U (a single chondrule has 1.8 ppm), and phosphates from 1 ppb to 3.4 ppm. L5 Elenovka phosphates have the consistently highest U concentrations with all above 1 ppm. Pb concentration ranges from 3 ppb to 6 ppm (a single phosphate has anomalously high 63 ppm). Silicates have a maximum of 2.8 ppm Pb, but the average is only 70 ppb. More than half of the phosphates have over 1 ppm Pb. There is no correlation between chemical class or petrologic type and the abundances of U and Pb, and concentrations vary between samples from the same meteorite.

$^{238}U/^{204}Pb$ also has a wide range, from 0.120 – 926. The range is similar for silicates and phosphates. For phosphates, high $^{238}U/^{204}Pb$ samples have high U and Pb concentrations, but not all samples with high U and Pb concentration have high $^{238}U/^{204}Pb$. Silicates all have lower U concentrations than phosphates, and high $^{238}U/^{204}Pb$ is not associated with high U concentration, but rather with low Pb concentration.

Because leachates were not analyzed, it is not known if, for the more radiogenic samples, it was primarily common or radiogenic Pb that was leached. Reverse discordance for some analyses indicates preferential leaching of U over Pb (Amelin et al., 2002). The most consistently radiogenic samples are from L5 Elenovka, with $^{238}U/^{204}Pb$ ranging from 480-926 (excluding one phosphate with $^{238}U/^{204}Pb$ only 73). H4 Ankober is also fairly radiogenic, as are the single measurements from each of L6 Kunashak and Pervomaisky.

Several of the previously analyzed H5 Richardton chondrules and fractions had $^{238}U/^{204}Pb$ over 1,000 and Göpel et al. (1994) reported phosphates with $^{238}U/^{204}Pb$ as high as 3400. Two L5 Elenovka phosphates, with $^{238}U/^{204}Pb$ of 764 and 926 are more radiogenic than the Richardton phosphates, all but one of which have $^{238}U/^{204}Pb < 311$. Similar to Richardton, pyroxene fractions from Elenovka were found to contain very radiogenic Pb. Kyrmka and Bjurböle pyroxene fractions do not. Most chondrules do not have highly radiogenic Pb, though some do, especially those from H4 Ankober and H6 Kidairat.

For the silicates and chondrules, only samples with low Pb concentration have highly radiogenic Pb with $^{238}U/^{204}Pb$ greater than 100. For some phosphates, especially the most radiogenic, high Pb concentration correlates with highly radiogenic Pb. This provides further confirmation of the observation of Göpel et al. (1994) that chondritic phosphates form with high U/Pb and therefore have highly radiogenic Pb. However, Saratov and Bjurböle phosphates have low

$^{206}Pb/^{204}Pb$ despite high total Pb concentration. No Krymka phosphates are radiogenic. Krymka might be a special case though. Krymka is a LL3.1, one of the least metamorphosed ordinary chondrites. Phosphates are not generally found at all in type 3 meteorites, and phosphate abundance and grain size increase with increasing petrologic type. Göpel et al. were unable to study phosphates from any type 3 meteorites on account of their small grain size and scarcity. Amelin et al. (2005) have discussed the possibility that U in chondrules actually resides in phosphate grains armoured within chondrules, and concluded that this is most likely not the case.

Compared with Bouvier et al.'s Elenovka data, the current data is for the most part more radiogenic. This is most likely, as pointed out by Bouvier et al., because of our more aggressive leaching. One Elenovka phosphate, however, is the least radiogenic of all the Elenovka analyses from either study. Richardton phosphates exhibit a similar range of $^{206}Pb/^{204}Pb$.

4.2.1 H class meteorites

H5 Orlovka has the most consistent dates among the H class meteorites reported here. Two point U-Pb concordia and Pb-Pb isochron regressions for silicate fractions yield 4559.5 ± 0.8 Ma and 4558.8 ± 1.0 Ma respectively. Pb-Pb model dates are 4559.3 ± 0.8 and 4562.4 ± 2.1 Ma. Three Orlovka phosphate fractions were analyzed. Two yield Pb-Pb model dates of 4560 ± 5 and 4555 ± 2 Ma, and the third has a much younger date of 3844 Ma. This sample is much less radiogenic than the others, with $^{238}U/^{204}Pb$ of 41, while all other Orlovka samples are over 150.

The data from the other two H type chondrites, H4 Ankober and H6 Kidairat, are less precise. No U data was collected for either meteorite. Ankober Pb is radiogenic, but ratios for all samples are almost equivalent, so a Pb-Pb

isochron plot is not meaningful. Two Pb-Pb model dates are unrealistically old, and the other five yield a weighted average of 4559.9 ± 2.8 with a mean square of weighted deviates (MSWD) of 1.9.

H6 Kidairat chondrules scatter on the Pb-Pb isochron plot (Figure 2) and yield 4539 ± 9, with a poor fit, with MSWD of 42. Pb-Pb model dates scatter greatly, and vary from 4543-4405 Ma, but model dates of chondrules with $^{206}Pb/^{204}Pb > 80$ have a range of just 4543-4520 Ma. All of the Kidairat dates are younger than H5 Richardton.

4.2.2 L class meteorites

Two chondrules and one silicate fraction from L4 Saratov have model dates of about 4559 Ma, and another chondrule and two fractions have slightly older model dates of about 4564. A weighted average of all model dates gives 4563 ± 2 (MSWD =5). A Pb-Pb isochron regression (Figure 3a) yields 4559 ± 12 (MSWD = 5). On the concordia diagram, the two silicate fractions plot near concordia, and the chondrules and chondrule fragments define a discordia chord with an upper intercept at 4563.3 ± 2.7 (MSWD = 5.5) (Figure 3b). These dates agree well with one another and are resolvable from the single phosphate analysis which yields a model date of 4530.1 ± 5.9 Ma.

Five chondrules from L6 Barwell were analyzed. Model dates scatter. The Barwell chondrules do not define a line on the concordia plot. A Pb-Pb isochron regression gives a much older date than the model dates, 4525 ± 26 Ma (Figure 4). All Barwell analyses have Pb ratios close to modern terrestrial Pb values. Two L6s, Kunashak and Pervomaisky, both have very radiogenic Pb, with corrected (CDT) $^{206}Pb/^{204}Pb$ of 674 and 599 respectively. Model dates for these meteorites are 4091 and 4431 respectively. Pervomaisky exhibits high shock features (Dunaway et al, 2006; Semenenko and Golovka, 1994).

L5 Elenovka is one of the most extensively studied meteorites in this paper with analyses of two chondrules, four silicate fractions (pyroxenes), and three phosphate fractions. Both silicates and phosphates give consistent U-Pb and Pb-Pb results. For silicates, two chondrules and four pyroxene fractions from chondrules all plot near concordia and yield a U-Pb concordia intercept date of 4554 ± 1 Ma (MSWD = 0.43) (Figure 5). The same samples define a Pb-Pb isochron date of 4555.0 ± 2.7 Ma (MSWD = 0.53), and Pb-Pb model ages average 4554.59 ± 0.49 Ma (MSWD = 0.49) (Figure 6). Two phosphates fractions are concordant at 4538 ± 9, and together with the third phosphate give a U-Pb concordia intercept date of 4535 ± 1 Ma (MSWD = 0.56) (Figure 7). The three fractions give a Pb-Pb isochron date of 4535 ± 1 Ma (MSWD = 0.11), and Pb-Pb model dates average 4537 ± 6 Ma (MSWD = 24). The model dates of the phosphates with higher $^{238}U/^{208}Pb$, over 750, agree at 4535.4 ± 1 Ma, while the third, with a slightly older model date of 4540 ± 1 has considerably less radiogenic Pb with $^{238}U/^{208}Pb$ of only 70. The silicate and phosphate dates are well resolved within the errors. Elenovka pyroxene fractions are among the most radiogenic samples analyzed here. All pyroxene fractions have $^{206}Pb/^{204}Pb > 500$.

4.2.3 L/LL class meteorites

Analyses of five chondrules from the unnamed Antarctic L/LL3 – one of which was analysed separately as two fragments – yield a Pb isochron date of 4499 ± 34 Ma (MSWD = 45) (Figure 8). Four model dates are in fairly close agreement with an average of 4501.4 ± 3.9 Ma and a Pb isochron regression through these chondrules yields 4503 ± 13 Ma (MSWD = 2.7), and U-Pb concordia plot for these four chondrules yields 4500 ± 5 (MSWD = 1.2). Two of these analyses are fragments of the same chondrule. The two chondrules with anomalously high Pb-Pb model dates (4530 and 4570 Ma) also have anomalously

low Rb/Sr (see below section 6.1). These two chondrules exhibit severe bleaching after leaching in 3N HCl and 2N HNO_3. Pb in this meteorite is not very radiogenic.

L/LL4 Bjurböle data exhibit a great deal of scatter for both Pb-Pb and U-Pb plots, and many samples exhibit reverse discordance. The Pb-Pb isochron regression gives 4569 ± 9, and the U-Pb concordia regression yields a concordia intercept of 4548 ± 14. Both regressions have high MSWDs (Figures 9a and 9b). Most model dates are between 4545 and 4555 Ma. Three U-Pb analyses of L/LL6 Holbrook yield concordant dates at 4556 ± 10 Ma. Isochron and model ages agree at 4555 (Figure 10). One chondrule fragment has an older model-date, 4561 Ma, and this same analysis, when regressed with the other chondrules skews the isochron regression to 4563, though within the relatively large errors, it still overlaps 4555 Ma. Generally speaking the L/LL data obtained from these analyses is not precise enough to resolve from other meteorites.

4.2.4 LL class meteorites

LL3 Krymka has among the most analyses but the data scatter greatly. The concordia and isochron plots both yield dates of about 4547 Ma with large errors and high MSWDs (Figures 11a and 11b). The model dates also scatter a fair amount. Ten model dates agree to within about 15 Ma and average 4547 ± 4 Ma, while four others scatter much more. If only these are regressed, the MSWDs are reduced, but the dates and errors are not changed substantially. Unlike the phosphates from other meteorites studied here, the Krymka and Bjurböle phosphate Pb is less radiogenic than the silicate Pb, with phosphate $^{238}U/^{204}Pb$ ranging from 0.1-3.1, while the other chondritic phosphates range from 12-926. Krymka phosphate data also have large errors.

Four LL5 Tuxtuac chondrule analyses regressed on a U-Pb concordia plot yield an intercept date of 4099 ± 29 Ma (MSWD = 0.02) (Figure 12a). Model dates scatter around 4100 Ma. But an imprecise Pb-Pb isochron regression yields 4493 ± 50 Ma (Figure 12b). Tuxtuac Pb is not radiogenic, and the model dates are probably artifacts of an inaccurate common Pb correction.

5. Discussion

5.1 Relative chronology of different classes and petrologic types

A timeline of meteorite studied here is presented in Figure 13. H5 Orlovka results indicate an age of about 4560 Ma for silicates and about 4555 Ma for phosphates. Previously published results from H5 Richardton (Amelin et al., 2005) gave silicate and phosphate ages of 4563 ± 2 and 4551 ± 3 Ma, respectively. Because the Orlovka dates are calculated from two point isochrons, the most that can be reliably said is that H5 Orlovka silicates appear to be of similar same age, or perhaps just slightly younger than H5 Richardton while their phosphate ages may be a few Ma older than those from Richardton. If the Orlovka phosphates are indeed older than Richardton phosphates, this would indicate faster cooling for Orlovka, but additional data would be required to establish this. Both Orlovka and Richardton are H5, and therefore in a classic onion-shell model of the H parent body, Orlovka would have to be more shallowly buried than Richardton, but still deep enough to heat up to type 5 temperatures of 973-1023 K (Dodd, 1981).

H4 Ankober chondrules have very radiogenic Pb with $^{206}Pb/^{204}Pb$ ranging from 247-3514. However, they do not yield as precise dates as H5 Richardton. All Ankober dates are similar to the 4563 ± 2 Ma age of H5 Richardton. This is to be expected since the type 4 EOCs are less altered than type 5, and unless otherwise disturbed, should be expected to preserve a more primary age. The

data are not precise enough to determine if H4 dates can be resolved from H5. They are no more than a few Ma younger than the oldest dated chondrules (e.g. Allende: 4566.2 ± 2.5 Ma (Amelin and Krot, 2007)) and CAIs (Amelin et al., 2002). At the resolution currently attained for the best samples, it might be possible to determine whether H4 chondrule ages are resolved from H5 chondrule ages, and thus to assess if they preserve primary chondrule formation ages or if, like the type 5 chondrules, they record cooling from thermal metamorphism. The overlap between the very old ages of H5 Richardton and H4 Ankober chondrules also allows for the possibility that type 5 material did not experience high enough temperatures to disturb U-Pb systematics. The estimated Pb closure temperature for Pb in chondritic pyroxenes is 1055 ± 106 K (Amelin et al., 2005), which roughly overlaps with the estimated maximum temperature attained by type 5 ordinary chondrites. It is possible then that both type 4 and type 5 chondritic silicates preserve chondrule formation ages.

Kidairat was the subject of a test of the utility of Electric Pulse Disaggregation (EPD) for meteorites. EPD is supposed to break rocks along mineral grain boundaries and it was hoped that it would be superior to mechanical crushing in that whole chondrules would be freed, intact, from the surrounding matrix. This was not found to be the case. EPD conveniently broke the meteorite into more evenly sized fragments than mechanical crushing did, but the degree to which chondrules were broken and/or separated from the matrix was similar to the results with mechanical crushing. The model-dates for the EPD chondrules, which were disaggregated in water, also exhibit much more scatter than the mechanically crushed ones. A Pb-Pb isochron regression with only the mechanically crushed samples yields 4538.2 ± 9.7 with a reasonable MSWD of 1.8. This is only a three point regression and there is very little spread and therefore this is a very tentative date. But it is possible that the EPD process

disturbed the Pb in the meteorite. If that is the case, the mechanically crushed samples might reflect the age of these chondrules, and the young age would date the cooling of type 6 through the pyroxene closure temperature.

The H meteorites provide a good example of the different quality of chronometric information that can be obtained from U-Pb in meteorites. H5 Richardton exhibits the most robust U-Pb system, yielding precise dates and clearly resolving the ages of different phases. Based on a relatively small data set, H5 Orlovka appears similarly to preserve intact U-Pb and yields ages nearly as old as Richardton. H4 Ankober yields old dates, which is to be expected from a meteorite that has undergone even gentler thermal processing than Richardton, but the data are not precise. H6 Kidairat give the youngest dates, although imprecise. The bulk of the data from the H class meteorites reported here support the picture of the H body as generally fitting a classic onion shell model (Trieloff et al., 2003).

The data from L5 Elenovka are the best EOC ages determined in this study. The good agreement between U-Pb concordia and Pb-Pb isochrons, as well as Pb-Pb model dates, suggest that these dates reliably reflect the Pb closure ages of the silicates and phosphates. Elenovka silicate ages, 4555 ± 1 Ma, are well resolved from phosphate ages, 4535 ± 1 Ma. The implications for the thermal history of the L parent body are discussed below.

The L6 silicate ages (Barwell, Kunashak and Pervomaisky) are so young and inconsistent that they could be artifacts of disturbance. Barwell Pb is not radiogenic, but Kunashak and Pervomaisky Pb is highly radiogenic. Kunashak is shocked though, which likely accounts for the disturbed U-Pb. The 4563 ± 2 Ma age from Saratov L4 silicates is older than the 4554 ± 1 Ma of silicates from Elenovka L5 and is about the same age as H4 Ankober and H5 Richardton (Amelin et al., 2005). The phosphate ages from both L class meteorites accord at

about 4535 Ma, significantly younger than phosphate ages of 4550-4555 Ma from the H class. This would seem to indicate a more protracted cooling history, suggesting that the L parent body was significantly larger than the H parent body. Type 4 meteorites have an estimated maximum temperature of 800-973 K (Miyamoto et al., 1980; Dodd, 1981). The maximum temperature of 973 overlaps with the range of Pb closure temperatures in pyroxene, 1055 ± 106 K, meaning that the L4 silicate dates could be the ages of the chondrules themselves. Otherwise, they reflect an early stage in the cooling of the L parent body.

The data from LL3 Krymka give a date of about 4547 Ma. As type 3.1, it has undergone minimal thermal metamorphism, and would therefore be the best candidate to preserve an old or even primary age. However, Pb-Pb data for the silicate fractions from this meteorite scatter widely. For example, fractions 10 and 11 have nearly the same $^{206}Pb/^{204}Pb$ – 41.3-41.1 respectively, but $^{207}Pb/^{206}Pb$ is 0.750 and 0.726 respectively. In a closed system model with only radiogenic and CDT Pb, $^{207}Pb/^{206}Pb$ and $^{206}Pb/^{204}Pb$ should correspond, and discrepancies lead to unrealistic model ages. Discrepancies in the Krymka model ages indicate an open systems or additional Pb components. There is some evidence suggesting that the LL body was subjected to late impacts that disturbed various isotopic systems (e.g. Dixon et al., 2004) but those impacts occurred significantly later, at about 4270 Ma. The relatively young scattered data for the LL samples studied here may be due to partial resetting from impact disturbance on the LL parent body.

Unlike H5 Richardton and L5 Elenovka, LL3 Krymka phosphate Pb is less radiogenic than silicate Pb. The same is true for L4 Saratov and L/LL4 Bjurböle. The less radiogenic Pb in these more primitive meteorites supports the suggestion that chondritic phosphates concentrate U and exclude Pb as they grow during thermal metamorphism (Göpel et al., 1994) and indicate that it is

only the type 5 and 6 chondrites whose phosphate has concentrated sufficient U to have highly radiogenic Pb. We did not analyze phosphates from any type 6 meteorites, but they too would be expected to have high U concentrations corresponding to highly radiogenic Pb. This is the case for phosphates from type 6 chondrites studied by Göpel et al. However, they also found highly radiogenic Pb in on H4 phosphate, Ste. Marguerite.

5.2 Thermal history of the L parent body

From the difference in U-Pb ages of L5 Elenovka silicates and phosphates, we can estimate the cooling rate of the L parent body from a peak at the silicate Pb diffusion closure temperature through the closure temperature of phosphates. Closure temperatures depend on, among other things, grain size and the cooling rate itself. The closure temperature increases with faster cooling and larger grain size. Using closure temperature estimates for apatite: 759 ± 56 K, and pyroxene: 1055 ± 106 K, from Amelin et al. (2005) based on Cherniak (2001) and Cherniak et al. (1991) and the time difference between Elenovka silicates and phosphates: 20 Ma, an estimate of the cooling rate for the L parent body is about 14.8 ± 6 K/Ma. More precisely, this would be the cooling rate of the L5 material in the L parent body. Since both closure temperatures depend on the cooling rate, the difference between closure temperatures can be estimated more precisely than the absolute closure temperatures as 296 ± 50 K, which gives a more precise cooling rate estimate of 14.8 ± 2.6 K/Ma (Figure 14).

This cooling rate is nearly 50% lower than the H5 Richardton cooling rate of 25.7 ± 9 K/Ma and suggests that the L parent body was larger than the H parent body. Cooling more slowly, L silicates remain above their closure temperatures for longer than H, and this explains the absolute time difference between silicate/chondrule ages and phosphate ages between H5 and L5. This

also suggests that the silicate ages are in fact timing the end of metamorphism, rather than chondrule formation, since otherwise L5 Elenovka silicates would be expected to preserve a primary age closer to 4560 Ma. As the parent bodies continue to cool, the faster cooling H5 cools past the phosphate Pb closure temperature in 12 Ma, while the more slowly cooling L5 takes 20 Ma. This is inconsistent with other models that make the H and L bodies the same size, or even have the L body smaller than the H (Miyamoto, et al, 1981; Bennet and McSween et al., 1996). These models, however, do not use measured cooling rates as a parameter to constrain parent body accretion and heating.

L/LL6 Holbrook data is not precise, but all dates indicate an old age of about 4555 Ma. This is approximately the same age as the other L/LL, Bjurböle, which is type 4. The old age for a type 6 chondrite does not accord with a classic onion-shell model. If the body did indeed form as a layered body, there could have been an early impact that excavated type 6 material which then cooled quickly. The L/LL meteorites studied here exhibit an apparent inverse relationship between age and petrologic type.

6. Rb-Sr

6.1 Results and Discussion

Rb concentrations range from 0.26-115 ppm. Sr concentrations range from 2.3-152 ppm (one fraction has anomalously high 784 ppm). Concentration ranges of Sr are similar for silicates and phosphates for the different meteorites, but phosphates tend to have less Sr, with an average concentration of 44 ppm, vs. 89 ppm for silicates. Rb is far more concentrated in silicates than in phosphates, with a silicate average of 15 ppm, and phosphate average of 0.88. Rb and Sr concentrations as well as isotopic ratios are shown in Table 6, and summarized in Figures 15a-15c. $^{87}Sr/^{86}Sr$ in silicates is in all cases higher than it is in phosphates.

Phosphate Sr is relatively non-radiogenic, with $^{87}Sr/^{86}Sr$ ranging over 0.701-0.711. Apatite does not readily incorporate Rb, so low Rb/Sr and $^{87}Sr/^{86}Sr$ are expected (Podosek and Brannon, 1991). Silicate Sr is more radiogenic with a range of 0.722-1.312 (with the exception of two chondrules from L/LL3 Unnamed Antarctic with low $^{87}Sr/^{86}Sr$ and low Rb/Sr).

All studied samples have Rb/Sr < 1 except for four: two fragments of the same chondrule from the Unnamed Antarctic L/LL3, and two chondrules from LL3 Krymka. All four have Rb concentrations in the normal range, but Sr concentrations that are low compared with other silicate fractions. All four have correspondingly high $^{87}Sr/^{86}Sr$ indicating that this is not likely the result of disturbance. Nearly all phosphates have low Rb concentration, and therefore there is generally a correlation in phosphates between high Sr concentration and low Rb/Sr. Silicates, with considerably more variable Rb concentration, show no such correlation.

6.1.1 Rb-Sr dates

$^{87}Rb/^{86}Sr$ v. $^{87}Sr/^{86}Sr$ was plotted on Rb-Sr isochron diagrams for each meteorite, and for silicates and phosphates separately where more than a single sample was analyzed. No meaningful lines can be regressed through the phosphate data. The silicates and chondrules have a far wider range of $^{87}Sr/^{86}Sr$. Because initial $^{87}Sr/^{86}Sr$ in ordinary chondrites is fairly well constrained, model dates can also be calculated for the chondrules and fractions. Rb-Sr model dates assume that fractions formed with a given initial $^{87}Sr/^{86}Sr$ $(^{87}Sr/^{86}Sr)_i$. For the H chondrites these are calculated with $(^{87}Sr/^{86}Sr)_i = 0.69876 \pm 0.0040$ (Minster and Allègre, 1979), and for L and LL with $(^{87}Sr/^{86}Sr)_i = 0.69877 \pm 0.00012$ (Minster and Allègre, 1981). Model dates can be useful for revealing disturbances to the Rb-Sr system on a sample by sample basis.

6.1.2 Rb-Sr isochrons

Evensen et al. (1979) determined a Rb-Sr age for Richardton of 4467 ± 30 Ma (λ_{87} = 1.398 × $10^{-11}a^{-1}$, adjusted from the published value of 4390 Ma using λ_{87} = 1.42 × $10^{-11}a^{-1}$) with $(^{87}Sr/^{86}Sr)_i$ of 0.7003 ± 0.0007. The chondrules and silicate fractions studied here yield 4553 ± 110 Ma with $(^{87}Sr/^{86}Sr)_i$ of 0.6987 ± 0.0013. When regressed together with the Evensen et al. data, these yield a date of 4540 ± 72 Ma, $(^{87}Sr/^{86}Sr)_i$ = 0.69895 ± 0.00088 (MSWD 7.2) (Figure 16). The larger errors are at least partially the result of different regression programs. We use Isoplot 3.0 (Ludwig, 2003) and Evensen et al.'s data plotted with Isoplot yields a higher error than their published value: ± 97 Ma. The recalculated Evensen et al. data, even with its fairly large error, is resolved from U-Pb ages for Richardton silicates (4563 Ma) and phosphates (4551 Ma). But the Rb-Sr regression including both our new data and Evensen et al.'s data overlaps with Richardton U-Pb data.

Elenovka silicates do not have the same spread in $^{87}Sr/^{86}Sr$ that Richardton silicates do. All analyzed samples are between 0.744-0.749, and consequently yield a very imprecise date of 4783 ± 2400 Ma (Figure 17). This is in quite marked contrast to the precision of the U-Pb ages from the same samples of this meteorite. L/LL3 Unnamed Antarctic gives the best isochron fit, with 4455 ± 41 Ma and initial $^{87}Sr/^{86}Sr$ of 0.7026 (MSWD 0.58) (Figure 18).

6.1.3 Rb-Sr Model Dates

Rb-Sr model dates scatter quite widely for all meteorites. Model dates for Richardton span over 300 Ma and Elenovka model dates span 120 Ma compared with just a few Ma for Pb-Pb model dates. Elenovka Rb-Sr model dates are all older than the Pb-Pb model dates, and in most cases are older than the solar system. This suggests variable loss of Rb. Calculated with the bulk H initial $^{87}Sr/^{86}Sr$ (0.69876), Richardton chondrules and silicate dates are also older than

the Pb-Pb dates. Calculating with the Richardton value of 0.7003 (Evensen et al., 1979), produces younger ages, some of which are younger than the Pb-Pb dates. The large variability in these dates also attests to disturbed Rb-Sr systematics. Although model dates scatter widely, the silicates with $^{87}Sr/^{86}Sr$ above 0.8 cluster around 4500 Ma while nearly all those with lower $^{87}Sr/^{86}Sr$ have model dates that are far too old.

Another model approach which has been applied to chondritic phosphates is to calculate initial $^{87}Sr/^{86}Sr$ for individual samples by subtracting the radiogenic $^{87}Sr/^{86}Sr$ that would be generated by the decay of ^{87}Rb (based on measured $^{87}Rb/^{86}Sr$) over the course of 4560 Ma (the approximate age of the meteorite). Time intervals can then be calculated for the evolution of $^{87}Sr/^{86}Sr$ from a given reservoir to the calculated initial $^{87}Sr/^{86}Sr$. This interval will represent the time between the isolation of a body with a particular $^{87}Sr/^{86}Sr$ and the closure to Rb-Sr on the mineral scale (Brannon et al., 1988; Podosek and Brannon, 1991). This method has particularly been applied to chondritic phosphates because phosphates typically have low Rb/Sr. Consequently, they have low $^{87}Sr/^{86}Sr$, and the correction for radiogenic $^{87}Sr/^{86}Sr$ is small. Model intervals are then calculated from an initial reservoir that is assumed to have primitive Sr isotopic composition taken to be angrite $(^{87}Sr/^{86}Sr)_i$: 0.698955 ± 0.000004 (Hans et al., 2009) to the calculated $(^{87}Sr/^{86}Sr)_i$ for each sample. $^{87}Rb/^{86}Sr$ is assumed to be equal to the measured whole rock values for samples, 0.746 for Elenovka, 0.792 for Bjurböle, and 0.75 for the rest of the samples where whole rock values were not measured (Podosek and Brannon). Calculated $^{87}Sr/^{86}Sr$ for phosphates and silicates are shown in Table 6, along with the corresponding calculated time intervals.

Both the Rb-Sr model dates and model time intervals show large variation, with many unrealistically ancient dates. It is of note that the

phosphates in particular, which owing to their low Rb/Sr and $^{87}Sr/^{86}Sr$ are expected to be less sensitive to corrections required for the time interval calculations actually seem to have some of the most unrealistically old time intervals. This might be partially due to incorrect assumptions about the whole rock $^{87}Rb/^{86}Sr$ value during this time interval. Time intervals for Sr evolution are calculated with whole-rock $^{87}Rb/^{86}Sr$ rather than mineral $^{87}Rb/^{86}Sr$ on the assumption that on the whole rock scale, the chondrites can be considered a closed system following separation from a reservoir with given $^{87}Sr/^{86}Sr$, but closure at the mineral scale would not occur until later. Using mineral $^{87}Rb/^{86}Sr$ would require an assumption of closed system behaviour from the time of separation of the chondrite parent body from the nebular reservoir, which is highly unlikely due to metamorphism, and the fact that phosphates only grew during this metamorphism. The whole-rock $^{87}Rb/^{86}Sr$ in EOCs from the literature ranges from 0.107-1.6, leaving a wide range of possible choices for the calculations. Phosphate fractions from the same meteorite yield very different formation intervals, and consequently no single choice of $^{87}Rb/^{86}Sr$ will yield dates that agree. This in itself indicates that the model assumptions are not supported.

Podosek and Brannon (1991) presented model intervals from 14 ordinary chondrites, which also yielded complex data. Errors were large, and intervals for meteorites of the same class and type differed by as much as 67 Ma. Some intervals were negative, implying unrealistically that initial $^{87}Sr/^{86}Sr$ in these phosphates was lower than the most primitive known ratios. They suggested several ways to explain the data, including a non-uniform Sr composition in the early solar system, or the incorporation into phosphates of Sr that is not representative of the whole rock. In the former case, the model is incorrect because it assumes invariant $(^{87}Sr/^{86}Sr)_i$, and in the latter case, whole rock Rb/Sr

would be an incorrect choice for calculating the intervals, and local Rb/Sr could be variable, making it impossible to choose any single value for all model dates.

These explanations assume a two stage Rb-Sr evolution model, and heterogeneity in the initial conditions – $^{87}Sr/^{86}Sr$ and Rb/Sr. Disturbance of Rb-Sr, either by migration of Rb or addition of radiogenic Sr to the phosphates, at some point (or points) after crystallization will upset the model. The fact that some phosphates have calculated initial Sr model dates older than the Pb-Pb ages (and even older than the solar system) while others are significantly younger suggests that both of these processes may be in effect to varying degrees. Rb and Sr are easily mobilized in meteorites (Faure and Powell, 1972), and radiogenic Sr mobilized from the higher Rb/Sr phases might be taken up by the low Rb/Sr phosphates. Shock, impact induced heating, and terrestrial contamination are all possible causes for the disturbance to Rb-Sr. The fact that most ordinary chondrite samples plot near a 4560 Ma reference isochron (Figures 15a-15c) indicates that they formed at approximately the same time from the same, or similar reservoirs. Loss or gain of a few percent Rb will upset the model ages by tens of millions of years and the point will still plot near the reference isochron. There does not appear to be a simple model to explain Rb-Sr behaviour. At least one of the assumptions for the Rb-Sr chronometer is not met: homogeneous $^{87}Sr/^{86}Sr$ reservoir, formation of samples at the same time, and closed system behaviour.

6.2 Recalculation of old Rb-Sr meteorite data with the new decay constant

Many Rb- Sr studies of meteorites have used ^{87}Rb decay constants of 1.42 or $1.39 \times 10^{-11} a^{-1}$. The context of the Rb-Sr study of meteorites here invites a recalculation and comparison of a few meteorite ages from the literature.

Minster and Allègre (1979) plotted a whole-rock isochron for eight H chondrites yielding 4520 ± 50 Ma. This was calculated with $\lambda_{87} = 1.42 \times 10^{-11}a^{-1}$. Calculating with the newly measured value of λ_{87}, $1.3979 \times 10^{-11}a^{-1}$, gives 4594 ± 50 Ma. H3 Tieschitz, a primitive H chondrite, gives a date of 4530 ± 60 Ma with 1.42, and 4604 ± 60 adjusted to 1.398. Minster and Allègre interpret the whole-rock combined meteorite isochron and the H3 Tieschitz internal isochron as dating the condensation of the chondrites from the nebula. The H6 Guareña isochron is recalculated to 4553 ± 80 (4480 ± 80 with 1.42), is interpreted by Minster and Allègre as a metamorphic age. The recalculated date agrees within error with the Pb-Pb age of H5 Richardton, but with the 80 Ma error, it could easily reflect a later metamorphic age as well.

Minster and Allègre (1981) reported a similar study of LL chondrites. The LL whole rock isochron from 10 meteorites yielded 4486 ± 20 Ma and initial Sr ratio 0.69881 ± 0.00012. Recalculated with the new decay-constant this is adjusted to 4555 ± 20 Ma. LL3 Krymka U-Pb data give a date of approximately 4547 Ma, in agreement with the Rb-Sr whole rock isochron (recalculated). LL4 Soko Banja chondrules yielded 4452 ± 20 Ma, which is recalculated to 4521 Ma. With the 20 Ma error, this nearly overlaps either the Krymka Pb-Pb dates, or the L/LL3 Unnamed Antarctic, and cannot be put into a context without a more precise date. The Rb-Sr ages from the literature have large errors compared with U-Pb ages. Recalculating the Rb-Sr ages with the new decay constant results in increasing the ages by about 1.6%, or about 70 Ma older for meteorites between 4400-4560 Ma. Because the errors are large, the recalculated ages for the H meteorites do not demand an interpretation that is unambiguously different from the original interpretations, but they suggest faster cooling than would be inferred from the ages originally calculated with $1.42 \times 10^{-11}a^{-1}$. The LL isochrons have smaller errors, and the recalculated ages would suggest much faster cooling

than the original ages would. But because LL parent body history is complex, the data are not precise enough or extensive enough to draw further conclusions.

7. Conclusions

1) Like H5 Richardton, chondrules from other EOCs have highly radiogenic Pb and can be used for U-Pb and Pb-Pb dating.
2) The Pb-Pb isochron and model dates of L5 Elenovka chondrules and chondrule fragments, 4555 ± 3 Ma, is resolved from the phosphate date of 4535 ± 1.
4) The difference in ages between silicates and phosphates in L5 Elenovka can be used to estimate the cooling rate for the L parent body at 14.8 ± 2.6 K/Ma between approximately 1055-759 K.
5) Some ordinary chondrite chondrules and silicate fractions and phosphates have well behaved U-Pb systems, while others do not. This may reflect processes on the parent body, including shock, as well as terrestrial weathering and contamination.
6) For both H and L classes, at least some type 4 meteorites have the same age as type 5. The best data currently come from type 5 chondrites. Estimates for type 5 peak temperatures are between 973-1023 K (Dodd, 1981), and estimates for pyroxene Pb closure temperatures are in the same range. It is therefore possible that thermal alteration did not affect U-Pb in some chondritic pyroxenes.
7) Aggressive leaching of chondritic silicates can fractionate U from Pb, but is effective at removing common Pb.
8) U-Pb exhibits closed system behaviour in many ordinary chondrites. This is exemplified by good agreement between Pb-Pb isochrons and model dates, which suggests that although a single stage Pb evolution model might be

somewhat oversimplified, it is not far from reality. This is in marked contrast to Rb-Sr. While the Rb-Sr system in the EOCs does preserve generally ancient ages, as exhibited by whole rock measurements that yield, within error, the ages of the parent bodies, it seems doubtful that Rb-Sr will achieve the kind of high resolution chronology in meteorites given by U-Pb. This is likely due to disturbances to the Rb-Sr system. The general failure of Rb-Sr models to produce coherent fine resolution chronological information attests to a more complex response to heating, impact, and weathering for Rb-Sr than U-Pb.

9) Rb-Sr is almost certainly disturbed by the aggressive leaching that is required for precise U-Pb analysis. Sample preparation optimized for Rb-Sr analysis may produce better results.

8. References

Amelin, Y. and Krot, A.N. (2007) Pb isotopic age of the Allende chondrules. *Meteoritics & Planet. Sci.* **42**, 1321-1335.

Amelin Y., Krot A. N., Hutcheon I. D., and Ulyanov A. A. (2002) Lead isotopic ages of chondrules and Calcium-Aluminum-Rich inclusions. Science 297, 1678–1683.

Amelin, Y., Ghosh, A., and Rotenberg, E. (2005) Unraveling the evolution of chondrite parent asteroids by precise U-Pb dating and thermal modeling. *Geochim. Cosmochim. Acta* **69**, 505-518.

Anders, E. and Zadnik M.G. (1985a) A subclassification of unequilibrated ordinary chondrites based on volatile element content. *Meteoritics & Planet. Sci.* **20**, 602.

Anders, E. and Zadnik M.G. (1985b) Unequilibrated ordinary chondrites: A tentatitve subclassification based on volatile-element content. *Geochim. Cosmochim. Acta* **49**, 1281-1291.

Bennet, M.E. III and McSween H.Y. (1996). Revised model calculations for the thermal histories of ordinary chondrite parent bodies. *Meteoritics & Planet. Sci.* **31,** 783-792.

Blinova, A., Amelin, Y., and Samson, C. (2007) Constraints on the cooling history of the H-chondrite parent body from phosphate and chondrule Pb-isotopic dates from Estacado. *Meteoritics & Planet. Sci.* **42,** 1337-1350.

Bouvier, A., Blichert-Toft, J., Moynier, F., Vervoort, J.D., and Albarède, F. (2007) Pb-Pb dating constraints on the accretion and cooling history of chondrites. *Geochim. Cosmochim. Acta* **71**, 1583-1604.

Brannon, J.C., Podosek, F.A., and Lugmair, G.W. (1988) Initial $^{87}Sr/^{86}Sr$ and Sm-Nd chronology of chondritic meteorites. IN: *Lunar and Planetary Science*

Conference, 18th, Houston, TX, Mar. 16-20, 1987, Proceedings (A89-10851 01-91). Cambridge and New York/Houston, TX, Cambridge University Press/Lunar and Planetary Institute, 1988, p. 555-564.

Brearly, A.J. and Jones, R.H. (1998) Chondritic meteorites. In *Planetary Materials*, Ed. Papike, J.J. Mineralogical Society of America, Washington, D.C., 3-1 – 3-398.

Chambers, J.E. (2003) Planet formation. In *Treatise on Geochemistry*, Turekian, K.K. and Holland, H.D. eds. Elsevier, 7800 p.

Cherniak D.J. (2001). Pb diffusion in Cr diopside, augite, and enstatite and consideration of the dependence of cation diffusion in pyroxene and oxygen fugacity. *Chem. Geol.* **177,** 381-397.

Cherniak D.J., Lanford W.A., and Ryerson F.J. (1991). Lead diffusion in apatite and zircon using ion implantation and Rutherford Backscattering techniques. *Geochim. Cosmochim. Acta* **55,** 1663-1673.

Dixon, E.T., Bogard, D.D., Garrison, D.H., and Rubin, A.E. (2004) ^{39}Ar-^{40}Ar evidence fo early impact events on the LL parent body. *Geochim. Cosmochim. Acta* **68,** 3779-1390.

Dodd R.T. (1969). Metamorphism of the ordinary chondrites: A review. *Geochim. Cosmochim. Acta* **33,** 161-203.

Dodd R.T. (1981). *Meteorites : A Petrologic-Chemical Synthesis.* Cambridge University Press, Cambridge. 368 p.

Dodd R.T. (1986). *Thunderstones and Shooting Stars: The Meaning of Meteorites.* Harvard University Press, Cambridge, Mass. 196 p.

Dunaway, J.K., Moersch, J., and Taylor, L.A. (2006) Petrogenisis and potential pairing of the Kunashak and Park Forest chondrites. In *Lunar. Planet. Sci. XXXVII*, abstract #1891, Lunar and Planetary Institute, Houston.

Evensen, N.M., Carter, S.R., Hamilton, P.J., O'Nions, R.K., and Ridley, W.I. (1979) A Combined chemical-petrological study of separated chondrules from the Richardton Meteorite. *Earth Planet. Sci. Lett.* **42**, 223-236.

Faure, G. (1986) *Principles of Isotope Geology, 2nd Ed.* John Wiley & Sons, New York, Chichester, Brisbane, Toronto, Singapore, 589 p.

Faure, G. and Powell, J.L. (1972) *Strontium Isotope Geology*. Springer-Verlag, Berlin, Heidelberg, and New York, 188 p.

Göpel D., Manhès G., and Allègre, C.J. (1994). U-Pb systematics of phosphates from equilibrated ordinary chondrites. *Earth Planet. Sci. Lett.* **121,** 153-171.

Goswami, J.N. and Vanhala H.A.T. (2000) Extinct radionuclides and the origin of the solar system. In *Protostars and Planets IV*. Mannings, V., Boss, A.P., and Russell, S. eds., University of Arizona Press, Tucson, pp. 963-994.

Grady, M. (2000) *Catalogue of Meteorites*. The Natural History Museum, London.

Hans, U., Kleine, T., and Bourdon, B. (2009) The chronology of accretion and volatile depletion of differentiated protoplanets inferred from Rb-Sr systematics of angrites. In *40th Lunar Planet. Sci. Conf.* abstract #2440. Lunar and Planetary Institute, Houston.

Herd, R.K., Hunt, P.A., Venance, K.E., Killgore, M .B. (2003) Comparative textural and mineralogical studies of two primitive ordinary chondrites: Saratov (L4) and an unnamed (L/LL3) from Antarctica. In *Lunar and Planetary Science XXXIV*, Abstract #2058, Lunar and Planetary Institute, Houston (CD-ROM).

Hewins R.H. (1997). Chondrules. *Ann. Rev. Earth Sci.* **25,** 61-83.

Ludwig, K. (1993) PbDat v. 1.24.

Ludwig, K. (2003) Isoplot/Ex 3.0 – A geochronological toolkit for Microsoft Excel. Berkeley Geochronology Center Special Publication No. 4.

McSween H.Y. (1999). *Meteorites and Their Parent Planets.* 2nd ed. Cambridge, Cambridge University Press. 310 p.

Minster, J.-F. and Allègre, C.J. (1979) ^{87}Rb-^{86}Sr chronology of H chondrites: Constraint and speculations on the early evolution of their parent body. *Earth Planet. Sci. Lett.* **42**, 333-347.

Minster, J.-F. and Allègre, C.J. (1981) ^{87}Rb-^{86}Sr dating of LL chondrites. *Earth Planet. Sci. Lett.* **56**, 89-106.

Miyamoto M., Fujii N., and Takeda H. (1980). A model of the ordinary chondrite parent body (abstract). *Lunar Planet. Sci.* **11,** 737-739.

Miyamoto, M., Fujii, N., and Takeda, H. (1981) Ordinary chondrite parent body: An internal heating model. *Proc. Lunar Planet. Sci.* **12B**, 1145-1152.

Perron C., Bourot-Denise M., Marti K., Kim J.S., and Crozaz G. (1992). The metal-phosphate connection in chondrites. *Meteoritics & Planet. Sci.***27,** 275.

Podosek, F.A. and Brannon, J.C. (1991) Chondrite chronology by initial $^{87}Sr/^{86}Sr$ in phosphates? *Meteoritics & Planet. Sci.* **26**, 145-152.

Rubin, A.E. (1990) Kamacite and olivine in ordinary chondrites: Intergroup and intragroup relationships. *Geochim. Cosmochim. Acta* **54,** 1217-1232**.**

Sears D.W.K. (1978) *The Nature and Origin of Meteorites*. A. Hilger, Bristol. 187 pp.

Sememenko, V.P. and Golovko, N.V. (1994) Shock-induced black veins and organic compounds in ordinary chondrites. *Geochim. Cosmochim. Acta* **58**, 1525-1535.

Tatsumoto, M, Knight, R.J., and Allègre, C.J. (1973) Time differences in the formation of meteorites as determined from the ratio of lead-207 to lead-206. *Science* **180**, 1279-1283.

Trieloff, M., Jessberger, E.K., Herrwerth, I., Hopp, J., Fiénei, C., Ghélis, M., Bourot-Denise, M., and Pellas, P. (2003) Structure and thermal history of the H-chondrite parent asteroid revealed by thermochronometry. *Nature* **422**, 502-506.

Urey H.C. and Craig H. (1953). The composition of stone meteorites and the origin of meteorites. *Geochim. Cosmochim. Acta.* **4,** 36-82.

Urey, H.C. (1955) The cosmic abundances of potassium, uranium, and thorium and the heat balances of the Earth, the Moon, and Mars. *Proc. Nat. Acad. Sci. USA* **41**, 127-144.

Van Schmus W.R. and Wood J.A. (1967). A chemical-petrologic classification for the chondritic meteorites. *Geochim. Cosmochim. Acta* **31,** 747-765.

Wasson J.T. (1972). Formation of ordinary chondrites. *Rev. Geophys. Space Phys.* **10,** 711-759.

Wasson J.T. (1985). *Meteorites: Their Record of Early Solar-System History.* W.H. Freeman, New York. 267 p.

Wood, J.A. (2005) The chondrite types and their origins, In *Chondrites and the Protoplanetary Disk*, Krot, A.N., Scott E.R.D., and Reipurth, B. eds., Astronomical Society of the Pacific.

Table 1 - Meteorites and Shock and Weathering Classification

Class	Meteorite	Shock	Weathering	
H4	**Ankober**			Fall
H5	**Orlovka**			Find
H5	**Richardton**	S2	W2	Fall
H6	**Kidairat**			Fall
L4	**Saratov**	S2		Fall
L5	**Elenovka**	S2	W0	Fall
L6	**Barwell**	S3		Fall
L6	**Kunashak**	S4		Fall
L6	**Pervomaisky**			Fall
L/LL3	**Unnamed Antarctic**	S1-S2	Moderate	
L/LL4	**Bjurböle**	S1		Fall
L/LL6	**Holbrook**	S2		Fall
LL3.1	**Krymka**	S3		Fall
LL5	**Tuxtuac**	S2		Fall

Shock and weathering information from Grady (2000), Herd et al. (2003), and Dunaway et al. (2006)

Table 2 - Samples and Descriptions

Class	Meteorite	Fraction	Description	Cleaning
H4	**Ankober**	Chondrule 1	Large whole chondrule. Dark Grey.	
H4	**Ankober**	Chondrule 2	Large whole chondrule. Dark Grey.	
H4	**Ankober**	Chondrule 3	Whole chondrule. Dark Grey.	
H4	**Ankober**	Chondrule 4	Whole chondrule. Dark Grey.	
H4	**Ankober**	Chondrule 5	Whole chondrule. Light Grey.	
H4	**Ankober**	Fragment 6	Large chondrule fragment	
H4	**Ankober**	Fragment 7	Small chondrule fragment. Radial.	
H5	**Orlovka**	Fraction 1	Dark grey grains. Considerable orange staining.	
H5	**Orlovka**	Fraction 2	Light grey grains. Considerable orange staining.	
H5	**Orlovka**	Phosphate 1	Bulk phosphate fraction.	
H5	**Orlovka**	Phosphate 2	Grains with orange-yellow surface coating but without black inclusions.	
H5	**Orlovka**	Phosphate 3	Clear, yellow-reddish.	
H6	**Kidairat**	Chondrule 1	Mechanically crushed. Not washed	
H6	**Kidairat**	Chondrule E1	Grey, barred chondrule.	EPD
H6	**Kidairat**	Chondrule E2	Grey grains.	EPD
H6	**Kidairat**	Chondrule E3	Grey and clear, radial, chondrule fragment.	EPD
H6	**Kidairat**	Chondrule E4	Clear and white grains, with some opaque material.	EPD
H6	**Kidairat**	Chondrule E5	White grains - nearly whole chondrule.	EPD
H6	**Kidairat**	Chondrule E6	White grains - nearly whole chondrule.	EPD
H6	**Kidairat**	Chondrule M4	Clear grains, radial.	
H6	**Kidairat**	Chondrule M5	Mostly clear grains, some opaque material.	
H6	**Kidairat**	Chondrule M6	Large fragment	
H6	**Kidairat**	Chondrule E7	White and clear chondrule.	EPD
L4	**Saratov**	Chondrule 1	Dark chondrule with bleached rim	
L4	**Saratov**	Chondrule 2	Dark chondrule with bleached rim	
L4	**Saratov**	Chondrule 3	Small dark chondrule	
L4	**Saratov**	Fraction 1	Light grey grains. No staining.	
L4	**Saratov**	Fraction 2	Light grey grains. Considerable orange staining.	
L4	**Saratov**	Fragment 4	Light grey chondrule fragment. Prior to initial washing, encrusted in rusty material	
L4	**Saratov**	Phosphate	Mixture of orange-yellow, and colorless grains.	
L5	**Elenovka**	Chondrule 1	Light grey, semi-translucent chondrule with rare opaque inclusions. Crushed	
L5	**Elenovka**	Chondrule 2	Translucent with abundant black inclusions.	
L5	**Elenovka**	Pyroxene 1	> 100 mesh, medium to light grey fragments.	

Table 2 - Samples and Descriptions

Class	Meteorite	Fraction	Description	Cleaning
L5	**Elenovka**	Pyroxene 2	> 100 mesh, four fragments of light-grey material with slight yellow staining	
L5	**Elenovka**	Pyroxene 3	> 100 mesh. Light coloured grains and fragments with no or almost no visible dark inclusions.	
L5	**Elenovka**	Pyroxene 4	> 100 mesh. Light coloured grains and fragments with abundant dark inclusions.	
L5	**Elenovka**	Phosphate 1	Clear colorless phosphate fraction.	
L5	**Elenovka**	Phosphate 2	Yellow-orange phosphate fraction.	
L5	**Elenovka**	Phosphate 3	Mixture of yellow-orange grains, relatively clear.	
L6	**Barwell**	Chondrule 1	Large, light and medium grey chondrule.	
L6	**Barwell**	Chondrule 2	Light grey chondrule.	
L6	**Barwell**	Chondrule 3	~½ of a dark grey chondrule	
L6	**Barwell**	Chondrule 4	One light grey chondrule	
L6	**Barwell**	Chondrule 5	Most of one light grey chondrule.	
L6	**Kunashak**		Dark grey grains. Small troilite crystals dot the grains.	
L6	**Pervomaisky**		Small light grey grains.	
L/LL3	**Unnamed Antarctic**	Chondrule 1	Fragments. Acid bleaching visible, espeically on smaller fragments.	
L/LL3	**Unnamed Antarctic**	Chondrule 2	Slight bleaching of chondrule surface, no visible effect on interior.	
L/LL3	**Unnamed Antarctic**	Chondrule 3a	Acid washing - no visible effect.	
L/LL3	**Unnamed Antarctic**	Chondrule 3b	Acid washing - no visible effect.	
L/LL3	**Unnamed Antarctic**	Chondrule 4	Acid washing - strong bleaching.	
L/LL3	**Unnamed Antarctic**	Chondrule 6	Acid washing - minimal bleaching.	
L/LL4	**Bjurböle**	Chondrule 10	Finely crushed chondrule	
L/LL4	**Bjurböle**	Chondrule 11	Uncrushed chondrule	
L/LL4	**Bjurböle**	Chondrule 12	Finely crushed chondrule	
L/LL4	**Bjurböle**	Chondrule 13	Uncrushed chondrule	
L/LL4	**Bjurböle**	Chondrule 14	Finely crushed chondrule	
L/LL4	**Bjurböle**	Chondrule 15	Finely crushed chondrule	
L/LL4	**Bjurböle**	Chondrule 7	Finely crushed chondrule	
L/LL4	**Bjurböle**	Chondrule 8	Finely crushed chondrule	
L/LL4	**Bjurböle**	Chondrule 9	Finely crushed chondrule	
L/LL4	**Bjurböle**	Fraction 1	Light grey grains. Some troilite. Some rusty staining.	
L/LL4	**Bjurböle**	Fraction 2	Light grey grains with white rims.	
L/LL4	**Bjurböle**	Pyroxene 1	> 100 mesh, medium to dark grey grains and fragments. Fine grained and radial. Some intergrown with troilite.	
L/LL4	**Bjurböle**	Pyroxene 2	Medium to light grey chondrules and fragments. Coarse grained.	

Table 2 - Samples and Descriptions

Class	Meteorite	Fraction	Description	Cleaning
L/LL4	**Bjurböle**	Phosphate 2	Clear colorless grains with minor surface alteration, or rough surface or very tiny inclusions.	
L/LL4	**Bjurböle**	Phosphate 3	Clear colorless phosphate fraction.	
L/LL6	**Holbrook**	Chondrule E11	Chondrule fragment	EPD
L/LL6	**Holbrook**	Chondrule E12	Chondrule fragment	EPD
L/LL6	**Holbrook**	Chondrule E9	Chondrule fragment	EPD
L/LL6	**Holbrook**	Chondrule Fragments	Eight chondrule fragments from different chondrules	EPD
LL3	**Krymka**	Fraction 1	Dark grey grains. Slight orange staining.	
LL3	**Krymka**	Fraction 10	Assorted chondrule fragments.	
LL3	**Krymka**	Fraction 11	Dark to medium grey chondrule fragments.	
LL3	**Krymka**	Fraction 12	Medium to light grey chondrules and fragments. Fine grained.	
LL3	**Krymka**	Fraction 13	Fragments of barred and porphyritic chondrules. Olivine rich.	
LL3	**Krymka**	Fraction 2	Light grey grains. Some orange staining.	
LL3	**Krymka**	Fraction 3	Dark grey chondrule fragments, fine grained.	
LL3	**Krymka**	Fraction 4	Medium grey chondrule fragments. Fine grained.	
LL3	**Krymka**	Fraction 5	Fragments of porphyritic chondrules, mostly olivine rich.	
LL3	**Krymka**	Fraction 6	Fragments of barred and radial chondrules	
LL3	**Krymka**	Fraction 7	Light grey fragments with fine texture containing dark inclusions.	
LL3	**Krymka**	Fraction 8	Very light grey, yellowish chondrule fragments.	
LL3	**Krymka**	Pyroxene 1	> 100 mesh, medium to dark grey	
LL3	**Krymka**	Pyroxene 2	> 100 mesh, medium to dark grey	
LL3	**Krymka**	Phosphate 1	Bulk phosphate fraction.	
LL3	**Krymka**	Phosphate 2	Fraction with yellow coating and other imperfections.	
LL3	**Krymka**	Phosphate 3	Mixture of yellow-orange grains, relatively clear.	
LL5	**Tuxtuac**	Chondrule 1	Small dark grey chondrule	
LL5	**Tuxtuac**	Chondrule 2	½ of a dark grey chondrule	
LL5	**Tuxtuac**	Chondrule 3	Large chondrule fragment, some residual rust staining.	
LL5	**Tuxtuac**	Chondrule 4	½ of a chondrule	
LL5	**Tuxtuac**	Chondrule 5	Fragment of a dark grey fine grained chondrule	

EPD - Electric Pulse Disaggregation

Table 3 - U and Pb abundances and ratios

Class Meteorite	Fraction	Weight (mg)	U (ppm)	Pb (ppm)	$^{206}Pb/^{204}Pb$ (meas)[a]	% err	$^{206}Pb/^{204}Pb$ (corr)[b]	$^{208}Pb/^{204}Pb$ (corr)[b]	% err	$^{238}U/^{204}Pb$ (corr)[b]	% err	$^{238}U/^{206}Pb$ (corr)[b]	%err	$^{207}Pb/^{206}Pb$ (corr)[b]	% err	ρ 4/6-7/6
H4 Ankober	Chondrule 1	2.060	nd	0.0337	336.1	9.8	528.0	499.1	25.2	nd		nd		0.633 79	0.5	0.689
H4 Ankober	Chondrule 2	0.670	nd	0.0276	158.1	8.4	419.9	456.4	78.4	nd		nd		0.631 46	1.3	0.974
H4 Ankober	Chondrule 3	0.430	nd	0.0235	100.5	0.3	247.6	199.8	67.8	nd		nd		0.641 74	2.1	0.969
H4 Ankober	Chondrule 4	0.270	nd	0.0359	112.2	8.4	466.8	458.6	162.0	nd		nd		0.641 29	2.3	0.967
H4 Ankober	Chondrule 5	0.510	nd	0.0343	247.0	8.4	3514.0	2479.2	637.0	nd		nd		0.624 89	1.3	0.967
H4 Ankober	Fragment 6	1.140	nd	0.0460	424.1	5.2	964.8	702.6	56.5	nd		nd		0.626 72	0.4	0.951
H4 Ankober	Fragment 7	0.540	nd	0.0429	170.4	4.3	340.3	295.2	44.3	nd		nd		0.634 16	0.9	0.981
H5 Orlovka	Fraction 1	1.288	0.0210	0.0331	94.5	3.9	106.2	125.5	3.3	166.1	5.0	1.5648	1.5	0.665 28	0.3	0.884
H5 Orlovka	Fraction 2	2.730	0.0286	0.0677	564.7	6.0	678.9	609.8	5.8	625.3	6.2	0.9211	0.5	0.628 24	0.1	0.728
H5 Orlovka	Phosphate 1	0.035	3.4068	6.1296	24.8	1.8	25.4	42.3	0.9	40.9	10.1	1.6089	10.3	0.648 04	1.9	0.752
H5 Orlovka	Phosphate 2	0.066	0.1355	0.4106	118.2	43.5	218.7	312.7	41.8	191.9	48.7	0.8772	65.3	0.642 41	60.7	1.000
H5 Orlovka	Phosphate 3	0.151	0.2991	0.6699	240.3	4.7	267.3	188.7	4.1	241.6	7.5	0.9038	8.9	0.636 73	6.6	1.000
H6 Kidairat	Chondrule 1	1.530	nd	0.0205	92.5	13.4	118.2	225.6	13.5	nd		nd		0.644 28	0.8	0.968
H6 Kidairat	Chondrule E1	0.119	nd	0.0853	20.7	2.1	20.7	40.0	6.4	nd		nd		0.807 56	0.8	0.736
H6 Kidairat	Chondrule E2	1.459	nd	0.0893	53.7	2.0	55.8	107.1	3.3	nd		nd		0.695 53	0.3	0.792
H6 Kidairat	Chondrule E3	1.211	nd	0.1682	19.5	0.7	19.5	38.4	1.1	nd		nd		0.820 06	0.8	-0.004
H6 Kidairat	Chondrule E4	2.126	nd	0.0268	105.0	12.9	132.7	243.6	12.6	nd		nd		0.647 14	0.7	0.986
H6 Kidairat	Chondrule E5	1.501	nd	0.0265	100.7	19.4	140.0	252.4	19.0	nd		nd		0.647 23	0.9	0.988
H6 Kidairat	Chondrule E6	3.222	nd	0.0488	253.4	11.9	318.4	564.8	11.9	nd		nd		0.626 06	0.3	0.953
H6 Kidairat	Chondrule M5	0.374	nd	0.1085	128.0	30.0	205.4	390.6	29.9	nd		nd		0.630 75	1.0	0.984
H6 Kidairat	Chondrule M6	0.370	nd	0.0715	85.7	26.6	129.6	230.5	25.9	nd		nd		0.643 06	1.4	0.985
H6 Kidairat	Chondrule E7	0.253	nd	0.0379	25.3	6.4	27.2	51.5	6.6	nd		nd		0.770 07	1.5	0.944
L4 Saratov	Chondrule 1	3.700	0.0711	0.0267	82.6	2.6	87.3	89.6	2.5	543.3	3.6	6.2230	1.3	0.673 29	0.2	0.791
L4 Saratov	Chondrule 2	2.120	0.1240	0.0312	75.8	3.7	81.7	87.2	4.3	772.3	5.0	9.4559	1.5	0.676 63	0.3	0.772
L4 Saratov	Chondrule 3	1.680	0.1565	0.0315	44.8	2.2	46.8	55.8	1.2	589.7	4.1	12.6096	1.8	0.720 22	0.3	0.887
L4 Saratov	Fraction 1	4.282	0.0148	0.0423	64.4	0.5	65.5	70.8	0.4	55.3	0.9	0.8443	0.6	0.692 05	0.1	0.480
L4 Saratov	Fraction 2	4.833	0.0177	0.0464	70.3	0.5	71.3	63.7	0.3	60.9	0.9	0.8540	0.6	0.686 32	0.1	0.298
L4 Saratov	Fragment 4	0.770	0.3415	0.0542	43.5	2.9	45.9	62.3	2.7	774.0	5.3	16.8600	2.2	0.719 03	0.4	0.817
L4 Saratov	Phosphate	0.056	0.0665	0.4519	30.9		31.5	39.4	0.5	12.2	67.4	0.3857	67.4	0.755 91	1.7	0.980
L5 Elenovka	Chondrule 1	5.292	0.0181	0.0577	472.3	6.5	543.5	1002.5	6.5	511.8	6.8	0.9417	1.1	0.627 78	0.1	0.815
L5 Elenovka	Chondrule 2	4.298	0.0076	0.0234	330.2	14.9	441.4	707.7	14.7	401.7	15.8	0.9100	3.2	0.629 73	0.2	0.926
L5 Elenovka	Pyroxene 1	1.987	0.0196	0.0581	405.8	43.1	924.6	1616.9	43.0	908.1	44.0	0.9822	1.2	0.624 39	0.3	0.925
L5 Elenovka	Pyroxene 2	0.989	0.0142	0.0433	200.5	87.8	695.8	1237.8	87.4	673.1	90.4	0.9674	3.2	0.625 44	0.9	0.954
L5 Elenovka	Pyroxene 3	1.454	0.0216	0.0694	366.9	18.6	521.8	937.8	18.5	481.6	19.6	0.9230	3.3	0.628 40	0.2	0.956
L5 Elenovka	Pyroxene 4	3.465	0.0198	0.0628	541.0	11.4	683.0	1230.3	11.4	637.6	11.8	0.9336	1.5	0.626 36	0.1	0.869
L5 Elenovka	Phosphate 1	0.105	2.0449	3.8839	878.1	4.0	964.4	480.5	3.8	926.2	4.3	0.9604	1.2	0.616 22	0.1	0.425
L5 Elenovka	Phosphate 2	0.085	1.0144	2.1084	674.0	8.2	807.5	534.8	7.8	764.3	8.9	0.9465	2.9	0.617 09	0.1	0.710
L5 Elenovka	Phosphate 3	0.193	1.4551	3.9829	87.7	0.2	88.2	73.2	0.2	69.7	1.1	0.7900	1.0	0.665 21	0.1	-0.105

Table 3 - U and Pb abundances and ratios

Class Meteorite	Fraction	Weight (mg)	U (ppm)	Pb (ppm)	$^{206}Pb/^{204}Pb$ (meas)[a]	% err	$^{206}Pb/^{204}Pb$ (corr)[b]	$^{208}Pb/^{204}Pb$ (corr)[b]	% err	$^{238}U/^{204}Pb$ (corr)[b]	% err	$^{238}U/^{206}Pb$ (corr)[b]	%err	$^{207}Pb/^{206}Pb$ (corr)[b]	% err	ρ 4/6-7/6
L6 Barwell	Chondrule 1	10.500	0.0308	0.2036	21.1	0.1	21.1	40.3	0.2	10.5	20.2	0.4047	1.0	0.853 92	0.0	-0.749
L6 Barwell	Chondrule 2	2.090	0.0142	0.8330	18.0	0.1	18.0	37.7	0.4	1.1	1.9	0.5290	1.1	0.897 99	0.0	-0.667
L6 Barwell	Chondrule 3	2.180	0.0084	1.0534	17.4	0.1	17.4	37.1	0.3	0.5	3.1	0.4054	1.1	0.906 90	0.4	-0.080
L6 Barwell	Chondrule 4	1.250	0.0176	1.4205	17.6	0.1	17.6	37.4	0.2	0.8	2.5	0.5220	1.1	0.902 57	0.1	-0.573
L6 Barwell	Chondrule 5	1.140	0.0331	2.4206	17.7	0.1	17.8	37.4	0.4	0.9	1.9	0.3348	1.0	0.900 48	0.1	-0.572
L6 Kunashak		0.656	0.0219	0.0096	109.0	192.0	673.6	848.9	188.0	3612.6	198.0	5.3632	5.8	0.460 92	4.6	0.992
L6 Pervomaisky		2.690	0.0173	0.0197	372.6	18.6	599.2	580.5	18.0	1155.8	19.3	1.9288	0.9	0.577 59	0.3	0.943
L/LL4 Bjurböle	Chondrule 10	3.360	0.0068	0.0224	46.0	1.4	47.2	52.9	2.2	35.3	2.8	0.7462	1.7	0.714 03	0.2	0.831
L/LL4 Bjurböle	Chondrule 11	1.750	0.0347	0.0315	26.6	0.7	26.9	60.2	0.9	103.9	3.0	3.8658	1.8	0.784 03	0.2	0.689
L/LL4 Bjurböle	Chondrule 12	3.310	0.0127	0.0440	43.1	0.7	43.7	54.9	2.7	32.6	1.4	0.7462	0.9	0.721 99	0.1	0.573
L/LL4 Bjurböle	Chondrule 13	1.980	0.0175	0.0639	43.8	0.8	44.5	58.0	1.4	32.1	1.7	0.7204	1.1	0.715 67	0.1	0.686
L/LL4 Bjurböle	Chondrule 14	3.830	0.0030	0.0126	47.4	2.8	50.1	96.3	2.9	37.9	6.1	0.7564	4.0	0.706 84	0.4	0.902
L/LL4 Bjurböle	Chondrule 15	25.710	0.0010	0.0030	64.3	2.2	67.3	80.1	1.6	55.1	3.4	0.8195	1.6	0.686 74	0.2	0.784
L/LL4 Bjurböle	Chondrule 7	3.390	0.1243	0.4140	19.2	0.1	19.2	39.0	0.5	19.5	0.3	1.0136	0.3	0.831 24	0.0	-0.803
L/LL4 Bjurböle	Chondrule 8	3.420	0.0277	0.0776	73.7	0.7	74.9	76.7	0.6	62.8	1.1	0.8382	0.6	0.678 00	0.1	0.531
L/LL4 Bjurböle	Chondrule 9	1.900	0.0193	0.0500	81.0	2.1	84.7	68.4	1.2	70.3	2.9	0.8295	1.2	0.669 29	0.2	0.781
L/LL4 Bjurböle	Fraction 1	2.437	0.0337	0.1022	57.6	0.3	58.3	67.1	0.3	47.6	0.7	0.8164	0.5	0.698 06	0.1	0.254
L/LL4 Bjurböle	Fraction 2	1.016	0.0601	0.1470	103.3	1.0	106.8	93.8	0.8	96.0	1.4	0.8991	0.6	0.661 12	0.1	0.655
L/LL4 Bjurböle	Pyroxene 1	2.203	0.0343	0.0900	80.2	1.4	83.7	80.2	1.0	72.8	1.9	0.8697	0.6	0.673 62	0.1	0.829
L/LL4 Bjurböle	Pyroxene 2	2.054	0.0208	0.0664	54.0	1.3	56.2	67.6	0.9	44.4	2.2	0.7901	1.0	0.700 19	0.2	0.814
L/LL4 Bjurböle	Phosphate 2	0.311	0.0056	1.1777	19.8	0.5	19.8	38.5	0.6	0.3	40.5	0.0158	40.5	0.873 13	0.8	0.866
L/LL4 Bjurböle	Phosphate 3	0.230	0.1549	4.0869	19.8	0.1	19.9	38.4	0.2	2.5	7.0	0.1252	7.0	0.839 68	0.2	0.947
L/LL6 Holbrook	Chondrule E11	0.410	0.0191	0.0571	76.0	3.7	82.5	99.7	4.0	69.0	7.6	0.8368	5.9	0.674 33	0.3	0.911
L/LL6 Holbrook	Chondrule E12	0.400	0.0267	0.0711	164.0	8.0	197.4	224.6	7.3	178.0	9.8	0.9017	4.4	0.642 66	0.4	0.693
L/LL6 Holbrook	Chondrule E9	0.450	0.0098	0.0300	81.0	7.6	95.3	121.0	12.1	79.6	14.1	0.8349	10.4	0.667 90	0.5	0.956
L/LL6 Holbrook	Chondrule Fragments	0.990	nd	282.5190	292.0	0.7	292.7	324.1	1.5	nd		nd		0.638 02	0.1	-0.046
LL3 Krymka	Fraction 1	0.877	0.0123	0.0432	35.6	1.1	36.6	53.3	0.7	29.1	3.9	0.7955	3.2	0.743 19	0.2	0.612
LL3 Krymka	Fraction 10	0.800	0.0119	0.0614	30.2	0.5	41.3	48.3	6.4	17.2	0.7	0.7981	7.4	0.750 55	0.9	0.956
LL3 Krymka	Fraction 11	2.100	0.0055	0.0233	36.2	0.3	41.1	52.9	7.3	23.9	0.4	0.7209	7.0	0.726 75	1.1	0.973
LL3 Krymka	Fraction 12	2.320	0.0075	0.0270	45.3	0.3	38.0	61.1	0.4	33.6	0.4	3.5163	1.7	0.735 24	0.2	0.885
LL3 Krymka	Fraction 13	2.370	0.0063	0.0258	40.1	0.4	32.8	58.1	8.6	27.2	0.7	0.6233	7.6	0.749 23	0.9	0.960
LL3 Krymka	Fraction 2	1.295	0.0135	0.0544	35.3	0.6	35.8	53.1	0.4	25.0	2.5	0.6969	2.2	0.743 93	0.1	0.582
LL3 Krymka	Fraction 3	0.950	0.0125	0.0487	36.1	0.5	52.2	52.9	0.6	26.1	0.7	0.7928	5.0	0.703 54	1.0	0.979
LL3 Krymka	Fraction 4	1.720	0.0127	0.0454	44.0	0.3	49.0	60.3	0.8	33.3	0.5	0.7960	4.0	0.710 24	0.7	0.974
LL3 Krymka	Fraction 5	3.480	0.0756	0.0618	37.0	0.2	45.2	55.0	0.6	127.0	1.0	0.7268	5.4	0.714 52	0.9	0.957
LL3 Krymka	Fraction 6	3.680	0.0715	0.0463	40.0	0.2	44.9	57.0	1.0	169.8	1.1	0.7079	1.8	0.719 53	0.3	0.936
LL3 Krymka	Fraction 7	1.230	0.0134	0.0576	39.9	0.1	44.1	57.1	0.4	25.5	0.2	0.6751	4.6	0.710 28	0.8	0.970
LL3 Krymka	Fraction 8	2.350	0.0192	0.0756	43.0	0.2	41.7	60.6	0.3	29.8	0.5	4.3683	1.9	0.723 47	0.3	0.945

Table 3 - U and Pb abundances and ratios

Class Meteorite	Fraction	Weight (mg)	U (ppm)	Pb (ppm)	$^{206}Pb/^{204}Pb$ (meas)[a]	% err	$^{206}Pb/^{204}Pb$ (corr)[b]	$^{208}Pb/^{204}Pb$ (corr)[b]	% err	$^{238}U/^{204}Pb$ (corr)[b]	% err	$^{238}U/^{206}Pb$ (corr)[b]	%err	$^{207}Pb/^{206}Pb$ (corr)[b]	% err	ρ 4/6-7/6
LL3 Krymka	Pyroxene 1	1.269	0.0121	0.0394	63.4	5.1	72.5	88.5	4.0	56.0	7.5	0.7718	2.7	0.685 29	0.5	0.895
LL3 Krymka	Pyroxene 2	1.650	0.0099	0.0363	38.3	1.9	40.3	57.3	1.2	30.1	4.3	0.7480	2.5	0.731 21	0.3	0.850
LL3 Krymka	Phosphate 1	0.160	0.0019	0.0889	19.2	1.1	18.8	38.9	1.0	1.4	231.0	0.0733	231.0	0.852 35	1.4	0.862
LL3 Krymka	Phosphate 2	0.220	0.0013	0.0313	22.4	5.2	23.2	43.6	3.7	3.1	248.0	0.1341	248.1	0.816 90	6.9	0.963
LL3 Krymka	Phosphate 3	0.567	0.1215	63.1158	17.9	0.1	18.0	37.9	0.2	0.1	8.1	0.0067	8.1	0.868 35	0.2	0.756
LL3 Unnamed Antarctic	Chondrule 1	8.270	0.0165	0.1314	16.7	0.1	16.7	38.4	0.2	7.7	0.4	0.4609	0.4	0.887 01	0.1	-0.518
LL3 Unnamed Antarctic	Chondrule 2	13.510	0.0443	0.4950	14.1	0.1	14.1	34.0	0.2	4.8	1.5	0.3415	1.5	0.932 50	0.1	-0.820
LL3 Unnamed Antarctic	Chondrule 3a	36.610	0.0178	0.1029	22.4	0.2	22.5	45.7	0.2	13.1	2.3	0.5831	2.3	0.808 22	0.1	-0.397
LL3 Unnamed Antarctic	Chondrule 3b	24.410	0.0193	0.1129	22.8	0.1	22.8	46.1	0.2	13.1	0.6	0.5727	0.6	0.804 80	0.1	-0.592
LL3 Unnamed Antarctic	Chondrule 4	12.760	0.0058	0.1069	12.5	0.4	12.5	40.5	0.5	3.1	0.8	0.2488	0.7	0.984 44	0.2	-0.034
LL3 Unnamed Antarctic	Chondrule 6	6.640	0.0319	0.3352	14.2	0.1	14.3	33.7	0.2	5.1	0.4	0.3596	0.4	0.928 68	0.1	-0.547
LL5 Tuxtuac	Chondrule 1	0.930	0.0173	1.9329	17.3	0.1	17.3	37.1	1.4	0.5	3.6	0.5201	1.1	0.908 25	0.1	-0.458
LL5 Tuxtuac	Chondrule 2	2.830	1.8504	0.6761	17.5	0.1	17.5	37.4	1.3	169.9	0.3	0.4866	1.0	0.904 18	0.1	-0.367
LL5 Tuxtuac	Chondrule 3	6.950	0.0094	0.3061	18.4	0.2	18.4	38.8	1.2	2.0	2.7	0.4326	2.6	0.888 28	0.1	-0.138
LL5 Tuxtuac	Chondrule 4	3.750	0.0134	0.4767	16.9	0.6	16.9	36.3	0.6	1.7	39.4	0.5241	25.1	0.917 31	7.1	-0.001
LL5 Tuxtuac	Chondrule 5	0.590	0.0143	2.8810	17.1	0.1	17.1	36.8	0.4	0.3	6.8	0.5509	1.1	0.911 42	0.1	-0.601

[a] Measured $^{206}Pb/^{204}Pb$. Errors are 2σ%

[b] Corrected for fractionation, spike, and procedure blank.

Table 4 - Radiogenic Pb and Pb isotopic ratios and model dates

Class	Meteorite	Fraction	$^{206}Pb^*/^{238}U^a$	% err	$^{207}Pb^*/^{235}U^a$	% err	ρ 6/8-7/5	$^{207}Pb^*/^{206}Pb^{*a}$	% err	$^{206}Pb^*/^{238}U$ Date	$^{207}Pb^*/^{235}U$ Date	(CDT primordial) $^{207}Pb^*/^{206}Pb^*$ Date	2σ err
H4	**Ankober**	Chondrule 1	nd		nd		nd	0.625 32	0.35	nd	nd	4568.0	5.0
H4	**Ankober**	Chondrule 2	nd		nd		nd	0.620 71	0.33	nd	nd	4557.2	4.8
H4	**Ankober**	Chondrule 3	nd		nd		nd	0.623 60	0.58	nd	nd	4564.0	8.4
H4	**Ankober**	Chondrule 4	nd		nd		nd	0.631 84	0.67	nd	nd	4583.0	9.6
H4	**Ankober**	Chondrule 5	nd		nd		nd	0.623 61	0.34	nd	nd	4564.0	4.9
H4	**Ankober**	Fragment 6	nd		nd		nd	0.622 05	0.14	nd	nd	4560.4	2.0
H4	**Ankober**	Fragment 7	nd		nd		nd	0.620 89	0.21	nd	nd	4557.7	3.0
H5	**Orlovka**	Fraction 1	0.583	1.56	50.078	1.56	0.996	0.622 93	0.14	2961	3994	4562.4	2.1
H5	**Orlovka**	Fraction 2	1.071	0.48	91.775	0.48	0.993	0.621 59	0.06	4693	4600	4559.3	0.8
H5	**Orlovka**	Phosphate 1	0.394	9.53	20.806	2.00	0.983	0.383 19	2.00	2140	3130	3844.4	28.0
H5	**Orlovka**	Phosphate 2	1.091	9.18	93.579	0.35	0.999	0.621 81	0.35	4757	4619	4559.8	5.0
H5	**Orlovka**	Phosphate 3	1.068	5.56	91.264	0.11	1.000	0.619 80	0.11	4684	4594	4555.1	1.5
H6	**Kidairat**	Chondrule 1	nd		nd		nd	0.604 83	0.24	nd	nd	4519.6	3.4
H6	**Kidairat**	Chondrule E1	nd		nd		nd	0.563 45	1.47	nd	nd	4416.5	21.5
H6	**Kidairat**	Chondrule E2	nd		nd		nd	0.613 44	0.21	nd	nd	4540.2	3.0
H6	**Kidairat**	Chondrule E3	nd		nd		nd	0.559 23	2.20	nd	nd	4405.5	32.1
H6	**Kidairat**	Chondrule E4	nd		nd		nd	0.612 53	0.13	nd	nd	4538.0	1.9
H6	**Kidairat**	Chondrule E5	nd		nd		nd	0.614 55	0.18	nd	nd	4542.8	2.6
H6	**Kidairat**	Chondrule E6	nd		nd		nd	0.611 60	0.09	nd	nd	4535.8	1.3
H6	**Kidairat**	Chondrule M5	nd		nd		nd	0.608 19	0.21	nd	nd	4527.7	3.0
H6	**Kidairat**	Chondrule M6	nd		nd		nd	0.607 23	0.30	nd	nd	4525.4	4.3
H6	**Kidairat**	Chondrule E7	nd		nd		nd	0.595 59	0.96	nd	nd	4497.3	13.9
L4	**Saratov**	Chondrule 1	0.144	1.31	12.305	1.32	0.992	0.621 65	0.17	865	2628	4559.4	2.4
L4	**Saratov**	Chondrule 2	0.094	1.65	8.028	1.66	0.987	0.621 40	0.27	577	2234	4558.9	3.9
L4	**Saratov**	Chondrule 3	0.064	2.02	5.468	2.01	0.996	0.624 36	0.19	397	1896	4565.7	2.7
L4	**Saratov**	Fraction 1	1.016	0.64	87.340	0.64	0.993	0.623 46	0.08	4520	4550	4563.7	1.1
L4	**Saratov**	Fraction 2	1.018	0.65	87.511	0.66	0.991	0.623 34	0.09	4527	4552	4563.4	1.3
L4	**Saratov**	Fragment 4	0.047	2.56	4.046	2.55	0.991	0.620 61	0.35	298	1644	4557.0	5.0
L4	**Saratov**	Phosphate	1.827	67.30	153.470	67.30	1.000	0.609 18	0.41	6700	5118	4530.1	5.9
L5	**Elenovka**	Chondrule 1	1.044	1.10	89.143	1.10	0.999	0.619 45	0.06	4608	4571	4554.3	0.8
L5	**Elenovka**	Chondrule 2	1.076	3.18	91.881	3.18	1.000	0.619 47	0.10	4708	4601	4554.3	1.4
L5	**Elenovka**	Pyroxene 1	1.008	1.29	86.089	1.29	0.995	0.619 49	0.13	4494	4536	4554.4	1.9
L5	**Elenovka**	Pyroxene 2	1.020	3.50	87.037	3.47	0.997	0.618 92	0.28	4532	4547	4553.1	4.1

Table 4 - Radiogenic Pb and Pb isotopic ratios and model dates

Table 4 - Radiogenic Pb and Pb isotopic ratios and model dates

Class	Meteorite	Fraction	$^{206}Pb^*/^{238}U^a$	% err	$^{207}Pb^*/^{235}U^a$	% err	ρ 6/8-7/5	$^{207}Pb^*/^{206}Pb^{*a}$	% err	$^{206}Pb^*/^{238}U$ Date	$^{207}Pb^*/^{235}U$ Date	(CDT primordial) $^{207}Pb^*/^{206}Pb^*$ Date	2σ err
L5	**Elenovka**	Pyroxene 3	1.064	3.30	90.922	3.30	1.000	0.619 72	0.08	4672	4590	4554.9	1.1
L5	**Elenovka**	Pyroxene 4	1.057	1.52	90.280	1.52	0.999	0.619 73	0.06	4648	4583	4555.0	0.9
L5	**Elenovka**	Phosphate 1	1.031	1.23	86.936	1.23	0.999	0.611 45	0.06	4568	4545	4535.5	0.9
L5	**Elenovka**	Phosphate 2	1.044	2.93	88.034	2.93	1.000	0.611 39	0.07	4610	4558	4535.3	1.0
L5	**Elenovka**	Phosphate 3	1.132	1.03	95.746	1.03	0.998	0.613 24	0.07	4881	4642	4539.7	1.0
L6	**Barwell**	Chondrule 1	1.383	1.04	96.384	1.07	1.040	0.505 49	0.20	5598	4649	4257.3	2.9
L6	**Barwell**	Chondrule 2	0.912	1.12	59.142	1.18	1.120	0.470 29	0.30	4179	4160	4150.7	4.4
L6	**Barwell**	Chondrule 3	1.147	1.08	72.453	1.99	1.080	0.458 23	1.65	4925	4363	4112.2	24.5
L6	**Barwell**	Chondrule 4	0.905	1.06	57.718	1.14	1.060	0.462 48	0.34	4155	4135	4125.9	5.0
L6	**Barwell**	Chondrule 5	1.421	1.03	90.922	1.11	1.030	0.463 95	0.34	5701	4590	4130.6	5.0
L6	**Kunashak**		0.184	6.77	11.457	7.22	0.991	0.451 89	1.02	1088	2561	4091.4	15.2
L6	**Pervomaisky**		0.510	0.99	40.062	1.00	0.995	0.569 25	0.10	2658	3772	4431.4	1.5
L/LL3	**Unnamed Antarctic**	Chondrule 1	0.957	0.44	80.404	0.52	0.897	0.609 23	0.06	4334	4469	4530.2	3.4
L/LL3	**Unnamed Antarctic**	Chondrule 2	1.001	1.55	82.595	1.59	0.985	0.598 39	0.05	4477	4496	4504.1	4.1
L/LL3	**Unnamed Antarctic**	Chondrule 3a	1.004	2.33	82.688	2.34	0.997	0.597 30	0.06	4487	4497	4501.4	2.5
L/LL3	**Unnamed Antarctic**	Chondrule 3b	1.034	0.57	85.217	0.60	0.973	0.597 45	0.05	4584	4527	4501.8	2.0
L/LL3	**Unnamed Antarctic**	Chondrule 4	1.019	1.33	88.017	2.41	0.821	0.626 03	0.21	4536	4559	4569.6	22.0
L/LL3	**Unnamed Antarctic**	Chondrule 6	0.965	0.46	79.119	0.63	0.870	0.594 70	0.06	4359	4453	4495.1	4.7
L/LL4	**Bjurböle**	Chondrule 10	1.076	1.79	91.676	1.79	0.997	0.617 87	0.14	4709	4599	4550.6	2.0
L/LL4	**Bjurböle**	Chondrule 11	0.169	2.19	14.308	2.17	0.993	0.613 54	0.25	1007	2770	4540.4	3.7
L/LL4	**Bjurböle**	Chondrule 12	1.055	0.98	89.926	0.99	0.990	0.618 19	0.14	4643	4579	4551.3	2.0
L/LL4	**Bjurböle**	Chondrule 13	1.098	1.16	92.737	1.17	0.994	0.612 54	0.13	4777	4610	4538.0	1.9
L/LL4	**Bjurböle**	Chondrule 14	1.077	4.20	91.402	4.19	0.999	0.615 78	0.22	4710	4596	4545.7	3.2
L/LL4	**Bjurböle**	Chondrule 15	1.052	1.69	89.806	1.69	0.994	0.619 43	0.19	4632	4578	4554.2	2.8
L/LL4	**Bjurböle**	Chondrule 7	0.510	0.33	40.329	0.39	0.911	0.573 98	0.16	2655	3779	4443.5	2.3
L/LL4	**Bjurböle**	Chondrule 8	1.045	0.61	88.917	0.61	0.989	0.617 25	0.09	4611	4568	4549.1	1.3
L/LL4	**Bjurböle**	Chondrule 9	1.073	1.27	91.056	1.28	0.994	0.615 40	0.14	4700	4592	4544.8	2.1
L/LL4	**Bjurböle**	Fraction 1	1.029	0.47	88.045	0.48	0.984	0.620 48	0.08	4562	4558	4556.7	1.2
L/LL4	**Bjurböle**	Fraction 2	1.015	0.59	86.608	0.60	0.993	0.618 66	0.07	4518	4542	4552.4	1.0
L/LL4	**Bjurböle**	Pyroxene 1	1.022	0.66	87.296	0.66	0.993	0.619 52	0.08	4539	4550	4554.5	1.2
L/LL4	**Bjurböle**	Pyroxene 2	1.056	1.06	90.199	1.06	0.993	0.619 57	0.13	4646	4582	4554.6	1.8
L/LL4	**Bjurböle**	Phosphate 2	33.591	40.50	3088.240	40.50	1.000	0.666 79	0.82	22844	8159	4660.8	11.4

Table 4 - Radiogenic Pb and Pb isotopic ratios and model dates

Class	Meteorite	Fraction	$^{206}Pb^*/^{238}U$[a]	% err	$^{207}Pb^*/^{235}U$[a]	% err	ρ 6/8-7/5	$^{207}Pb^*/^{206}Pb^*$[a]	% err	$^{206}Pb^*/^{238}U$ Date	$^{207}Pb^*/^{235}U$ Date	(CDT primordial) $^{207}Pb^*/^{206}Pb^*$ Date	2σ err
L/LL4	Bjurböle	Phosphate 3	4.242	7.04	353.652	7.04	1.000	0.604 59	0.18	10680	5961	4519.1	2.5
L/LL6	Holbrook	Chondrule E11	1.060	5.93	90.544	5.93	1.000	0.619 42	0.15	4659	4586	4554.2	2.2
L/LL6	Holbrook	Chondrule E12	1.057	4.38	90.293	4.39	0.998	0.619 73	0.29	4649	4584	4555.0	4.2
L/LL6	Holbrook	Chondrule E9	1.081	10.50	92.464	10.50	1.000	0.620 49	0.19	4724	4607	4556.7	2.7
L/LL6	Holbrook	Chondrule Fragments	nd		nd		nd	0.622 65	0.13	nd	nd	4561.8	1.8
LL3	Krymka	Fraction 1	0.937	3.32	80.035	3.32	0.996	0.619 36	0.31	4263	4462	4554.1	4.5
LL3	Krymka	Fraction 10	1.212	0.59	101.257	0.68	0.947	0.605 95	0.23	5118	4699	4522.3	8.3
LL3	Krymka	Fraction 11	1.127	0.36	95.327	0.43	0.895	0.613 38	0.19	4866	4638	4540.0	6.1
LL3	Krymka	Fraction 12	1.073	0.29	90.924	0.34	0.901	0.614 50	0.15	4700	4591	4542.7	2.3
LL3	Krymka	Fraction 13	1.134	0.54	95.589	0.64	0.882	0.611 41	0.30	4886	4641	4535.4	6.7
LL3	Krymka	Fraction 2	1.062	2.24	90.372	2.24	0.997	0.616 93	0.17	4666	4584	4548.4	2.4
LL3	Krymka	Fraction 3	1.026	0.55	90.844	0.61	0.953	0.642 09	0.19	4552	4590	4606.3	4.3
LL3	Krymka	Fraction 4	1.047	0.41	88.902	0.45	0.951	0.615 92	0.14	4618	4568	4546.0	3.6
LL3	Krymka	Fraction 5	0.218	1.03	18.487	1.04	0.991	0.614 44	0.14	1272	3015	4542.5	6.1
LL3	Krymka	Fraction 6	0.181	1.04	15.321	1.05	0.995	0.612 83	0.11	1074	2835	4538.7	2.2
LL3	Krymka	Fraction 7	1.205	0.21	100.256	0.29	0.727	0.603 49	0.20	5097	4689	4516.4	4.4
LL3	Krymka	Fraction 8	1.133	0.50	96.501	0.52	0.973	0.617 69	0.12	4884	4650	4550.2	2.1
LL3	Krymka	Pyroxene 1	1.129	2.88	97.062	2.86	0.996	0.623 34	0.27	4872	4656	4563.4	3.9
LL3	Krymka	Pyroxene 2	1.028	2.73	87.663	2.70	0.996	0.618 54	0.25	4558	4554	4552.2	3.7
LL3	Krymka	Phosphate 1	6.885	231.00	573.003	231.00	1.000	0.603 61	1.54	13312	6450	4516.7	21.6
LL3	Krymka	Phosphate 2	4.467	247.00	383.834	247.00	1.000	0.623 26	2.47	10950	6044	4563.2	34.6
LL3	Krymka	Phosphate 3	71.771	8.07	6063.790	8.08	1.000	0.612 76	0.17	27638	8844	4538.6	2.3
LL5	Tuxtuac	Chondrule 1	0.887	1.07	55.653	1.17	0.939	0.454 87	0.40	4095	4099	4101.2	6.0
LL5	Tuxtuac	Chondrule 2	0.964	1.06	61.166	1.18	0.933	0.460 04	0.43	4352	4193	4118.0	6.3
LL5	Tuxtuac	Chondrule 3	1.145	2.62	74.477	2.73	0.974	0.471 88	0.62	4919	4390	4155.7	9.2
LL5	Tuxtuac	Chondrule 4	0.857	25.10	53.462	40.78	0.616	0.452 27	32.10	3991	4059	4092.7	477.2
LL5	Tuxtuac	Chondrule 5	0.827	1.07	51.479	1.16	0.952	0.451 31	0.36	3886	4021	4089.6	5.3

nd = not determined

[a] Corrected for fractionation, spike, blank, and primordial Pb isotopic composition from Tatsumoto et al. (1973) as initial common Pb.

Table 5 - Pb-Pb isochron and U-Pb concordia dates

	Meteorite	Fraction	U-Pb date (Ma)		Pb-Pb isochron date (Ma)	
H4	**Ankober**	Chondrules				
H5	**Orlovka**	Silicates	4559.5	± 0.76	4558.8	± 1
H6	**Kidairat**	Chondrules			4539	± 9
L4	**Saratov**	Chondrules & Silicates	4563.3	± 2.7	4559	± 12
L5	**Elenovka**	Pyroxenes & Chondrules	4554	± 1	4555	± 3
L5	**Elenovka**	Phosphates	4535	± 1	4535	± 1
L6	**Barwell**	Chondrules			4526	± 27
L/LL3	**Antarctic**	Chondrules			4499	± 34
L/LL4	**Bjurböle**	Chondrules	4548	± 14	4569	± 9
L/LL6	**Holbrook**	Chondrules	4556	± 10	4563	± 10
LL3	**Krymka**	Chondrules	4547	± 12	4543	± 40
LL5	**Tuxtuac**	Chondrules	4099	± 29	4493	± 50

Table 6 - Rb-Sr Data

Type	Sample	Fraction	$^{207}Pb/^{206}Pb$ Model Age (Ma)	err	[Rb] (ppm)	[Sr] (ppm)	$^{87}Rb/^{86}Sr$[a]	$^{87}Sr/^{86}Sr$	2σ	Sr model date (Ma)[b]	Model $(^{87}Sr/^{86}Sr)I$[c]	ΔT from Angrites[d] (Ma)
H5	Orlovka	Silicate Fraction	4562.41	2.06	2.67	13.95	0.555 10	0.738 41	0.000 09	4934 ± 54	0.701 90	281
H5	Orlovka	Silicate Fraction	4559.3	0.81	2.10	11.54	0.527 90	0.733 66	0.000 03	4578 ± 51	0.698 94	-1
H5	Orlovka	Phosphate 1	3844.4		16.68	212.44	0.226 33	0.708 98	0.000 42	3149 ± 144	0.694 09	-464
H5	Orlovka	Phosphate 2	4559.8		0.62	29.81	0.060 23	0.703 88	0.000 23	5800 ± 335	0.699 92	92
H5	Orlovka	Phosphate 3 (#2)	4555.12		0.60	37.41	0.046 29	0.704 94	0.000 06	8916 ± 298	0.701 89	281
H5	Richardton	Chondrule 1	4571.56	1.00	21.40	105.48	0.556 16	0.736 59	0.002 79	4707 ± 339	0.700 01	101
H5	Richardton	Chondrule 2	4558.99	2.84	31.60	40.72	2.130 90	0.842 54	0.012 63	4674 ± 399	0.702 40	329
H5	Richardton	Chondrule 3	4553.1	0.75	10.00	36.63	0.762 51	0.748 21	0.000 45	4495 ± 61	0.698 06	-85
H5	Richardton	Chondrule 4	4559.65	1.59	17.40	61.06	0.779 46	0.751 03	0.000 03	4643 ± 48	0.699 77	77
H5	Richardton	Chondrule 6	4563.24	1.59	14.70	116.79	0.345 92	0.722 35	0.002 80	4715 ± 544	0.699 60	62
H5	Richardton	Chondrule 8	4560.82	1.04	5.30	24.47	0.619 20	0.738 69	0.000 06	4470 ± 49	0.697 97	-94
H5	Richardton	Bromo Lights			115.53	784.10	0.396 17	0.725 18	0.000 01	4615 ± 56	0.699 12	16
H5	Richardton	Bromo Lights			3.82	15.13	0.680 46	0.741 96	0.000 17	4403 ± 50	0.697 21	-166
H5	Richardton	Olivine - MI Heavy +100			7.69	11.04	1.890 58	0.822 36	0.000 17	4532 ± 45	0.698 02	-89
H5	Richardton	Opx +100 MI Lights			93.42	113.33	2.242 79	0.847 23	0.000 02	4588 ± 44	0.699 73	74
H5	Richardton	Opx +100 MI Lights			60.37	152.25	1.070 81	0.769 92	0.000 03	4604 ± 46	0.699 50	52
H5	Richardton	Opx +100 MI Lights			31.60	40.72	2.130 90	0.842 54	0.012 63	4674 ± 399	0.702 40	329
H5	Richardton	Phosphate 1	4554.01	1.33	0.58	57.84	0.028 94	0.701 27	0.000 01	5853 ± 459	0.699 36	39
H5	Richardton	Phosphate 2	4555.37	0.73	0.64	22.90	0.081 16	0.701 66	0.000 02	2475 ± 173	0.696 32	-252
H5	Richardton	Phosphate 4	4559.65	1.59	1.78	46.21	0.111 33	0.703 92	0.000 05	3217 ± 130	0.696 60	-225
H5	Richardton	Phosphate 5	4551.86	0.75	0.35	72.81	0.013 99	0.700 67	0.000 01	8990 ± 903	0.699 75	76
L4	Saratov	Silicate Fraction 1	4563.65	1.11	5.07	6.96	2.127 98	0.840 83	0.000 10	4627 ± 46	0.700 88	184
L4	Saratov	Phosphate 1	4530.05		0.55	80.09	0.019 67	0.701 42	0.000 05	9062 ± 576	0.700 13	112
L5	Elenovka	Chondrule 1	4554.29	0.83	22.40	82.14	0.746 37	0.749 19	0.000 01	4680 ± 50	0.700 10	110
L5	Elenovka	Chondrule 2	4554.34	1.39	10.10	38.98	0.719 51	0.747 13	0.000 03	4657 ± 50	0.699 81	82
L5	Elenovka	Chondrule 3			38.40	150.47	0.692 38	0.744 40	0.000 88	4570 ± 96	0.698 87	-8
L5	Elenovka	Pyroxene 3	4554.94	1.12	15.60	57.67	0.741 47	0.748 33	0.000 04	4633 ± 50	0.699 57	59
L5	Elenovka	Pyroxene 4	4554.95	0.94	13.90	50.40	0.758 41	0.748 84	0.000 07	4577 ± 49	0.698 96	1
L5	Elenovka	Pyroxene 5			11.10	42.34	0.727 60	0.748 02	0.000 05	4689 ± 50	0.700 17	116
L5	Elenovka	Phosphate 1	4535.45	0.88	0.56	66.85	0.024 13	0.700 91	0.000 07	6088 ± 496	0.699 32	35
L5	Elenovka	Phosphate 2	4535	1.00	0.78	44.76	0.050 09	0.702 21	0.000 05	4752 ± 245	0.698 91	-4
L5	Elenovka	Phosphate 3	4539.67	1.03	0.73	57.97	0.036 30	0.702 13	0.000 03	6335 ± 327	0.699 74	75
L6	Kunashak	Silicate Fraction	4091.43	15.17	11.93	16.51	2.097 05	0.763 93	0.000 05	2191 ± 23	0.626 02	-7000
L6	Pervomaisky	Silicate Fraction	4431.41	1.47	8.83	16.19	1.586 62	0.803 06	0.000 04	4558 ± 46	0.698 71	-23
L/LL3	Unnamed Antarctic	Chondrule 1	4530.17	3.40	3.17	64.06	0.146 81	0.710 28	0.020 47	5405 ± 8692	0.700 63	160
L/LL3	Unnamed Antarctic	Chondrule 2	4504.09	4.05	44.14	52.41	2.305 58	0.851 54	0.002 43	4593 ± 83	0.699 91	91
L/LL3	Unnamed Antarctic	Chondrule 3a	4501.44	2.46	31.90	10.75	8.445 60	1.242 45	0.000 04	4466 ± 43	0.687 01	-1140
L/LL3	Unnamed Antarctic	Chondrule 3b	4501.82	2.01	30.56	9.28	9.444 76	1.311 85	0.000 06	4503 ± 43	0.690 71	-787
L/LL3	Unnamed Antarctic	Chondrule 4	4569.61	22.02	1.64	49.04	0.108 30	0.707 45	0.008 80	5517 ± 5175	0.700 32	131

Table 6 - Rb-Sr Data

Type	Sample	Fraction	$^{207}Pb/^{206}Pb$ Model Age (Ma)	err	[Rb] (ppm)	[Sr] (ppm)	$^{87}Rb/^{86}Sr$[a]	$^{87}Sr/^{86}Sr$	2σ	Sr model date (Ma)[b]	Model $(^{87}Sr/^{86}Sr)I$[c]	ΔT from Angrites[d] (Ma)
L/LL3	Unnamed Antarctic	Chondrule 6	4495.09	4.65	26.94	151.38	0.484 05	0.733 16	0.004 25	4914 ± 584	0.701 32	226
L/LL4	Bjurböle	Silicate Fraction 1	4556.7	1.22	3.75	15.17	0.716 55	0.747 25	0.000 06	4687 ± 50	0.700 13	106
L/LL4	Bjurböle	Silicate Fraction 2	4552.44	1.04	3.05	15.85	0.556 54	0.736 24	0.000 18	4664 ± 56	0.699 64	61
L/LL4	Bjurböle	Phosphate 1	4590	11.00	0.65	44.85	0.041 76	0.701 72	0.000 07	4894 ± 294	0.698 98	2
L/LL4	Bjurböle	Phosphate 2	4660.75	11.00	4.02	58.96	0.197 01	0.707 64	0.000 02	3152 ± 72	0.694 68	-386
L/LL4	Bjurböle	Phosphate 3 (#2)	4519.07	2.00	0.57	59.51	0.027 84	0.702 46	0.000 06	8911 ± 417	0.700 63	151
LL3	Krymka	Silicate Fraction 1	4554.09	4.51	12.55	6.70	5.592 76	1.074 21	0.000 13	4651 ± 45	0.706 39	710
LL3	Krymka	Silicate Fraction 2	4548.38	2.41	10.98	6.27	5.213 59	1.047 59	0.000 08	4636 ± 45	0.704 71	549
LL3	Krymka	Phosphate 1	4516.7		0.26	2.30	0.322 65	0.708 94	0.000 46	2221 ± 103	0.687 72	-1073
LL3	Krymka	Phosphate 2	4563.18		0.26	9.55	0.078 99	0.703 38	0.000 19	4063 ± 211	0.698 19	-73
LL3	Krymka	Phosphate 3	4538.56		1.18	16.64	0.204 71	0.710 96	0.000 03	4140 ± 75	0.697 49	-140

[a] $^{87}Rb/^{87}Sr$ errors are estimated at 1%

[b] H chondrite model dates (including Richardton) are calculated with assumed $^{87}Sr/^{86}Sr$ of 0.69876 (Minster and Allègre, 1979). L, L/LL, and LL chondrite model dates are calculated with assumed $^{87}Sr/^{86}Sr$ of 0.69877 (Minster and Allègre, 1981).

[c] Radiogenic $^{87}Sr^*/^{86}Sr$ generated by measured $^{87}Rb/^{86}Sr$ in 4560 Ma subtracted from measured $^{87}Sr/^{86}Sr$

[d] Calculated interval required for $^{87}Sr/^{86}Sr$ to evolve from Angrite Sr composition (0.698955 - Hans et al., 2009) to the calculated model initial $^{87}Sr/^{86}Sr$ for each sample from whole rock $^{87}Rb/^{86}Sr$ for each chondrite. WR data is available only for Elenovka (0.746), Bjurböle (0.792). For the other meteorites 0.75 is used.

Figure 1a – H chondrites Pb-Pb summary plot

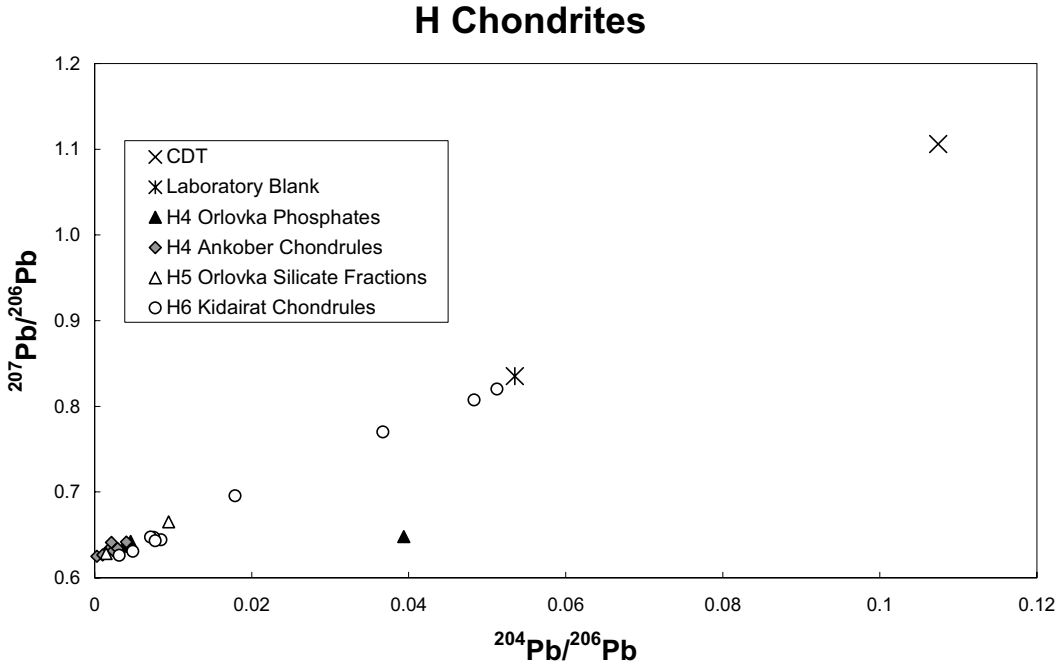

Figure 1b – L chondrites Pb-Pb summary plot

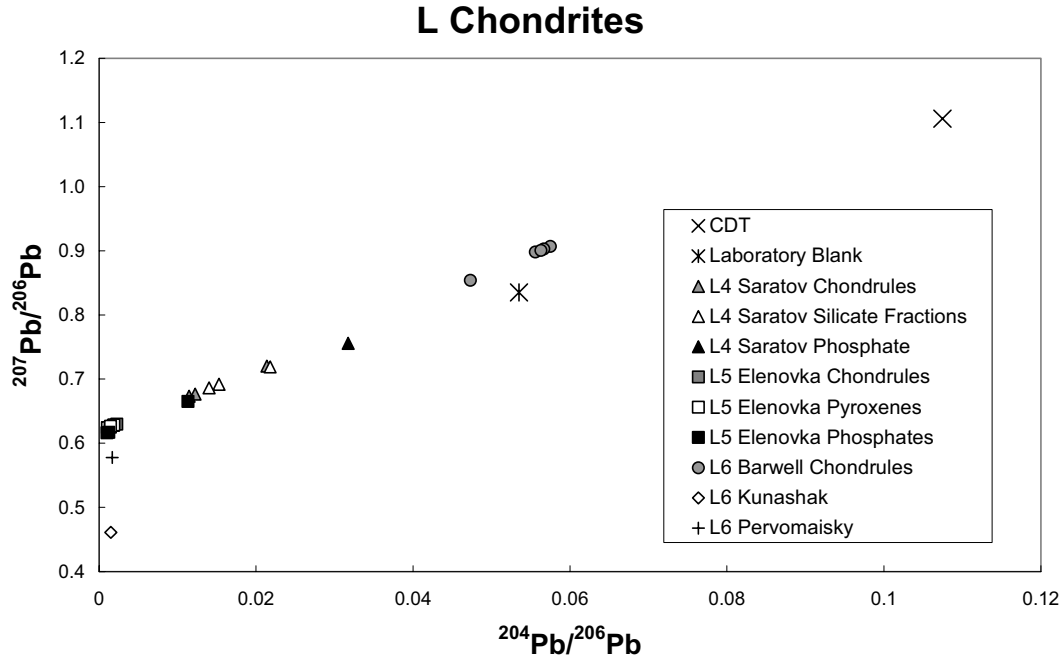

Figure 1c – L/LL chondrites Pb-Pb summary plot

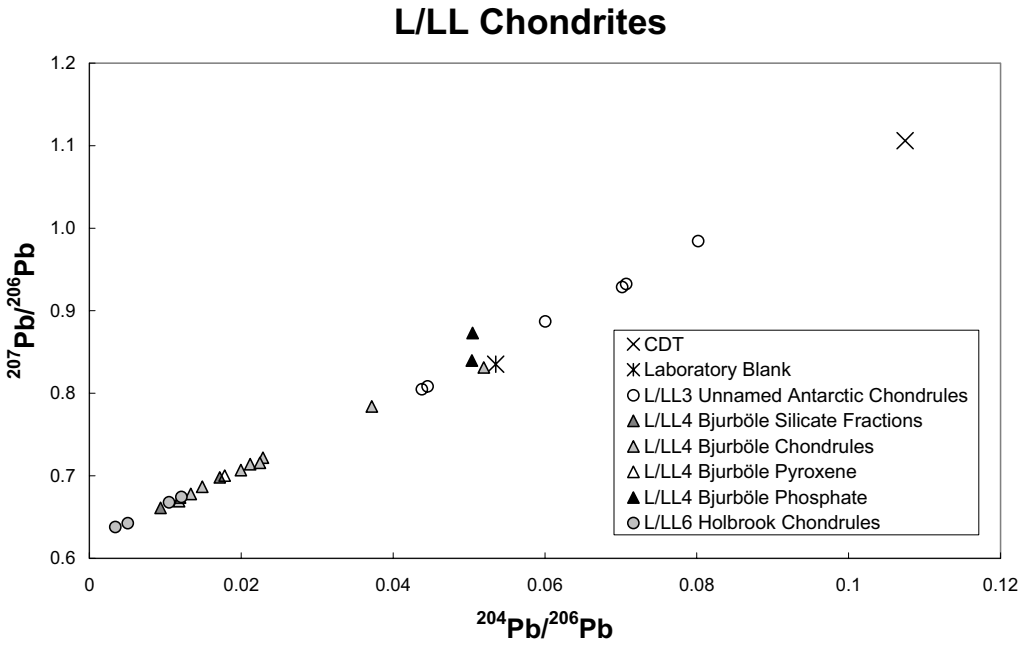

Figure 1d – LL chondrites Pb-Pb summary plot

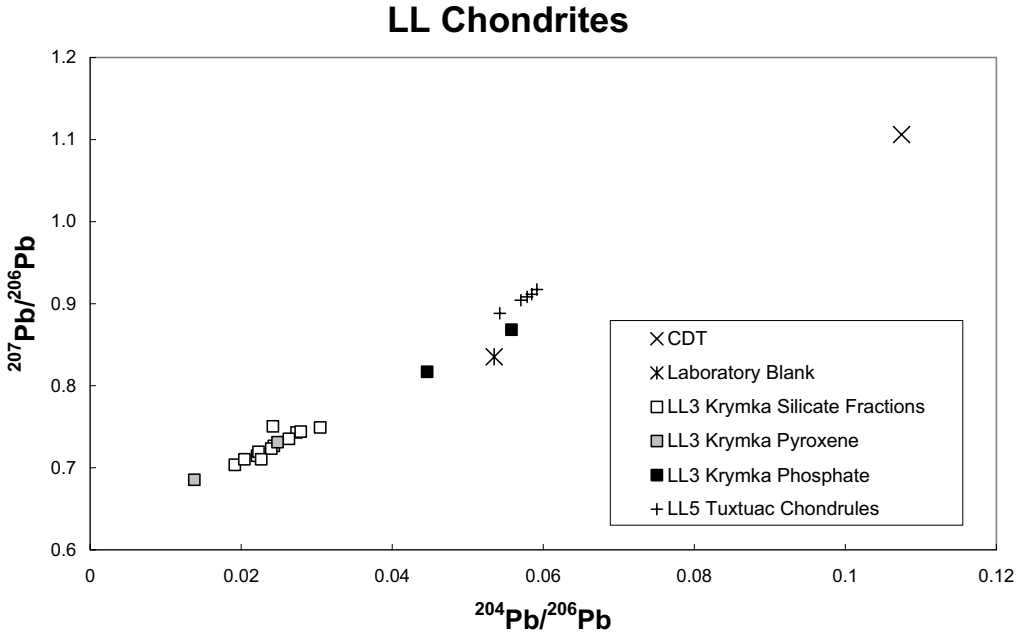

Figure 2 – H6 Kidairat Pb-Pb isochron regression

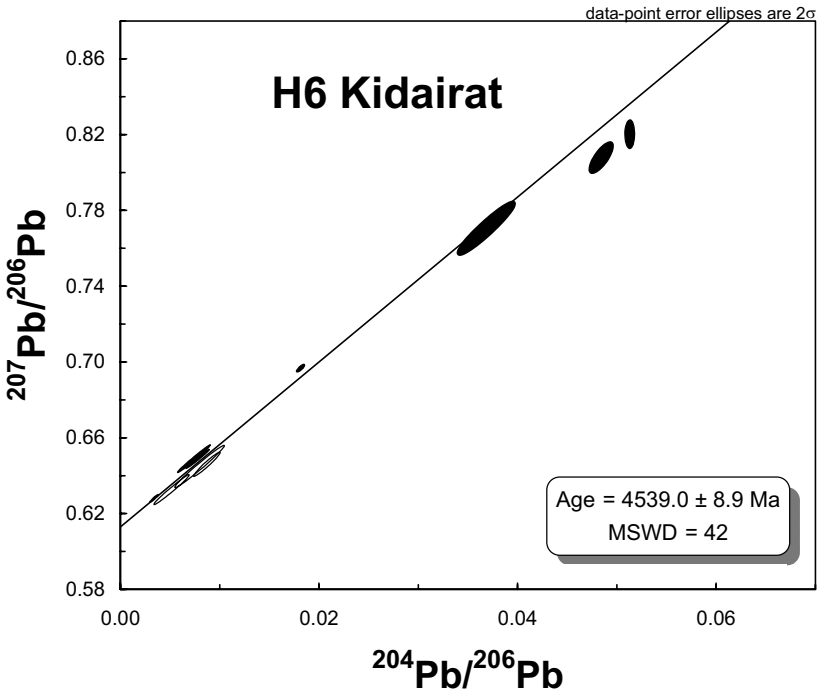

Filled symbols are chondrules crushed by electric pulse disaggregation. Open symbols are mechanically crushed chondrules.

Figure 3a – L4 Saratov Pb-Pb isochron regression

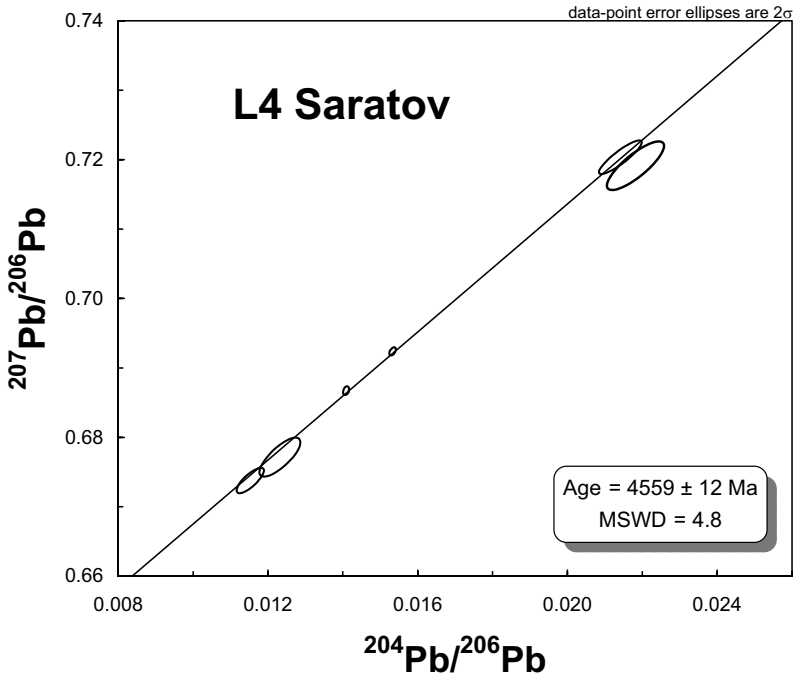

Figure 3b – L4 Saratov U-Pb concordia plot

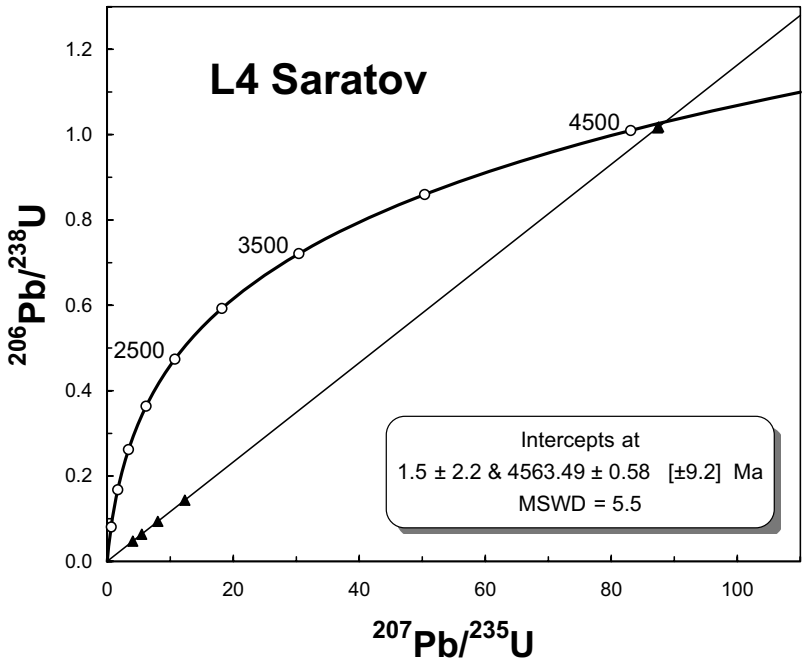

Figure 4 – Barwell Pb-Pb isochron regression

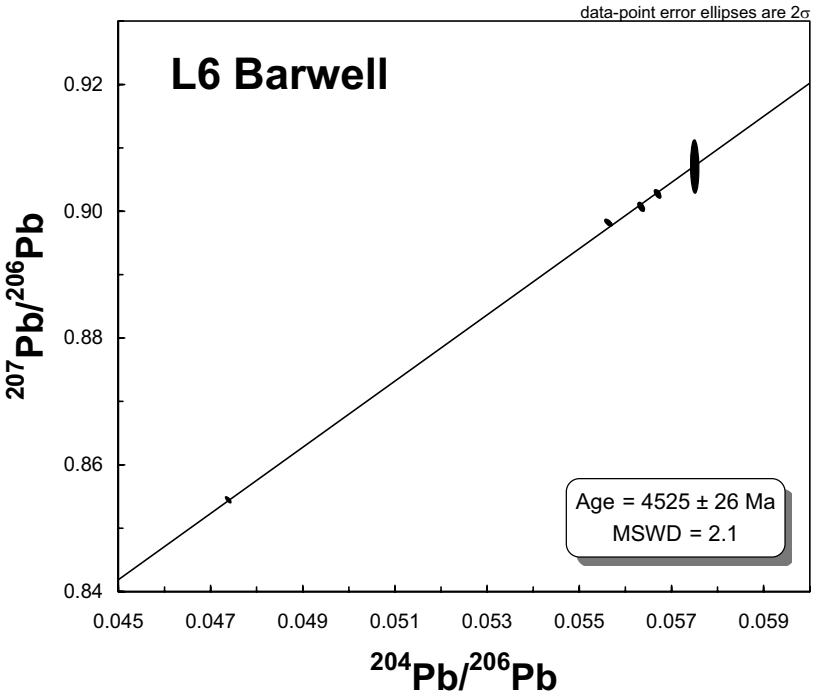

Figure 5 – L5 Elenovka silicates U-Pb concordia plot

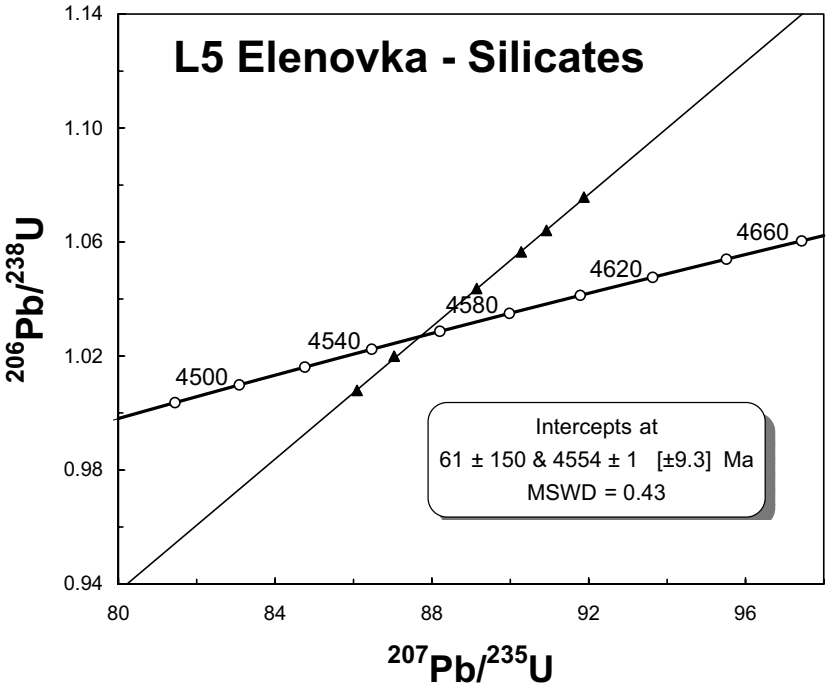

Figure 6 – L5 Elenovka silicates and phosphates Pb-Pb isochron regression

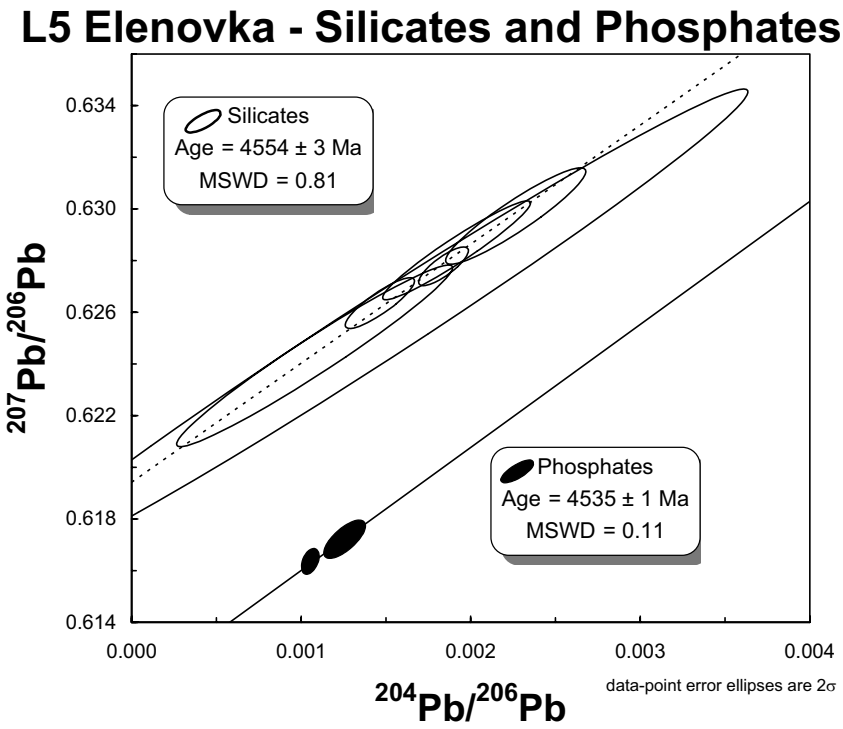

Figure 7 – L5 Elenovka phosphates U-Pb concordia plot

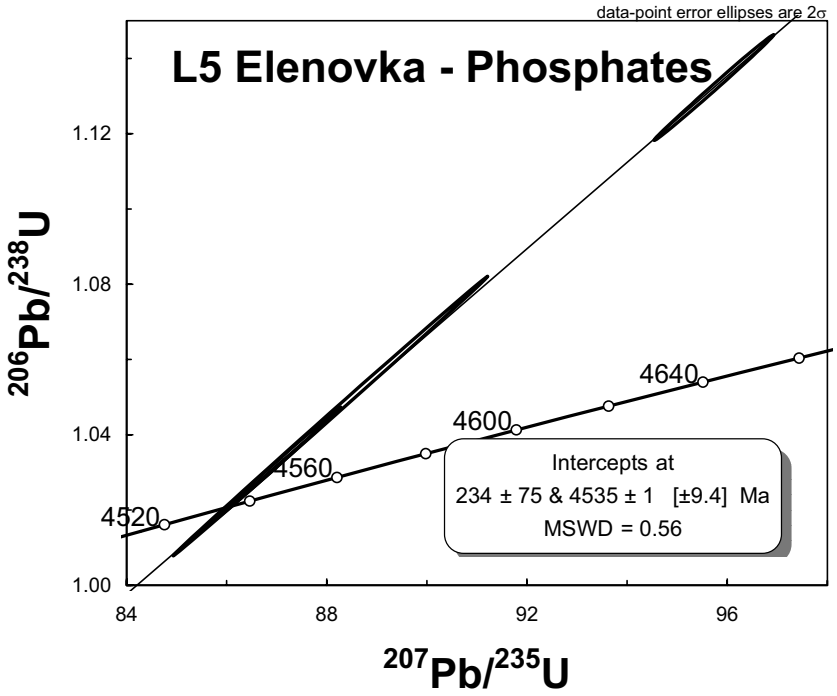

Figure 8 - L/LL3 Unnamed Antarctic Pb-Pb isochron regression

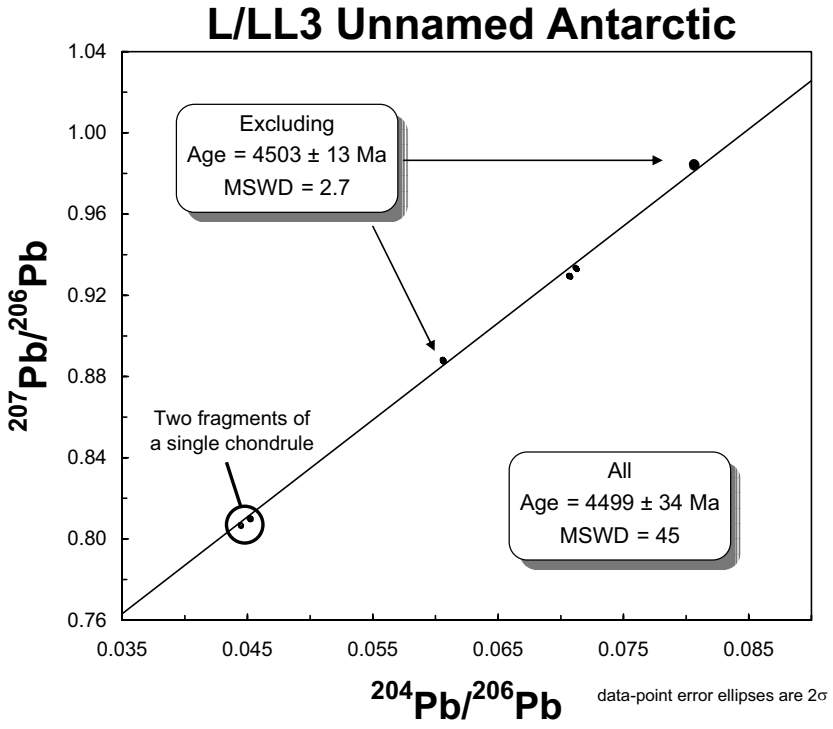

Figure 9a - L/LL4 Bjurböle Pb-Pb isochron regression

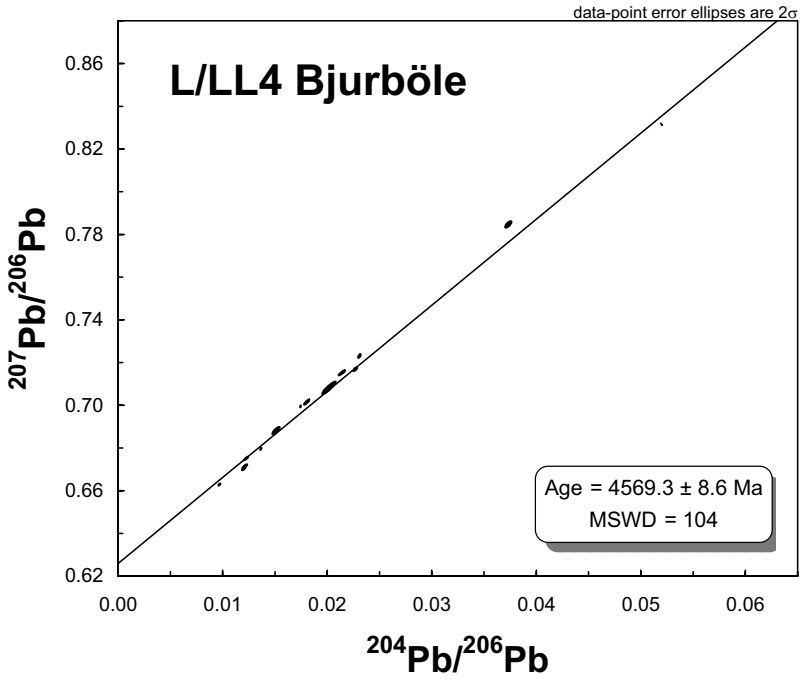

Figure 9b – L/LL4 Bjurböle U-Pb concordia plot

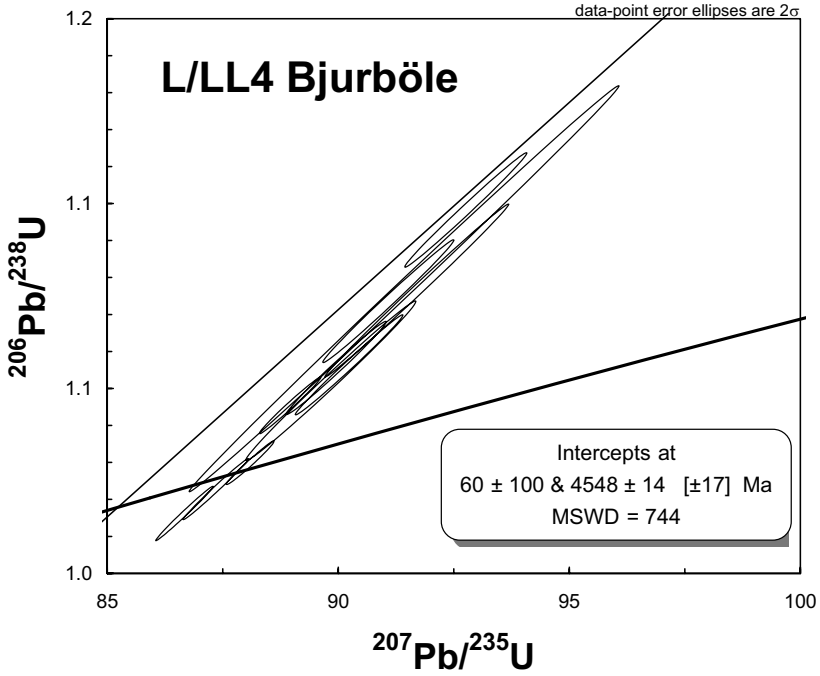

Figure 10 – L/LL6 Holbrook Pb-Pb isochron regression

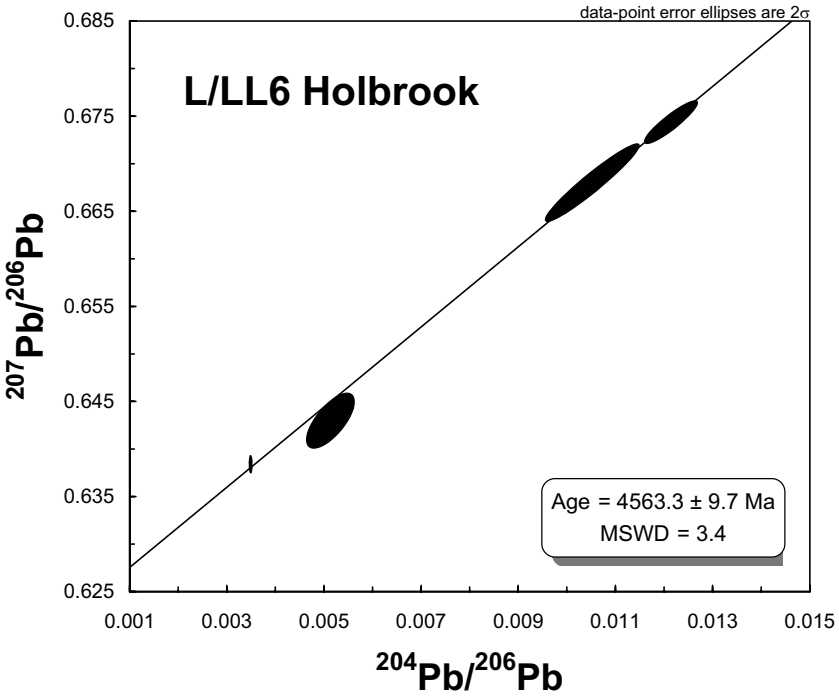

Figure 11a – LL3.1 Krymka Pb-Pb isochron regression

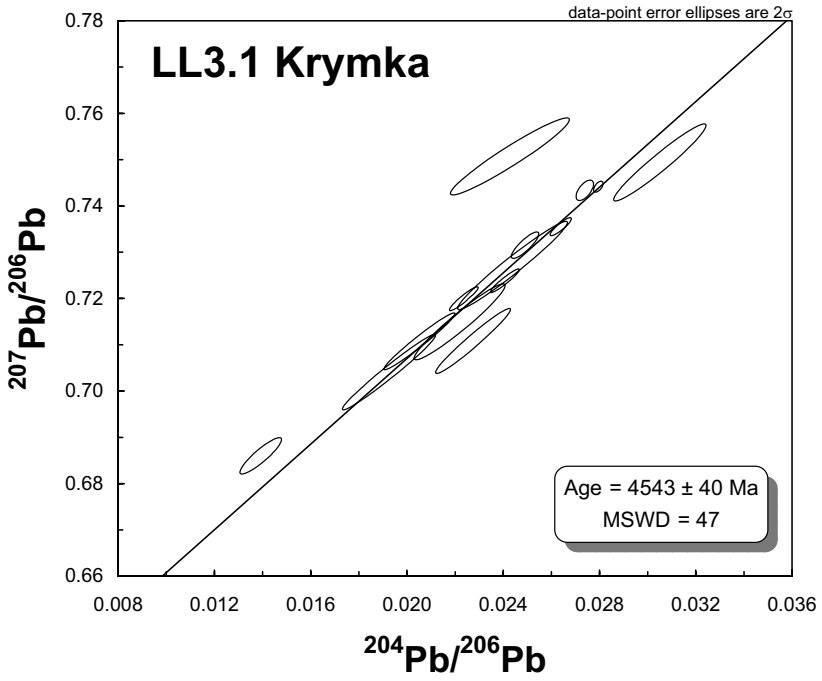

Figure 11b – LL3.1 Krymka U-Pb concordia plot

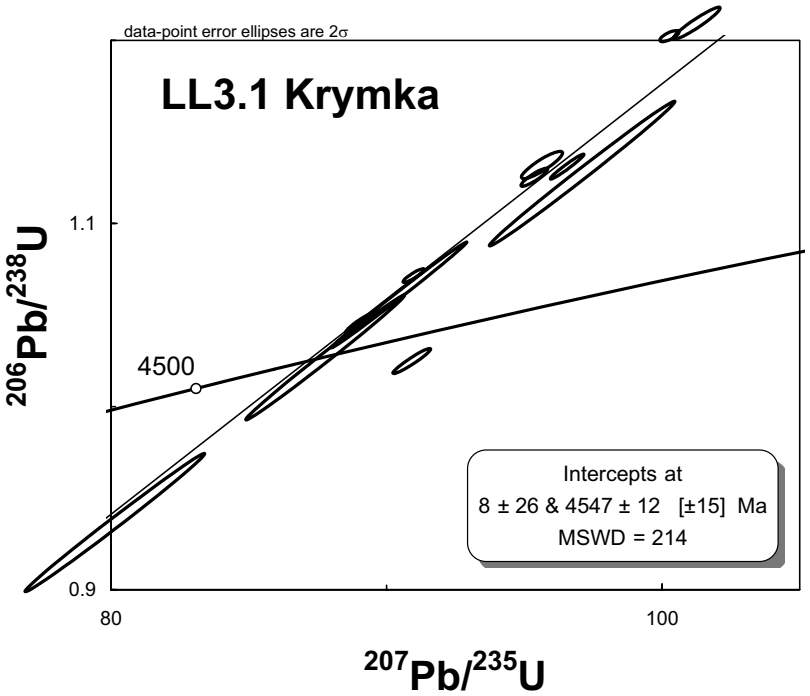

Figure 12a – LL5 Tuxtuac Pb-Pb isochron regression

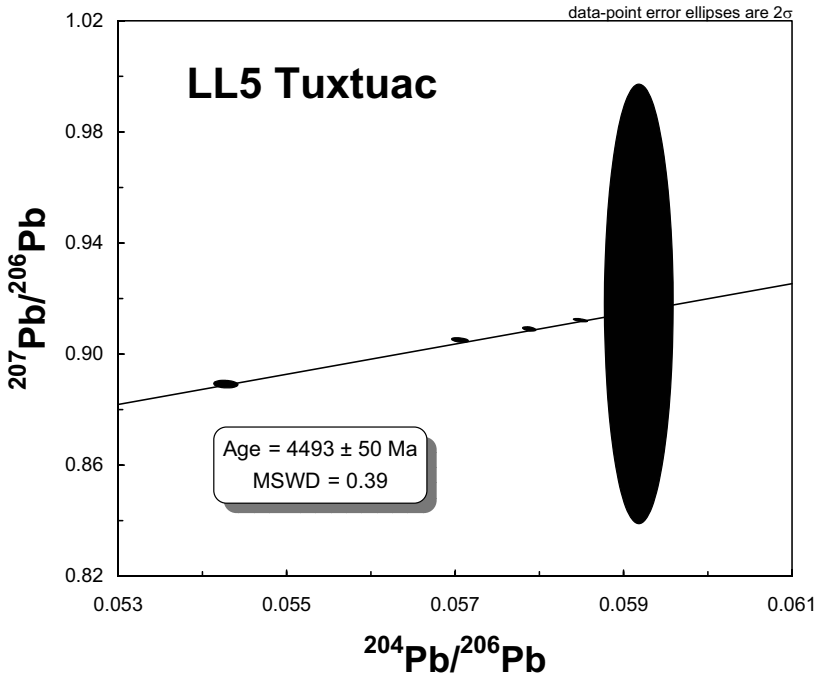

Figure 12b – LL5 Tuxtuac U-Pb concordia plot

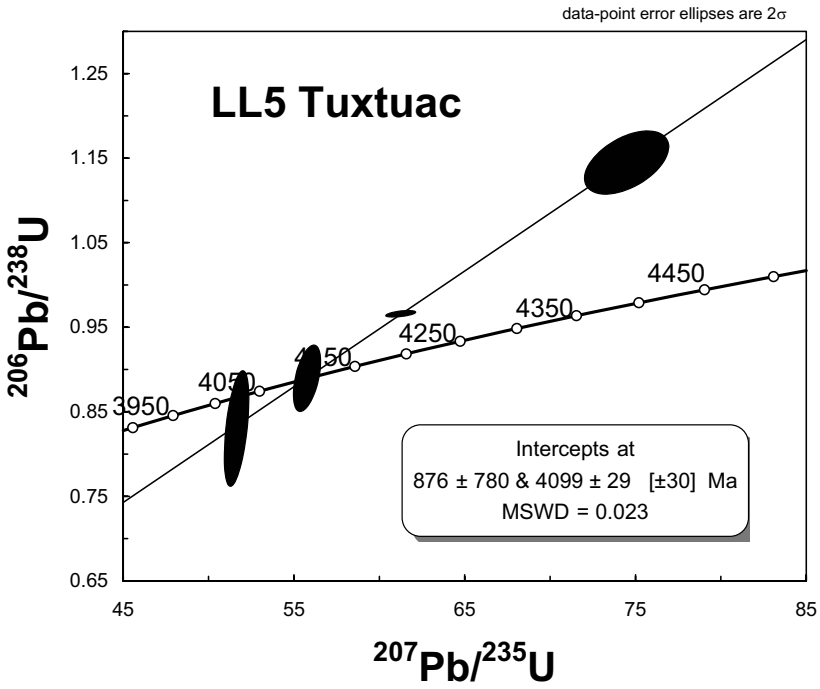

Figure 13 – Meteorite timeline

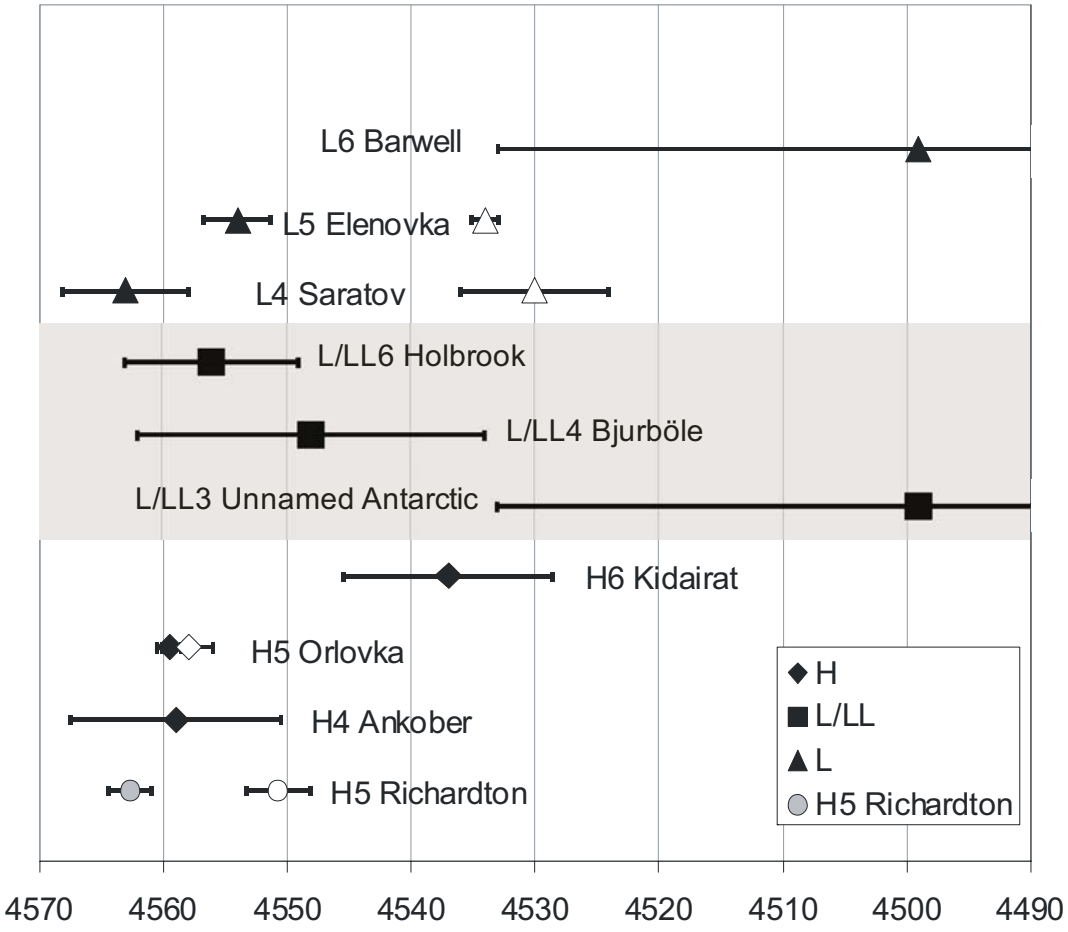

Filled symbols are silicates, open symbols are phosphates

Figure 14 – Closure temperature vs. age plot for L5 Elenovka silicates and phosphates.

Both 1, estimate of absolute closure temperatures for silicates and phosphates, and 2, estimate of the difference between closure temperatures for silicates and phosphates, yield a cooling rate of 14.8 K/Ma. The uncertainty is reduced for 2, from 6 to 2.6 Ma.

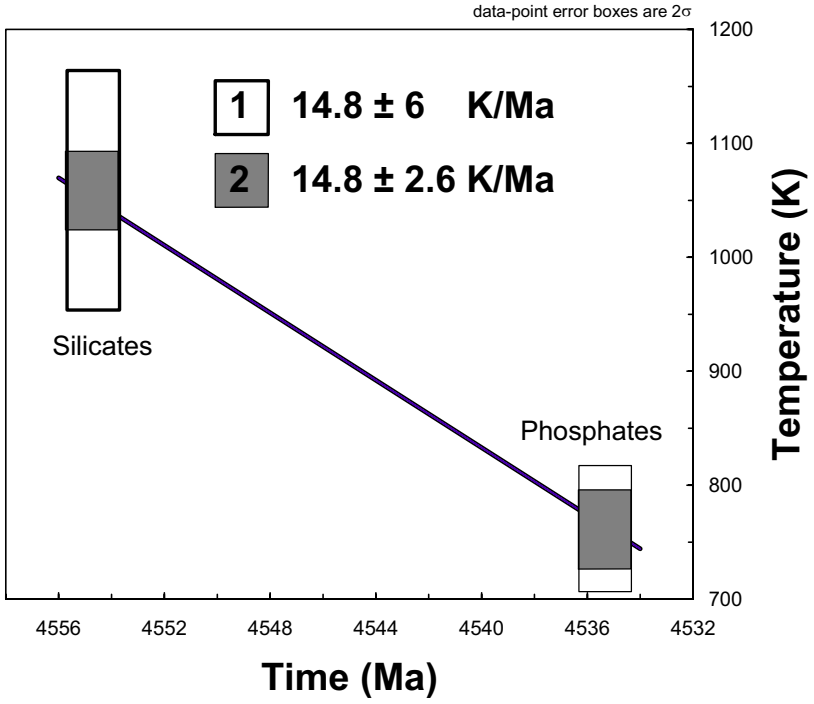

Figure 15a – Summary plot of Rb-Sr data for H meteorites with 4560 Ma reference line

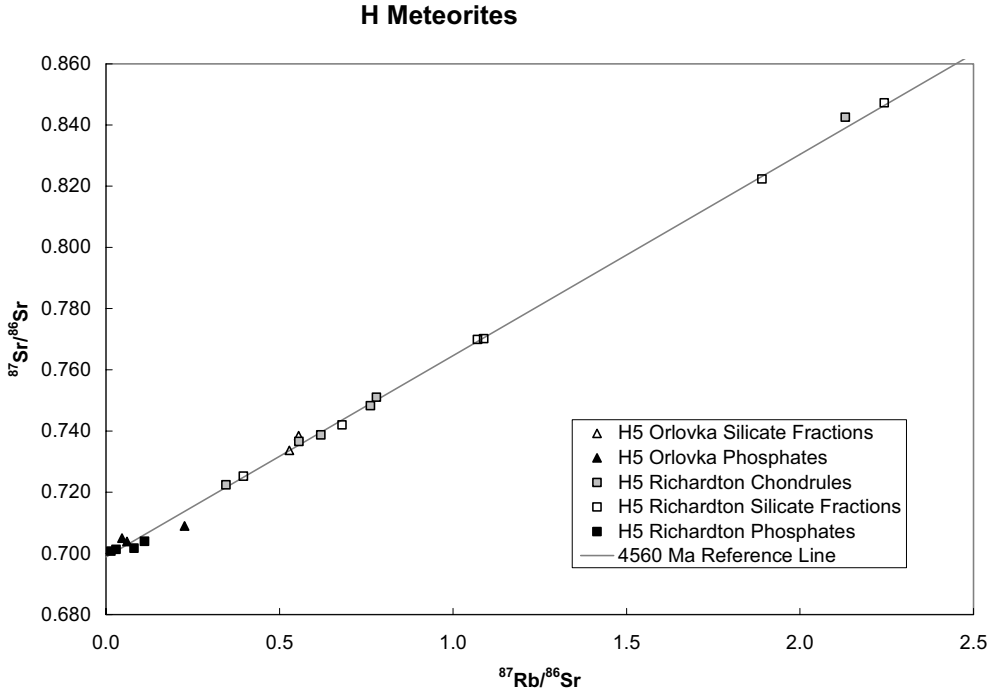

Figure 15b – Summary plot of Rb-Sr data for L meteorites with 4560 Ma reference line

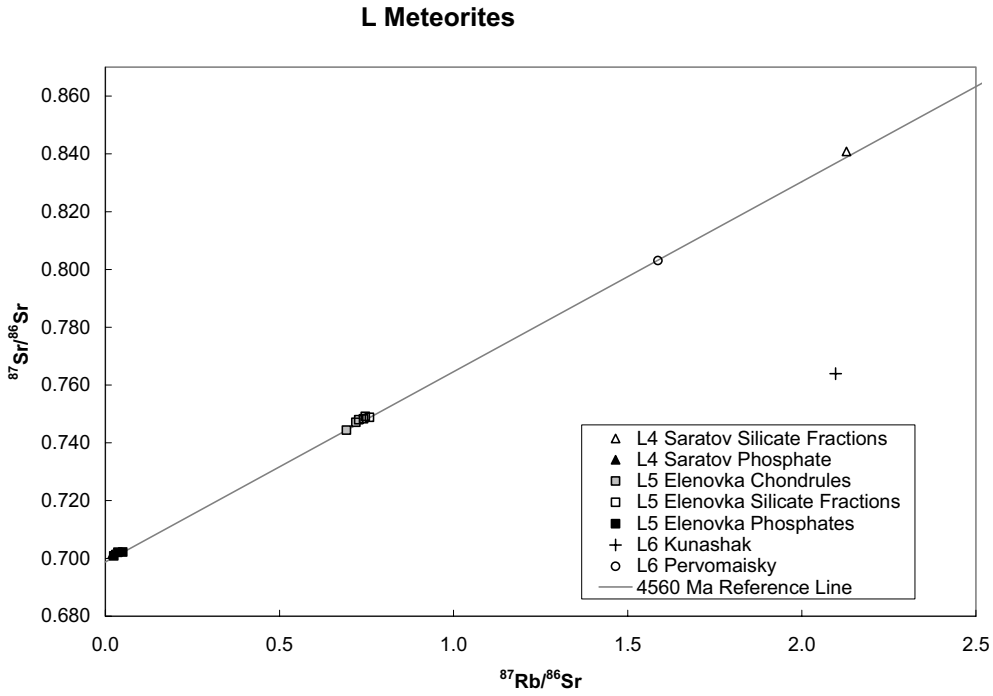

Figure 15c – Summary plot of Rb-Sr data for L and L/LL meteorites with 4560 Ma reference line

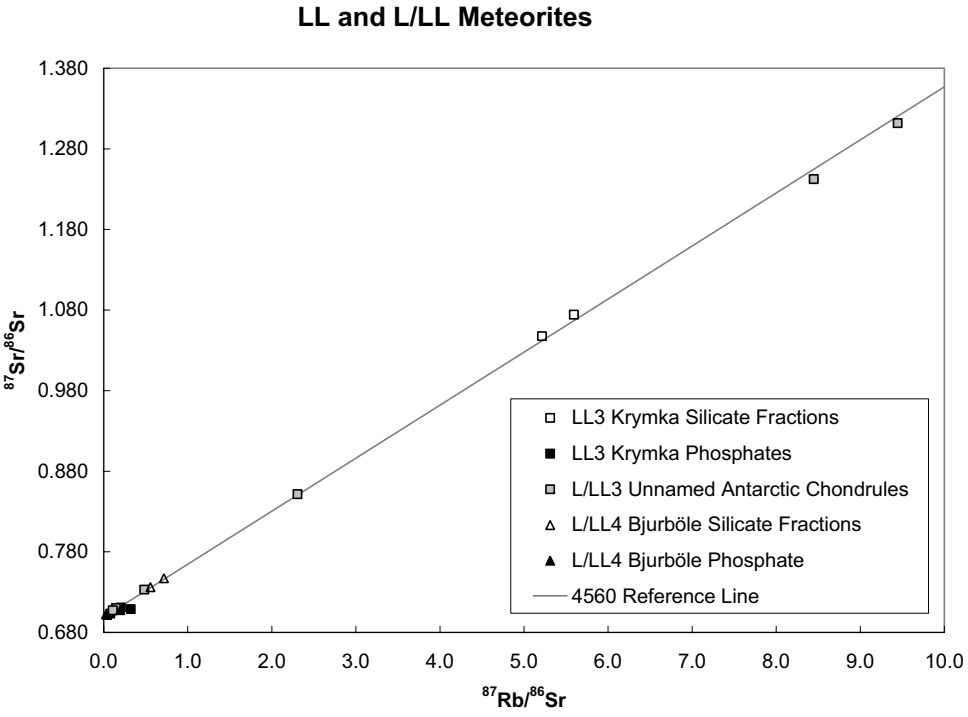

Figure 16 – H5 Richardton Rb-Sr isochron regression. Data from this study with data from Evensen et al., 1979.

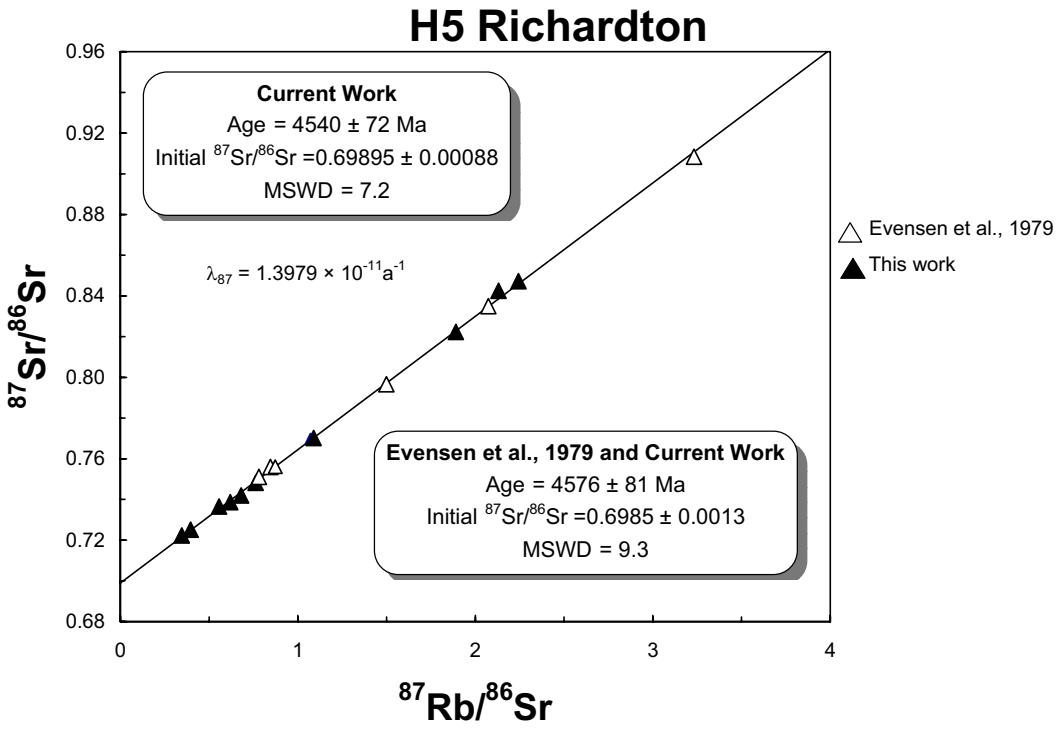

Figure 17 – L5 Elenovka silicates Rb-Sr isochron regression

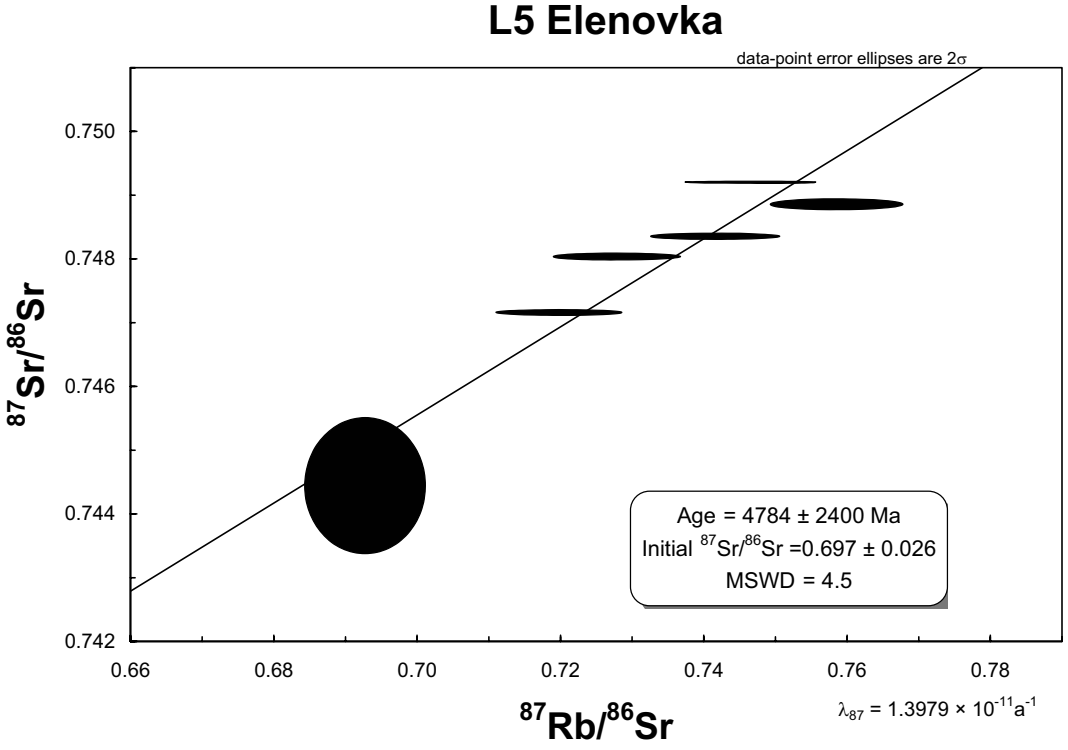

Figure 18 – L/LL3 Unnamed Antarctic chondrules Rb-Sr isochron regression

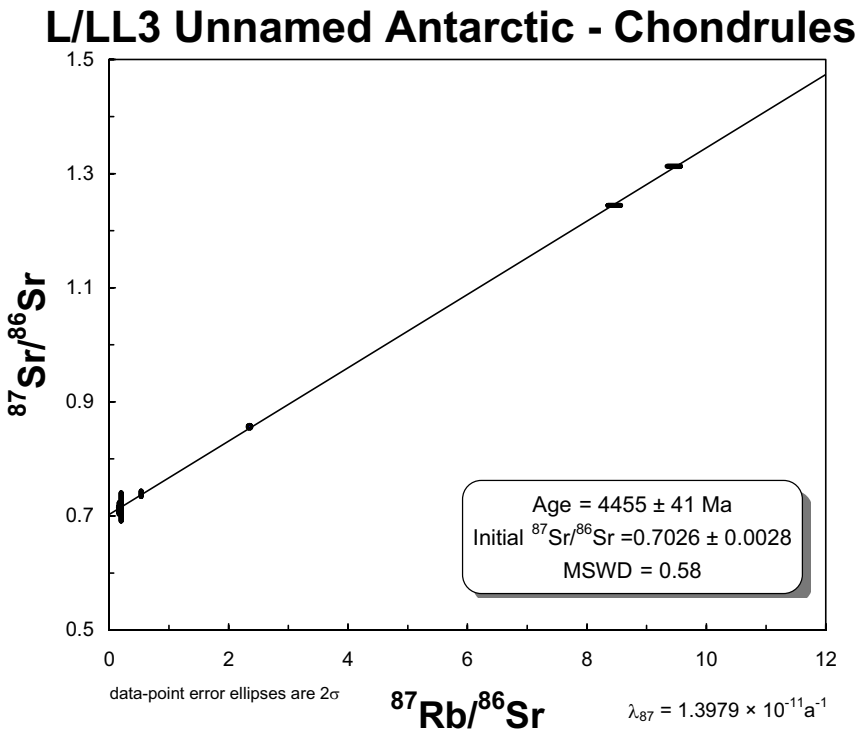

Conclusions

1. The decay constant of ^{87}Rb

The decay constant of ^{87}Rb (λ_{87}) has been measured by a $^{87}Sr^*$ accumulation experiment. This is the first measurement of its kind in over 30 years. λ_{87} is determined to be $1.3979 \pm 0.0026 \times 10^{-11}a^{-1}$. The precision is almost four times better than the previous accumulation experiment which yielded $1.419 \pm 0.012 \times 10^{-11}a^{-1}$. Only one other measurement, by geological age comparison, has comparable precision. Accuracy is ensured by careful constraints on all sources of uncertainty. Accuracy is further attested to by the good agreement with five other λ_{87} measurements since 1980, four by age comparison, and one by direct counting. The convergence of these measurements indicates that the value of $1.42 \times 10^{-11}a^{-1}$ is approximately 1.6% too high.

Despite making every effort to constrain all uncertainties the measurements scatter outside of their analytical errors indicating either an unaccounted for source of uncertainty, or a non-random bias that is unidentified. This presents a quandary for analyzing the data and choosing a best value for λ_{87}. If there is a random bias that has been overlooked, then the analytical errors must be larger than the current estimates, which requires that the errors be expanded but that all measurements be averaged. On the other hand, if the bias is systematic, the biased measurements should be excluded and only the unbiased ones should be averaged. Unfortunately, the available information is not sufficient to choose between these scenarios. Instead, I have compromised by expanding the errors and averaging all data – to take into account the possibility of underestimated analytical errors. The expanded errors encompass the lower

values that would be the accurate ones if there is a systematic bias. This choice has compromised precision for accuracy.

Preparation of a double-spike has greatly enhanced the precision of the measurements. Early measurements with a Sr spike enriched only in ^{84}Sr had large analytical errors. This was due primarily to the highly radiogenic nature of the measured Sr, which gave very weak ^{86}Sr and ^{88}Sr signals. The consequent large analytical errors in $^{86}Sr/^{88}Sr$ yielded imprecise corrected $^{87}Sr/^{86}Sr$ which was used for calculating the decay constant. The double-spike increased the analytical precision by an order of magnitude over measurements made with the ^{84}Sr spike. The Sr concentration of the double-spike is also better constrained than the ^{84}Sr spike, enhancing the accuracy of the measurements.

2. U-Pb and Rb-Sr in ordinary chondrites

U-Pb has previously been demonstrated to be a high precision cosmochronometer for chondrules, chondritic silicates, and chondritic phosphates (Göpel et al., 1994; Amelin et al., 2005), resolving time differences between these chondrite components. These time differences combined with estimates of Pb closure temperatures in pyroxenes and apatite allowed for estimation of the cooling rate of H5 Richardton as it cooled from metamorphic temperatures shortly after accretion. Following up on that work, I have analyzed U-Pb and Rb-Sr in thirteen additional ordinary chondrites with the aim of further resolving H parent body history, and putting similar constraints on the L and LL parent bodies.

The results of my study show that the U-Pb system has approximated closed system behavior in some meteorites, but not in others. L5 Elenovka had the most precise U-Pb data from both silicates and phosphates, and like Richardton exhibits an age difference between chondrules/silicates and

phosphates. Both silicates and phosphates are younger than in Richardton, and the time difference between Elenovka silicates and phosphates is longer as well. Elenovka silicates are 4555 Ma compared with 4563 Ma for Richardton. Phosphates are 4535 Ma compared with 4551 Ma for Richardton. This corresponds to an estimated cooling rate for Elenovka of 14.8 ± 2.6 K/Ma over the temperature range from 1055 – 759 K. This is about 50% lower than the 25.7 ± 9 K/Ma estimated for H5 Richardton. The slower cooling rate and younger absolute ages for a meteorite of the same petrologic type as Richardton, but from the L parent body, suggests that the L body was larger than the H body. This conflicts with H and L parent body models by Miyamoto et al. (1981) and Bennet and McSween (1995) which predict bodies of similar size for both H and L, but which do not use cooling rates to constrain the models.

L4 Saratov chondrules are approximately the same age as H5 Richardton chondrules and are 5-8 Ma older than L5 Elenovka chondrules. Both Richardton and Elenovka are type 5, and should have experienced similar temperatures during parent body heating. The Pb closure temperature of pyroxene, approximately 1055 ± 106 (Amelin et al., 2005), is very close to the estimated peak temperature for type 5 meteorites, 998 ± 25 (Dodd, 1981). Consequently, it is possible that some type 5 meteorites never reached high enough temperatures to disturb U-Pb systematics. In this case, chondrule/silicate ages would preserve the primary age of the chondrules and Richardton chondrules would not reflect the cooling history of the parent body. This would then explain why H5 Richardton chondrules have the same age as L4 Saratov chondrules. On the other hand, type 4 material was heated to between 800-973 K (Dodd, 1981; Miyamoto et al., 1980) and even Saratov might reflect an early stage of cooling rather than primary chondrule ages. In this case, the 8 Ma between Richardton

and Elenovka further attest to considerably faster cooling in the H parent body than in the L. It must also be noted that the 4 and 5 type material span a spectrum, and Elenovka might have been deeply buried within the type 5 while Richardton was a more shallow within the 5 zone which would also account for the age differences between meteorites ostensibly of the same type. Although imprecise, the young dates for H6 Kidairat, around 4540 Ma, also support an onion-shell model for the H parent body.

Most Rb-Sr data plot near the 4560 Ma isochron, indicating that broadly the ordinary chondrite Rb-Sr preserves ancient ages, and has not been reset completely over the coarse of solar system history. However, the data do not define precise isochrons, indicating that there has been some disturbance to Rb-Sr systematics. The lack of agreement between Rb-Sr model ages, and the unrealistically old model dates calculated for some meteorite fractions indicate that this disturbance has been variable. Both Rb and Sr are easily leached Rb-Sr, and comparison with Pb-Pb demonstrates that the Pb-Pb system is far more resistant to disturbance than Rb-Sr.

3. Directions for further research

The λ_{87} measurements presented here are the most precise reported. However, the excess scatter leaves the ^{87}Rb decay constant open to further revision in the future, and there is sufficient $RbClO_4$ salt for additional measurements. As suggested in Chapter 1, it would be worthwhile to revisit these measurements on perhaps a decadal basis, when the Sr in the salt will be more radiogenic, and improvements in analytical methods may circumvent the currently unidentified source of uncertainty.

The λ_{87} study may act as a model for other accumulation type measurements of decay-constants. $\lambda^{187}Re$ was measured by accumulation by

Lindner et al. (1989). λ^{40}K and λ^{176}Lu have been the subject of debate (Begemann et al., 2001). And even λ^{235}U and λ^{238}U, the best known decay constants for geochronology, have been subject to revision recently (Schön et al., 2004; Schoene et al, 2006). These might all be candidates for accumulation experiments.

U-Pb has been demonstrated to be a precise and accurate chronometer for ordinary chondrites, capable of putting important constraints on the thermal history of the chondrite parent bodies. However, as demonstrated here, not all chondrites give equally high quality data. Meteorites have been subject to complex histories involving thermal alteration, impact(s), and terrestrial interaction. The aim should be data of the quality of H5 Richardton and L5 Elenovka for silicates and phosphates when possible, for ordinary chondrites of all chemical classes and petrologic types. Data from more equilibrated type 6 meteorites will further constrain the cooling history of the parent bodies, while data from more primitive type 4 and 3 meteorites will tell us about the early thermal history, and perhaps the interval between chondrule formation and accretion. This would greatly enhance our picture of the early history of the solar system.

4. References

Amelin, Y., Ghosh, A., and Rotenberg, E. (2005) Unraveling the evolution of chondrite parent asteroids by precise U-Pb dating and thermal modeling. *Geochim. Cosmochim. Acta* **69**, 505-518.

Begemann F., Ludwig K.R., Lugmair G.W., Min K., Nyquist L.E., Patchett P.J., Renne P.R., C.-Y. Shih, Villa I.M., and Walker R.J. (2001) Call for an improved set of decay constants for geochronological use. *Geochim. Cosmochim. Acta* **65**, 111-121.

Bennet, M.E. III and McSween H.Y. (1996). Revised model calculations for the thermal histories of ordinary chondrite parent bodies. *Meteoritics* **31,** 783-792.

Dodd, R.T. (1981) *Meteorites: A Petrologic-Chemical Synthesis*. Cambridge University Press, Cambridge, 368 p.

Göpel D., Manhès G., and Allègre, C.J. (1994). U-Pb systematics of phosphates from equilibrated ordinary chondrites. *Earth Planet. Sci. Lett.* **121,** 153-171.

Lindner, M., Leich, D.A., Russ, G.P., Bazan, J.M., and Borg, R.J. (1989) Direct determination of the half-life of ^{187}Re. *Geochim. Cosmochim. Acta* **53**, 1597-1606.

Miyamoto, M., Fujii, N., and Takeda, H. (1980) A model of the ordinary chondrite parent body (abstract). *Lunar Planet. Sci.* **11**, 737-739.

Miyamoto, M., Fujii, N., and Takeda, H. (1981) Ordinary chondrite parent body: An internal heating model. *Proc. Lunar Planet. Sci.* **12B**, 1145-1152.

Schoene, B., Crowley, J.L., Condon, D.J., Schmitz, M.D., and Bowring, S.A. (2006) Reassessing the uranium decay constants for geochronology using ID-TIMS U-Pb data. *Geochim. Cosmochim. Acta* **70**, 426-445.

Schön, R., Winkler, G, and Kutschera, W. (2004) A critical review of experimental data for the half-lives of the uranium isotopes ^{238}U and ^{235}U. *Appl. Radiat. Isot.* **60**, 263-273.

Appendix A

Calibration of Concentration of a 84Sr Spike

This appendix describes the procedure for measuring the concentration of the ^{84}Sr spike used for the first group of measurements of λ_{87}, Sr#3–Sr#18.

1.0 Pipettes for spike and $SrCO_3$ solution

A pipette was prepared for aliquoting the spike. The pipette was designed to minimize evaporation and maximize reproducibility. The pipette was made from Teflon® tubing, heated and stretched on both sides to create a reservoir between two extremely narrow outlets. A mark was made on the pipette to indicate how much to fill it. The empty pipette was weighed repeatedly. It was then weighed repeatedly with MQ H_2O in order to test the reproducibility and to measure evaporation from the pipette when full. The empty pipette weight is 0.33596 ± 0.00007 g. The weight with MQ H_2O is 0.44952 ± 0.00017. This results in a net weight of 0.11356 ± 0.000 17 (0.15%).

2.0 Preparation of the ^{84}Sr spike

The ^{84}Sr was prepared by diluting a mixed ^{85}Rb-^{84}Sr spike already in use in the laboratory. Because the spike was to be mixed with grams of $RbClO_4$, and no Rb isotopic measurements were required, the ^{85}Rb in the spike had no effect on the λ_{87} measurements. The concentration of the spike prior to dilution was approximately 0.69666 ± 0.01986 μg/g. The spike was prepared from SRM-988 with certified isotopic composition of Sr (NBS, 1973):

$^{86}Sr/^{84}Sr = 0.000589$

$^{87}Sr/^{84}Sr = 0.000098$

$^{88}Sr/^{84}Sr = 0.000386$

And isotopic abundances:

$^{84}Sr = 0.99892$

$^{86}Sr = 0.00059 \pm 0.00001$

$^{87}Sr = 0.00010 \pm 0.00001$

$^{88}Sr = 0.00039 \pm 0.00001$

Approximately 6 g of this spike were diluted in 70 g of water in a 125 mL FEP Nalgene® bottle.

3.0 Preparation of calibration solutions from SRM-987 $SrCO_3$ and $SrCl_2$

A total of five calibrating solutions were prepared, four from SRM-987 $SrCO_3$, and one from $SrCl_2$ obtained from Alfa Aesar®. Initially, two solutions, ROM 1.0 and ROM 2.0, were prepared from SRM-987 at the Royal Ontario Museum (ROM) in Toronto. A 1 gram ampoule of SRM-987 $SrCO_3$ was obtained. The salt was weighed and dried in two small Al-foil dishes. Weighing of all salts, flasks, vials, and solutions was with an OHAUS Analytical *Plus*® (AP250D-O) analytical balance. After preliminary weighing, the salt was dried in an oven at 115 °C for two hours, cooled in a desiccator, and reweighed. It was then returned to the oven overnight, and following cooling, was weighed again. Two 100 mL Kimax® volumetric flasks for the master solutions were weighed.

The $SrCO_3$ powder was transferred to the volumetric flasks. Because the transfer was not quantitative, the salt was reweighed in the volumetric flasks, and the difference between the flask weight with and without the salt was taken as the weight of the salt. This resulted in an uncertainty in the salt weight of approximately 0.1%. This is about an order of magnitude greater than the error of the salt weighed in the Al-foil dishes.

Following weighing, water and HNO_3 were added to the volumetric flasks. When the $SrCO_3$ was completely dissolved, additional water was added. Flask ROM 1.0 was filled to the 100 mL fill line. Flask ROM 2.0 was not completely filled, allowing room in the bottle to swirl and mix the solution. The concentrations of the two initial stock solutions are: ROM 1.0: 1,124,566 ± 1,039 ng Sr/g and ROM 2.0: 1,481,978 ± 1,712 ng Sr/g (Table 1).

3.1 Dilute concentrated calibration solutions

The planned working concentration for the spike was about 10 ng Sr/g. The two stock solutions were diluted approximately 100,000 times in two stages. Details of the weights of each solution are found in Table 1. 0.13944 g of ROM 1.0 and 0.13895 g of ROM 2.0 were pipetted out of the flasks and weighed in 7 mL Savillex® vials. These solutions were then transferred to bottles ROM 1.1 and ROM 2.1 respectively. In order to ensure quantitative transfer, the vials were rinsed five times each, and the rinses decanted into the bottles with the solution to be diluted. The bottles were filled with approximately 100 g of water. For the second stage, over 1 g of solution was diluted. Approximately 1 g of each solution was pipetted into the next bottles, ROM 1.2 and ROM 2.2, and weighed in those bottles. Those bottles were then filled with approximately 100 g of water, completing the dilution of the first two solutions.

3.2 Preparation of calibrating solutions GSC 1.2 and 2.2

Because of inconsistencies in the measurements of the concentrations of the spike using these two solutions, a second set of solutions were prepared at the Geological Survey of Canada (GSC) in Ottawa. The preparation of these solutions was similar to the preparation of the first two. Instead of weighing SRM-987 directly in the bottles, the salt was weighed in quartz crucibles. GSC 1.0 started with 0.15439 g and GSC 2.0 with 0.27486 `g of $SrCO_3$. The salt

was transferred into 1000 mL polypropylene bottles. Each crucible was rinsed 20 times, with the rinses decanted into their corresponding bottles to ensure quantitative transfer. HNO_3 was added, and following dissolution these bottles were filled with MQ H_2O. These were again diluted in two stages, into 1000 mL bottles. The solution to be diluted was weighed in Savillex® vials, and approximately 5-9 g of solution were weighed and diluted at each stage. Additional HNO_3 was added at each stage of dilution.

3.3 Preparation of ROM 3.0 from $SrCl_2$

A fifth calibrating solution, ROM 3.2, was prepared from $SrCl_2$. Approximately 5 g of $SrCl_2$ were obtained from Alfa Aesar® in a sealed glass ampoule under argon. The entire 5 g of $SrCl_2$ was used. The salt was weighed as the difference between full and empty ampoule. The dilution procedure was the same as for the GSC solutions. Solution for dilution was weighed in 3 mL Savillex® vials and the final bottle is 1000 mL FEP.

4.0 Calibrating the spike

Weighed aliquots of the calibrating solutions were mixed with aliquots of spike, equilibrated by heating on a hotplate in Savillex® vials, and dried down with H_3PO_4. Samples were loaded on Re filaments with Ta_2O_5 slurry and isotopic ratios were measured on a mass spectrometer. Measurements were made on the VG 354 at the Jack Satterly Geochronology Laboratory (JSGL) at the University of Toronto, and on the Triton at the GSC. Spike concentrations were calculated from measurements of isotopic ratios in the mixtures, weights of aliquots of spike and calibrating solution, and isotopic ratios of SRM-987 and SRM-988.

5.0 Results

Concentrations of individual solutions and dilutions are shown in Table 1. Concentrations of dilute solutions used for calibrations range from 11 – 25 ng Sr/g solution.

Detailed results of calibrations are shown in Table 2, and summarized in Figures 1 and 2. Measurements of GSC 1.2, GSC 2.2, and ROM 2.2 have the best reproducibility, and agree with one another. ROM 1.2 scatters more than those three solutions, and yield a slightly lower concentration. ROM 3.2, prepared from $SrCl_2$, scatters very widely, with most measurements yielding a higher concentration. A weighted average of all five solutions yields a spike concentration of 13.252 ± 0.058 (0.44%) ng ^{84}Sr/g solution (MSWD 3.2). A weighted average of the three more precise solutions yields 13.256 ± 0.023 (0.18%) ng ^{84}Sr/g solution (MSWD 0.82).

6 Discussion

6.1 Precision of spike calibration

This spike was calibrated at the working concentration of about 20 ng Sr/g. The advantage of calibrating a spike at the working concentration is that there are no further dilutions, so the spike that is actually used for the experiment is the one that is calibrated. If it must be diluted after calibration, there are no further checks on those dilutions. The drawback, however, is the sensitivity of the measurements to blank. This sensitivity was not considered when deciding to calibrate the spike at low concentration, and probably contributed to the scatter in the data. Typical procedure blanks for Rb-Sr chemistry are 10-60 pg. For approximately 3 g of spike mixed with 3 g of calibrating solution, the addition of 10 pg of common Sr will lower the apparent

concentration by approximately 0.02%. This may have contributed to some of the scatter in the data, as well as overall inaccuracy.

It was only in the process of the calibration of the spike that it was discovered that the Teflon® bottles in which both the calibration solutions and the spike were stored are permeable, and tend to lose between 0.08-0.18% per year. Because the weight of the bottles had not previously been tracked, it is difficult to quantify the magnitude of this effect. Though water generally diffuses out of the bottles, increasing the concentration, at least one bottle was observed to gain weight over time. This bottle, however, was kept in a humid atmosphere. There is no evidence of a time dependent change in λ_{87} measurements made with this spike, but most of the measurements were not precise enough for this effect to be noticeable. In addition, there was no accounting for evaporation from vials as spike and calibrating solutions were transferred into them for weighing.

6.2 ^{84}Sr spike compared with ^{84}Sr-^{86}Sr double-spike

The uncertainty of the concentration of the ^{84}Sr spike is only slightly greater than that of the ^{84}Sr-^{86}Sr double-spike. The uncertainty in the ^{84}Sr spike concentration is 0.18% when averaging only the three solutions which agree best. The ^{84}Sr-^{86}Sr double-spike is determined to 0.11%. Individual measurements of the ^{84}Sr-^{86}Sr spike concentration are in much better agreement than those of the ^{84}Sr spike, and it is uncertainty in the isotopic composition that increase the uncertainty on the concentration from about 0.4% to 0.11%. The full range of measurements is considerably smaller for the ^{84}Sr-^{86}Sr spike. The ^{84}Sr spike measurements span a range of 1.4%, while the ^{84}Sr-^{86}Sr spike range just 0.14%, and this is reduced to 0.06% if JSGL 2.4 measurements are excluded.

A final comparison between spikes relates not to the precision and accuracy of the concentration, but to the increased precision in λ_{87} measurements that the double-spike permits. The 2σ percent error on fractionation corrected $^{87}Sr/^{86}Sr$ in the λ_{87} measurements with the ^{84}Sr spike range from 0.05-0.58%, with an average of 0.22% (excluding one measurement that is extremely precise, primarily because of the very large number of measurements taken). By contrast, for measurements of λ_{87} with the double-spike, these errors are reduced to 0.004-0.14%, with an average of 0.02%. And only one measurement has an error as high 0.14%. The next highest is 0.04%. Thus, the double-spike achieves an average increase in precision of λ_{87} measurements from 0.22% to 0.04%.

7 Reference

NBS (National Bureau of Standards) (1973) Certificate of Analysis Standard Reference Material 988. Strontium-84 Spike Assay and Isotopic Solution Standard.

Table 1 - Preparation and Dilution of ^{84}Sr Spike Calibrating Solutions

Master Solution

Solution	Salt (g)	Sr (g)	Empty Bottle (g)	2σ	Solution (g)	Concentration (ng Sr/g solution)	2σ
ROM 1.0	0.191 38	0.113 58	63.561 7	± 0.000 1	101.00	1,124,550	± 1,039
ROM 2.0	0.201 70	0.119 71	53.770 1	± 0.000 0	80.78	1,481,956	± 1,712
ROM 3.0 ($SrCl_2$)	5.199 08	2.873 63	101.384 7	± 0.011 8	814.90	3,526,343	± 92
GSC 1.0	0.154 39	0.091 63	99.65	± 0.1	1010.55	90,676	± 42
GSC 2.0	0.274 86	0.163 14	100.4	± 0.1	1015.30	160,569	± 33

First Dilution

	Solution Diluted	Empty Bottle	2σ	Solution	Concentration (ng Sr/g solution)	2σ
ROM 1.1	0.139 44	30.689 29	± 0.000 22	122.613 5	1,279	± 1.428 51
ROM 2.1	0.138 95	38.351 64	± 0.099 75	115.860 5	1,777	± 2.605 25
ROM 3.1 ($SrCl_2$)	1.271 30	102.785 2	± 0.013 09	586.0	7,650	± 0.000 07
GSC 1.1	5.451 33	100.3	± 0.1	771.7	641	± 0.465 82
GSC 2.1	7.735 82	100.1	± 0.1	906.2	1,371	± 0.361 33

Second Dilution

	Solution Diluted	Empty Bottle	2σ	Solution	Concentration (ng Sr/g solution)	2σ
ROM 1.2	1.175 55	32.577 40	± 0.000 21	113.080 55	13.295 23	± 0.016 68
ROM 2.2	1.238 50	34.790 84	± 0.000 29	111.526 59	19.736 38	± 0.038 55
ROM 3.2 ($SrCl_2$)	1.355 44	224.72	± 0.01	599.62	17.292 75	± 0.001 00
GSC 1.2	6.942 24	54.8	± 0.1	408.9	10.876 30	± 0.020 21
GSC 2.2	8.746 84	54.4	± 0.1	476.8	25.145 44	± 0.010 00

All solutions except ROM 3.0 were prepared from SRM-987 $SrCO_3$

[1] ROM 1.0 and ROM 2.0 were prepared in Kimax® 100 mL volumetric flasks

Table 2 - ^{84}Sr Spike Calibration Measurements

	Calibrating Solution	Calibrating Solution (g)	^{84}Sr Spike (g)	^{84}Sr/^{86}Sr	molar concentration ^{84}Sr (nmol ^{84}Sr/g solution)	weight concentration ^{84}Sr (ng ^{84}Sr/g solution)
Mix-1	**GSC 1.2**	3.024 19	0.297 29	1.301 76	0.158 08	13.264 85
Mix-17	**GSC 1.2**	3.019 03	1.005 00	4.257 65	0.157 88	13.248 07
Mix-18	**GSC 1.2**	3.033 79	1.008 38	4.247 66	0.157 74	13.236 58
Mix-2	**GSC 1.2**	3.042 59	0.298 55	1.297 61	0.157 84	13.244 80
Mix-3	**GSC 1.2**	3.043 44	0.298 31	1.297 34	0.157 98	13.256 26
Mix-4	**GSC 1.2**	3.041 17	0.298 57	1.299 80	0.158 03	13.261 18
Mix-41	**GSC 1.2**	2.001 91	0.477 86	3.076 35	0.158 14	13.269 72
Mix-42	**GSC 1.2**	2.012 48	0.503 02	3.217 26	0.158 08	13.265 20
Mix-59	**GSC 1.2**	1.496 34	0.499 20	4.274 16	0.158 16	13.271 35
Mix-60	**GSC 1.2**	1.498 13	0.503 14	4.298 54	0.158 02	13.259 58
Mix-20	**GSC 2.2**	3.032 22	1.007 93	1.874 38	0.157 99	13.248 82
Mix-43	**GSC 2.2**	2.008 54	0.505 32	1.434 79	0.158 19	13.265 54
Mix-44	**GSC 2.2**	2.014 93	0.508 56	1.438 70	0.158 13	13.260 46
Mix-5	**GSC 2.2**	3.016 10	0.298 40	0.599 77	0.158 25	13.270 09
Mix-51	**GSC 2.2**	1.002 21	1.010 80	5.593 04	0.159 01	13.334 06
Mix-52	**GSC 2.2**	1.015 09	1.005 17	5.489 10	0.158 91	13.325 25
Mix-6	**GSC 2.2**	3.031 78	0.298 98	0.597 64	0.158 14	13.260 83
Mix-61	**GSC 2.2**	1.496 42	0.503 63	1.902 47	0.158 46	13.288 01
Mix-62	**GSC 2.2**	1.498 11	0.502 92	1.900 47	0.158 69	13.307 34
Mix-7	**GSC 2.2**	3.032 17	0.298 92	0.597 82	0.158 24	13.269 73
Mix-8	**GSC 2.2**	3.033 98	0.299 54	0.598 29	0.158 15	13.261 64
Mix-10	**ROM 1.2**	3.024 32	0.501 82	1.739 21	0.155 71	12.988 15
Mix-11	**ROM 1.2**	3.024 68	0.502 38	1.742 38	0.155 84	12.999 66
Mix-12	**ROM 1.2**	3.025 14	0.503 16	1.745 24	0.155 89	13.003 56

Table 2 - ^{84}Sr Spike Calibration Measurements

	Calibrating Solution	Calibrating Solution (g)	^{84}Sr Spike (g)	^{84}Sr/^{86}Sr	molar concentration ^{84}Sr (nmol ^{84}Sr/g solution)	weight concentration ^{84}Sr (ng ^{84}Sr/g solution)
Mix-9	**ROM 1.2**	3.018 06	0.497 49	1.730 31	0.155 91	13.004 81
#1 F4	**ROM 1.2**	0.113 61	0.113 58	10.270 49	0.157 75	13.158 47
#2 H1	**ROM 1.2**	0.113 50	0.113 54	10.061 77	0.154 41	12.880 04
#4 I3	**ROM 1.2**	0.113 56	0.113 60	10.106 63	0.155 11	12.938 14
#5 K1	**ROM 2.2**	0.113 61	0.113 58	6.967 21	0.157 19	13.189 97
#6 K4	**ROM 2.2**	0.113 50	0.113 54	7.011 57	0.158 10	13.266 81
Mix-13	**ROM 2.2**	3.013 58	0.503 26	1.220 97	0.157 88	13.248 40
Mix-14	**ROM 2.2**	3.021 46	0.503 03	1.213 57	0.157 36	13.204 53
Mix-15	**ROM 2.2**	3.022 66	0.502 52	1.212 63	0.157 45	13.212 43
Mix-16	**ROM 2.2**	3.024 63	0.503 56	1.215 57	0.157 63	13.227 39
Mix-53	**ROM 3.2**	1.005 42	1.004 98	8.003 20	0.158 50	13.300 01
Mix-54	**ROM 3.2**	1.005 83	1.004 02	7.953 69	0.157 72	13.234 78
Mix-55	**ROM 3.2**	1.002 61	1.003 90	8.180 02	0.161 76	13.573 98
Mix-56	**ROM 3.2**	1.005 08	1.003 64	8.161 05	0.161 82	13.579 01
Mix-57	**ROM 3.2**	1.003 03	1.004 67	8.192 08	0.161 95	13.589 50
Mix-58	**ROM 3.2**	1.006 23	1.005 00	8.162 47	0.161 82	13.578 53
Mix-63	**ROM 3.2**	1.491 48	0.504 17	2.769 45	0.159 47	13.381 30
Mix-64	**ROM 3.2**	1.504 01	0.504 91	2.747 26	0.159 26	13.363 49
Mix-65	**ROM 3.2**	1.508 22	0.504 06	2.741 26	0.159 61	13.393 52
Mix-66	**ROM 3.2**	1.509 61	0.503 81	2.781 69	0.162 25	13.614 89
Mix-67	**ROM 3.2**	1.006 87	0.302 97	2.576 99	0.166 41	13.964 02
Mix-68	**ROM 3.2**	1.005 29	0.498 80	4.229 87	0.167 30	14.038 14
Mix-69	**ROM 3.2**	0.964 00	1.006 82	8.720 89	0.165 46	13.884 35
Mix-70	**ROM 3.2**	1.000 17	1.010 97	8.423 31	0.165 07	13.850 97

Figure 1 - Concentration of ^{84}Sr spike measured against all five calibrating solutions

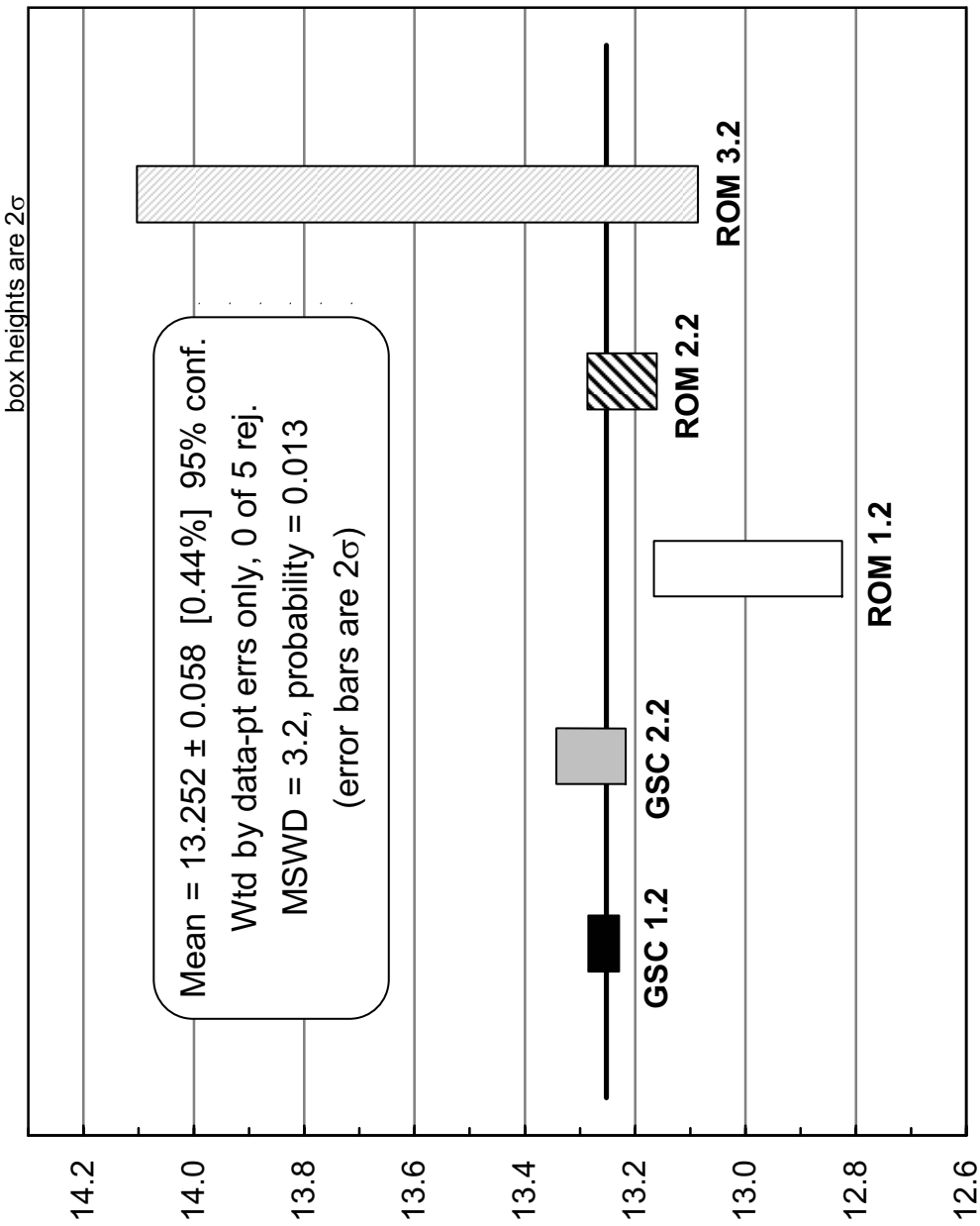

Figure 2 - Concentration of ^{84}Sr spike measured against calibrating solutions that yield best agreement

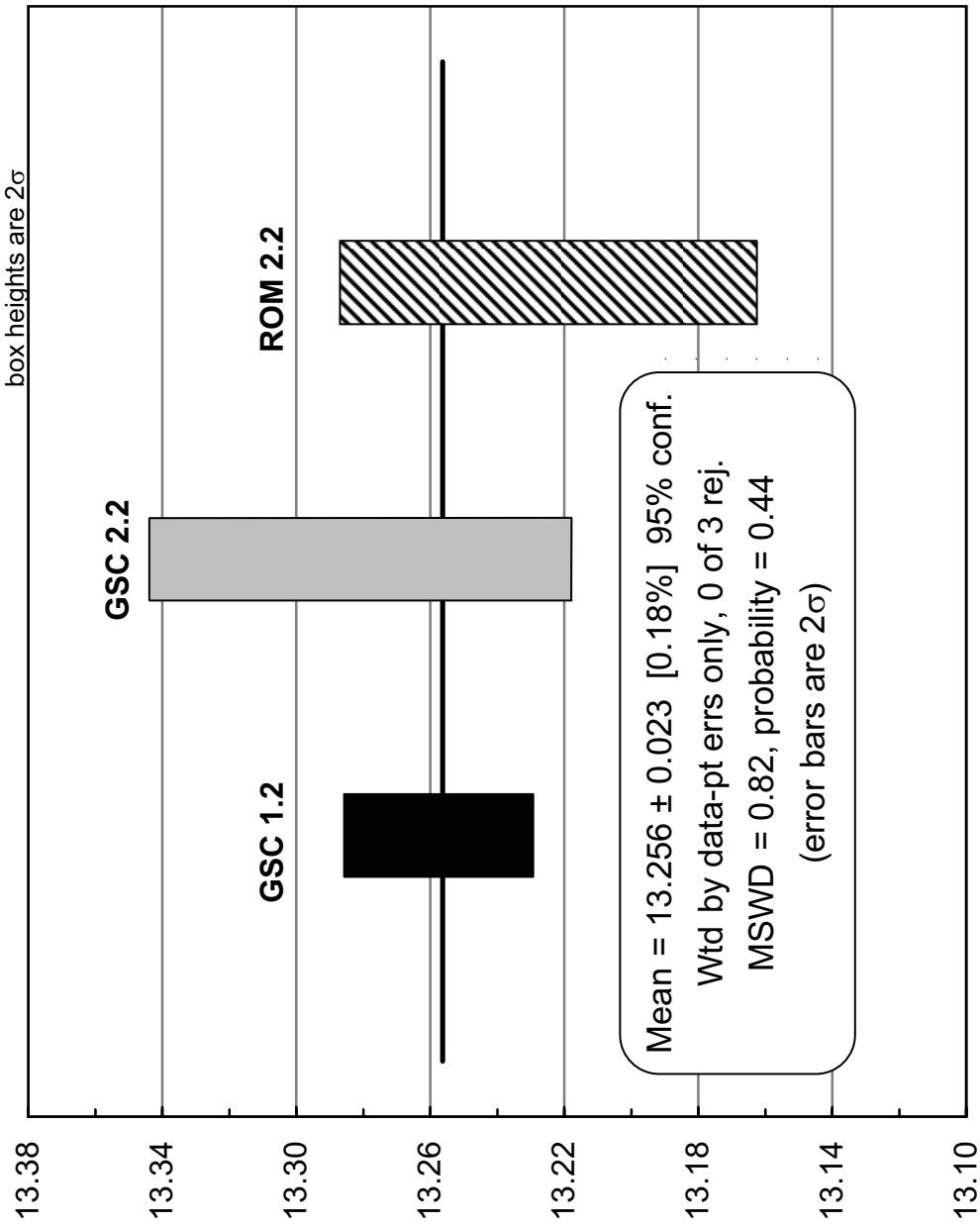

Appendix B – Washing and Leaching of Meteorite Specimens

Phosphates

Ultrasonic 15 minutes in ethanol
Ultrasonic distilled acetone 30 seconds
Rinsed 2x with distilled acetone
Dissolved in 1N HBr and 6N HCl

Silicates

Chond Sil 3

L/LL4	Bjurböle	Fraction 1
L/LL4	Bjurböle	Fraction 2
L6	Kunashak	
LL3	Krymka	Fraction 1
LL3	Krymka	Fraction 2
H5	Orlovka	Fraction 1
H5	Orlovka	Fraction 2
L6	Pervomaisky	
L4	Saratov	Fraction 1
L4	Saratov	Fraction 2

HCl + Ethanol - ultrasonic 30 min
Rinse with Acetone
4N HNO_3 on hot plate for 30 min
MQ rinse
2N HCl on hot plate - 30 min
Rinse:
MQ
MQ
Acetone
Acetone

Chond Sil 4

L5	Elenovka	Pyroxene 3

L5 Elenovka Pyroxene 4
L5 Elenovka Chondrule 1
L5 Elenovka Chondrule 2

Rinse in Ethanol
Rinse in acetone
30 min in 7N HNO_3 on hot plate, some grains slightly stick to bottom of beaker
Dilute with MQ - briefly ultrasonic to release stuck grains
Rinse MQ
2N HCl on hot plate for ~ 1 hour
Rinse with MQ
Rinse 3x with distilled acetone

Chond Sil 5

LL3 Unnamed Antarctic Chondrule 1
LL3 Unnamed Antarctic Chondrule 2
LL3 Unnamed Antarctic Chondrule 3a
LL3 Unnamed Antarctic Chondrule 3b
LL3 Unnamed Antarctic Chondrule 4
LL3 Unnamed Antarctic Chondrule 6

Samples rinsed in Ethanol
Rinsed in acetone
3N HCl on hot-plate at "4" (surface T 170 °C) - 1 hour
Some grains stick to the bottoms of the beakers - and solutions yellow slightly
Ultrasonic for 10-30 seconds to release these grains
Rinsed with MQ
2N HNO_3 on hot plate at "4" (170 °C) - 30 min
Acid is clear and colorless after this cleaning stage
Rinse with MQ
Rinse with distilled acetone 2x

Chond Sil 10

LL3 Krymka Fraction 3

LL3	Krymka	Fraction 4
LL3	Krymka	Fraction 5
LL3	Krymka	Fraction 6
LL3	Krymka	Fraction 7
LL3	Krymka	Fraction 8
LL3	Krymka	Fraction 10
LL3	Krymka	Fraction 11

Fractions are picked from +100 mesh crushed bulk meteorite.
Washed in ultrasonic in 4N HNO_3 - 30 min
Rinsed with acetone
Ultrasonic in 6N HCl + ethanol 1:1 mixture - 30 min. Repeated twice.
Rinsed with ethanol several times
Final picking - fragments are sorting according to their appearance
Rinsed with distilled acetone, air dried, and weighed
Selected fractions finely crushed in Al_2O_3 mortar

Chond Sil 11

L/LL4	Bjurböle	Chondrule 7	Finely crushed chondrule
L/LL4	Bjurböle	Chondrule 8	Finely crushed chondrule
L/LL4	Bjurböle	Chondrule 9	Finely crushed chondrule
L/LL4	Bjurböle	Chondrule 10	Finely crushed chondrule
L/LL4	Bjurböle	Chondrule 11	Uncrushed chondrule
L/LL4	Bjurböle	Chondrule 12	Finely crushed chondrule
L/LL4	Bjurböle	Chondrule 13	Uncrushed chondrule
L/LL4	Bjurböle	Chondrule 14	Finely crushed chondrule
L/LL4	Bjurböle	Chondrule 15	Finely crushed chondrule
H6	Kidairat	Chondrule 1	Mechanically crushed. Not washed
H6	Kidairat	Chondrule E1	Grey, barred chondrule.

Same as Chond Sil 10
Chondrules 10-15 were abraided prior to washing
Chondrules were crushed finely in Al_2O_3 mortar after initial washing and weighing.
Chondrules 11 and 13 were not crushed
Final washing:
Rinsed 2x in acetone
Rinsed with MQ

Cleaned ultrasonically in 2N HCl 4x

Chond Sil 12

H6	Kidairat	Chondrule E2	Grey grains.
H6	Kidairat	Chondrule E3	Grey and clear, radial, chondrule fragment.
H6	Kidairat	Chondrule E4	Clear and white grains, with some opaque material.
H6	Kidairat	Chondrule E5	White grains - nearly whole chondrule.
H6	Kidairat	Chondrule E6	White grains - nearly whole chondrule.
H6	Kidairat	Chondrule M4	Clear grains, radial.
H6	Kidairat	Chondrule M5	Mostly clear grains, some opaque material.
H6	Kidairat	Chondrule M6	Large fragment
H6	Kidairat	Chondrule E7	White and clear chondrule.

Grains were washed in small glass beakers in ultrasonic bath in 1:1 mixture Ethanol & 6N HCl

1) After two hours:
    - Chondrule 1 Cloudy and yellow
    - Chondrule 2 Almost no change
    - Chondrule 3 Slighty yellow
    - Chondrule 4 Slighty yellow
    - Chondrule 5 Slighty yellow

2) After 1.5 hours
    - Chondrule 1 Cloudy
    - Chondrule 2 No change
    - Chondrule 3 Slighty yellow
    - Chondrule 4 Slighty yellow
    - Chondrule 5 Slighty yellow

3) Additional 0.5 hour
    - All Clear

4) Additional 0.5 hour
    - All Clear

Final washing
    - 4 cycles, 10 minutes ultrasonic bath in 3.1 N HCl

Chond Sil 15

ER01-105	L/LL6	Holbrook	Chondrule E9	Chondrule fragment
ER01-109	L/LL6	Holbrook	Chondrule E11	Chondrule fragment
ER01-111	L/LL6	Holbrook	Chondrule E12	Chondrule fragment
ER01-113	L/LL6	Holbrook	Chondrule Fragments	Eight chondrule fragments from different chondrules
ER01-119	LL5	Tuxtuac	Chondrule 1	Small dark grey chondrule

Same as Chond Sil 12

Chond Sil 16

LL5	Tuxtuac	Chondrule 1	Small dark grey chondrule
LL5	Tuxtuac	Chondrule 2	½ of a dark grey chondrule
LL5	Tuxtuac	Chondrule 3	Large chondrule fragment, some residual rust staining.
LL5	Tuxtuac	Chondrule 4	½ of a chondrule
LL5	Tuxtuac	Chondrule 5	Fragment of a dark grey fine grained chondrule
L6	Barwell	Chondrule 1	Large, light and medium grey chondrule.
L6	Barwell	Chondrule 2	Light grey chondrule.
L6	Barwell	Chondrule 3	~½ of a dark grey chondrule
L6	Barwell	Chondrule 4	One light grey chondrule
L6	Barwell	Chondrule 5	Most of one light grey chondrule.

Same as Chond Sil 12

Chond Sil 17

H4	Ankober	Chondrule 1	Large whole chondrule. Dark Grey.
H4	Ankober	Chondrule 2	Large whole chondrule. Dark Grey.
H4	Ankober	Chondrule 3	Whole chondrule. Dark Grey.
H4	Ankober	Chondrule 4	Whole chondrule. Dark Grey.
H4	Ankober	Chondrule 5	Whole chondrule. Light Grey.
H4	Ankober	Fragment 6	Large chondrule fragment
H4	Ankober	Fragment 7	Small chondrule fragment. Radial.
L4	Saratov	Chondrule 1	Dark chondrule with bleached rim
L4	Saratov	Chondrule 2	Dark chondrule with bleached rim

L4	Saratov	Chondrule 3	Small dark chondrule
L4	Saratov	Fragment 4	Light grey chondrule fragment. Prior to initial washing, encrusted in rusty material

Initial: 4x cycles 1:1 EtOH and 6N HCl - 0.5 hour/cycle
Final: 4x cycles, 10 min. ultrasonic in 6N HCl